AN APPLICATION OF VAN-DER-WAALS' FORCES IN MICRO-MATERIAL HANDLING.

by

STEPHEN MATOPE

PROMOTOR: DR. ANDRE F. VAN DER MERWE

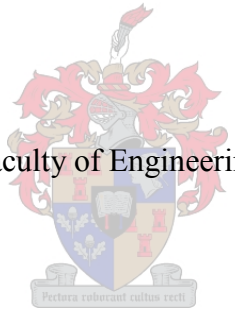

Faculty of Engineering

Dissertation presented for the degree of Doctor of Philosophy in Engineering at the University of Stellenbosch

Department of Industrial Engineering

December 2012

DECLARATION

By submitting this thesis/dissertation electronically, I declare that the entirety of the work contained therein is my own, original work, that I am the sole author thereof (save to the extent explicitly otherwise stated), that reproduction and publication thereof by Stellenbosch University will not infringe any third party rights and that I have not previously in its entirety or in part submitted it for obtaining any qualification.

December 2012

ABSTRACT

This doctoral dissertation focuses on the application of Van-der-Waals' forces in micro-material handling. A micro-material handling system consists of four main elements, which include: the micro-gripper, the micro-workpart, the picking up position and the placement position. The scientific theoretical frameworks of Van-der-Waals' forces, presented by Van der Waals, Hamaker, London, Lifshitz, Israelachvilli, Parsegian, Rumpf and Rabinovich, are employed in exploring the extent to which these forces could be applied in a micro-manufacturing situation. Engineering theoretical frameworks presented by Fearing, Bohringer, Sitti, Feddema, Arai and Fukuda, are employed in order to provide an in-depth synthesis of the application of Van-der-Waals' forces in micro-material handling. An empirical or pragmatic methodology was adopted in the research.

The Electron Beam Evaporation (e-beam) method was used in generating interactive surfaces of uniform surface roughness values. E-beam depositions of copper, aluminum and silver on silicon substrates were developed. The deposition rates were in the range of 0.6 – 1.2 Angstrom/s, at an average vacuum pressure of 2×10^{-6} mbar. The topographies were analysed and characterised using an Atomic Force Microscope and the corresponding *rms* surface roughness values were obtained. The Rumpf-Rabinovich equation, which gives the relationship of the exerted Van-der-Waals' forces and the *rms* surface roughness values, is used to numerically model the results. In the final synthesis it is observed that the e-beam depositions of copper are generally suited for the pick-up position. Aluminum is suited for the micro-gripper and silver is suited for the placement position in an optimised micro-material handling system.

Another Atomic Force Microscope was used in order to validate the numerically modelled results of the exerted Van- der-Waals' forces. The aim was to measure the magnitude of Van-der-Waals' forces exerted by the e-beam depositions and to evaluate their applicability in micro-material handling operations. The measurements proved that Van-der-Waals' forces exerted by the samples could be used for micro-material handling purposes on condition that they exceeded the weight of the micro-part being handled.

Three fundamental parameters, ie: material type, geometrical configuration and surface topography were used to develop strategies of manipulation of micro-materials by Van-der-Waals' forces. The first strategy was based on the material type variation of the interactive

surfaces in a micro-material handling operation. This strategy hinged on the fact that materials have different Hamaker coefficients, which resulted in them experiencing a specific Van-der-Waals' forces' intensity during handling. The second strategy utilised variation in the geometrical configuration of the interacting surfaces. The guiding principle in this case was that, the larger the contact area was, the greater the exerted Van-der-Waals' forces would be In the analytical modelling of Van-der-Waals' forces with reference to geometrical configuration, a flat surface was found to exert more force than other configurations. The application of the design, for purposes of manufacturing and assembling (DFMA) criteria, also proved that flat interactive surfaces have high design efficiency. The third strategy was based on surface roughness. The rougher the topography of a given surface was, the lesser the Van-der-Waals' forces exerted were. It was synthesised that in order for a pick-transfer-place cycle to be realised, the root-mean-square (*rms*) interactive surface roughness values of the micro-part (including the picking position, the micro-gripper, and the placement position) should decrease successively. Hybrid strategies were also identified in this research in order to deal with some complex cases. The hybrids combined at least two of the aforementioned strategies.

ACKNOWLEDGEMENTS

I am very thankful to Dr. Andre F. Van der Merwe, my study leader, who was inspirational in conducting of this PhD research. His expertise in guiding me in this research is second to none. Without him, this research would not have been successful.

I would also again, like to acknowledge the support I received from my wife, Jasmine. She supported me unhesitatingly as I completed my research. May God reward her abundantly. On the same note, I would like to thank my daughters, Ishetendwai and Ishekudzwai,as well as my son, Mbirikunashe, who were very considerate when I spent much time on this research.

I greatly appreciate the support I received from the Industrial Engineering Department's staff and students. Their constructive opinions led to the success of this dissertation. I am greatly indebted to the staff of iThemba Laboratories (Cape Town, South Africa) and Particle Engineering Research Center (Florida University, USA) who provided the scientific resources required for the completion of this research. The Electronics, Process Engineering, Polymer Science, Geology and Textile Departments of Stellenbosch University also aided substantially in the provision of laboratory equipment required in this research.

I also thank the Chemnitz University of Technology staff (Germany) for their superb support by allowing me to spend three months at their campus during my studies. I am again very grateful to the German Research Foundation (DFG), the special research field SFB/TR 39, for funding my research during that period.

Finally, I would like to, above all, thank Almighty God, who granted me the resources, good health, wisdom, intelligence and diligence to accomplish this research.

TABLE OF CONTENTS

LIST OF FIGURES

LIST OF TABLES

GLOSSARY

- 'AFM' – atomic force microscope
- 'Ag' - Silver
- 'A_H' - Hamaker coefficients,
- 'Al' - Aluminum
- 'Cu' – Copper
- 'DFG' - German Research Foundation
- 'DFMA' - design for manufacturability and assemblability
- 'DFMA' - Design For Manufacturability and Assembly
- 'Hamaker coefficient' is a chemical property of matter which reflects the intensity of the Van-der-Waals' forces exerted by a given substance (Parsegian, 2006).
- 'H_j' - jump-in distance of an AFM probe
- 'mbar' – millibar, a pressure unit.
- 'MEMS' - micro-electro-chemical systems
- 'Micro-gripper' is an end effector of a micro-robot which interacts with micro-work part in a pick-transfer-place cycle.
- 'Micromanipulation' is the task of grasping, moving, reorienting and repositioning of micro-scale objects (Krishnan and Saggere (2011))
- 'Micro-manufacturing' refers to the processing of raw materials in the microscopic range, from 10 mm down to 1µm.
- 'Micro-material handling' refers to a system in which micro-work parts are transferred by micro-grippers from a pick-up position to a placement position in a micro-manufacturing environment.
- 'Micro-object', 'micro-workpart', 'micro-workpiece', 'micro-part' are used interchangeably and refer to the micro-material or micro-bodies of dimensions 10 mm down to 1µm, which have to be moved from one position to another. The definition is attained by combining the following definitions: Atsushi et al (2011), refer to micro-objects as items with outer dimensions, ranging from several hundred microns to several millimetres. Nah and Zhong (2007), state that a micro-part has a diameter less than 1mm, but do not mention anything to do with the length. The maximum dimension of a micro-part used in this research is 10 mm as given by Attia and Alock (2011), and Cao et al (2004).

- 'Micro-robots' are industrial machines that are programmed to perform functions within a work-volume of 30 mm x 30 mm x 30 mm, in a manufacturing environment.
- 'MST' - micro systems technology
- 'Non-retarded Hamaker coefficient' refers to the Hamaker coefficient where there is no time delay in the transmission of electric and magnetic signals between interacting charges of given materials.

- 'p_{Boyle}' - Boyles' pressure
- 'PhD' – Doctor of philosophy
- 'Pick-up position' or 'picking position' refers to a place from which a micro-work part is taken or lifted up during micro-material handling.
- 'Placement position' refers to the place onto which a micro-work part is released or placed at the end of a transfer operation.
- '*rms*' – root-means-square of surface roughness
- 'Root mean square' (*rms*) is a measure of the roughness of a given surface topography. It is the square root of the arithmetic average of the squares of the asperity heights along equally spaced points on a trace (Rabinovich et al, 2000; Matope et al, 2010)
- 'Substrate' refers to the material onto which e-beam depositions are made.
- 'Van-der-Waals' forces' may be simply defined as natural attractive forces which exist between two particles or surfaces which are in close proximity (Fukuda T. & Arai F., 1999; Parsegian, 2006). An advanced definition would be that Van der Waals' forces are short-range forces, acting when surfaces are sufficiently close together, and are due to spontaneous electrical and magnetic polarisations that cause a fluctuating electromagnetic field within the medium and the gap between the surfaces involved (Debrincat, D.P., Solnordal, C.B., Van Deventer, J.S.J., 2008; Zhang, H.W., Wang, J.B., Ye, H.F., Wang, L., 2007).
- 'C_m' – operation cost
- 'E-beam' refers to the electron beam evaporation method and is also in some cases used as an adjective to describe the type of deposition produced by this method.
- '*g*' – gravitational acceleration
- '*H*'- shortest surface-to-surface separation distance between interacting micro-parts
- 'H_o' – possible shortest surface-to-surface separation distance between interacting surfaces which are in the closest proximity.

- 'N_m' - minimum number of theoretically needed parts for DFMA
- 'p_{vdW}' - Van der Waals pressure
- 'R' – radius
- 'Researcher' refers to the author of the PhD dissertation, who is Stephen Matope.
- 'T' - absolute temperature in Kelvins
- 'T_m' – operation time for DFMA
- 'zJ' - zepto-Joule, where 1 zJ = $1x10^{-21}$ J
- 'γ' – surface tension constant
- 'θ' – angle's value
- 'λ' - the peak-to-peak distance of the surface roughness asperities
- 'ρ' – density

1 CHAPTER 1: INTRODUCTION

1.1 Background

The market for micro-products is on the rise (Qin, 2006). The demand for micro-components, which includes: micro-sensors, micro-chips, micro-parts for cellphones and micro-robots has increased steadily over the last decade (Hesselbasch and Raatz, 2007). Figure 1-1 shows a growth rate of 16% per year, from $12 billion in 2004 to $25 billion in 2009, across a spectrum of 26 micro-electro-chemical systems/micro systems technology (MEMS/MST)'s products as postulated by the NEXUS report (Salomon, 2005). This trend is also confirmed by the MINAM Position Paper (2011). However; the micro-manufacturing industry is experiencing challenges in meeting the demand for micro-products due to inappropriate micro-material handling technology being used.

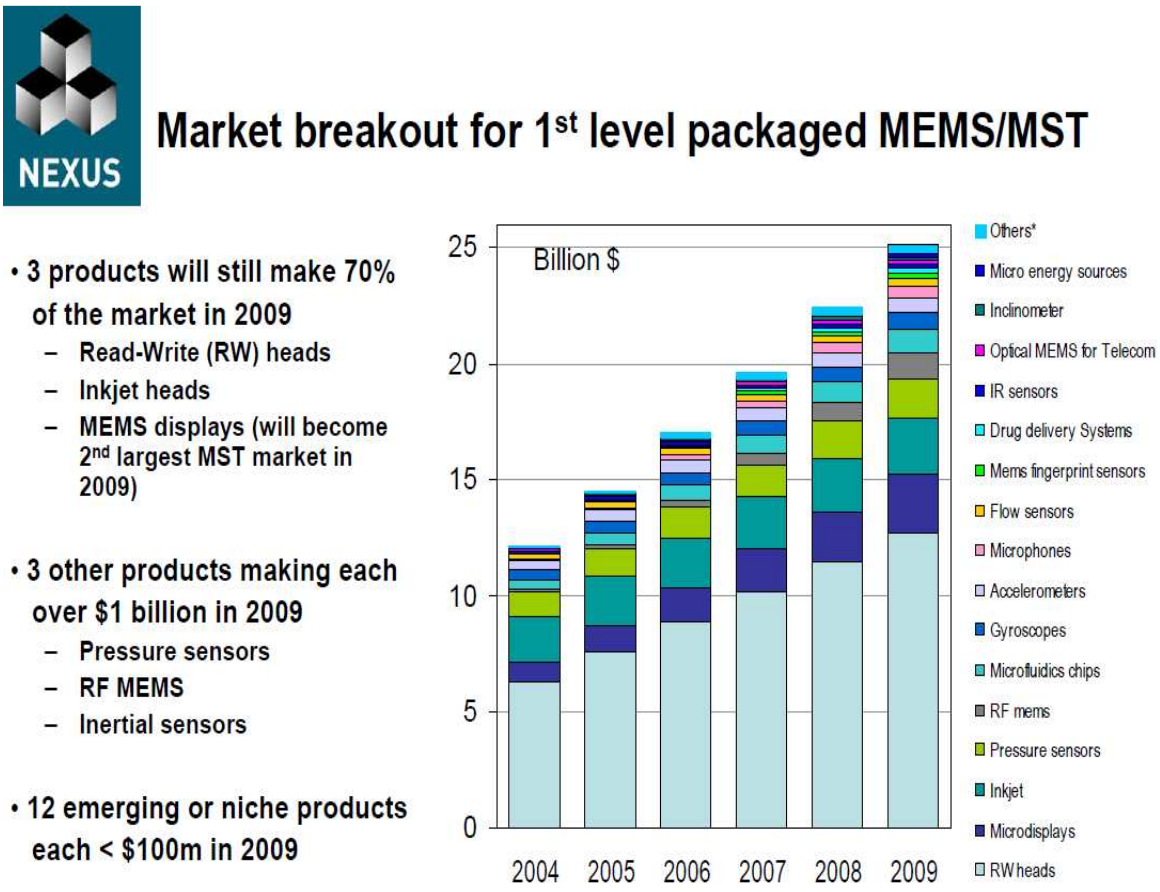

Figure 1-1 Demand increase for micro-products (Salomon, 2005)

Macro-machines have been used to mass produce micro-products to meet the demand. However, these conventional machines have failed. This has led to the development of micro-factories, similar to the one shown in Figure 1-2 (Okazaki Y., Mishima N., and Ashida K., 2004).

These consist of micro-machines which are miniature versions of conventional machines, but more efficient than the former. The micro-machines have almost the same number of components as the conventional versions (Okazaki Y., Mishima N., and Ashida K., 2004). However; conventional micro-material handling instruments are still being used with these micro-machines.

Figure 1-2 Microturning system in a carry box (courtesy NANO Co.) (Okazaki Y., Mishima N., and Ashida K., 2004)

Some of the conventional instruments are actuated by mechanical, electrical, electromagnetic, pneumatic and hydraulic forces. (A.J. Sanchez-Salmeron, R. Lopez-Tarazon,R. Guzman-Diana, C. Ricolfe-Viala , 2005) However; they have proven to be unsuitable for micro-manipulation due to the imposition of mechanical strains, polarization, oxidation and residual stresses (to mention, just a few). They occupy a large amount of space and impair the vision

and precision required in micro-material handling. They are made up of numerous parts which result in them having a low design efficiency according to DFMA principles (Boothroyd, 1994).

On the other hand, adhesive forces add to the dilemma of micro-material manipulation (Rollot, Y., Regnier, S., Guinot, J.C. , 1999). Whilst making it easy to pick a micro-workpart, they also make it difficult to release (Bohringer K.F., Fearing R.S., Goldberg K.Y., 1999). Gravity cannot initiate an effective release in cases where micro workparts are of masses less than 1×10^{-6} kg (Sanchez J. A, 2010) because the adhesive forces supersede it (Fukuda T. & Arai F., 1999; Fearing, 1995; Bohringer K.F., Fearing R.S., Goldberg K.Y., 1999). This leaves a technological gap which needs to be filled as far as efficacy in micro-material handling is concerned.

1.2 Problem Statement

Adhesive forces hinder the efficient picking and releasing of a micro-part (Fearing, 1995; Fukuda and Arai, 1999). These forces are composed of electrostatic, surface tension and Van-der-Waals' forces (Neugebauer et al, 2011). Although these forces are a problem in micro-material handling systems, some researchers have identified how they can be used profitably. There has been extensive research on how surface tension forces can be used effectively in the handling of micro-materials (Lambert P. , 2007; Lambert P., Seigneur F., Koelemeijer S., and Jacot J., 2006). However; they are not applicable in either vacuum or aqueous environments (Lambert, 2007). As for electrostatic gripping and releasing, several authors have completed research in this area (Neugebauer R., Koriath H.-J., Muller M., June 2010; Hesselbach J., Wrege J., Raatz A., 2007; Biganzoli F., Fantoni G., 2008). However; electrostatic forces do not work in aqueous conditions (Lambert, 2007).

Limited research has been done in the application of Van-der-Waals' forces in micro-material handling especially preceding 2007 (Lambert P. , 2007) when this research was first embarked upon. These forces can work in almost all environments, including vacuum and aqueous conditions (Neugebauer, R., Koriath, H-J., Van der Merwe, A. F., Müller M. and Matope, S., 2011). Articles have been written on the planning for the application of Van-der-Waals' in micro-material handling (Feddema J.T., Xavier P., and Brown R., 1999), but no significant research has been conducted on the application of the forces. On the other hand, it is evident that these forces are used in nature, as in the case of geckoes (Autumn, 2002).

Geckoes use Van-der-Waals' forces in scaling surfaces of any orientation (Autum K., Sitti M., Liang Y.A., Peattie A.M., Hansen W. R., Sponberg S., Kenny T.W., Fearing R., Israelachvili J.N., Full, R.J., 2002). Although these forces are considered weak (Reich R.A., Stewart P.A., Bohaychick J., Urbanski,J.A., 2003; Bhushan, 2003) they are proving to be strong enough to prevent the massive geckoes (relative to the mass of micro-part) from dropping down from inverted surfaces.

Therefore; this research aims at applying Van-der-Waals' forces in the handling of micro-materials in a given manufacturing environment. The null hypothesis is that Van-der-Waals' forces can be utilised in micro-material handling. The alternative hypothesis is that Van-der-Waals' forces are inapplicable in micro-material handling operations.

In the event that the null hypothesis is proven true, then the main research question and sub-questions would be:
Research Question: What strategies should be employed to utilise Van-der-Waals' forces reliably in micro-material handling?
Sub-question 1: What are Van-der-Waals' forces?
Sub-question 2: Why should they be used in a micro-material handling system?
Sub-question 3: Which parameters greatly influence Van-der-Waals' forces?
Sub-question 4: What are the components of a micro-material handling system?
Sub-question 5: How can Van-der-Waals' forces be used to realise a reliable micro-material handling operation?
Sub-question 6: What strategies should be employed to use Van-der-Waals' forces effectively in a micro-material handling operation?

The research objectively identifies the main parameters upon which Van-der-Waals' forces depend. It then characterises the micro-material handling components and develops three fundamental micro-material handling strategies. These originate from material type, geometrical configuration and surface topography. It subsequently presents a hybrid strategy for complicated micro-material handling operations.

With reference to Figure 1.3, the criteria for a reliable pick-transfer-place cycle in micro-material handling is that the picking place (A) should exert less force on the micro-part (B) than the micro-gripper (C), and the placement position should exert more force than the

micro-gripper. In this case, the weight of the micro-part should be less than the Van-der-Waals' forces exerted by the gripper.

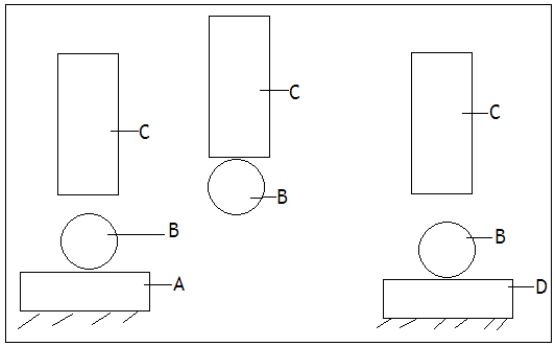

Figure 1.3 Micro-material handling system

The benefits of using Van-der-Waals' forces in micro-material handling are that they do not require any external energy supply for gripping purposes. They do not induce the development of oxide layers as in the case of surface tension and do not pollute the environment. Neither do they leave residual charges as in the case of electrostatic forces nor residual strains as in the case of vacuum-force actuated grippers (Neugebauer, R., Koriath, H-J., Van der Merwe, A. F., Müller M. and Matope, S., 2011). High productivity, reliability and efficacy of a micro-material handling system could be realised by utilising these forces because they overcome the challenges experienced when releasing a micro-part.

1.3 Road Map

The study matches research findings from the scientific and engineering disciplines in order to achieve its objectives. On the scientific side, the work done by Hamaker (1937) on different intensities of Van-der-Waals' forces exerted by different materials because of their unique nature, is employed in this research (Parsegian, 2006; Hamaker, 1937). Lifshitz' (1956) research on the calculation of the Hamaker coefficients using quantum theory instead of the additive method, is also considered (Lifshitz, 1956). This theory takes into cogniscence, the fact that Van-der-Waals' forces (among a group of atoms) are affected by an interference of electron clouds caused by the adjacent atoms. The work by Parsegian (2006) and Israelachvili (2011) is used to interpret how geometrical parameters affect the intensity of the exerted Van-der-Waals' forces between interacting bodies (Israelachvili, 1972; Israelachvili, 2011; Parsegian, 2006). The works by Rumpf (1990) and Rabinovich et al (2000) are used to understand the effect of surface roughness on the exerted Van-der-Waals' forces between

interacting surfaces (Rabinovich I. Y., Adler J. J., Ata A., Singh K. J., and Moudgil M.B., 2000; Rumpf, 1990; Rabinovich Y. I, Adler J. J., Ata A., Singh R.K. , Moudgil B. M., 2000).

In the engineering discipline, research done by Arai and Fukuda (1995),in understanding adhesive forces, is applied (Arai F, Ando D., Fukuda T., Nonoda Y., Oota T, 1995; Fukuda T. & Arai F., 1999). The work done by Fearing (1995) and Bohringer et al (1999), which highlights the predominance of adhesive forces over gravity, is also employed (Fearing, 1995; Bohringer K.F., Fearing R.S., Goldberg K.Y., 1999). The research by Sitti et al (2003), Aksak et al (2007) and Murphy et al (2011) on the application of gecko-hair-like micro-structures in the design of wall-climbing robots is adapted for micro-material handling purposes (Michael P. Murphy, Casey Kute, Yi˘git Mengüç and Metin Sitti, 2011; Murphy, M. P. and Sitti, M, 2007; Aksak, B., Murphy, M., and Sitti, M. , 2007; Sitti, M. & Fearing, R. , 2003).

The ensuing Chapter 2 covers the literature review on micro-material handling, in which the parameters influencing Van-der-Waals' forces are identified, and a comparison is made of the forces active in micro-material handling systems. Chapter 3 details the methodology and the approaches employed whilst conducting this research. It further details experimental work executed in order to achieve the objectives of this research. Chapter 4 highlights the research findings and the analysis and Chapter 5 sets out the conclusions and recommendations.

Furthermore; Appendix A includes the abstracts of articles published in peer-reviewed and accredited journals and conferences as academic outputs of this research. Appendix B includes a letter of collaborative research with iThemba laboratories. Appendix C contains the researcher's report of his work as a research scientist at Chemnitz University of Technology, Germany (where an invitation was extended to him as a result of the outputs of his PhD studies). Appendix D includes communication with Florida University as a proof of collaborative research initiated as a result of this study. Appendix E contains tables of Hamaker coefficients. Appendix F includes properties of e-beam deposited materials. Appendix G contains copies of the original e-beam evaporation log-sheets as proof that the e-beam depositions were actually conducted on the stated dates over a period of two years. Appendix H includes X-ray diffraction (XRD) graphs of the e-beam deposited samples to prove their purity. Appendix I includes the manufacturer's specifications of the polyurethane materials used in this study. Appendix J includes Van-der-Waals' Forces and other properties measured by the Asylum MFP 3 D-Bio Atomic Force Microscope model with version 6.22A

software as validation of the results of this study. Appendix K carries experimental samples and equipment. Appendix L contains polyurethane graphs of preloads and the exerted Van-der-Waals forces plotted against time. Finally, Appendix M contains the papers published in accredited journals as well as regional and international conferences as research outputs of this PhD study.

2 CHAPTER 2: LITERATURE REVIEW

2.1 Introduction

This chapter highlights the discovery of the Van-der-Waals' forces and explores their application in solid state materials. It also sheds light on other active forces in the micro-range which include adhesive forces such as surface tension and electrostatic forces. The application of these forces are analysed and their limitations revealed. This analysis finally leads to a synthesis on the application of Van-der-Waals' forces in micro-material handling systems.

2.2 Van-der-Waals' forces

2.2.1 Definition of Van der Waals' forces

Van-der-Waals' forces are adhesive forces which cause particles to adhere to surfaces. They are caused by spontaneous electrical and magnetic polarisations when surfaces are positioned sufficiently close together. The polarisations develop a fluctuating electromagnetic field that is generally attractive in nature, yielding the Van-der-Waals' forces (Debrincat, D.P., Solnordal, C.B., Van Deventer, J.S.J., 2008; Zhang, H.W., Wang, J.B., Ye, H.F., Wang, L., 2007).

Van-der-Waals' forces exist even in the event of the interacting objects being electrically neutral and even when they do not carry electric or magnetic moments (Buhmann, S.Y. & Welsch, D.G., 2007). They arise from quantum zero-point fluctuations; ie: the fluctuating charge and current distributions of the interacting objects and the vacuum fluctuations of the transverse electromagnetic field (Buhmann, S.Y. & Welsch, D.G., 2007).

The Van-der-Waals forces embody three types of forces, firstly the force between two permanent dipoles - referred to as Keesom force (Van Oss C.J., Good R. J., 1989; Parsegian V.A., Ninham B.M., 1970; Halsey T.C. and Toor W., 1990)), secondly the force between a permanent dipole and a corresponding induced dipole - known as Debye force (Munday, J.N., Capasso, F., Parsegian, V. A and Bezrukov S.M., 2008; Feng S. and Li T., 2006), and thirdly the force between two instantaneously induced dipoles also referred to as London dispersion force (French, 2000; F.M., 1963; Jacobi N., Cysanak G, 1975; Tan G.-L., Lemon M.F., French R. H., 2003; Bowen W.R., Jenner F., 1995))

2.2.2 In gases

The Van-der-Waals' forces were discovered by Johannes Diderik Van der Waals in his 1873 Ph.D dissertation on 'Pressure, Volume and Temperature of Dense Gases' (Parsegian, 2006). He developed his Van-der-Waals' equation from Boyles' Law (Equation 2.1) which states that the product of pressure and volume of a gas is constant provided that the container of gas does not leak (Parsegian, 2006).

$$p_{Boyle}V = NkT \qquad \text{Equation 2.1}$$

Where

- p_{Boyle} is the Boyles' pressure in N/m^2
- V is the volume of the container of the gas in m^3
- N is the number of molecules
- k is the universal Boltzmann constant in J/K
- T is the absolute temperature of the gas in Kelvins (K).

Parsegian (2006) says Johannes Diderik Van der Waals studied dense gases and found that their particles occupied a specific volume, b, which would leave an effective free volume of $(V\text{-}b)$ in a given container. When this volume is divided by the number of particles (atoms) it is referred to as Van-der-Waals' volume. If the particles are considered spherical, a Van-der-Waals' radius can be calculated for each atom using the volume of a sphere's formula.

The volume of $(V\text{-}b)$ allows the particles to move around in the container. Equation 2.2 reveals the initial Van der Waals' equation for dense gas (Parsegian, 2006).

$$\left(p_{vdW} + \frac{a}{V^2}\right)(V - b) = NkT \qquad \text{Equation 2.2}$$

Where:

- p_{vdW} is the Van der Waals' pressure at the internal side of the walls of gas container in N/m^2.
- V is the volume of the container in m^3
- b is the positive volume occupied by the gas particles in m^3
- $(V\text{-}b)$ is the volume of a gas in a container excluding the volume of the particles in m^3.
- $\frac{a}{V^2}$ is the difference between p_{Boyle} and p_{vdW} in N/m^2, the latter being less than the former due to the attraction of particles.

- N is the number of gas molecules
- k is the universal Boltzmann constant in J/K
- T is the absolute temperature of the gas in Kelvins (K).

When pressure was measured at the internal side of the walls of the gas container, it was found experimentally that p_{vdW} was less than p_{Boyle} by a value equivalent to $\frac{a}{V^2}$.

This revealed that there were forces of attraction between the gas particles that yielded a pressure to the magnitude of $\frac{a}{V^2}$. These forces were then called Van-der-Waals' forces. The forces varied according to the average separation distance of the particles. For the same quantity of gas: the smaller the volume of the gas container, the higher the forces were and the larger the volume, the less the forces were.

2.2.3 Van-der-Waals' forces in solids and the nature of Van-der-Waals' forces

Van-der-Waals' forces are not only present in gases, but also in liquids and solids (Parsegian, 2006). In 1937, H.C. Hamaker published an influential paper on Van-der-Waals' forces between interacting macro-bodies (Hamaker, 1937). Hamaker is accredited as 'the first to deal with such interactions between two interacting solids. He used the principle of energy summations employed in London's treatment of Van der Waals interactions between atoms and molecules (London, 1942). The Van-der-Waals' forces' interaction between the two bodies can also be calculated by integration of all pairs of atoms and molecules (Xie, 1997). During 1948, H.B.G. Casimir formulated the Van-der-Waals' forces interactions between two parallel metal plates (Casimir H. B. G., Polder D., 1948). In the 1950's, Lifshitz continued the work of Casimir by introducing a third media between the two parallel metal plates, instead of a mere vacuum as in the previous cases (Lifshitz, 1956).

It was experimentally proved that Van-der-Waals' forces do not vary linearly with separation distance between particles or surfaces under examination. Figure 2-1 shows the non-linearity of the forces with respect to inter-atomic distances between two carbon nanotubes (Zhang, H.W., Wang, J.B., Ye, H.F., Wang, L., 2007). The Van-der-Waals' forces can either be repulsive or attractive depending on the distances between the atoms under consideration as shown in Figure 2-1. Under normal circumstances Van-der-Waals' forces are repulsive at separation distances less than the Van-der-Waals' radius and attractive at greater distances.

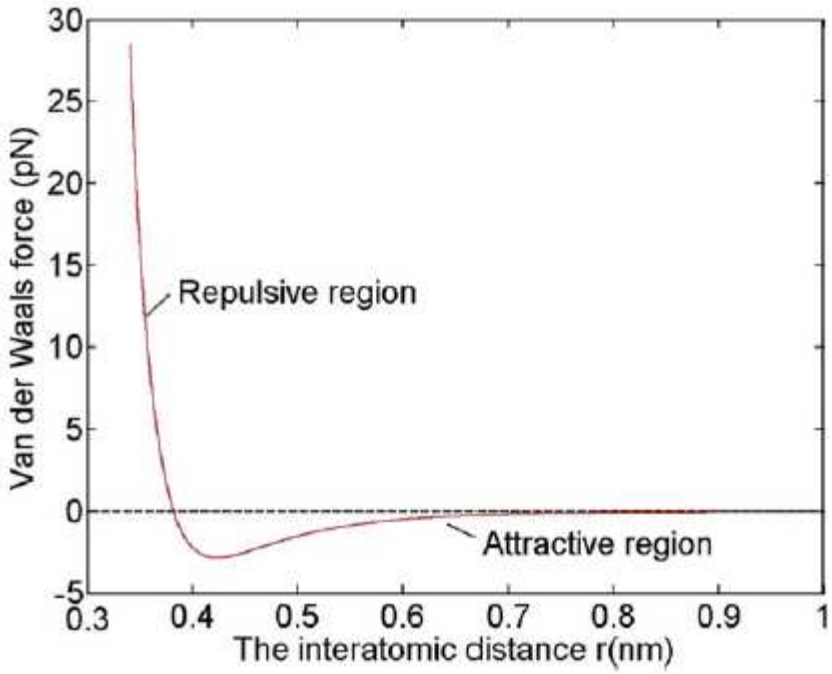

Figure 2-1 Van der Waals'' forces versus atomic distance in carbon nano-tubes (Zhang, H.W., Wang, J.B., Ye, H.F., Wang, L., 2007)

Batsanov (2001) highlighted various methods of obtaining Van-der-Waals radius for various materials (Batsanov, 2001). He postulated the values given in Figure 2-2. It is evident in the figure that the Van-der-Waals' radius generally decreases from left to right across the periodic table, and increases from top to bottom.

Li 2.2 2.63	Be 1.9 2.23											B 1.8 2.05	C 1.7 1.96	N 1.6 1.79	O 1.55 1.71	F 1.5 1.65
Na 2.4 2.77	Mg 2.2 2.42											Al 2.1 2.40	Si 2.1 2.26	P 1.95 2.14	S 1.8 2.06	Cl 1.8 2.05
K 2.8 3.02	Ca 2.4 2.78	Sc 2.3 2.62	Ti 2.15 2.44	V 2.05 2.27	Cr 2.05 2.23	Mn 2.05 2.25	Fe 2.05 2.27	Co 2.0 2.25	Ni 2.0 2.23	Cu 2.0 2.27	Zn 2.1 2.24	Ga 2.1 2.41	Ge 2.1 2.32	As 2.05 2.25	Se 1.9 2.18	Br 1.9 2.10
Rb 2.9 3.15	Sr 2.55 2.94	Y 2.4 2.71	Zr 2.3 2.57	Nb 2.15 2.46	Mo 2.1 2.39	Tc 2.05 2.37	Ru 2.05 2.37	Rh 2.0 2.32	Pd 2.05 2.35	Ag 2.1 2.37	Cd 2.2 2.37	In 2.2 2.53	Sn 2.25 2.46	Sb 2.2 2.41	Te 2.1 2.36	I 2.1 2.22
Cs 3.0 3.30	Ba 2.7 3.05	La 2.5 2.81	Hf 2.25 2.52	Ta 2.2 2.42	W 2.1 2.36	Re 2.05 2.35	Os 2.0 2.33	Ir 2.0 2.34	Pt 2.05 2.37	Au 2.1 2.41	Hg 2.05 2.25	Tl 2.2 2.53	Pb 2.3 2.53	Bi 2.3 3.52	Po	At
		Th 2.4 2.75	U 2.3 2.65													

Figure 2-2 Recommended crystallographic (upper figures) and equilibrium (lower figures) van der Waals' radii (in Angstroms) (Batsanov, 2001)

In the micro-range, Van-der-Waals' forces are a dominating contributor to the adhesion (DelRio, F.W., De Boer, M.P., Knapp, J.A, Reedy, E.D. (Jr), Clews, P.J., Dunn, M.L., 2005; Debrincat, D.P., Solnordal, C.B., Van Deventer, J.S.J., 2008). They also cause small particles to agglomerate (Debrincat, D.P., Solnordal, C.B., Van Deventer, J.S.J., 2008) (Eichenlaub, S., Kumar, G., Beaudoin, S., 2006).

The main parameters which influence Van-der-Waals' forces include: material type, geometrical configuration of interacting materials, the topography of the interacting surfaces (surface roughness), humidity, temperature and pressure. The geometric parameters upon which the Van-der-Waals' forces depend include radius, length, separation distance, height and included angles (Tanaka, M., Komagata, M., Tsukada, M., Kamiya, H. , 2008; Fatikow, S., Seyfried, J., Fahlbusch, S., Buerkle, A., Schmoeckel, F. , 2000). These forces vary inversely as the square of the separation distance, *H*, of the interacting surfaces as shown in Equation 2.3 (Parsegian, 2006) in some cases

$$F \propto \frac{1}{H^2} \qquad \text{Equation 2.3}$$

The Hamaker theory estimates that the Van-der-Waals' force, *F*, between two equal-sized spherical particles is given as in Equation 2.4 (Weber W. M., Hrenya M. C., 2007; Thoreson, E.J., Mart, J. and Burnham, N.A., 2006; Fatikow, S., Seyfried, J., Fahlbusch, S., Buerkle, A., Schmoeckel, F. , 2000). The assumptions for all the stated equations (unless otherwise stated) are that the interactive surfaces are ideally smooth. Again these formulae cater for non-retarded Van-der-Waals' forces which normally occur in separation distances of less than 10 nm (Parsegian, 2006; Butt, H-J., Cappella, B. and Kappl, M., 2005). For larger separation distances, the Van-der-Waals' forces are normally retarded. Although the effect of Van-der-Waals' forces is detected in the retarded region, it would be reduced because of an increased separation distance. The retarded region extends to separation distances of 100 nm or several 100nm, and even to longer distances of up to 8μm as in the case of metals (Israelachvili, 2011).

$$F = -\frac{A_H R}{12H^2} \qquad \text{Equation 2.4}$$

Where *R* is the sphere's radius in *m*, A_H is the Hamaker coefficient in *J*. *H* is the shortest surface-to-surface separation distance between the spheres in *m*. As the radius increases, the force increases.

When two unequal spheres are interacting, the Van-der-Waals' forces are given in Equation 2.5 (Fatikow, S., Seyfried, J., Fahlbusch, S., Buerkle, A., Schmoeckel, F. , 2000; Israelachvili, 2011)

$$\boldsymbol{F = -\frac{A_H}{6H^2}\frac{R_1 R_2}{R_1 + R_2}} \qquad \text{Equation 2.5}$$

Where R_1 and R_2 are the radius of the two spheres in *m* and the other symbols maintain their previously stated definitions.

In the case of interaction between a sphere and a flat surface, the forces increase directly with radius and decrease with an increase in separation distance (Gotzinger M., Peukert W., 2003). The Van-der-Waals' forces for a sphere-flat surface interaction are given by Equation 2.6 (Takahashi, K., Berengueres, J.O.L., Obata, K.J., Saito, S., 2006; Weber W. M., Hrenya M. C., 2007; Thoreson, E.J., Mart, J. and Burnham, N.A., 2006).

$$F = -\frac{A_H R}{6H^2} \qquad \text{Equation 2.6}$$

Where R is the radius of the sphere in *m* and the other symbols maintain their previously stated definitions.

When two flat surfaces are interacting, the flat-flat surface interaction is shown by Equation 2.7 (Fatikow, S., Seyfried, J., Fahlbusch, S., Buerkle, A., Schmoeckel, F. , 2000; Israelachvili, 2011).

$$f = -\frac{A_H}{6\pi H^3}\ per\ unit\ area \qquad \text{Equation 2.7}$$

Where *f* is the Van-der-Waals' force per unit area in N/m^2, and the other symbols are defined as previously stated.

When the cone interacts with a flat surface in that its tip is pointing onto the flat surface, a cone-flat surface interaction is developed. The formula for the Van-der-Waals' force, *F*, exerted by such an arrangement is shown in Equation 2.8 (Fatikow, S., Seyfried, J., Fahlbusch, S., Buerkle, A., Schmoeckel, F. , 2000; Israelachvili, 2011)

$$\boldsymbol{F = -\frac{A_H tan^2\theta}{6H}} \qquad \text{Equation 2.8}$$

Where θ is the half-cone angle in *degrees* and the other symbols maintain their earlier stated definitions.

When a cylinder lies horizontally interacting with a flat surface, the interaction is termed cylinder-flat surface interaction. The Van-der-Waals' forces for such an arrangement are shown in Equation 2.9 (Fatikow, S., Seyfried, J., Fahlbusch, S., Buerkle, A., Schmoeckel, F. , 2000; Israelachvili, 2011)

$$\boldsymbol{F = -\frac{A_H R^2}{6H^3}} \qquad \text{Equation 2.9}$$

Where *R* is radius of the cylinder in *m* and the other symbols are defined as before.

In all the considered cases, as the separation distance increases, the force decreases (Weber W. M., Hrenya M. C., 2007), and the interactive surface areas vary directly as the Van-der-Waals' forces (Oliveira, 1997).

The Van-der-Waals' force, *F*, between interacting solid surfaces can be generalised by Equation 2.10 (Matope, S and Van der Merwe, A. F., 2010),

$$F = -\frac{A_H Y^x}{NH^n} \qquad \text{Equation 2.10}$$

Where:

A_H - Hamaker coefficient in *J*,

H - The shortest surface-to-surface separation distance between two substances *m*,

n- An exponent of *H* greater than zero,

Y- Dimensional parameter of micro-material under consideration e.g. radius, length, included angle or a ratio of dimensional properties in *m or suitable SI units*,

x- An exponent (greater than zero) of Y,

N- A constant greater than zero.

Conventionally, the Van-der-Waals' forces are considered attractive in nature and are given a negative sign (-) in their formulae (Oliveira, 1997) (Luckham, 2004).

It should also be noted that Van-der-Waals' forces vary again inversely as the surface roughness (Rabinovich I. Y., Adler J. J., Ata A., Singh K. J., and Moudgil M.B., 2000). The rougher the surface, the less the Van-der-Waals' forces exerted; the smoother the surface, the greater the Van-der-Waals' forces (Fearing, 1995; Vogeli B. & von Kanel H., 2000; Zhou Y. and Nelson B.J., 1999) (Lambert P. & Delchambre A., 2003). For an effective picking, the gripper should have a lower value of the root mean square (*rms*) than the picking position's substrate in order for a greater force to be exerted on the micro-workpart by the gripper. As for an efficient release, the placement position's substrate should have a lowers *rms* value than the gripper's.

Added to that, in order to initiate release in some difficult cases, a thin film of helium liquid can be injected between the interacting surfaces of a micro-gripper and the micro-workpart to introduce repulsive Van-der-Waals' forces. Helium easily permeates through cavities because of its small atoms and low relative dielectric permittivity ($\varepsilon = 1.057$). It also naturally produces a repulsive Van-der-Waals' force due to of its negative Hamaker coefficient (Israelachvili, 2011; Parsegian, 2006). Repulsive Van-der-Waals' forces also occur across thin liquid films of hydrocarbon on alumina (Blake, 1975) and quartz (Gee et al., 1989).

Nevertheless, Van-der-Waals' forces are not the only active forces in the micro-domain.

2.3 Comparison of active forces in the micro-range and their applicability in micro-material handling operations

It should be noted that Van-der-Waals' forces do not solely influence the adhesion of matter in the micro-range. Gravity, electrostatic and surface tension are among others that do. These forces also affect the handling of micro-materials to some degree. Other forces that may be used for micro-material manipulation encompass magnetic, electrical, electromagnetic, mechanical, pneumatic and hydraulic forces. The latter forces are also regarded as conventional macro-scale forces. However; they impose large straining forces on the handled micro-materials which are already fragile in nature (Biganzoli F., Fantoni G., 2008), hence imposing limitations in their application in micro-material handling.

In general, industry has resorted to the use of vacuum forces for micro-material handling purposes. However; they have short-comings with regard to the size of the micro-materials they can handle and have some limitations as to the required accuracy in picking and placing of the micro-object. Adhesive forces, that is: Van-der-Waals' force, electrostatic forces and surface tension force or capillary forces (Fukuda T. & Arai F., 1999) can be used with great success in micro-material handling. These forces dominate over gravity in the micro-range as shown in Figures 2.3 and 2.4 (Fukuda T. & Arai F., 1999; Fearing, 1995; Bohringer K.F., Goldberg K.Y., Cohn M., Howe R., and Pisano A., 1998).

Micro-materials of masses less than $1x10^{-6}$ Kg are difficult to release by gravity since the adhesive forces predominate over it (Sanchez J. A. , 2010). Figure 2-3 shows how rapidly adhesive forces surpass gravity in their intensity as a micro-workpart decreases in size..

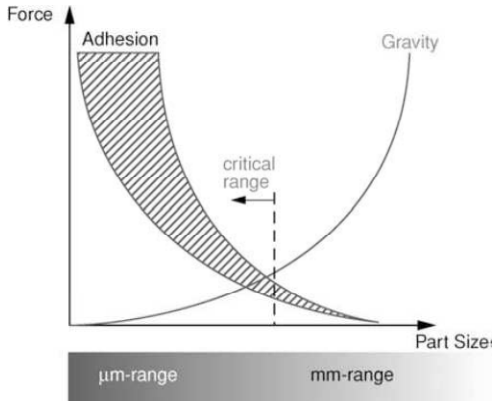

Figure 2-3 Comparison of adhesion and gravity in the micro-range (Sanchez J. A. , 2010)

Fearing (1995) takes the comparison of the adhesive forces and gravity further as shown in Figure 2.4. Forces experienced between a silicon sphere of density 2300 Kg/m^3, of radius ranging from 1µm to 1 mm, and a flat plane are analytically modelled. Gravity drops drastically as the micro-workpart decreases in size (radius). Surface tension or capillary forces dominate over other forces in this micro-range, followed by Van-der-Waals' forces and then electrostatic forces (Fearing, 1995; Bohringer K.F., Fearing R.S., Goldberg K.Y., 1999). In this analysis 1% of the Van-der-Waals' forces is plotted for an atomically smooth surface (Fearing, 1995) to compensate for the fact that Van-der-Waals' forces decrease rapidly with separation distance and also that they are greatly affected by surface roughness. This percentage also takes care of the effects of retardation. Even so, according to the conditions used in the experiments, the Van-der-Waals' forces are more prominent than electrostatic forces and gravity, at micro-level as indicated in Figure 2-4.

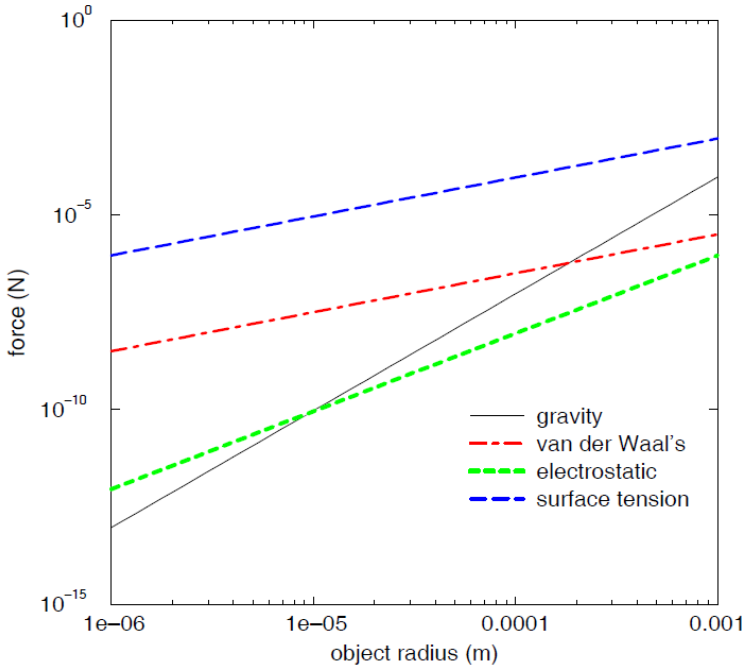

Figure 2-4 Comparison of forces acting in the micro-range (Fearing, 1995; Bohringer K.F., Fearing R.S., Goldberg K.Y., 1999)

Further on in this section a different comparison of the adhesive forces is executed in conjunction with gravitational and vacuum forces, with respect to separation distance as shown in Figure 2-6.

The gravitational force, F_g is given by Equation 2.11,

$$F_g = \rho g V \qquad \text{Equation 2.11}$$

Where ρ – density in kg/m^3, g – gravitational acceleration in m/s^2, and V – Volume in m^3 (the maximum volume should comply with the upper limit of mass of 1x10^{-6} Kg (Sanchez J. A. ,

2010). In this case the separation distance has negligible effect since the distances are too small.

Vacuum forces, F_{vac} are analytically modelled using the Equation 2.12 proposed by Dini et al (2009) derived from Bernoulli's principle of fluid dynamics for an incompressible fluid of uniform flow (Dini G., Fantoni G. and Failli F., 2009).

$$F_{vac} = \frac{\rho Q^2}{2\pi H^2}\left[ln\frac{r_{ext}^2}{r_{int}^2} - \frac{1}{2}\left(\frac{r_{ext}^2 - r_{int}^2}{r_{int}^2}\right)\right] \qquad \text{Equation 2.12}$$

Where ρ – density of air in kg/m^3, Q – flow rate of air m^3/s, H – separation distance in m, r_{int} – internal radius of vacuum pipe in m, r_{ext} – external radius of vacuum pipe in m.

The parameters used by Zesch et al (1997) in the design of a pipette vacuum gripper are used for the analytical modelling in Figure 2-6. The parameters are: air density, ρ – $1.22521 Kg/m^3$; air flow rate, Q = 1.2 x $10^{-4} m^3/s$; internal radius of gripper, r_{int} – $2.5x10^{-5} m$ (which gives a limit to the minimum dimension of the micro-workpart to be picked or else it might be sucked in); and external radius of gripper, r_{ext} – $5.0x10^{-5}$ m (Zesch W., Brunner M., Weber A., 1997).

However; it should be noted that the disadvantages of vacuum actuated grippers include the following:

1. There is a limit to the size of their internal micro-hole construction since it becomes difficult to manufacture as the diameter decreases.
2. This in turn limits the size of micro-parts they pick as micro-workpieces can get sucked into the vacuum channels. Zech et al (1997) used their gripper in picking diamond particles ranging from 300µm down to 50µm (and no further than that) with a success factor of 75% (Zesch W., Brunner M., Weber A., 1997).
3. Micro-workparts cannot easily be released (Huang X., Chang L. and Ming W., 2010). Zech et al (1997) had to use an external probe to release the other 25% of their diamond particles (Zesch W., Brunner M., Weber A., 1997).
4. The precise release of a micro-workpart is difficultto achieve (Zesch W., Brunner M., Weber A., 1997; Huang X., Chang L. and Ming W., 2010; Guoliang C. & Xinhan H., 2004).
5. The vacuum mechanism is adversely affected by humidity levels.
6. They impose high mechanical strain on micro-workparts.

7. They do not work well with porous micro-materials (Vandaele V., Lambert P. and Delchambre A., 2005).
8. They do not work in a vacuum environment since they depend on outside pressure (Vandaele V., Lambert P. and Delchambre A., 2005).
9. Requires a pneumatic system which may include pumps, valves and controllers (Huang X., Chang L. and Ming W., 2010).
10. Not suitable for collapsible and soft materials which easily get drawn into the vacuum channels, clogging the system (Vandaele V., Lambert P. and Delchambre A., 2005).

Surface tension grippers do not have most of the disadvantages that vacuum grippers have. When picking a micro-part, a liquid is introduced between the interacting surfaces of the micro-gripper and the micro-part. The surface tension between the interacting surfaces of the gripper and the micro-part should be greater than that between the latter and the substrate of the pick-up position. When releasing, the surface tension between the gripper and micro-workpart should be less than that between the micro-workpart and the placement position's surface. Since surface tension depends on the contact area, the interactive surfaces between the micro-gripper and micro-workpart should be larger than that between the workpart and the substrate. For a reliable release, the contact area between the micro-workpart and the placement position's substrate should be higher than with the gripper (Lambert P. , 2007). In cases where picking of a micro-material is a problem, a gripper is coated by a hydrophilic substance in order to reduce the contact angle to allow for the exertion of a stronger surface tension force on the micro-workpart during the picking process.

Since release proves to be a great challenge with micro-workpart, a micro-heater may be used to evaporate the water bridge between the micro-gripper and micro-workpart interactive surfaces (Arai F, Ando D., Fukuda T., Nonoda Y., Oota T, 1995), thus reducing the adhesive surface tension. Introduction of a dry stream of nitrogen aids in reducing the humidity level to a minimum. A hydrophobic coating may be integrated in a reconfigurable micro-gripper to reduce the surface tension on a micro-workpart during the release operation (Arai F, Ando D., Fukuda T., Nonoda Y., Oota T, 1995).

In some difficult cases, micro-particle release can be achieved by immersing into a liquid to nullify the surface tension force (Weisenhorn A.L., Hansma P.K., Albrecht T.R., Quate C.F., 1989). However; the micro-workpart should make contact with the surface of the placement

position so that Van-der-Waals' forces would affect the release (since they are active in aqueous conditions). Another option would be to release the micro-workpart in a vacuum where surface tension forces are normally reduced to a minimum (Lambert P. , 2007)**.** This is; however, difficult to achieve.

The surface tension force between two plates of the same material, with their separation distance small compared to their length, is given by Equation 2.13 (Lambert P. , 2007),

$$F_s = \frac{2\pi\gamma}{H} R^2 \cos\theta \qquad \text{Equation 2.13}$$

Where F_s represents the surface tension force in *N*, γ – surface tension constant in *N/m*, R – radius in *m* of the meniscus from the centre of the plates, which in this case is taken as $5x10^{-3}$ *m*, half the length of our largest work-part, H – separation distance in *m*. θ is the contact angle of a given liquid in *degrees*, water in this case. θ is taken to be equal to 0^o so that a maximum value of cos θ = 1 is used in order to obtain the upper limit.

Limitations of surface tension forces are: they cannot work in a vacuum; they form an oxide layer on corrosive materials; they cannot work for contact angles of 90^o (as in the case of water and silver), and cannot work for contact angles greater than 90^o (as in hydrophobic cases; for example, water on Teflon makes a contact angle of 180^o) because they become repulsive (Neugebauer, R., Koriath, H-J., Van der Merwe, A. F., Müller M. and Matope, S., 2011). On the other hand, electrostatic forces do not have these disadvantages.

Figure 2-5 shows an electrostatic gripper. To realise an effective picking operation, the voltage of the electrostatic gripper should be increased to its optimum level. The interactive contact areas between the micro-gripper and micro-workpart should be maximized to execute the picking. In some challenging cases, a dielectric material of high permittivity should be used to exert a greater electrostatic force on the micro-object to be picked.

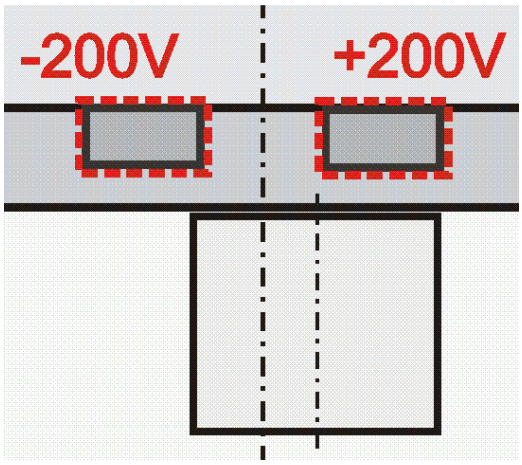

Figure 2-5 Electrostatic micro-gripper (Neugebauer R., Koriath H.-J., Muller M., June 2010)

When releasing, the micro-workpart and the gripper are grounded (Feddema J.T., Xavier P., and Brown R., 1999) using an anti-static mat (Matope, S & Van der Merwe, A. F. , 2010). The placement position's environment may also be ionised in order to discharge the micro-gripper and the miniature part (Lambert P. , 2007). However; these strategies only nullify the electrostatic force, and not Van-der-Waals' forces. Final release is achieved by Van-der-Waals' force when the micro-workpart contacts the surface of the placement position. Conductive materials that do not easily form insulating oxides may also be incorporated in a reconfigurable micro-gripper to act as part of an ejection mechanism (Fearing, 1995). This is; however, difficult to achieve at micro-scale.

The electrostatic force exerted between flat surfaces is given by Equation 2.14 (Kalkowski G., Risse S., Harnisch G., Guyenot V., 2001)

$$F_e = \frac{\varepsilon V^2}{2H^2} A \qquad \text{Equation 2.14}$$

Where F_e is the Electrostatic force in N; ε- permittivity in F/m (Farads/metre), V- Voltage across the micro-gripper and micro-workpart in V and is taken as $200V$ in this analytical modelling, a figure used in piezoceramic micro-handling (Neugebauer R., Koriath H.-J., Muller M., June 2010); A – interactive area of the plates in m^2 (largest area being 10 mm x 10 mm = 100 mm^2 = 1x 10^{-4} m^2); and H – separation distance in m.

Electrostatic forces have been used in the handling of automotive piezo-ceramic sensors of 10 mm length (Neugebauer R., Koriath H.-J., Muller M., June 2010), metallic cylinders of diameters within the range of 0.25-1mm and length of 1-4mm (Fantoni, 2003), glass spheres

of 100-800µm diameter;(Hesselbach J., Buttgenbach S., Wrege J., Butefisch S., and Graf C., 2001). However, they are not suited for sensitive integrated circuits' (IC) components (Peirs, 2001).

Limitations of electrostatic forces are: they require a dielectric coating; they cannot work in aqueous conditions; they leave residual charges on micro-workparts after operation and they require electrical supply or other charging means. It should be noted that the disadvantages of electrostatic and surface tension forces do not apply in the case of Van-der-Waals' forces (Neugebauer, R., Koriath, H-J., Van der Merwe, A. F., Müller M. and Matope, S., 2011).

The Van-der-Waals' force equation for flat-flat surface interaction is given by Equation 2.15 (Parsegian, 2006; Bohringer K.F., Fearing R.S., Goldberg K.Y., 1999)

$$\boldsymbol{F = -\frac{A_H}{6\pi H^3} A} \qquad \text{Equation 2.15}$$

Where F represents the Van-der-Waals' force in N, A_H – Hamaker coefficient in J, H – separation distance in m, A – contact area of the interactive surfaces in m^2.

Figure 2-6 shows the analytical modelling of vacuum forces and adhesive forces (using all equations from Equation 2.11 to Equation 2.15) with respect to separation distances ranging from $1x10^{-12}m$ to $1x10^{-3}m$. In this comparison, a flat micro-workpart of 10 mm x 10 mm cross-sectional area (not a sphere as examined by Bohringer et al (1999)), is considered. The materials which were compared to arrive at this summarized figure were piezoceramic, polystyrene, gold, copper, silicon, aluminum dioxide, silver and diamond.

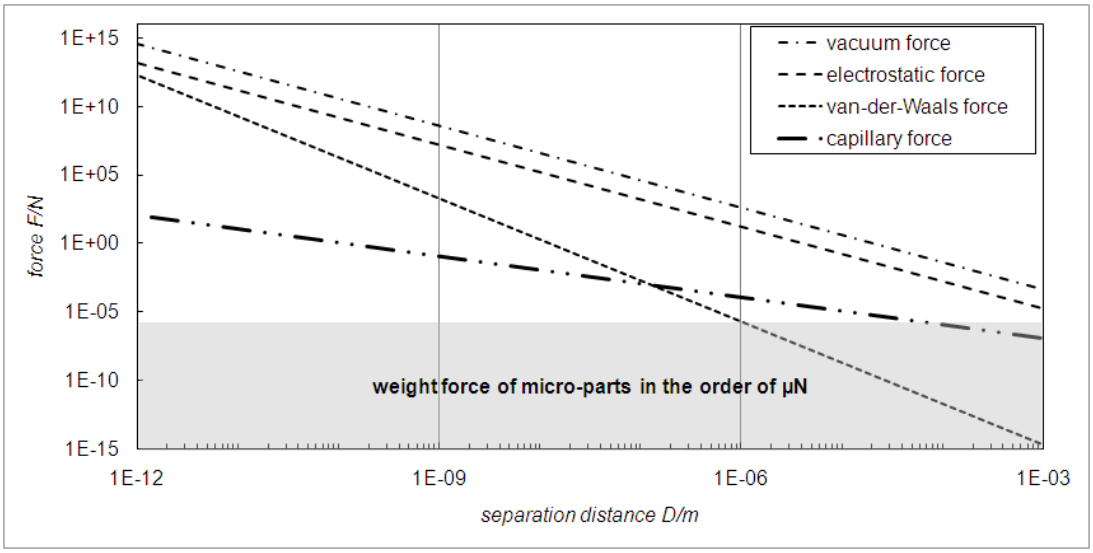

Figure 2-6 Comparison of forces active in the micro-range (Neugebauer et al, 2011)(Neugebauer, R., Koriath, H-J., Van der Merwe, A. F., Müller M. and Matope, S. , 2011)

It is evident in the analytical modelling in Figure 2.6; that vacuum forces predominate over others in the whole range of $1x10^{-12}$ *m* - $1x10^{-3}$ *m*, occupying the first position in magnitude and electrostatic the second. However, they cannot be used for a micro-workpart whose minimum dimension is equal to the internal radius of the gripper, for example in this case, $2.5x10^{-5}m$.

In the $1x10^{-12}$ *m* - $1x10^{-7}$ *m* range Van-der-Waals' forces occupy the 3rd, capillary or surface tension 4th and as anticipated gravity the 5th. In the $1x10^{-7}$ *m* - $1x10^{-6}$ *m* range capillary force (surface tension) surpasses Van-der-Waals' forces coming 3rd, the latter 4th, and gravity 5th. As for the $1x10^{-6}$ *m* - $1x10^{-4}$ *m* sub-section, capillary force is 3rd, gravity supersedes Van-der-Waals forces taking the 4th position and the latter 5th.

In the $1x10^{-4}$ m - $1x10^{-3}$ m, capillary force occupies the 3rd position, gravitational force 4th, and Van-der-Waals force 5th. Finally in the $1x10^{-4}m$ - $1x10^{-3}m$ region, gravity predominates over capillary force taking the 3rd position and the latter 4th, and as expected the Van-der-Waals forces occupy the 5th position.

It should be noted from Figure 2-6 that Van-der-Waals forces are short-range forces (Israelachvili, 2011) which dominate over gravity and capillary forces in the separation

distances less than $1\mu m$. Therefore, Van-der-Waals' forces are more effective when contact is realised between the interacting surfaces. Another limitation of Van-der-Waals' forces is that they require a clean environment.

However; the advantages of Van-der-Waals' forces over other adhesive forces are that they are applicable to all materials, can work in a vacuum, can work in aqueous conditions, are applicable in all states of matter and they do not require an external energy supply to be activated (Neugebauer, R., Koriath, H-J., Van der Merwe, A. F., Müller M. and Matope, S., 2011). Based on these arguments, this research further identifies how Van- der-Waals' forces can be reliably applied in a micro-material environment.

For optimum application of Van-der-Waals' forces to be realised, other forces should be eliminated or minimized (Lambert P. , 2007). Electrostatic force can be discharged by employing the anti-static apparatus with its accessories (Matope, S & Van der Merwe, A. F. , 2010). The surface tension force can be reduced by using a micro-heater to heat up the environment so that the humidity level is drastically reduced (Fukuda T. & Arai F., 1999) or by passing a continuous flow of dry nitrogen (Fearing, 1995; He M., Blum A.S., Aston D.E., Bueviage C., Overney R.M., Luginbuhl R., 2001; Zhou Y. and Nelson B.J., 1999). The electrostatic and surface tension forces may also be eliminated by immersing the interacting surfaces in a liquid.

2.3.1 General Micro-object release

Since releasing of work parts is the main challenge in a micro-material handling system, several authors postulate some possible ways of achieving an effective release. These include glueing the component to the substrate at the right place (Bohringer K.F., Fearing R.S., Goldberg K.Y., 1999; Bark C. & Binnenboese T., 1998). However; this does not work in a repeated pick-transfer-release cycle, especially for a micro-workpart which goes through several workstations in an assembly line. A relative motion between a component and the gripper, intended to strip off the component from an edge may also be used (Zech W., Brunner M., and Weber A., 1997) as shown in Figure 2-7 and Figure 2-8, but this compromises precision during object release. The term 'base material of medium A_H' refers to the fact that the placement position does not have the highest Hamaker coefficient value, but a middle value when compared to other interacting materials in the system, necessitating an improvement in the releasing mechanism.

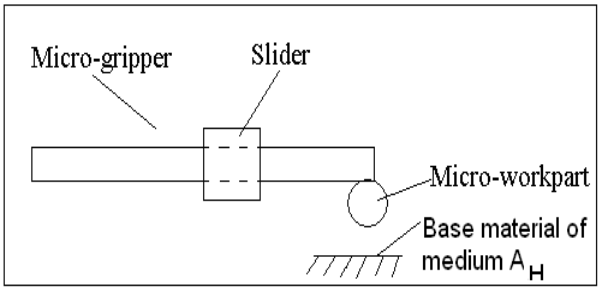

Figure 2-7 Picking and placing of a micro-workpart using a medium of lower A_H (Van der Merwe, A.F. & Matope, S. , 2009)

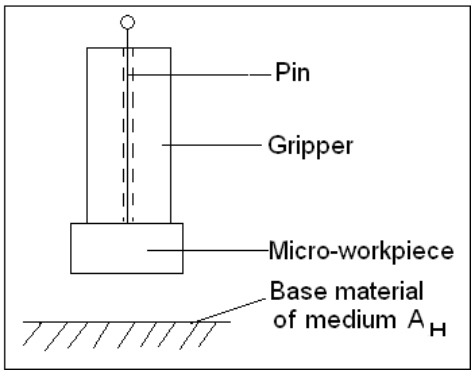

Figure 2-8 A pin of lower A_H used to place a micro-workpiece on the desired position (Van der Merwe, A.F. & Matope, S. , 2009).

Vibrations to perform the release task may be used (Bohringer K.F., Goldberg K.Y., Cohn M., Howe R., and Pisano A., 1998). However; as mentioned earlier, accuracy is reduced. A gas injection mechanism may also be employed where a small puff of gas blows away the micro-workpart from the gripper (Zech W., Brunner M., and Weber A., 1997), as shown in Figure 2-9, but precision is hampered.

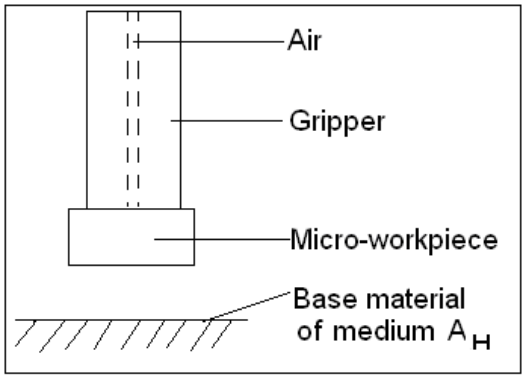

Figure 2-9 Air used as a media when placing a micro-workpiece.(Van der Merwe, A.F. & Matope, S., 2009)

A dynamic approach may be used in which a micro-gripper is further accelerated; for example, by shaking in order to release the micro-part (Haliyo D.S., Rollot Y., and Regnier, 2001). However; this would be suitable in cases where accurate placement is not required (Zech W., Brunner M., and Weber A., 1997). A relative orientation of the component and the gripper could be modified so that a release is easier to realise (Kasays T., Myazaki H., Saito S., and Sato T., 1998) (Feddema J.T., Xavier P., and Brown R., 1999; Lambert P. & Delchambre A., 2003), but as mentioned earlier, precision is compromised.

The longer the range of influence of the forces, the more difficult it is to release a picked micro-object. This renders the micro-grippers (whose operation is based on vacuum, electrostatic or surface tension) unsuitable for some precision micro-workpart positioning. These relatively long range forces would also tend to interact with the placement substrate, so that, instead of releasing the micro-workpart, they would also attract the substrate. If the substrate is not firmly fixed, it is picked together with the micro-workpart by the gripper.

Van-der-Waals' forces are short-range surface forces compared to other forces, as discussed earlier. They are significant in separation distances of 0 nm-100 nm of the interacting surfaces (Fearing, 1995; Scheeper P.R., Voorthuyzen J.A., Olthius W. and Bregveld, 1992; Lambert P. , 2007). This makes them applicable for the manipulation of one side of a micro-part, leaving the other for another manipulation; for example. a leasing operation. However; in order for Van-der-Waals' forces to work effectively, the interacting surfaces need to be smooth.

Systematically developed surface roughness of micro-workparts may be used profitably in material handling. A micro-gripper with a flexible surface may be used to grip a workpart as shown in Figure 2-10. It achieves this by taking the profile of the rough surface of the micro-workpiece during picking. A diaphragm with a built-in release mechanism is then used to realise the picking and placing. Upon release the diaphragm is stretched and its contact area with the workpart is decreased, thus releasing the work element as illustrated in Figure 2-10.

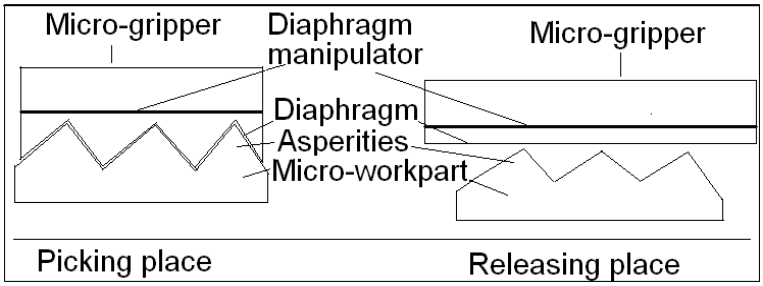

Figure 2-10 Gripper design incorporating a diaphragm to increase the area of contact on asperities (Matope, S & Van der Merwe, A. F. , 2010).

2.3.2 Calculation of the Hamaker coefficients, A_H

When two bodies *A* and *B* are interacting with a medium between them, the non-retarded Hamaker coefficient, A_H, summed over sampling frequencies is given by Equation 2.16 (Parsegian, 2006)

$$A_H = (3kT/2) \Sigma (\epsilon_A - \epsilon_m) / (\epsilon_A + \epsilon_m). (\epsilon_B - \epsilon_m) / (\epsilon_B + \epsilon_m) \qquad \text{Equation 2.16}$$

Where *k* is the Boltzmann constant = 1.3807 x 10^{-23} *J/K*; *T* is the temperature in Kelvins of the environment; ϵ_A, ϵ_m and ϵ_B are dielectric susceptibilities (no units because they are ratios) of material *A,* medium and material *B*.

It should be noted that the value of the dielectric susceptibility, ϵ, for a vacuum is equal to one, 1; for other materials ϵ is greater than 1 (Parsegian, 2006).

The Hamaker coefficient, A_H, for a specific material can also be calculated using an approximate method called the additive approach using Equation 2.17.

$$A_H = \pi^2 C \rho_1 \rho_2 \qquad \text{Equation 2.17}$$

Where A_H – Hamaker coefficient in *J*.

C – is the particle-particle pair interaction in *J*

ρ_1 – number of atoms per unit volume of substance 1 (corresponding to atoms of radius 0.2 nm)

ρ_2 – number of atoms per unit volume of substance 2 (corresponding to atoms of radius 0.2 nm)

Approximate values for unknown Hamaker coefficients, can be obtained by using some combination relationships in terms of known ones (Israelachvili, 2011). For example, a non-

retarded Hamaker coefficient for material 1 and 2 interacting across medium 3 is given in *J* by Equation 2.18.

$$A_{H132} \approx \sqrt{A_{H131}A_{H232}} \qquad \text{Equation 2.18}$$

From the above equation, Equation 2.19 can be deduced (Israelachvili, 2011)

$$A_{H12} \approx \sqrt{A_{H11}A_{H22}} \qquad \text{Equation 2.19}$$

where A_{H12} is the Hamaker coefficient in *J* for material 1 and 2 interacting across a vacuum (i.e., with no medium between them).

Two other useful relations for interactions involving three materials (material 1, 2 and 3) are given by Equation 2.20 and Equation 2.21 (Israelachvili, 1972).

$$A_{H131} = A_{H313} \approx A_{H11} + A_{H33} - 2A_{H13} \approx \left(\sqrt{A_{H11}} - \sqrt{A_{H33}}\right)^2 \qquad \text{Equation 2.20}$$

A combination of this equation with Equation 2-18 yields

$$A_{H132} \approx \left(\sqrt{A_{H11}} - \sqrt{A_{H33}}\right)\left(\sqrt{A_{H22}} - \sqrt{A_{H33}}\right) \qquad \text{Equation 2.21}$$

Since the amount of Van-der-Waals' forces experienced by an atom is influenced by the neighbouring atoms, Lifshitz' theory takes this into cogniscence by applying the continuum theory and treating a body as continuous media. According to Israelachvili (2011) , even though the full Lifshitz equation (Lifshitz, 1956; Dzyaloshinskii I.E., Lifshitz E.M., Pitaevskii L.P., 1961) includes the effects of retardation, there is no simple equation for calculating the Van-der-Waals' force at all separation distances, *H*. Numerical methods for calculating the Van-der-Waals' forces at all distances were postulated by Mahanty et al (1976), and Parsegian (2006) which involve solving the full Lifshitz equation. On the other hand, Russel et al (1999), have proposed various approximate equations for the computing of Van-der-Waals' forces for different dielectric media.

2.3.3 Measurement of the Van-der-Waals' forces at micro-level

The atomic force microscope (AFM) is used to measure Van-der-Waals' forces. A sample is placed on the AFM stage and the stylus of the AFM is brought into contact with it. When retracting the tip from the sample surface, the tip stays in contact with the surface until the cantilever force overcomes the adhesive tip–sample interaction. First measurements of this pull-off force or adhesion force F_{ad} were performed by Martin et al (1988), and Erlandsson et al (1988). Precision measurement of the Van-der-Waals' force in a fluid was executed using an AFM by Munday and Capasso (2007). In the most general case, the adhesion force F_{ad} is a combination of the electrostatic force F_{el}, the Van-der-Waals' force F_{vdW}, the meniscus or

capillary force F_{cap} and forces due to chemical bonds or acid–base interactions F_{chem} as given in *J* by Equation 2.22.

$$F_{ad}=F_{el}+F_{vdW}+F_{cap}+F_{chem}. \qquad \text{Equation 2.22}$$

The pull-off force curves provide valuable information on local material properties such as elasticity, hardness, Hamaker constant, adhesion and surface charge densities (Butt, H-J., Cappella, B. and Kappl, M., 2005). The AFM allows experimentation on length, time, force and energy at micro- and nano-scale levels. These experiments can be carried out under natural conditions (Butt, H.J., Berger, R., Bonaccurso, E., Chen, Y., Wang, J., 2007).

The AFM measures the force between its cantilever tip and the sample by monitoring the deflection, as shown in Figure 2-11 (Butt, H.J., Berger, R., Bonaccurso, E., Chen, Y., Wang, J., 2007; Butt, H-J., Cappella, B. and Kappl, M., 2005).

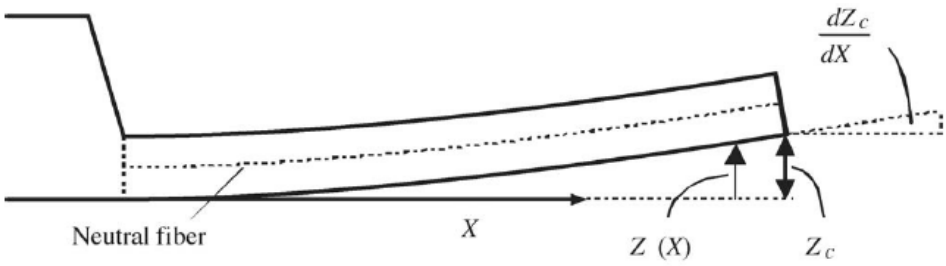

Figure 2-11 AFM cantilever with an exerted force at its end (Butt, H-J., Cappella, B. and Kappl, M., 2005).

With reference to Figure 2.11, X is the horizontal coordinate originating at the basis of the cantilever; Z(X) is the cantilever deflection at a position X; and Z_c is the cantilever deflection at its end.

At ambient conditions, a water neck forms between AFM tip and substrate due to capillary condensation and adsorption of thin water films at surfaces. This attractive interaction depends on the relative humidity and the hydrophilicity of tip and sample (Butt, H-J., Cappella, B. and Kappl, M., 2005).

For the AFM to measure Van-der-Waals' forces only on given samples, the measurements are conducted in a Faraday's box (which discharges electrostatic forces and prevents the interference from other forces which include magnetic, and electromagnetic force), at a humidity level around 20% (which is low enough to eliminate surface tension or capillary forces), where low or no loading forces are applied (to avoid development of a chemical bond

between the probe and the specimen) and also the contact time of the probe and the sample is reduced to a minimum to prevent the development of a chemical bond.

2.4 Dust challenges in the application of Van-der-Waals' forces

The environment for micro-manipulation should be clean and free of dust and small particles that could interfere with the microscopic objects being handled (Fukuda T. & Arai F., 1999).Dust should not be generated in the micro-manipulation process. Abrasion should be avoided and most of the micro-manipulation tasks should be based on pick-and-place motion and deformation achieved through pushing (Fukuda T. & Arai F., 1999). However; this is difficult to achieve because micro-manufacturing workpieces are already at a micron level and it is difficult to distinguish between a dust particle and a micro-workpiece (Matope, S. and Van der Merwe, A. F, 2010c).

A possible solution would be to control the humidity of the micro-manufacturing environment so that dust is trapped by the dampness. Optimisation has to be done experimentally to realise the appropriate level of humidity that would lead to an effective and efficient micro-environment. Furthermore, the condensed water on surfaces in humid atmospheres helps in the lubrication of the manufacturing process. This, incidentally, reduces abrasion and then leads to a reduction in the generation of dust (Rollot, Y., Regnier, S., Guinot, J.C. , 1999). However; the surfaces should be corrosion resistant.

Micro-vacuum cleaners may also be used to suck away the dust particles. The application of pneumatics at micron level is needed to identify the optimum suction pressures which remove nothing except the dust. Brownian motion and laws of flotation at micron level have to be studied and applied, aided by experimental results (Matope, S. and Van der Merwe, A. F, 2010c).

Magnetic and electromagnetic forces may be used to attract ferrous dust generated during micro-machining. The strength of the magnetic and electromagnetic forces can be varied experimentally in order to reach the optimum values suitable for specific materials. The strength of these forces may, unfortunately, interfere with Van-der-Waals' forces employed in the picking and placing of the micro-objects. This method has the disadvantage that it only applies to ferrous materials.

Electrostatic forces may be used to attract charged dust particles from the micro-manufacturing environment. However, the electrostatic forces may also interfere with the material handling activities executed by Van-der-Waals' forces.

2.5 Design for Manufacturability and Assemblability

Design for Manufacturability and Assemblability (DFMA) is a process for improving product design so as to reduce lead times using relatively simple and low-cost manufacturing and assembly processes, focusing on functionality and assemblability, concurrently (Boothroyd, 1994). The benefits of applying DFMA usually include improved quality and reliability, and a reduction in production equipment and part inventory.

Boothroyd and Dewhurst have formulated one of the most widely recognized DFA methodologies. The first step evaluates each part to determine whether it is essential in the design or is a candidate for elimination. The second step estimates the time taken to grasp, manipulate and insert the part during assembly (Stone, R.B., McAdams, D. A., Kayyalethekkel, V. J., 2004).

This method is based on two principles (Boothroyd, G. & Alting, L., 1992): the application of criteria to each part to determine if it should be separate from all other parts and estimation of the handling and assembly costs for each part using the appropriate assembly process. This method relies on an existing design which is iteratively evaluated and improved. Generally, the process follows these steps:

- Step 1: Select an assembly method for each part,
- Step 2: Analyse the parts for the given assembly methods,
- Step 3: Refine the design in response to shortcomings identified by the analysis,
- Step 4: Loop to step 2 until the analysis yields a sufficient design.

A part is evaluated as to whether it is really necessary (in the assembly) by asking three questions (Boothroyd, G. & Alting, L., 1992; Boothroyd, 1994):

- Does the part move relative to another part?
- Are the material properties of the part necessary?
- Does the part need to be a separate entity for the sake of assembly?

The list of all parts is then evaluated to obtain the minimum number of theoretically needed parts, denoted by N_m as in Table 2.1. Screws, bushes, stand-offs, washers and covers are

theoretically considered to be non-essential items in a design (Boothroyd, G. & Alting, L., 1992; Boothroyd, 1994).

Table 2.1 Sample Boothroyd-Dewhurst DFA worksheet

a	b	c	d	e	f	g	h	i*	Name of assembly
Part ID Number	Number of consecutive identical operations	2-digit handling code	Manual handling time/part	2-digit insertion code	Manual insertion time/part	Operation time (bd+f)	Operation cost	Essential part?	
Totals						T_m	C_m	N_m	

Where * - in column "i", denotes that one has to use "1" to represent that a part is essential, and "0" to represent that a part is not essential.

The method then assumes that the assembly time for a part is 3 seconds (*3s* in Equation 2.23). With that assumption, the design efficiency can be calculated using Equation 2.23 (Boothroyd, 1994; Stone, R.B., McAdams, D. A., Kayyalethekkel, V. J., 2004).

$$Design\ Efficiency = \frac{3sN_m}{T_m} \qquad \text{Equation 2.23}$$

Where *3s* is the assembly time of 3 seconds, N_m is the total number of essential parts, and T_m is the total operation time in seconds (s).

Figure 2.12 illustrated an application of DFMA principles to a motor drive assembly. *Design 1* shows the initial design and *Design 2* shows the final design after applying the DFMA principles. In the two designs the assembly times have been maintained as the same for the items which appear in both designs for comparison purposes. Otherwise the assembly times for Design 2 would be less because of high accessibility facilitated by the application of DFMA principles.

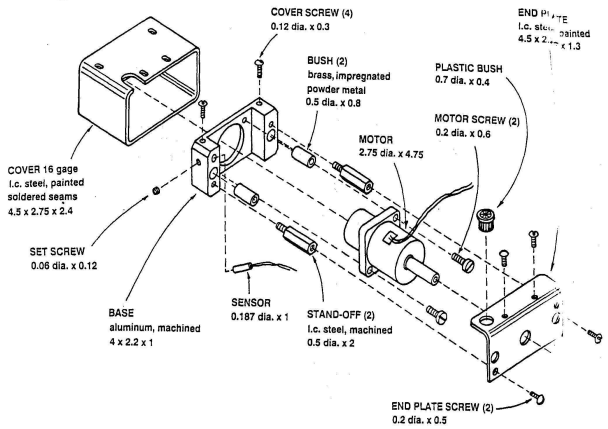

Design 1 Initial design (Jayaraman, 2003)

Part	Number of items.	Theoretical part count	Assembly time (s)
Base	1	1	3.5
Bushing	2	0	12.3
Motor sub.	1	1	9.5
Motor screw	2	0	21
Sensor Sub	1	1	8.5
Set Screw	1	0	10.6
Stand-off	2	0	16.0
End plate	1	1	8.4
End plate screw	2	0	16.6
Plastic bushing	1	0	3.5
Thread leads	-	-	5.0
Reorient	-	-	4.5
Cover	1	0	9.4
Cover screw	4	0	31.2
Totals	19	4	160.0
Design efficiency = (4 x 3)/160 = 7.5% (Jayaraman, 2003)			

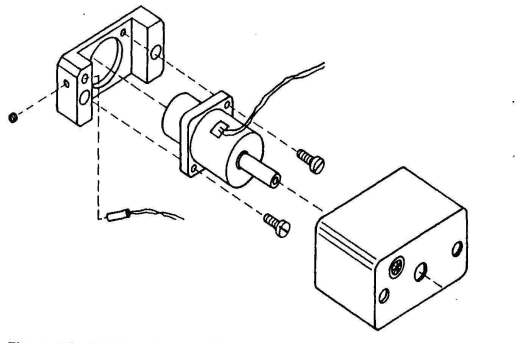

Design 2 Final design after applying the DFMA principles (Jayaraman, 2003).

Part	Number of items.	Theoretical part count	Assembly time (s)
Base	1	1	3.5
Motor sub.	1	1	9.5
Motor screw	2	0	21
Sensor Sub	1	1	8.5
End plate	1	1	8.4
Thread leads	-	-	5.0
Totals	6	4	55.9
Design efficiency = (4 x 3)/55.9 = 21%			

Figure 2-12 DFMA application for a motor drive assembly (Jayaraman, 2003), (Boothroyd, G. & Alting, L., 1992; Boothroyd, 1994)

A comparison of *Design 1* and *Design 2* shows that the former has 19 components and the latter only 6. When Equation 2.23 is applied *Design 2* has design efficiency of 21% and *Design 1* only 7.5% . Therefore, *Design 2* is 2.8 times better than *Design 1,* proving that DFMA principles (when applied) lead to higher design efficiency.

Tietje et al (2008) takes the DFMA principles further by postulating a suitable methodology for micro-assembly. They say that most of the DFMA apply to both the micro-domain and the macro-world. However; they comment that an update of the feeding, handling and gripping of micro-parts' design rules need to be updated. Tietje and Ratchev (2007) argue that in the micro-world Van-der-Waals' force, electrostatic force and surface tension force become dominant over gravity, necessitating a new methodology instead of methodologies which suit the macro-domain. Tietje and Ratchev (2007), and Tietje et al (2008)'s methodology is called design for micro-assembly (DFμA) and it facilitates:

1. Design improvements early in the design phase by capturing available micro-assembly process characteristics, and
2. Product-process analysis which provides a way to select and determine appropriate micro-assembly processes.

These two main points are captured and illustrated in the DFμA conceptual layout shown in Figure 2.13. This framework starts with the identification of requirements; followed by product design specification, and product assemblability analysis, which are evaluated with respect to the DFμA design guidelines. Thereafter the product process analysis, coupled with assembly process selection follows and these are analysed by a process capability model. A cost model is then used to determine a cost-effective decision. Finally, a sound and efficient product design is produced concurrently with selected suitable assembly processes.

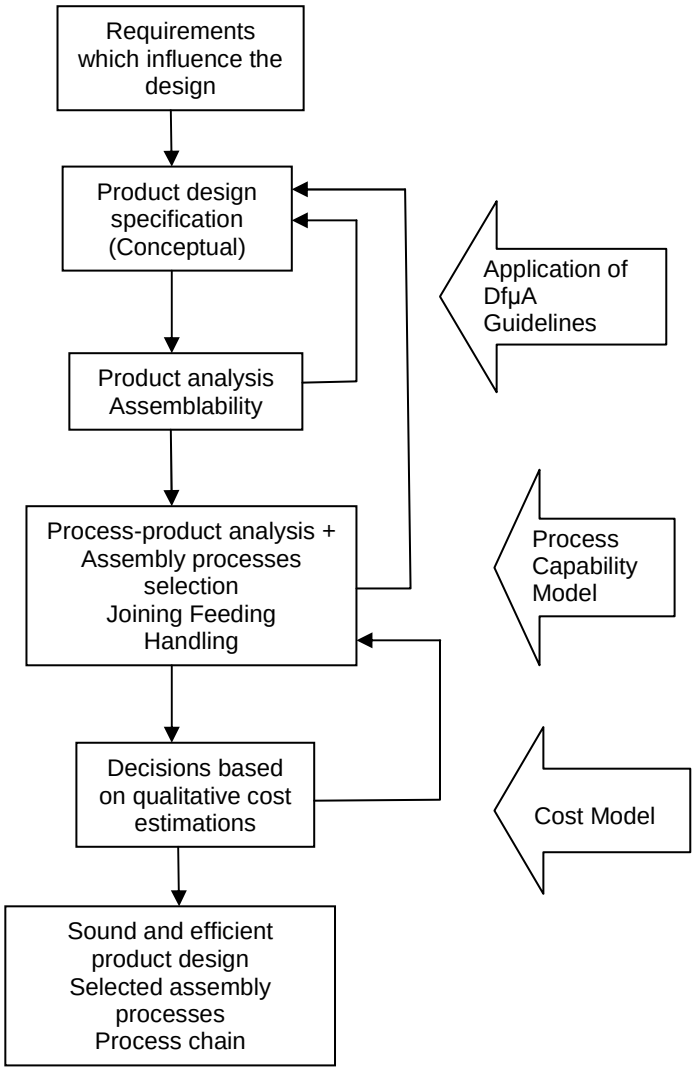

Figure 2-13 Conseptual DFμA Layout (Tietje and Ratchev (2007), Tietje et al (2008))

In their DFμA methodology, Tietje and Ratchev (2007) and Tietje et al (2008) establish rulesthrough the following questions:

1. What is particularly useful for a certain process?
2. Which techniques (e.g. certain joining techniques) should be avoided and under which circumstances?
3. Which techniques offer which advantages?

Finally, Tietje and Ratchev (2007) and Tietje et al (2008) also indicate a need for a supportive decision making method to enable cooperation of the models used in the DFμA methodology.

2.6 Parameters affecting Van-der-Waals' forces

2.6.1 Temperature

There is great evidence that Van-der-Waals' forces are also temperature-dependent in the case of solids and liquids as shown in Table 2.2 (Ninham, B.W., Parsegian, A.V. and Weiss, G.H., 1970). As indicated earlier in the calculation of the Hamaker coefficients, they depend on the thermal energy *kT* (where the Boltzmann constant, k = 1.3807 x 10^{-23} J/K and T is the absolute temperature in Kelvins of the environment) and dielectric susceptibilities of interacting materials as shown in Equation 2.16 (French, 2000).

Table 2.2 Non-retarded Hamaker Coefficients against temperature for Al_2O_3 (French, 2000).

Temperature	0 K	300 K	2000 K
Al_2O_3/vacuum/ Al_2O_3	164.85 zJ	164.851 zJ	164.864 zJ
Al_2O_3/water/ Al_2O_3	56.998 zJ	56.9786 zJ	56.8087 zJ
Al_2O_3/SiO_2/ Al_2O_3	26.1565 zJ	26.1568 zJ	26.1604 zJ
Al_2O_3/SiO_2/air]	240.4044 zJ	240.4047 zJ	240.4081 zJ

The units of the Hamaker coefficients in Table 2.2 are given in zepto-Joules (zJ), where 1 zJ is equal to 1x10^{-21} J. However; it is observed in the above case that the effect of temperature on the Hamaker coefficients is small, less than 0.2 zJ, as the temperature increases from 0 K to 2000 K.

2.6.2 Humidity

When two surfaces are interacting in environments of high humidity, Van-der-Waals' force would not be the only acting force. Surface tension would also be significant. However; at humidity levels below 30%, the effect of surface tension is almost eliminated (Rabinovich I. Y., Adler J. J., Ata A., Singh K. J., and Moudgil M.B., 2000). Podczek et al (1997), postulate that capillary forces can be removed at low relative humidity of about 5% (Podczeck, F., Newton J. M., James, M.B. , 1997).

A relative humidity value greater than 75% results in strong forces (which include surface tension) acting at the interface of interacting particles (Podczeck, F., Newton J. M., James,

M.B. , 1997). Takeuchi (2006) also asserts that when the relative humidity is higher than 50%, the water bridge adhesion force begins to contribute to some extent to the total adhesion forces of particles, and is most predominant at relative humidity levels higher than 70%, as shown Table 2.3 (Takeuchi, 2006) (Matope, S. and Van der Merwe, A. F, 2010c).

Table 2.3 Adhesion forces against humidity for toner particles (Takeuchi, 2006)

Relative humidity (%)	Average adhesion force (nN)
30	2.90
40	2.52
50	2.30
60	30.1
70	410

2.6.3 Material type variation

The intensity of Van-der-Waals' forces depends on the material type of the interacting surfaces, as mentioned earlier. The higher the Hamaker coefficient, A_H, the greater the intensity of the Van-der-Waals' forces between the interacting surfaces. The Hamaker coefficient is specific to given materials and has typical values, as shown in the Appendix E. The Hamaker coefficients for organic materials are generally less than those for inorganic materials, with the exception of some polymers like polyurethane. These materials can then be varied accordingly to increase the efficiency in the picking and releasing of micro materials. For example; polystyrene (of A_H = 79 zJ) may be used for the picking place, aluminum oxide (of A_H = 145 zJ) for the gripper, and copper (of A_H = 400 zJ) for the releasing place in the order of their increasing Hamaker coefficient values. The A_H values in vacuum are considered to be almost the same as those in air (Bergstrom, 1997). However, it should be noted that the effect of material type on Van-der-Waals' forces is low at times 'because the Hamaker coefficient are of the order of 10^{-21}J.

Polyurethane materials have been found to exert large amounts of Van-der-Waals' forces. The development of polyurethane gecko-setae-like micro- and nano-structures has enhanced Van-der-Waals' clamping of micro-parts (Glassmaker N. J., Jagota A., Hui, C. Y., Kim, J, 2004)(Geim, A. K., Dubonos, S. V., Grigorieva, I. V.; Novoselov, K. S.; Zhukov, A. A., Shapoval, S. Y., 2003; Bhushan, 2003). These are directional, hierarchical and high aspect ratio micro-structures with nano-fibres at the end, as in Figure 2-14 (Murphy M. P., Kute C.,

Mengüç Y. and Sitti M., 2011). They can firmly grip both micro- and macro-workparts (Murphy M. P., Kute C., Mengüç Y. and Sitti M., 2011) whose root-mean-square surface roughness values can be as high as 35µm. These numerous nano-fibres have the advantage that they can increase the surface's contact area by being in touch with the whole profile of a rough surface. Another advantage is that they are anisotropic allowing a relatively easy clamping and unclamping operation (Menon, C.; Murphy, M.; Sitti, M., 2004) (Murphy M.P., Kute C., Mengüç Y. and Sitti M., 2011) (Sitti, M. & Fearing, R. , 2003) (Murphy, M. P. and Sitti, M, 2007). Van-der-Waals' forces were experimentally proven by Murphy et al (2007) and Murphy et al (2011) to hold (in a fixed position) micro-robot masses of at least 0.1 kg on vertical walls. This corresponds to shearing forces of 0.981N magnitude.

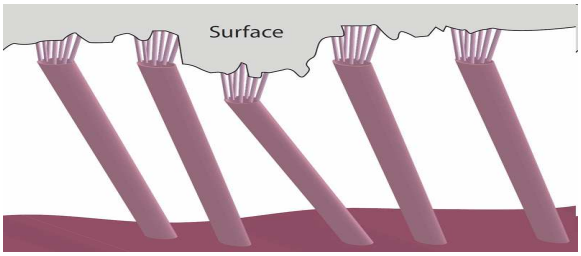

Figure 2-14 Directional and hierarchical polyurethane fibres (NanoRobotics Lab, 2011)

The polyurethane gecko-like setae and spatulae are produced by several methods. These include electron beam lithography (EBL) (Aksak, B., Murphy, M., and Sitti, M. , 2007); ultraviolet (UV) lithography as described by Aksak et al (2007) and Murphy et al (2009); and micro/nanomolding which also consists of three different methods: nano-embossed templates (Sitti, M. & Fearing, R. , 2003; Glassmaker N. J., Jagota A., Hui, C. Y., Kim, J, 2004; Menon, C.; Murphy, M.; Sitti, M., 2004; Aksak, B., Murphy, M., and Sitti, M. , 2007); self-organized nano-pore membranes (Sitti, M. & Fearing, R. , 2003; Glassmaker N. J., Jagota A., Hui, C. Y., Kim, J, 2004; Menon, C.; Murphy, M.; Sitti, M., 2004; Aksak, B., Murphy, M., and Sitti, M. , 2007); and directed self-assembly based micro/nano-hair growth (Sitti, M. & Fearing, R. , 2003; Glassmaker N. J., Jagota A., Hui, C. Y., Kim, J, 2004; Menon, C.; Murphy, M.; Sitti, M., 2004; Aksak, B., Murphy, M., and Sitti, M. , 2007).

As mentioned earlier, directional polyurethane fibres are anisotropic in nature. They exert more gripping force in one direction and less in the other, as shown in Figure 2-15. When this phenomenon is applied in micro-material handling, it enables an efficient gripping and releasing mechanism. A $1cm^2$ area of directional polyurethane microfiber array with 14^o

angled tips adhering to smooth glass can support approximately 100kPa in shear in the gripping direction, but only about 20 kPa in the releasing direction, as shown in Figure 2-15 (Murphy M., Aksak B., and Sitti M., 2009).

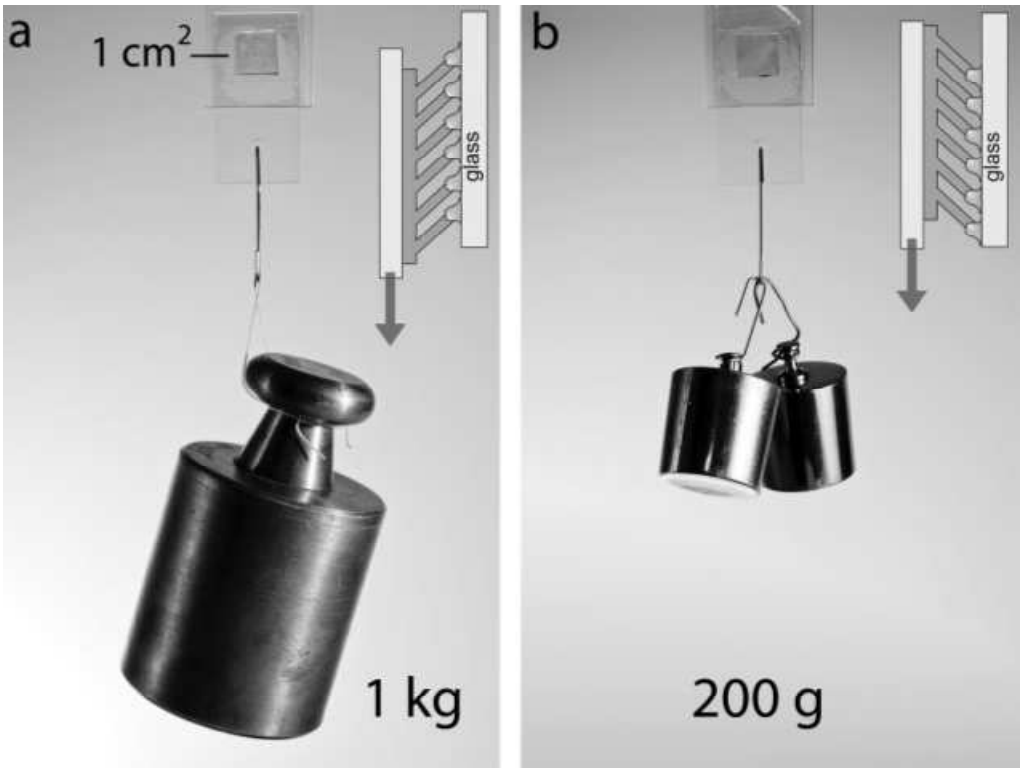

Figure 2-15 Directional polyurethane micro-fiber array.

Murphy et al (2009) proved that vacuum suction was not the principal source of adhesion in this scenario, but simply Van-der-Waals' forces. They hung a mass of 0.5 kg onto the 1cm^2 polyurethane pad in a vacuum of less than 0.01 atmosphere, and the load was sustained for 10 minutes (Murphy M., Aksak B., and Sitti M., 2009).

It should also be noted that Murphy et al (2007) and Murphy et al (2011) used preloads in order to obtain an optimum exertion of Van-der-Waals' forces on the interacting surfaces in their wall-climbing robots. Aksak et al (2007) also confirms that there is an optimum preload which yields an optimal Van-der-Waals' force for a given polyurethane material. They also observed that the soft polyurethane ST1060 with a shore hardness 60A, exerted higher Van-der-Waals' forces than a hard polyurethane ST1087 with a shore hardness 87A (Aksak et al, 2007).

2.6.4 Geometrical parameters variation and analysis

Once again, as mentioned earlier, Van-der-Waals' forces are dependent on the geometry of interacting surfaces of the micro-workparts, micro-grippers, picking position and placement position (Li, Q., Rudolph, V., Peukert, W. , 2006; Eichenlaub, S., Kumar, G., Beaudoin, S., 2006; Fukuda T. & Arai F., 1999; Tanaka, M., Komagata, M., Tsukada, M., Kamiya, H. , 2008). Van-der-Waals' forces vary directly with area. The forces increase with an increase in contact surface area. Van-der-Waals' forces also vary inversely as the separation distance as discussed earlier. They increase as the separation distance decreases until a cut-off distance, D_{cut}, is reached, as shown in Figure 2-16 (Weber W. M., Hrenya M. C., 2007).

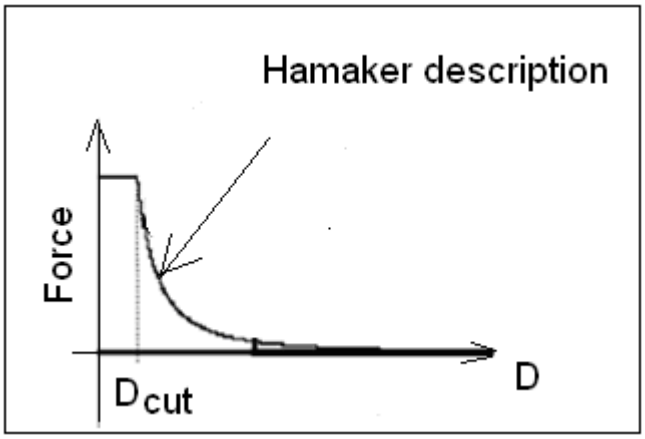

Figure 2-16 Cohesive force against separation distance (Weber W. M., Hrenya M. C., 2007)

Different geometrical configurations give different contact areas leading to different amounts of Van-der-Waals force being exerted between interacting surfaces. Analytical modelling of geometric parameters with respect to the exerted Van-der-Waals forces is executed (in the following paragraphs under this section) so as to identify the optimum solutions. The geometrical configurations include the flat-flat, sphere-sphere, sphere-flat, cone-flat, and cylinder-flat interactions. The geometrical parameters examined include radius, separation distance, half-cone angle and surface roughness of micro-grippers. The analysis is made with respect to least one of the following: radius of curvature ($1\mu m$ to $10\ \mu m$ range), separation distance ($1nm$ to $10\ nm$ range), included-half-cone angles (0^o to 90^o range) and surface roughness ($0.1nm$ to $1.0\ nm$ range), and a Hamaker coefficient of 1×10^{-21}J is assumed in the

analytical modelling. A synthesis is made aimed at optimising the efficacy of a given micro-material handling system.

Sphere-sphere surface interaction

Figure 2-17 shows the sphere-sphere interaction where D is the shortest separation distance between the interacting surfaces, R_1 is the radius of the smaller sphere and R_2 the radius of the bigger sphere.

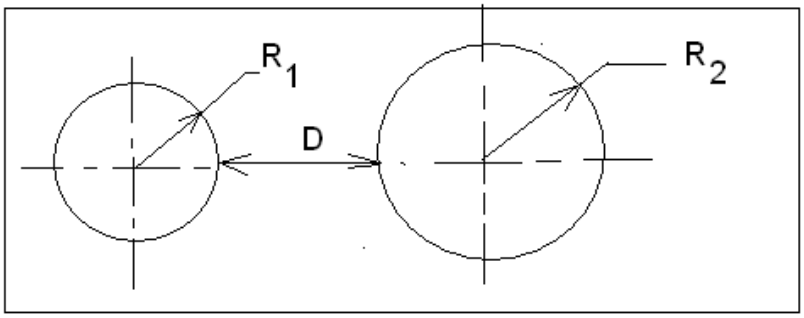

Figure 2-17 Sphere-sphere surface interaction with a separation distance D in between (Van der Merwe, A. F. and Matope, S., 2010)

Equation 2.5 is used in the analytical modelling of the Van-der-Waals' forces with respect to radius of the interacting spheres leading to the generation of the graphs in Figure 2-19 (for sphere-sphere interactions).

Sphere-flat surface interaction

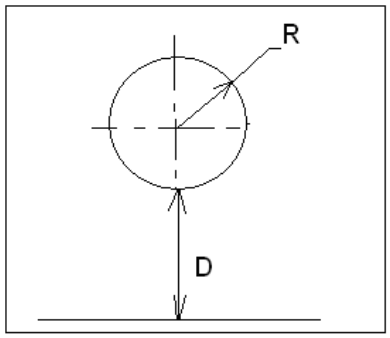

Figure 2-18 Sphere-flat surface interaction with a separation distance D in between (Van der Merwe, A. F. and Matope, S., 2010)

Figure 2-18 is a schematic representation of the sphere-flat surfaces' interaction. Equation 2.6 is used to analytically model the exerted Van-der-Waals' forces and is plotted on the same axes with the sphere-sphere interactions, for comparison purposes, as in Figure 2-19. In this

case, the comparison base is the radius of the sphere(s). R1 is the radius of one sphere and R2 of the other.

The graphs are straight line graphs as long as R2 is dependent upon R1. It can be observed that twice as much Van-der-Waals' forces are experienced on a sphere-flat interactive surfaces as compared to sphere-sphere (where R2 = R1) interactions.

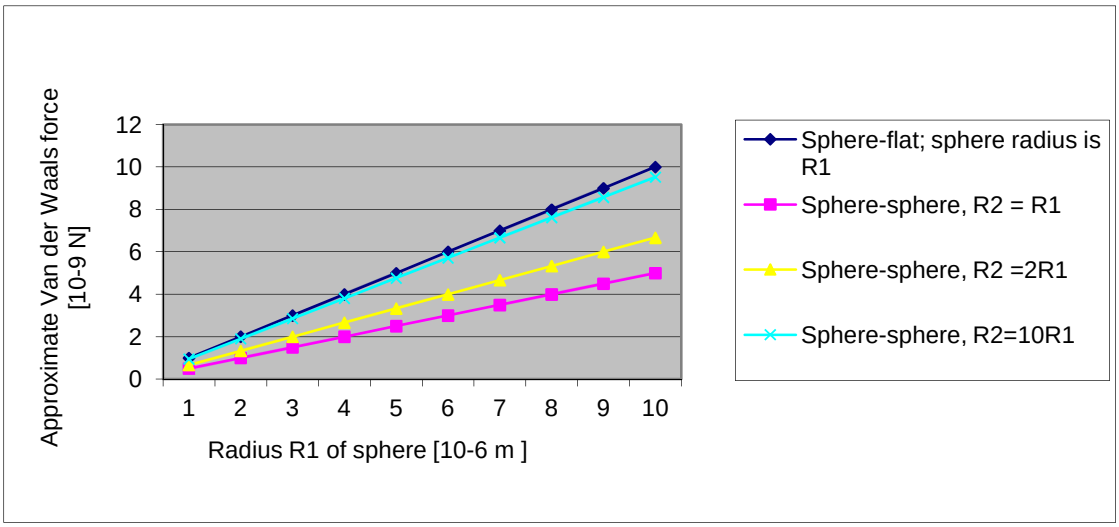

Figure 2-19 Sphere-sphere and sphere-flat surface comparison with respect to radius (Van der Merwe, A. F. and Matope, S., 2010)

As the radius R2 increases to 2R1 and then to 10R1, the gradient of the force-radius curve increases, approaching that of sphere-flat interactive surface as shown in Figure 2-19. As R2 increases to higher values, the intensity of the exerted Van-der-Waals' forces approaches that of a flat surface (Takeuchi, 2006). On the other hand, flat-flat surface interaction exerts the largest force because it affords the largest contact area. Therefore; for an optimum solution, the picking place of a micro-workpiece should be spherical (since adhesion force is less) and the releasing place should be flat (resulting in more attractive Van der Waals' for the work-piece).

Again Equation 2.5 is used for the analytical modelling in Figure 2-20 that depicts a sphere-sphere interaction with the radius of the larger sphere, R2, increasing while the radius of the smaller sphere, R1, is constant at given values. As the radius R2 increases, the Van-der-

Waals' force intensity increases. The smaller the particle (that is the smaller is the R1), the easier it is to pick it.

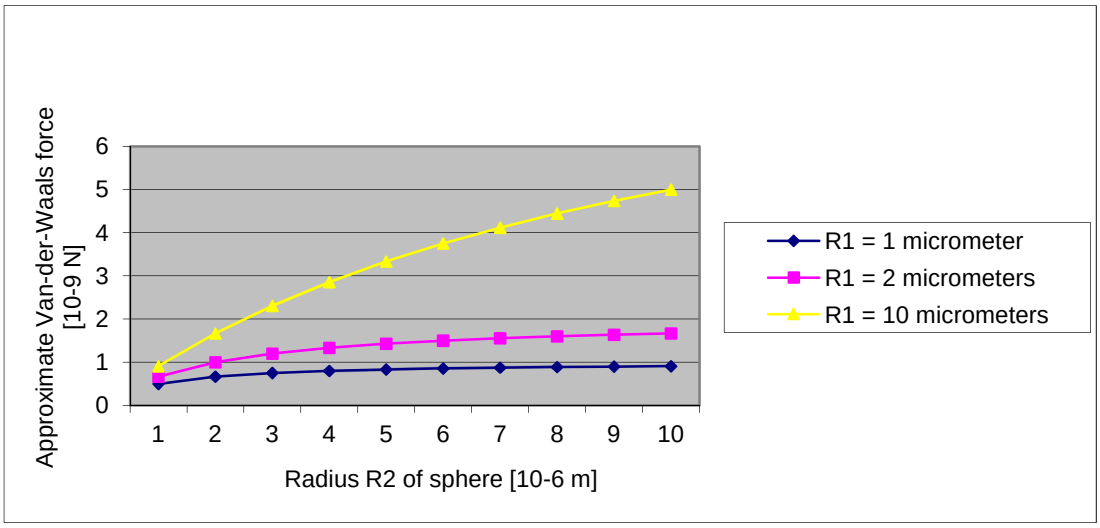

Figure 2-20 Sphere-sphere interaction with the radius of the larger sphere, R2, increasing while the radius of the smaller sphere, R1, is constant at given values (Van der Merwe, A. F. and Matope, S., 2010)**.**

It is evident from Figure 2-20 that as the radius of a gripper increases, the intensity of the Van-der-Waals' forces increases proportionately, and a decrease in radius leads to a decrease in the force. Therefore; in an optimisable micro-material handling system, the gripper should be designed in such a way that its radius is expandable when inflated, thus increasing the intensity of the Van-der-Waals' forces; and deflated when placing the micro-workpart, as shown in Figure 2-21. With this kind of design, the micro-gripper can pick and release both spherical and planar micro-workparts.

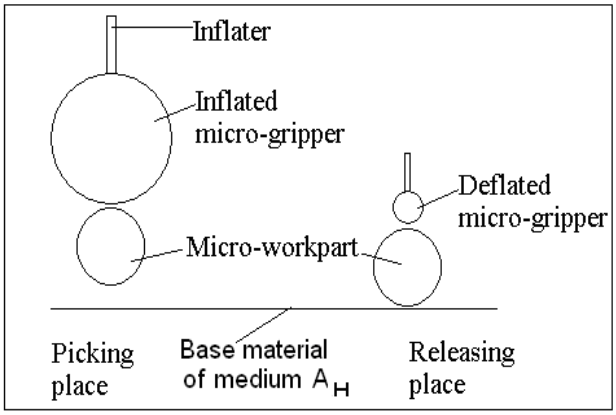

Figure 2-21 An inflatable micro-gripper of variable radius (Van der Merwe, A. F. and Matope, S., 2010)

However; there are some limitations ascribed to this design because it does not afford the required contact area for some micro-workparts for an effective picking and placing cycle. This is taken care of in the ensuing cylindrical design.

Cylinder-flat surface

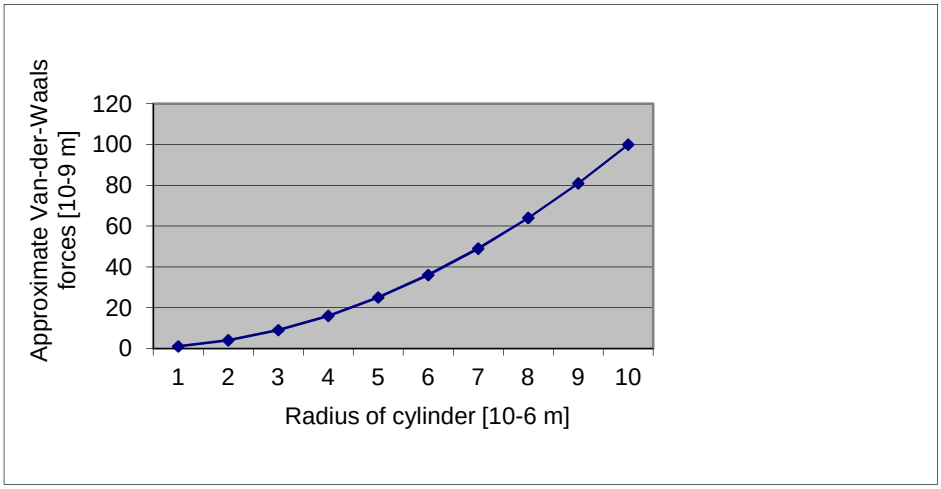

Figure 2-22 Cylinder-flat surface against radius (Van der Merwe, A. F. and Matope, S., 2010)

Figure 2-22 shows the plot of Van-der-Waals' forces against radius for a cylinder-flat surface interaction, an analytical modelling of Equation 2.9. The Van-der-Waals' forces in this case are more pronounced than in sphere interactions. The main reason for this is that a sphere has a point contact whilst a cylinder has a line contact with flat surfaces. Theoretically, a line consists of numerous points connected together. Hence, more Van-der-Waals' forces are experienced on a cylindrical surface than on the spherical. This implies that the picking place should be spherical and the releasing place cylindrical for greater efficiency and effectiveness. By the same token, the gripper should be expandable in order to vary its radius. When picking a micro-work, it should have a bigger radius than when releasing. From Figure 2-22 it is evident that, as the radius of the cylinder increases to infinite (cylinder's contact area becoming flatter), the Van-der-Waals' forces rapidly increase proving that a flat-flat surface's interaction exerts the largest force because it affords the largest contact area.

Sphere-sphere, sphere-flat, cylinder-flat surfaces comparison

Figure 2-23 shows the comparison of the sphere-sphere, sphere-flat surface, and cylinder-flat surface interactions. For analytical modelling purposes, the radius, R, of the elements

increases from 1 µm to 10 µm. It is evident that for the same materials and separation distance equal to 1µm, the cylindrical surface exerts more Van-der-Waals' forces than the spherical surfaces.

Therefore; a cylindrical micro-gripper exerts more force than a spherical one. Hence, when large amounts of Van-der-Waals' forces are required in micro-material handling, a cylindrical gripper should be used. However; it should be noted that a flat-flat surface's interaction affords the largest contact area and hence the greater Van-der-Waals' forces as explained earlier.

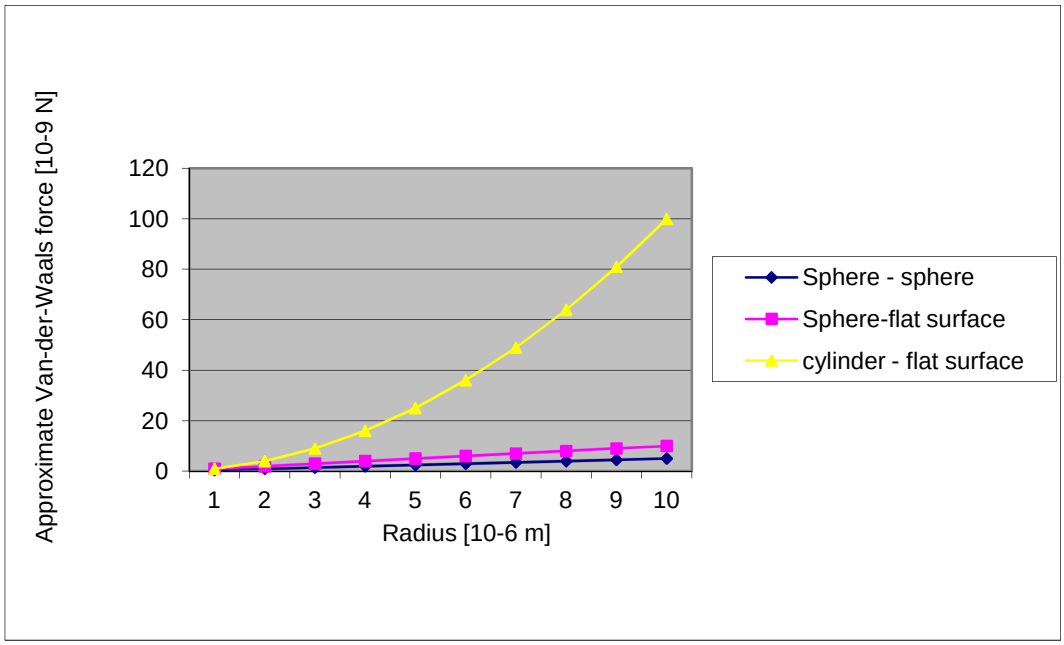

Figure 2-23 Comparison of geometries: sphere-sphere, sphere-flat, cylinder-flat surfaces with respect to radius, R. The sphere-sphere interactive surface consists of two equal spheres of radius R (Van der Merwe, A. F. and Matope, S., 2010)**.**

Cone-flat surface and cone angle analysis

As for a cone-flat interaction (illustrated in Figure 2-24), the Van-der-Waals' forces vary, as the square of the tangent of the included-half-cone angle, as shown in Equation 2.8. Figure 2-25 shows the analytical modelling of the forces. The Van-der-Waals' forces increase sharply after the half-cone angle of 60^{o} (semi-aperture cone angle) reaching a maximum of 90^{o}. At this maximum angle, the configuration would be a flat-flat surface interaction, proving that this configuration exerts more force than the cone-flat surface interactive surface.

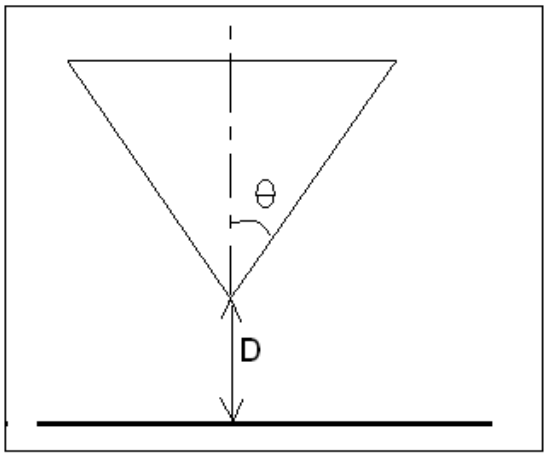

Figure 2-24 Cone-flat surfaces interaction (Van der Merwe, A. F. and Matope, S., 2010)

Figure 2.24 shows the cone with half-cone angle, Θ, interacting with a flat surface which is D micrometers away.

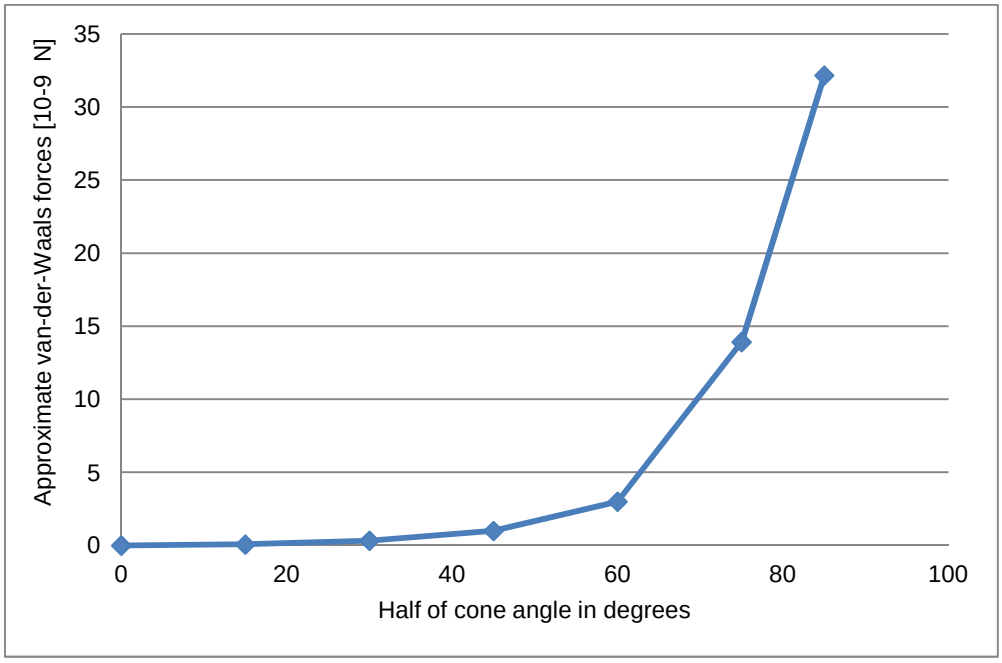

Figure 2-25 Van der Waals for cone-flat surface against included-half-cone angle (Van der Merwe, A. F. and Matope, S., 2010)**.**

Therefore; a gripper can be manufactured so that when picking the included-half-cone angle would be greater than 60^{o} and on releasing less than 60^{o} as shown in Figure 2-26. The conical configuration can be achieved mechanically by having numerous pin-like structures conically mounted to a diaphragm. The manipulation of the diaphragm (contraction or expansion)

would vary the cone angle much like an umbrella mechanism. Furthermore, a centre pin which protrudes in and out of the peak of the cone angle, may also be used to improve the picking and releasing mechanism.

However; the design efficiency of such a gripper would be low due to its high part count.

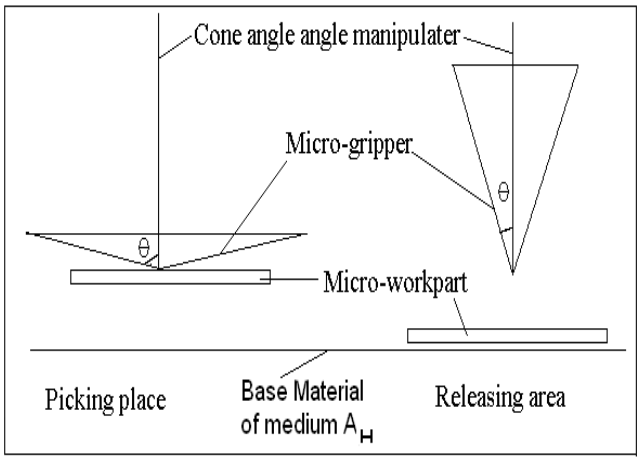

Figure 2-26 Conical design of a micro-gripper showing bigger half-cone angle when picking and a smaller when releasing (Van der Merwe, A. F. and Matope, S., 2010)

Similarly, the shape of the picking place can be manipulated. The picking place should have a small cone angle (to reduce the adhesive force of the base material) and the releasing place should have a large angle.

However; when the DFMA criteria by Boothroyd and Dewhurst (as detailed in Section 2.5 and Equation 2.23) is applied, the conical gripper is found to have a low design efficiency since it requires too many components in its construction. A flat surfaced gripper proves to have a better design efficiency since it has a low part-count. Furthermore, it is observed that the flat-flat interactive surface exerts the highest intensity of Van-der-Waals' forces as compared to cone-flat, cylinder-flat, sphere-flat and sphere-sphere interactive surfaces. Therefore, in this study, a flat surfaced configuration of interactive surfaces would be given first preference for material handling purposes.

2.6.5 Surface roughness variation

Surface roughness, as mentioned earlier, refers to the unevenness of the topography of a given substance. The effect of surface roughness has been studied and particles could be treated as smooth when the surface asperities are less than 0.01 μm (Xie, 1997). The surface asperities

rather than the parent particles dominate the Van-der-Waals' forces when they (surface asperities) are more than $0.1\mu m$ (Xie, 1997). There are several approaches to the consideration of surface roughness. These include the asperity radius and the root-mean-square of the spacing of the asperities.

When two rough surfaces are in contact, the crests of the asperities would be in top-to-top contact as shown in Figure 2-27 (Li, Q., Rudolph, V., Peukert, W. , 2006; DelRio, F.W., De Boer, M.P., Knapp, J.A, Reedy, E.D. (Jr), Clews, P.J., Dunn, M.L., 2005)

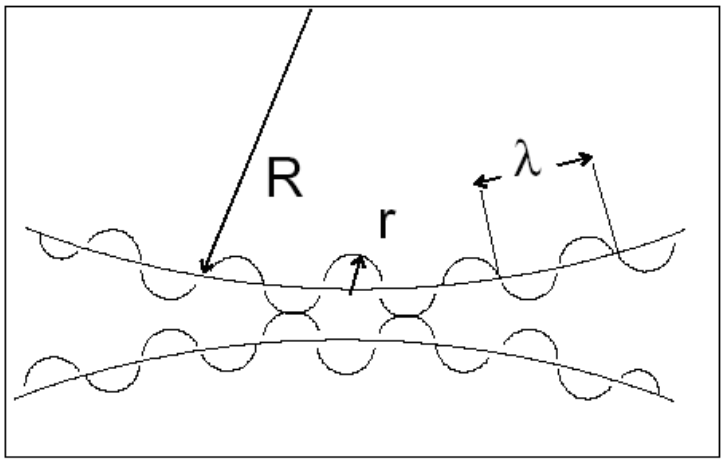

Figure 2-27 Objects with asperities in top-to-top contact

The objects in Figure 2-27 have radius, *R*; asperity radius, *r*; and asperity wavelength, λ (Rabinovich I. Y., Adler J. J., Ata A., Singh K. J., and Moudgil M.B., 2000). The general formula for the adhesive Van-der-Waals' forces, *F* in *N*, taking into consideration the existence of asperities at micro-level is given by Equation 2.24. (Li, Q., Rudolph, V., Peukert, W. , 2006):

$$F = \alpha A \qquad \text{Equation 2.24}$$

Where: α is the intrinsic adhesiveness defined as the adhesive force exhibited on a unit effective surface area (Li, Q., Rudolph, V., Peukert, W. , 2006) measured in Nm^{-2} *or* $Kgm^{-1}s^{-2}$, *A* is the effective surface contact area in m^2.

Roughness may be used to increase grip by employing pin-like structures actuated by an intelligent gripper. These pins would contact the whole profile of the asperity as shown in Figure 2-28. When picking, sufficient pins are protruded so that they form an elastic bond with the rough surface of the micro-workpiece. Upon releasing the workpiece, sufficient pins are retracted to allow for the placement of an object – mimicking gecko satae (Filippov, A.E. & Popov,V., 2006). Furthermore, a soft material (for example, polyurethane) may be used to

capitalise on surface roughness, as mentioned earlier. With reference to Figure 2-28, when the pins are replaced by polyurethane material and pressed against hard rough surfaces, it embeds itself into the irregular profiles of the hard material leading to an increase in contact area. This results in more Van-der-Waals' forces being experienced.

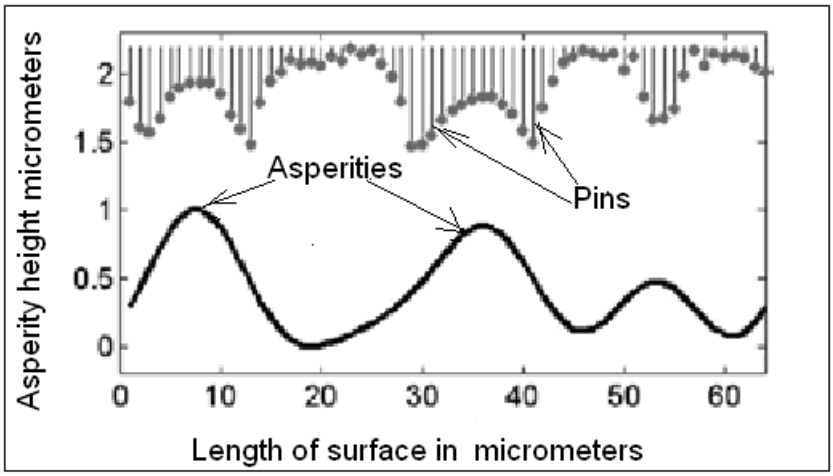

Figure 2-28 Diaphragm with pins (satae) to increase the area of contact,(Filippov, A.E. & Popov,V., 2006)

Rumpf studied the effect of root-mean-square (rms) surface roughness on the Van-der-Waals' forces' intensity (Rabinovich I. Y., Adler J. J., Ata A., Singh K. J., and Moudgil M.B., 2000). The non-contact and contact interaction of a spherical particle and flat surface were examined. Rabinovich took the study further and came up with the Rumpf-Rabinovich equation (given as Equation 2.25) which numerically models the Van-der-Waals' forces experienced when a smooth spherical micro-work part interacts with a flat surface (Li, Q., Rudolph, V., Peukert, W. , 2006; Komvopoulos, 1996; Suresh L. and Walz Y. J. , 1997; Eichenlaub S., Gelb A., Beaudoin S., 2004; Rabinovich Y. I, Adler J. J., Ata A., Singh R.K. , Moudgil B. M., 2000; Rabinovich I. Y., Adler J. J., Ata A., Singh K. J., and Moudgil M.B., 2000). For the rough flat sample, the dispersion adhesion force can be calculated using Equation 2.25 which incorporates a correction factor of *+1.48 rms.*

$$F = \frac{A_H R}{6H_o^2}\left[\frac{1}{1+\frac{R}{1.48rms}} + \frac{1}{\left(1+\frac{1.48rms}{H_o}\right)^2}\right] \qquad \text{Equation 2.25}$$

Where F is the Van der Waals force in N, A_H is the Hamaker coefficient (a chemical property of matter which reflects the intensity of the Van-der-Waals' forces exerted by a given substance in J) as mentioned earlier, (Parsegian, 2006)), *rms* is the root-mean-square surface

roughness value of the flat surface in *m*, *R* is the radius of the smooth spherical micro-work part in *m*, H_o is the shortest separation distance between interacting micro-parts in *m*.

The first component in the square brackets of Equation 2.25 reveals the effect of surface roughness (in *rms* values in *m*) in the non-contact region and is represented by [2.26] (also referred to as the non-contact term in this study) (Li, Q., Rudolph, V., Peukert, W. , 2006; Komvopoulos, 1996; Suresh L. and Walz Y. J. , 1997; Eichenlaub S., Gelb A., Beaudoin S., 2004)

$$\frac{1}{1+\frac{R}{1.48rms}} \qquad [2.26]$$

The second component which shows the effect of surface roughness for a contact interaction is given by [2.27] (also referred to as a contact term in this study).

$$\frac{1}{\left(1+\frac{1.48rms}{H_O}\right)^2} \qquad [2.27]$$

In practice, when the surfaces are in contact, the separation distance can be taken as $H_0 = 0.3$ nm, since surface roughness would prevent a total contact.

Van-der-Waals' forces are numerically modelled with respect to surface roughness based on the contact term [2.27] to give Figure 2-29. The contact term is chosen because it is a power function and would override the non-contact term given in Equation 2.26 (Matope, S., Van der Merwe, A. F., Nkosi, M., Maaza, M. and Nemutudi R., 2011). This reasoning is applied in the methodology and numerically modelling of Van-der-Waals' forces in Chapter 3 and Chapter 4.

In the figure it is revealed that the rougher the surface of a given sample is, the less is the intensity of the exerted Van-der-Waals' forces. An increase in the *rms* value of the surface roughness, at a constant separation distance (in this case assumed to be 1 nm), leads to a decrease in the Van-der-Waals' force intensity as shown in Figure 2-29. (Rabinovich I. Y., Adler J. J., Ata A., Singh K. J., and Moudgil M.B., 2000; Eichenlaub, S., Kumar, G., Beaudoin, S., 2006; Thoreson, E.J., Mart, J. and Burnham, N.A., 2006).

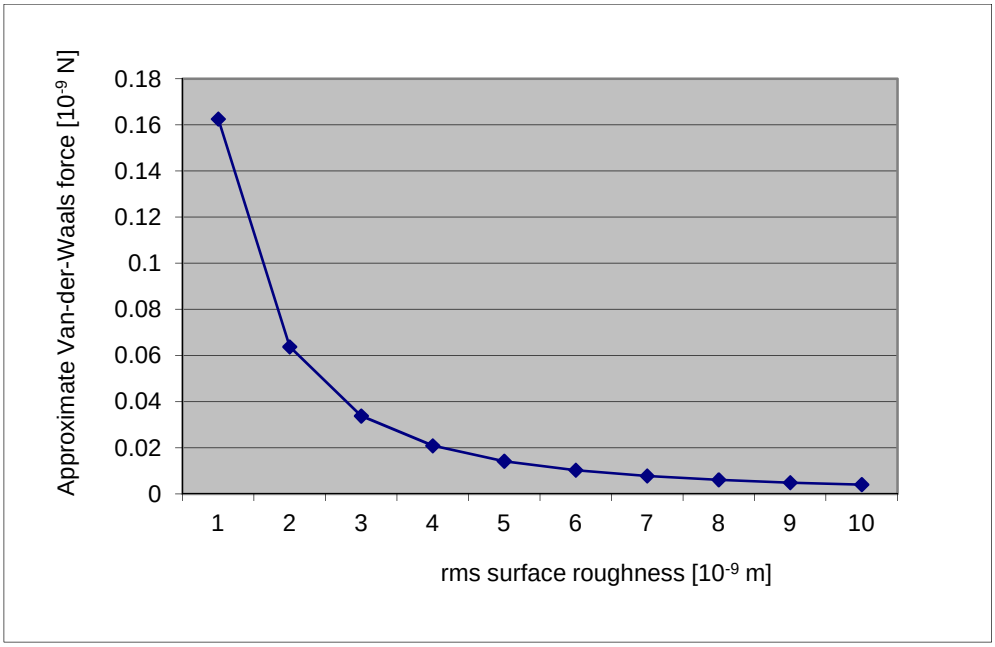

Figure 2-29 Effect of a *rms* roughness on Van-der-Waals forces at specific separation distances (Van der Merwe, A.F. & Matope, S. , 2009)

Surface roughness also may be manipulated on gripper's surfaces by ensuring that the micro-workparts fit themselves between adjacent asperities or into grooves as shown in Figure 2-30, giving them two areas of contact which increases the exerted Van-der-Waals' forces. In such a scenario, materials with low Hamaker coefficients may pick workparts from bases of high Hamaker coefficient values, by virtue of their increased contact area.

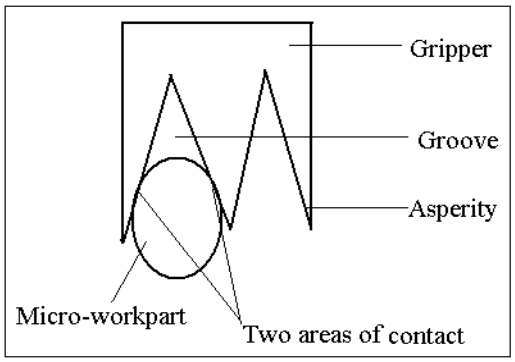

Figure 2-30 Surface roughness and increase in area of contact.

Furthermore; for a rough flat sample, within the framework of mono-roughness numerical model, the theoretical dispersion adhesion force (Van-der-Waals' force) can be calculated using Equation 2.28 which is an improved version of Equation 2.25 because it takes into consideration the peak-to-peak distance of asperities of the surface roughness (Rabinovich Y.

I, Adler J. J., Ata A., Singh R.K. , Moudgil B. M., 2000). Equation 2.28 is also referred to as Rabinovich's formula.

$$F = \frac{A_H R}{6H_0^{\,2}}\left[\frac{1}{(1+58R\cdot rms/\lambda^2)} + \frac{1}{(1+1.82rms/H_0)^2}\right] \qquad \text{Equation 2.28}$$

Where λ is the peak-to-peak distance of the asperities in *m* of the surface roughness and the other symbols carry the same meaning as stated earlier.

Again a correction factor of separation distance equal to *+1.48 rms*, is applied to Equation 2.6 in order to obtain a formula for non-contact dispersion force between a rough plane and smooth sphere, resulting in Equation 2.29. This equation is used in Section 4.3.1 to numerically model the Van-der-Waals' forces' extending curves (graphs produced when the AFM probe gradually approaches the specimen until contact is realised) for rough surfaces. These extending curves are labelled "3" and are compared with experimental graphs for analysis purposes. (Rabinovich I. Y., Adler J. J., Ata A., Singh K. J., and Moudgil M.B., 2000). It should be noted that Equation 2.29 gives information about the Van-der-Waals' forces experienced (at a specific separation distance) when a probe (or a micro-part) approaches a given surfaces. However, the total adhesive Van-der-Waals' forces are given by Equation 2.28 which has been given earlier.

$$F = A_H R/6(H+1.48rms)^2 \qquad \text{Equation 2.29}$$

Derivative of the force Equation 2.6 for smooth samples with respect to separation distance *H* is given by Equation 2.30.

$$F = A_H R/3H^3 \qquad \text{Equation 2.30}$$

When a probe of the atomic force microscope (AFM) is brought to close proximity with an interactive surface, it experiences an attractive force and jumps into contact with the surface after reaching a certain threshold-separation distance. For the jump-in distance, H_j, the force derivative is equal to the spring constant of the AFM cantilever as represented by Equation 2.31,

$$dF/dH(H=H_j) = k \qquad \text{Equation 2.31}$$

Therefore; the theoretical jump-in distance for smooth samples can be calculated using Equation 2.32 (a combination of Equation 2.30 and Equation 2.31),

$$H_j = \sqrt[3]{A_H R/(3k)} \qquad \text{Equation 2.32}$$

However; for a rough flat surface interacting with a smooth sphere, the theoretical force derivative of Equation 2.29 yields Equation 2.33

$$dF/dH = A_H R/(3(H+1.48RMS)^3) \qquad \text{Equation 2.33}$$

Therefore, the theoretical jump-in distance for a rough sample interacting with a smooth sphere is given by be Equation 2.34 (a combination of Equation 2-33 and Equation 2.31)

$$Hj = \sqrt[3]{A_H R/(3k)} - 1.48RMS \qquad \text{Equation 2.34}$$

It should also be noted that surface roughness predominates over material type in determining the amount of Van-der-Waals' forces exerted by a given interactive surface. This is evidenced by the fact that the *rms* surface roughness value is of the order of 10^{-9} *m* and the Hamaker coefficient is of the order of 10^{-21} *J,* as indicated in Appendix E. Furthermore, *rms* surface roughnesses of the micro-parts can be varied (for manipulation purposes) for any given material, whilst the Hamaker coefficient is always constant for a specific material.

2.7 E-beam evaporation

The e-beam evaporation method is used to generate surfaces of relatively uniform surface roughnesses (Matope, S., Van der Merwe, A. F., Nkosi, M., Maaza, M. and Nemutudi R., 2011). The substrates on which the depositions are made can be silicon or any other material. For a uniform surface roughness to be achieved, the substrates need to be smooth with an *rms* surface roughness values of less than 10 *nm*. The materials to be e-beam evaporated are placed in a crucible and positioned below the silicon substrates. The evaporated materials can be of any type, but preferably inorganic materials; for example, pure metals. The depositions can be made with respect to time or film thickness (Matope, S., Van der Merwe, A.F., Nemutudi R., Nkosi, M., Cele, M., and Maaza, M., 2010).

2.8 Conclusion

The Van-der-Waals' forces have been found to be adhesive in nature and they are effective when the separation distance between the interacting surfaces is in the nano-range. The greatest Van-der-Waals' force is exerted when contact between the interacting surfaces is achieved. It has also been analytically proved that flat-flat interactive surfaces exert the largest Van-der-Waals' forces as compared to others, which included the flat-cone, flat-sphere and sphere-sphere geometrical configurations. Therefore; flat interactive surfaces will be given preference in this study. Furthermore; surface roughness seem to predominate over

material type in influencing the exerted Van-der-Waals' forces in certain classes of materials (for example metals) because the *rms* surface roughness values are of the order of 10^{-9} *m* (generally for smooth samples) and materials have Hamaker coefficients of the order of 10^{-21} *J*. In addition, Van-der-Waals' forces vary inversely as the surface roughness, but varies directly as the Hamaker coefficient. This again gives surface roughness an upper-hand in influencing the exerted Van-der-Waals forces than material type. It was also highlighted that *rms* surface roughness values for a given material can be varied for micro-manipulation purposes, while the Hamaker coefficients are normally constant for a specific material. Therefore, this study focuses intensely on the application of Van-der-Waals' forces in a micro-material handling system based on surface roughness variation, although there would be reference to material type of flat (geometrically configured) samples. In the subsequent chapter, the methodology of the research is explained.

3 CHAPTER 3: METHODOLOGY

3.1 Introduction

In this study, an empirical or pragmatic methodology is employed to validate the applicability of Van-der-Waals' force in a micro-material handling system. Empirical research refers to research based on experimentation or observation aimed at testing a hypothesis (experiment-resources.com). Its main objectives are to prove relevancy of theory by working in a real world environment. The reason for using this method is that it helps to integrate research and practice. The advantages of Empirical research are: it responds appropriately to the dynamics of situations, it respects contextual differences, its helps to build scientifically acquired knowledge and it affords the opportunity to meet standards of professional research (experiment-resources.com). However; it produces poor results when insufficient data is available. The Empirical cycle includes five stages: the observation stage, where data is collected and empirical facts are organized; the induction stage, where a hypothesis is formulated; the deduction stage, where the consequences of the newly gained empirical data is construed; the testing stage, where the hypothesis is tested with the new empirical data; and finally, the evaluation stage, where the outcomes of the testing are analysed and synthesised to get a final judgment of the validity of a given hypothesis (experiment-resources.com). Analytical modelling, numerical modelling and experimental measurements are used in obtaining results.

The null hypothesis that Van-der-Waals' forces can be used in micro-material handling was experimentally tested. The alternative hypothesis was that Van-der-Waals' forces cannot be used because of their adhesive nature. To test the null hypothesis, the independent parameters upon which the Van-der-Waals' forces were dependent, were identified. As reflected in the literature review, these were: material type, geometrical configuration and surface roughness. These three form the fundamental strategies upon which Van-der-Waals' forces can be applied in a micro-material handling operation. The first strategy involves the application of material type variation of the interactive surfaces of the micro-part, micro-gripper, picking position and the placement position. The second strategy utilises geometrical configuration, and surface roughness variation makes up the third strategy of the interactive surfaces involved in a given micro-material handling system. A hybrid strategy is used as a final resort in complicated situations.

The analytical modelling in Section 2.6.4 proved that a flat surfaced geometrical configuration exerted the largest Van-der-Waals forces. Therefore, most experiments were conducted using flat surfaces in this research. Again from the discussion in Section 2.6.5 and Section 2.7 *rms* surface roughness variation seem to have more influence over the exerted Van-der-Waals' forces than material type variation. The following numerical modelling formulae: Rumpf-Rabinovich's formula and Rabinovich's formula were used in the analysis of the results. These formulae were used because they give a reliable relationship between the exerted Van-der-Waals' forces and the *rms* surface roughness values of a given micro-part or sample. Rabinovich's numerical modelling formula has the added advantage that it takes care of peak-to-peak distances of the surface roughness as discussed in Section 2.6.5. This formula again gives a better indication as to whether the Van-der-Waals forces are the only prevalent forces in a given experimental set-up.

The samples included copper, aluminium, silver and polyurethane. Turning operations, lapping, polishing and e-beam depositions were used in the preparation of samples. Measuring instruments, which included the optical microscope, scanning tunnelling microscope, scanning electron microscope and the atomic force microscopes, were used to examine the samples. Softwares (compatible with these instruments) were used to analyse and characterise the surfaces of the samples. Later atomic force microscopes were used to measure the Van-der-Waals' forces exerted by selected samples. The XRC 100 motoman robot was used to experiment with the micro-material handling capabilities of the specimens. Furthermore; the samples were tested in the handling of IC circuit components.

Experimental data was also collected from laboratory work conducted at iThemba laboratories, Cape Town; SENROB Robotics Laboratory, University of Stellenbosch (US); Metrological Laboratories, US; Electronics Laboratory, US; Material Examination Laboratory of the Geology Laboratory, US; Material Examination Laboratory of the Process Engineering Laboratory, US. Further experimental data and validation was obtained from international collaborative research with the Particle Engineering Research Center, Florida University, United States of America (USA). Constructive criticism was also obtained through another international collaboration with the Institute for Machine Tools and Forming Technology, Chemnitz University of Technology, Germany.

3.2 Surface preparation: Top-down approach

Initially, the researcher employed a top-down approach in preparing the surfaces of the samples. Four types of materials were used for the micro-material handling system. These were copper, aluminum, polyvinyl chloride (PVC) and Teflon. These materials were used because they were commonly available in industrial applications. The other criterion used was the distinct Hamaker coefficient values, with the metals having higher values than the non-metals, as in Appendix E. In this case, Teflon has the lowest Hamaker coefficient, making it suitable for the picking position's base; copper has the highest value, making it fit for the placement position's base; and aluminum has a middle value, making it suitable for the gripper.

Three cylindrical (100 mm long) samples of each material were prepared (by the researcher) with diameters of 20mm, 10mm and 5mm, respectively. The surfaces were initially smoothed using the most suitable turning operation on a lathe machine. An initial Van-der-Waals' force actuated micro-material handling operation was attempted manually, as shown in Figure 3-1. The gripper was made of aluminium, the picking base was made of Teflon and the placement base was made of copper. In order to ensure that Van-der-Waals' forces were dominant in the exercise, the researcher conducted the experiment on an electrostatic dissipating mat. The antistatic mat was designed in such a way that it discharged all the electrostatic force of any equipment which came into contact with it. An antistatic plug was used to connect the mat to the electrical power supply throughout the duration of the experiments in order to avoid any development of electrostatic charge on all the apparatus. An antistatic crocodile clip was used to hold and discharge the grippers. Again an antistatic wrist band was strapped on the wrist of the researcher in order to discharge him of any electrostatic force. Non-ferrous materials and apparatus were used to avoid the effect of magnetic forces. Methanol was used to clean the apparatus. The experiments were carried out in the US Metrological Laboratory.

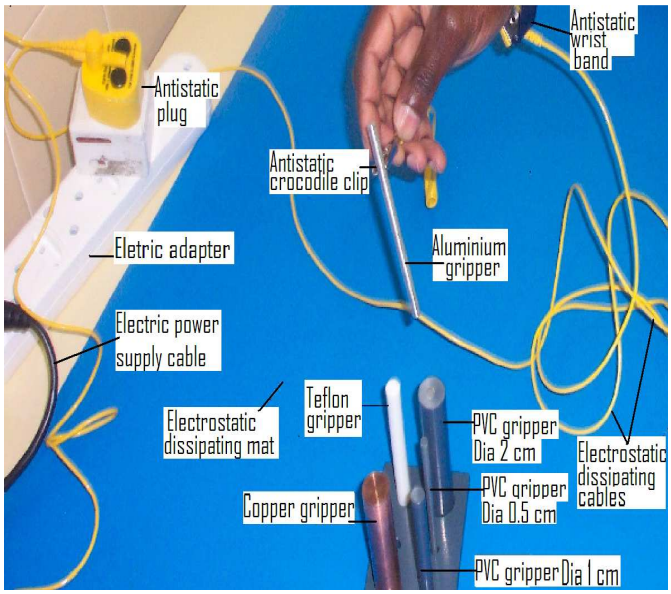

Figure 3-1 Experimental design using anti-static mat.

However; the researcher's hand's vibrations and non-repeatability of the positioning of the gripper with initial uniform pressure on the micro-parts prevented reliable results. Subsequently, the motoman robot was used by the researcher in the picking and placing of micro-parts, as indicated in Figure 3-2.

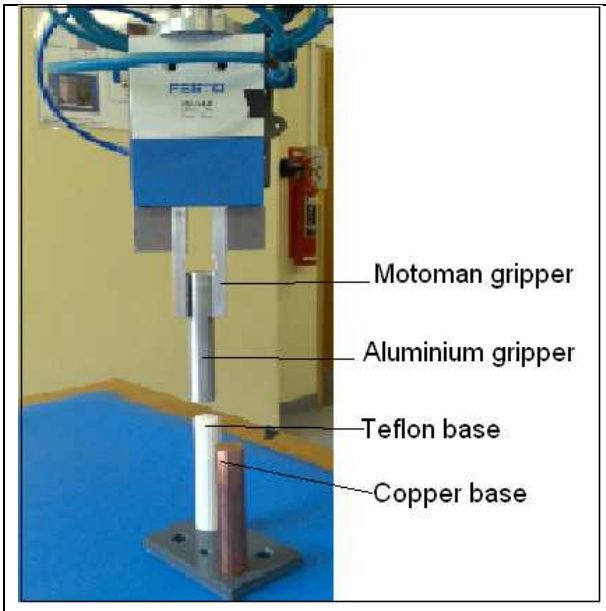

1. Experimental set-up on the Motoman

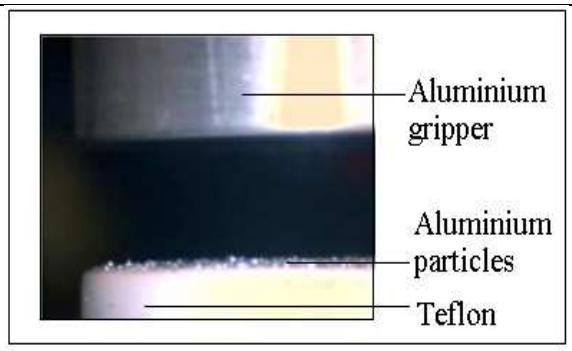

2. Aluminium gripper approaching the aluminum particles on Teflon.

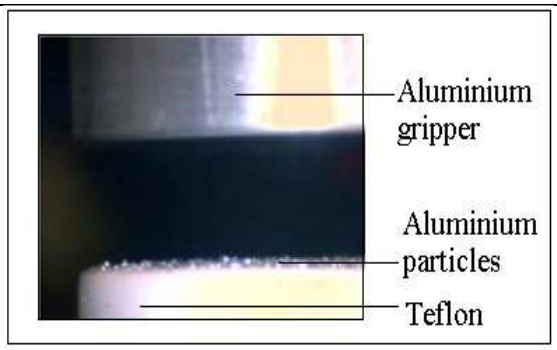

3.Aluminium gripper approaching the aluminum particles on Teflon.

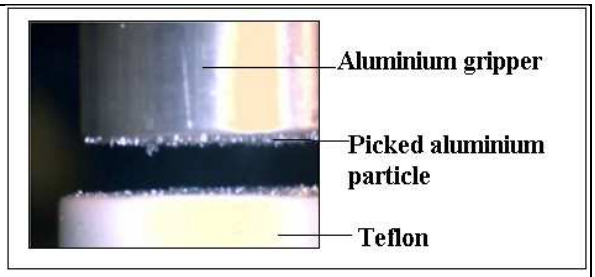

4.Aluminium gripper after picking the aluminum particles from Teflon

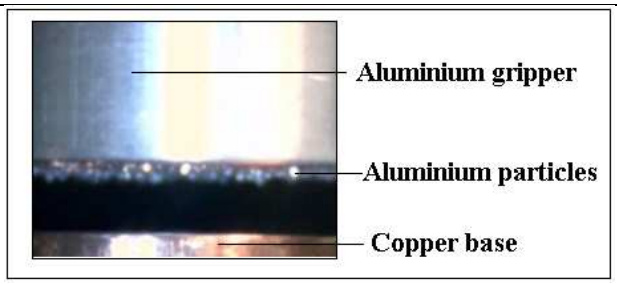

5.Aluminum gripper with aluminium particles approaching the copper base

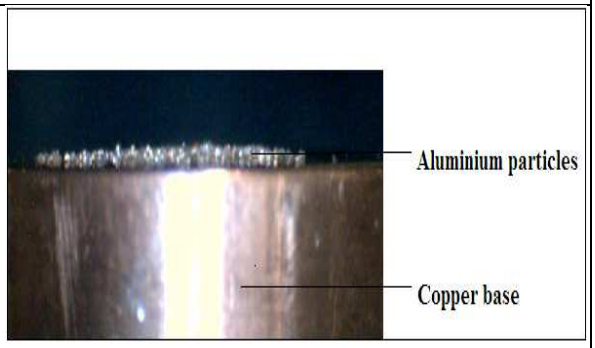

6.The aluminium particles attracted from the aluminum gripper onto the copper base

Figure 3-2 Material handling using aluminum gripper

The parts of the motoman, which were in contact with the samples, were earthed again using the anti-static mat and its accessories. With such a system in place, aluminium micro-parts, shown in Figure 3-3, were picked by the aluminium gripper from the Teflon surface (which had the lowest Hamaker coefficient) and deposited onto the copper surface (which had the highest Hamaker coefficient of the three).

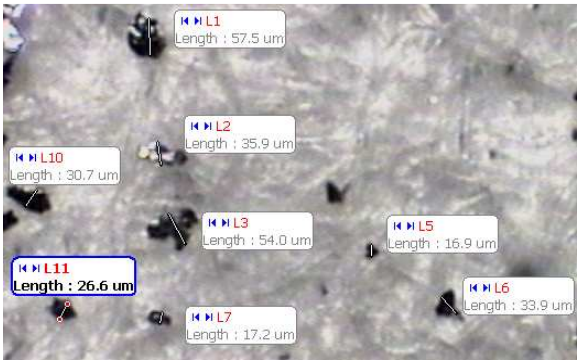

Figure 3-3 Aluminium particles

However; some micro-parts remained stuck to the aluminium gripper, which theoretically should not be the case. This necessitated the researcher to examine the surfaces under an

optical microscope. Rough surfaces with circular grooves, formed by the turning tool's trajectory, were observed as shown in Figure 3-4. The micro-parts (33.9 µm and 35.9 µm in Figure 3.3) were found embedded into the grooves (some 55.7µm and 55.8µm wide as in Figure 3.4) and were mechanically trapped so that no effective picking and placing of all the micro-parts was realised.

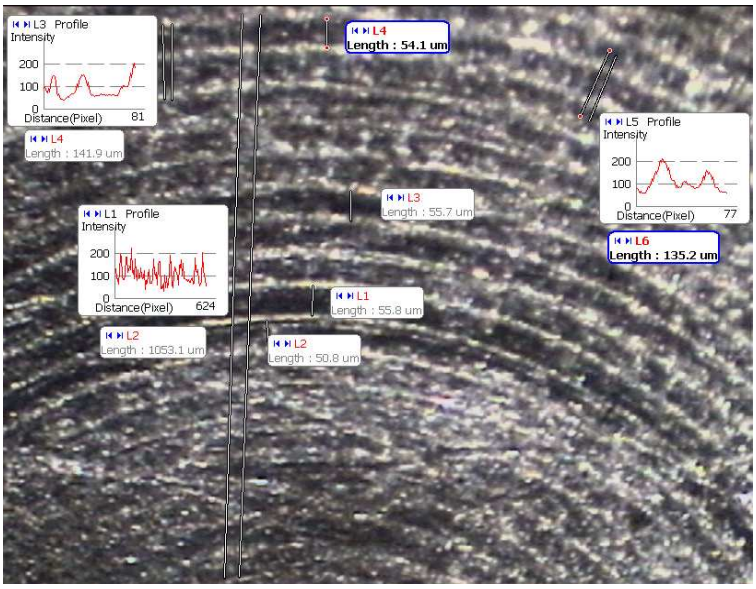

Figure 3-4 Turning grooves

Therefore; further surface smoothing through lapping, was required. The lapping machines needed short samples in order to fit into their sample holders. Four samples of copper, aluminum, PVC and Teflon, (each of 5 mm and 10 mm in diameter) were prepared by the researcher. To ensure secure gripping and uniform treatment during lapping, they were put into a mould and a resin was poured over them and cured. A large fixture disc (25 mm in diameter and 10 mm in height) using the four samples as integral parts, was developed, as shown in Fig. 1 in Appendix K. This disc was then mounted to the polishing machine and guaranteed the four specimens to be subjected to the same lapping conditions, the objective being to produce surfaces of uniform finish.

Different grades of lapping discs were used by the researcher, starting with the coarsest and ending with the finest. The discs were magnetically clamped to the large circular base of the lapping machines used. A DAP-2 Dia Duo Struers lapping machine with weights to press the sample against the lapping disc was used first (Fig. 2 in Appendix K). However; its polishing capabilities were hampered since it did not have a damping mechanism for vibrations.

The researcher then used the Struers RotoPol-35 lapping machine which had a better damping rubber mechanism (Fig. 3 in Appendix K). The samples were securely held in the small holes

of the mounting disc. A mechanically actuated screw punch (with conical rubber fixtures as shown in Fig 3 in Appendix K) exerted a force on the samples so as to remain in contact with the rotating lapping disc during the process. Lapping for 15 minutes was executed at rotational speeds of 150 rpm for coarse grades, namely MD Piano 220, 600 and 1200. Final polishing, by the researcher, with fine grits discs of 9 µm, 6 µm, 3 µm and 1µm was conducted separately for 1 hour at a rotational speed of 250 rpm. During the lapping process, the specimens were gently rotated so as to ensure uniformity on the generated surface structure.

The researcher used the scanning tunnelling microscope shown in Fig. 4 in Appendix K, to examine the four polished samples of copper, aluminium, PVC and Teflon. Since PVC and Teflon were non-conductors of electricity, all four samples were coated with gold so that their surfaces could be uniformly characterized.

An atomic force microscope was later used for analysis. Unfortunately, some deep scratches on the samples were present as indicated in Figure 3-5 (atomic force micrograph of aluminum), caused by the initial coarse grinding process. The *rms* surface roughness values for the lapped aluminium, copper, polyvinyl chloride and Teflon were 5.11 nm, 4.08 nm, 7.6 nm and 24.3 nm respectively. The scratches caused the surface roughness to be unevenly distributed, drastically affecting the determination of the appropriate Van-der-Waals' force values for a given sample. This traditional surface preparation involving lapping may also lead to surface hardening and plastic deformation of the work-part. It may also result in foreign materials; for example the debris produced by the grinding, polishing or lapping tool; being imbedded into the surface being prepared. The researcher then decided to use a bottom-up approach, in which he used the electron beam evaporation method to deposit metal coatings on silicon substrates, leading to the production of characterisable surfaces with an evenly distributed surface roughness.

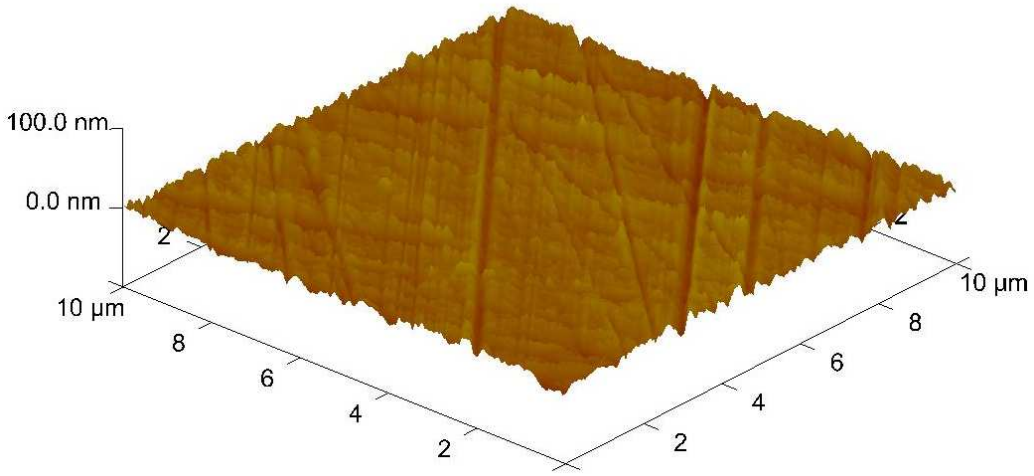

Figure 3-5 Surface roughness micrograph of lapped aluminium

3.3 Surface preparation: Bottom-up approach

The bottom-up approach involved the use of the electron beam evaporation (e-beam) method. This bottom-up approach was used because (as discussed earlier in Section 3.2) it afforded the production of a surface which was: evenly distributed, free of scratches, not hardened, not plastically deformed, without foreign inclusions and relatively homogenous in its nature. An e-beam machine at iThemba laboratories, Cape Town, shown in Fig.5 in Appendix K, was used for this operation. Mr. Mthobisi Cele and Dr Mlungisi Nkosi (specialists in operating the e-beam machine) in the Material Research Department, iThemba Labs, Cape Town, assisted the researcher in carrying out the e-beam depositions over two years, 2010 and 2011, as indicated in the Evaporator Sheets in Appendix G in which the first names of the researcher and those of the assistants are stated. The original records of these evaporator sheets are in the e-beam machine's usage log-book maintained in the Material Research Department at iThemba Labs in Cape Town, South Africa.

Up to three different elements could be evaporated sequentially during each e-beam operation. The elements were placed in crucibles, shown in Fig 6 in Appendix K. The crucibles were cleaned before each e-beam evaporation procedure to avoid possible contamination by remains of previously evaporated materials.

Silicon Substrate Preparation

Silicon substrates, 76.2 ± 0.5mm in diameter, 100 ± 0.5 degrees in orientation, 350 - 400 microns in thickness, P type/Boron, 1-20 ohm-cm resistivity and polished on one side, were

sliced by the researcher into 10 mm x 10 mm substrates using a diamond point tool on a Karl Suss – HR 50 machine in Fig. 7 in Appendix K. The researcher washed the substrates consecutively in an ultrasonic bath of methanol, acetone and trichloroethylene. Later the substrates underwent a second cycle of ultrasonic bath in acetone, methanol, de-ionised water and in 20% hydrofluoric acid solution respectively. Each ultrasonic bath was 5 minutes in duration. The ultrasonic bathing machine, shown in Fig. 8 in Appendix K, was used. The substrates were then rinsed in de-ionised water. The purpose of the cleaning was to remove all the oxide layers, greasy materials and other contaminants.

The researcher then dried the samples using a stream of dry nitrogen gas and later mounted them on aluminium sample holders, as illustrated in Fig. 9 in Appendix K.

The E-beam Deposition

Copper, aluminium and silver were selected for e-beam deposition. In these experiment 99.999% pure copper shots, 2.6mm in diameter; 99.9% pure aluminum wires and 99.99% pure silver shots, 3mm in diameter, were used. The other accompanying properties of the materials are shown in Appendix F. The depositions were made on the washed silicon substrate. Unfortunately, PVC and Teflon could not be deposited using this method since they are polymers. Silver was also included in the examination because it is another common industrial material which has high electrical and thermal conductivity as well as a high Hamaker coefficient. Copper, aluminium and silver were separately put by the researcher into the e-beam crucibles shown in Fig. 6 in Appendix K.

The silicon substrates which were mounted on aluminum holders were then placed on an indexing guide (Fig. 10 in Appendix K) as illustrated in Fig. 11 in Appendix K. These were assembled above the crucible, in the top part of the e-beam machine.

After the materials in the crucibles were preheated to reduce spattering and gaseous outbursts, the e-beam deposition was carried out. The pressure during deposition was within the range of 1×10^{-7} and 3×10^{-6} mbar. An electron gun, consisting of a tungsten filament, produced electrons that were focused onto the target sample in the crucible by a magnetic field, as in Figure 3.6.

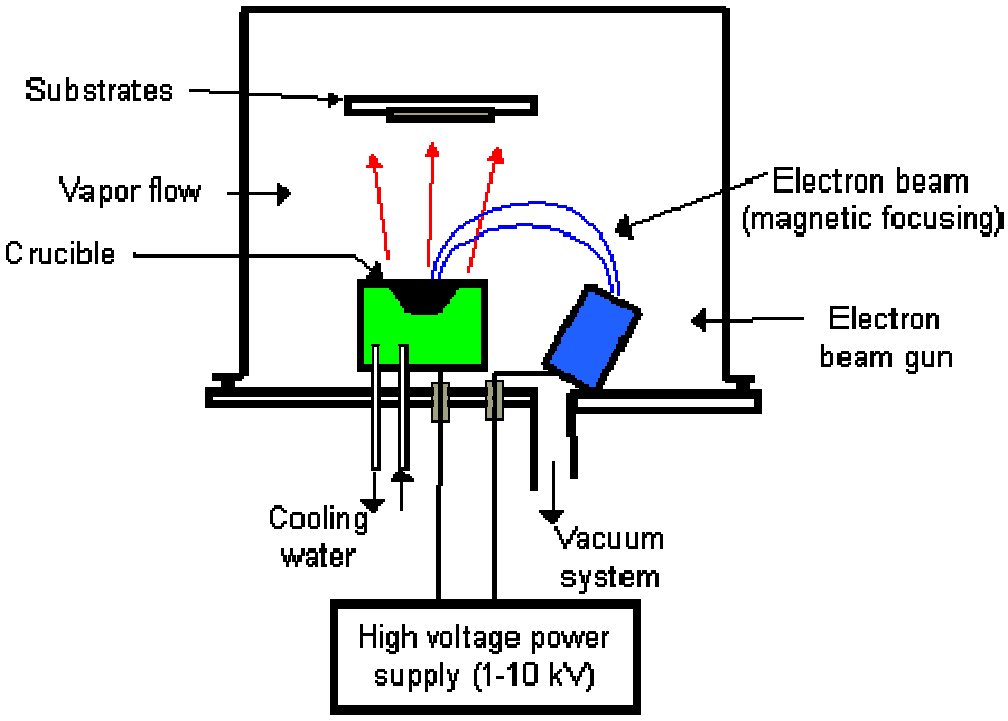

Figure 3-6 Diagram of e-beam experimental set-up (Courtesy: iThemba Labs).

The electron-beam was so strong that its energy vaporised the target sample in the crucible. The vapour was deposited on the silicon substrates mounted above in the e-beam top chamber. Film thickness was measured by a quartz monitor during evaporation. The accumulation of material on the vibrating quartz crystal caused a change in the crystal's frequency. This information was then fed into a microprocessor which calculated the rate of evaporation as well as the thickness of the deposited film.

The system was fitted with a shutter (Figure 3-7) that could be opened or closed by means of magnets, as shown in Figure 3-8. Before the experiments began the shutter always stayed closed to shield the silicon substrates from the e-beam vapour produced below in the crucibles. When the e-beam deposition had to take place, the shutter was opened by the researcher (using the magnetic mechanism in Figure 3-8) for e-beam deposition to take place on the targeted silicon substrate for a specified duration. At the end of the required duration, the researcher closed the shutter to stop the e-beam deposition. The durations were 2, 5, 7, 10, 15 and 20 minutes, respectively and they were randomly selected. The e-beam depositions were done at a rate within 0.6 – 1.2 *Angstrom/s*. After the completion of each period of e-

beam deposition, the next targeted silicon substrate was indexed into position above the shutter.

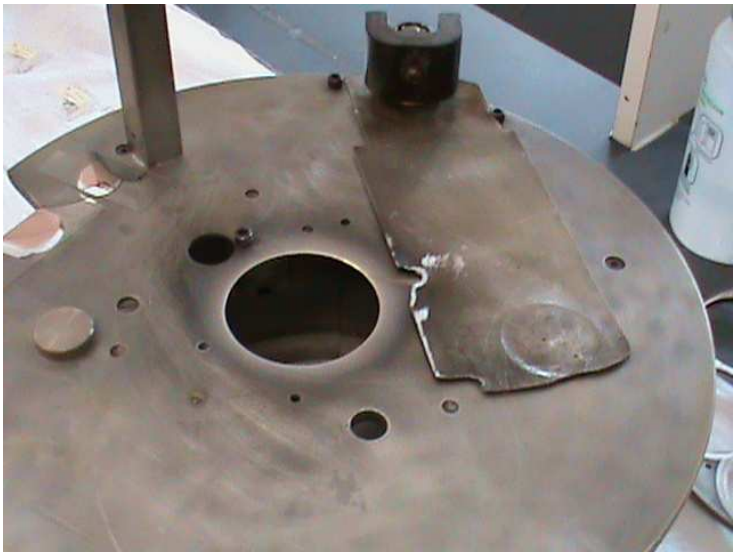

Figure 3-7 Shutter of the e-beam machine open (Courtesy: iThemba Labs).

Figure 3-8 Magnets for the opening and closing mechanism of the shutter (Courtesy: iThemba Labs)

The researcher repeated this process until all the substrates on the six sample holders were e-beam deposited. The top part of the e-beam was switched off and allowed to cool under vacuum conditions for two hours. The vacuum was then broken and the e-beam deposited samples shown in Figure 3-9 were retrieved.

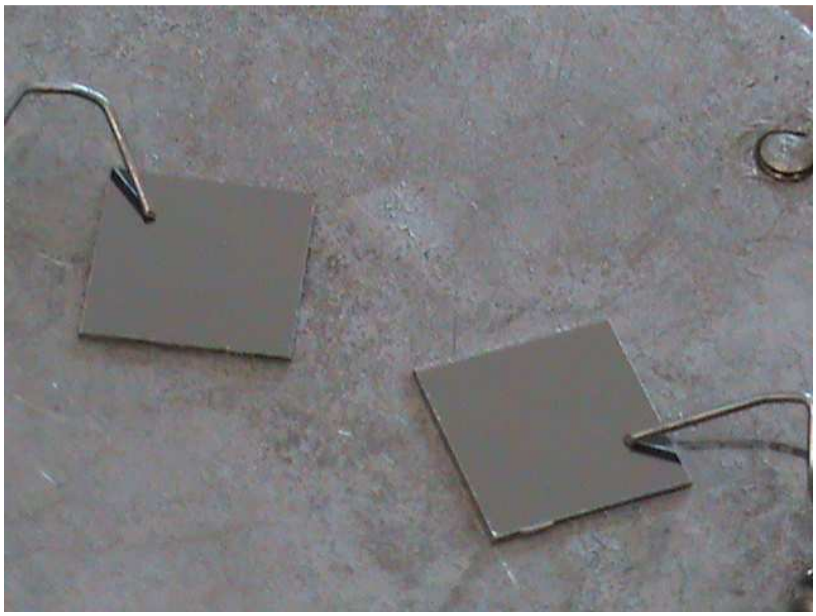

Figure 3-9 E-beam deposited samples (Courtesy: iThemba Labs)

The e-beam depositions were examined using the X-ray diffraction (XRD) machine shown in Figure 3-10 and found to be free of contaminants. The results are shown in Appendix H.

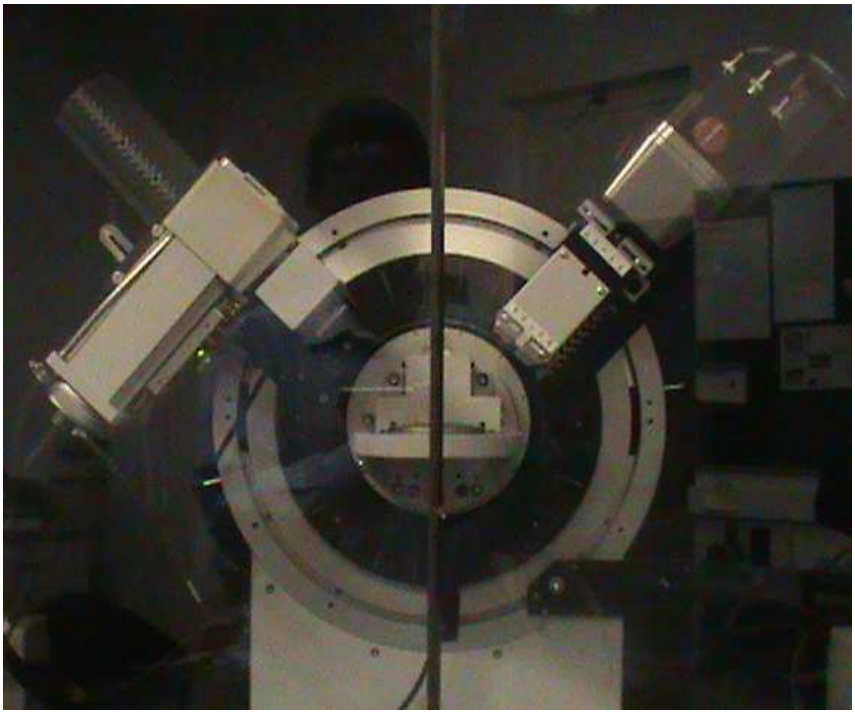

Figure 3-10 X-ray diffraction machine (Courtesy: iThemba Labs)

3.4 Surface Analysis of E-beam Depositions

The Veeco NanoMan V Atomic Force Microscope (AFM), shown in Figure 3-11, was used to examine the e-beam deposited samples. Dr. Mlungisi Nkosi (a specialist in the use of the

AFM) in the Material Research Department, iThemba Labs, Cape Town, assisted the researcher in measuring the surface roughnesses of the samples with the AFM. The specifications of the AFM cantilever used during the imaging are:

1. Material: 0.01 – 0.025 *Ohm-cm* Antimony (n) doped Si
2. Thickness: 2.5-3.5 μm; Length: 200 – 250 μm; Width: 23 – 33 μm; Resonance Frequency (f_o): 60 – 100 *kHz*; Spring Constant: 1-5 *N/m*
3. Coating: a) Front side: i) Top layer: 10-250 *nm* Co/Cr, and
   ii) Bottom layer: 1-10 *nm* Cr
   b) Back Side: ii) Top layer: 10-250 *nm* Co/Cr, and ii) Bottom layer: 1-10 *nm* Cr

The AFM obtains information about a surface when its tip interacts with a given surface. A laser beam is directed to the back side of the cantilever near the tip and reflected onto a photon detector. The laser beam will be reflected to different spots of the photon detector when the cantilever bends, thus the photon detector can monitor the motion of the cantilever over the scanned topography.

The samples' topography was scanned in the tapping mode (as opposed to the contact mode) to ensure a longer lifespan of the AFM probe. In tapping-mode, the cantilever keeps vibrating when the tip is scanning across the surface; the signal is measured at every point when the tip is touching to the surface. When the vibrating cantilever comes close to the surface, the amplitude and phase of the vibrating cantilever may change. Those changes in the vibration amplitude or phase are recorded because they are related to the changes in the profiles of the topographies being scanned. Low driving amplitudes were first set in order to prevent penetration into the sample and breaking of the tip.

The Nanoscope version 7.3 software was used to analyse the scanned surfaces so as to characterize them in terms of their 2D and 3D surface roughness. The Rumpf-Rabinovich method was employed to numerically model the intensity of the Van-der-Waals' forces exerted by the surfaces, based on the root-mean-square (*rms*) surface roughness values, using Equation 2.25. Since the contact term in the equation was a power function of *rms* values, the numerical modelling of Van-der-Waals' force in Section 4.3 was based on it (contact term) since it dominated a non-power function (which in this case was the non-contact term) as discussed in Section 2.6. For numerical modelling purposes, the separation distance, *H*, was taken as 1 nm since in such separation distances the Van-der-Waals forces are non-retarded.

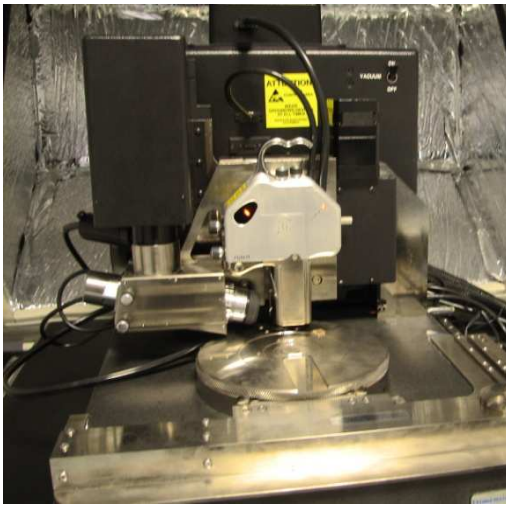

Figure 3-11 Veeco NanoMan V Atomic Force Microscope (Courtesy: iThemba Labs)

The researcher assisted by Mr. Ulrich Butner, a specialist in the use of the scanning microscope, in the Electronics Engineering Department, Stellenbosch University used the scanning electron microscope in Figure 3-12 to re-examine some samples previously examined by the AFM as a way of validating the findings. This machine produced 2D topography of the scanned surfaces.

Figure 3-12 Scanning Electron Microscope (Courtesy: Micro-electronics labs, Univ. of Stellenbosch)

3.5 Validation of Experiments on E-beam Deposited Materials

Another Atomic Force Microscope model, Asylum MFP 3 D- Bio with version 6.22A software was used to measure the actual Van-der-Waals' forces exerted by the e-beam

deposited samples. A research link created with Florida University' as a result of this study' afforded such an opportunity. Prof Y.I. Rabinovich, a specialist in measuring Van-der-Waals' forces, in the Particle Engineering Research Center, Florida University, USA, assisted in measuring the Van-der-Waals' forces exerted by the samples prepared by the researcher. The aim of the experimentation was to obtain practical evidence in validating the numerically modelled Van-der-Waals' forces (in Section 4.2) regarding their applicability in micro-material handling.

The experimental conditions were as follows:

- Temperature: 23^{o}C
- Atmospheric Pressure: 101.325 Pa
- Humidity level: 20% (which is low enough to eliminate surface tension or capillary forces)

To eliminate the effect of electrostatic force, the measurements were done inside a box coated by a grounding metal, referred to as a Faraday cage. This cage is insulated from interference of other forces which include magnetic, electromagnetic and forces due to vibrations. Low or no loading forces (about 1 nN) were applied to avoid plastic deformation and the development of a chemical bond between the probe and the specimen. The contact time of the probe and the sample was short, ranging from 3 – 10 seconds, to prevent the development of a chemical bond. Further experiments were also conducted at humidity levels of 40% (twice as much as that used earlier) in order to observe whether there was any effect of surface tension forces at a higher humidity levels to the measured Van-der-Waals' forces.

The experiments were conducted using the AFM cantilever with a silica sphere tip of 2.5 μm radius with an *rms* surface roughness value of 0.2 *nm*. Silica was used because it was relatively stable and had a relatively low Hamaker coefficient of 6.6 x 10^{-20}J which made it a suitable comparison base for the Van-der-Waals forces measured (Parsegian, 2006). If significant Van-der-Waals' forces' difference were to be observed on the e-beam generated surfaces or any other surface measured, then it indicated that Van-der-Waals' forces could be utilized in micro-material handling operations. (The experimental AFM measuring arrangement for the exerted Van-der-Waals' forces was as shown in Figure 3-13).

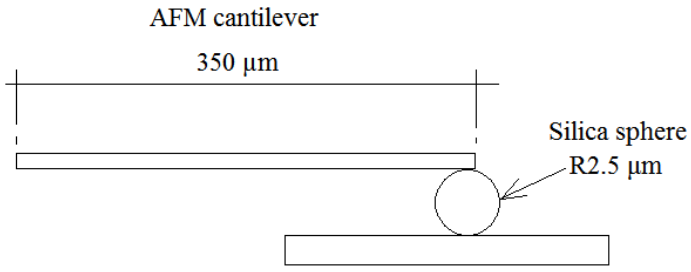

Figure 3-13 Arrangement of the AFM cantilever and e-beam specimen.

Experiments were conducted in two batches: batch number 1 and batch number 2. The first batch (batch number 1) consisted of three samples which were e-beam deposited during the second half of 2010 on the dates stated on the e-beam evaporation sheets contained in Appendix G. The three samples were Cu 5.1, Cu 20.1 and Ag 20.1 (where Cu refers to copper, Ag refers silver; the first digit refers to the e-beam deposition time, and the second digit to the batch number 1). These samples were chosen because the numerical modelling (in Section 4.2) had shown that Cu 20.1 exerted the lowest Van-der-Waals' forces because it had the highest *rms* surface roughness value, and Ag 20.1 exerted the highest Van-der-Waals' forces because it was the smoothest surface with the lowest *rms* value. Confirmation of this scenario was required through the actual measurement of the exerted Van-der-Waals' forces. Cu 5.1 was included in the sample because it had a median *rms* value and offered the opportunity to improve the comparison base.

The type of AFM cantilevers used to measure the Van-der-Waals' forces were Mikromasch NSC12/tipless/AIBS. These were of two types: one of a spring constant, k, (0.17 *N/m* and 350 µm in length) and the other of a spring constant, k, (0.27 *N/m* and 300 μm in length). Cantilevers with a spring constant, *k,* of 0.27 *N/m* were used for some copper specimens; and one with k = 0.17 *N/m* was used for silver, aluminium and some copper specimens because the former had run out of stock. The velocity of approach and retract of the silica sphere mounted on the tip of the AFM cantilever was 2 µm/s. The experimentally obtained interactive Hamaker coefficient of silica with either copper or aluminum was 7.7 x 10^{-20}J, and silica with silver was 1.5 x $10^{-19}J$. These values were used in the numerical modelling of the Van-der-Waals' forces.

In the second batch of experiments, six metallic samples and two polyurethane samples were examined. These were e-beam deposited during the second half of 2011 on the dates stated in Appendix G. These comprised of two specimens of copper (Cu 5.2 and Cu 20.2), two samples

of silver (Ag 5.2 and Ag 20.2) and two samples of aluminium (Al 5.2 and Al 20.2); where the first digit refers to the duration of the e-beam deposition time and the second refers to the batch number of 2. Cu 5.2 and Cu 20.2 and Ag 20.2 were included in the batch in order to determine any inconsistency from the first batch. Al 5.2 and Al 20.2 samples were included as a result of the numerical modelling of Van-der-Waals' forces in Section 4.3 proving aluminium to be suitable for the micro-gripper material since it had median forces when compared to the other two. The other reason was to maintain the 5 minute and 20 minute e-beam deposition comparison base. Ag 5.2 was also included to enhance this comparison base. Polyurethane samples of shore hardness 30A (polyurethane 30) and the other of shore hardness 60A (polyurethane 60) were included since they exerted large amounts of Van-der-Waals' forces, as stated in Section 2.6.

Extending (approaching) curves were plotted to identify whether Van-der-Waals' forces were the only forces acting on a given sample by comparing the experimental curves to numerically modelled curves. Extending curves are obtained when the AFM spherical silica probe is gradually brought closer to the specimen until it "jumps" into contact with it.

Retracting curves were plotted, depicting the amount of Van-der-Waals' forces which are exerted between surfaces in contact. These graphs are obtained when the AFM spherical silica probe is gradually pulled away from the specimen until it is detached. At least ten Van-der-Waals' forces' measurements were taken per given sample. Their statistical distributions are shown in Appendix J, and Section 4.3 summarises the findings. Extending curves allow for the identification of the active forces on interacting surfaces. They reveal the "jump-in points" which indicated the possible type of forces which may be active in a given scenario. Retracting curves reveal the amount of detachment (adhesion) force, be they Van-der-Waals', electrostatic or any other force. Comparisons between theoretical and experimental curves were conducted leading to a detailed analysis.

3.6 Experiments on Polyurethane Material

With reference to Section 2.6.3, polyurethane materials were found to exert large amounts of Van-der-Waals' forces. Therefore; the researcher experimented on their applicability in micro-material handling. Two types of polyurethane, that is; polyurethane 30 (polyurethane with a shore hardness of 30 A, trade name – VytaFlex 30) and polyurethane 60 (polyurethane with a shore hardness of 60A, trade name – VytaFlex 60) were experimented with by the

researcher. These materials were supplied by AMT Composites – Smooth-On Company in Cape Town. It should be noted that the softer the material, the greater the contact area, since a soft material elastically deforms into the surface profile of a given interactive surface. This leads to the exertion of more Van-der-Waals' forces by a softer material than a harder one. Therefore; these two offer a sound comparison base to validate the given notion since one has a hardness value half the magnitude of the other. The manufacturer's codes of the used polyurethane 30 were: Code - Sm169, SO# - 66670B, LOT# - 1010377; the codes of polyurethane 60 were: Code - Sm154, SO# - 61870B, LOT#1011085. Their mechanical properties and manufacturer's specifications are shown in Appendix I. Each component had two parts, A and B, (liquid ingredients) which were later mixed by the researcher in equal parts as per the manufacturer's formula. Thorough mixing took place for at least 3 minutes. The mix was poured into moulds by the researcher and subsequently cured under atmospheric conditions in order to produce flat micro-grippers, as shown in Figure 3-14. Added to that, 1 mm radii spherical grippers were produced by dipping metallic needles into a polyurethane mix and then suspended in the air in order to dry under atmospheric conditions.

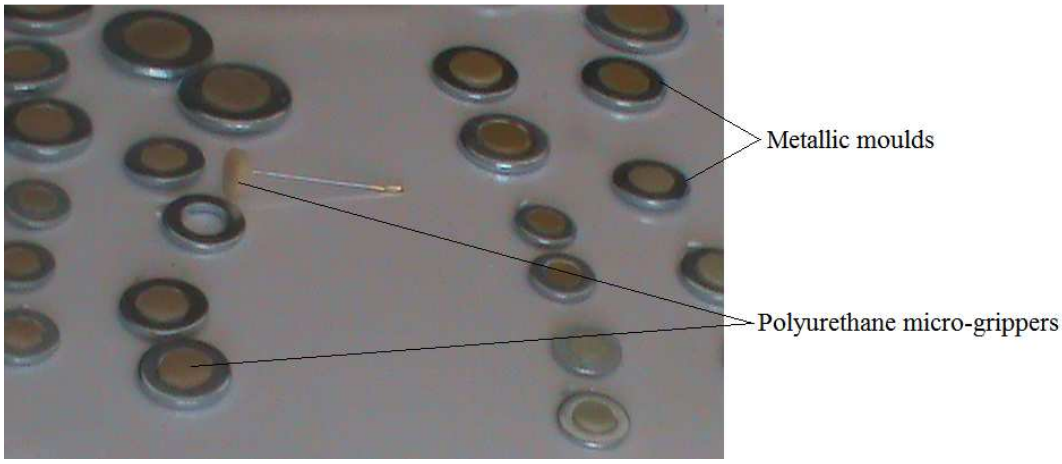

Figure 3-14 Diagram of moulds for circular polyurethane grippers, with one gripper removed from the mould in the first left row

With regard to the measurement of the exerted Van-der-Waals' forces, the haptic-force-feedback system (a system which measures contact force) incorporated in the motoman's end effector, was used by the researcher in the SENROB laboratory at Stellenbosch University. The haptic-force-feedback system used was the Gamma F/T Mux transducer supplied by ATI Industrial Automation. The experimental arrangement is shown in Figure 3.15. The polyurethane gripper was lowered until contact was reached and a preload was applied after contact. The polyurethane micro-gripper was then slowly detached while the haptic feedback

system recorded the corresponding Van-der-Waals' adhesive forces. The approaching and retraction speed of the polyurethane micro-grippers was 0.1mm/s for all the measurements taken. This was the lowest speed achievable with the Motoman SDA 10 robot. This lowest speed was used so as to avoid shock loads on the polyurethane gripper. The anti-static mat and its accessories were used to discharge the equipment of any electrostatic forces.

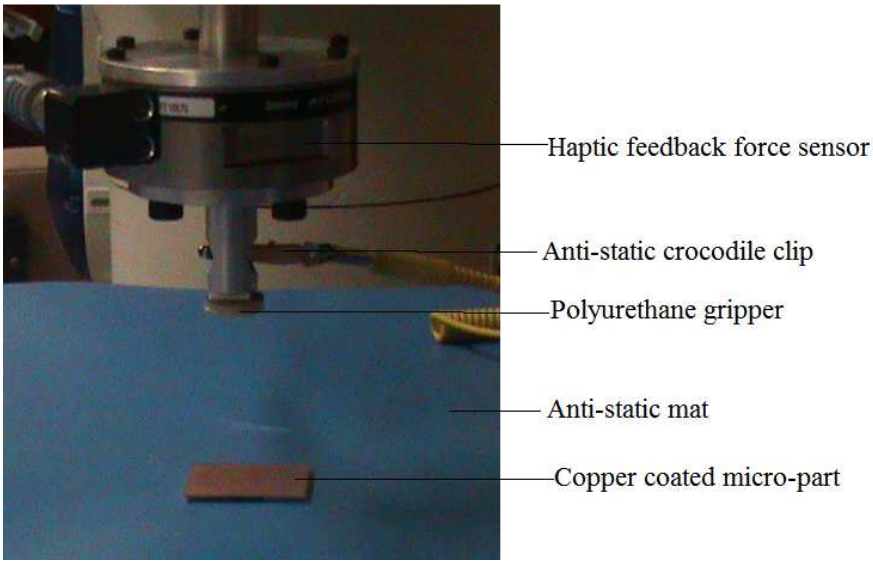

Figure 3-15 Experimental arrangement for measuring the Van-der-Waals' forces exerted by a polyurethane micro-gripper on a copper coated micro-part

Preloads between 0.05N and 0.25N were applied on 8-mm radius polyurethane grippers and the corresponding adhesive Van-der-Waals' forces were measured. It was found that beyond a pre-load of 0.20 N, there were no significant changes in the Van-der-Waals' forces exerted on a given specimen. Therefore; preloads of 0.20 N were used for the comparison of 8-mm radii micro-grippers of polyurethane 30 and polyurethane 60 (similar to what Murphy et al (2011) and Murphy et al (2007) did in their Van-der-Waal's force actuated wall climbing robots which used polyurethane material; and also similar to what Aksak et al (2007) did in testing the Van-der-Waals' forces exerted by their polyurethane material). The accuracy of the haptic feedback system was of the order of 0.01N, such that the Van-der-Waals' force of other smaller radii grippers (R6, 5, 3, 2, 1.5 mm) could not be measured as the forces were too small to be detected by the given system.

The measurements of Van-der-Waals' forces were analysed to identify the type of interactive surfaces appropriate for the picking position, placement position and micro-gripper in a reliable micro-material handling operation. These experiments were conducted in controlled

environments which discharge the equipment of electrostatic force. Attempts were made to pick and place micro-materials, which included integrated circuit (IC) components and e-beam deposited micro-parts.

This methodology was applied in this research and the findings were detailed and analysed as set out in the following chapter.

4 CHAPTER 4: NUMERICAL MODELLING, EXPERIMENTAL RESULTS, ANALYSIS AND EVALUATION

This chapter presents the findings on the Van-der-Waals' forces exerted by the metallic e-beam deposited coatings and polyurethane samples. It carries the *rms* surface roughness values of the metallic and polyurethane samples. It further presents the numerical models of the corresponding Van-der-Waals' forces exerted by these samples. Furthermore, it presents the experimental results of the measured Van-der-Waals' forces exerted by these samples. Finally this chapter presents the analysis and evaluation of the experimentally measured Van-der-Waals' forces as to their applicability in micro-material handling operations.

4.1 Surface Roughness Characterisation

The AFM micrographs and scanning electron micrographs of the silicon substrate; and e-beam depositions of copper, aluminium and silver are shown as from Figure 4-1 to Figure 4-15. Appendix J also carries some micrographs of other samples not contained in this section. The Nanoscope Version 7.3 software was used to produce both the micrographs and the *rms* surface roughness values of the generated surfaces. It is evident that the topographies vary in their profiles, hence their *rms* values vary. Table 4.1 summarises the characterization of the e-beam depositions carried in the figures contained in this section. The properties include *rms* surface roughness values, layer thicknesses of the e-beam coatings and the duration of the depositions.

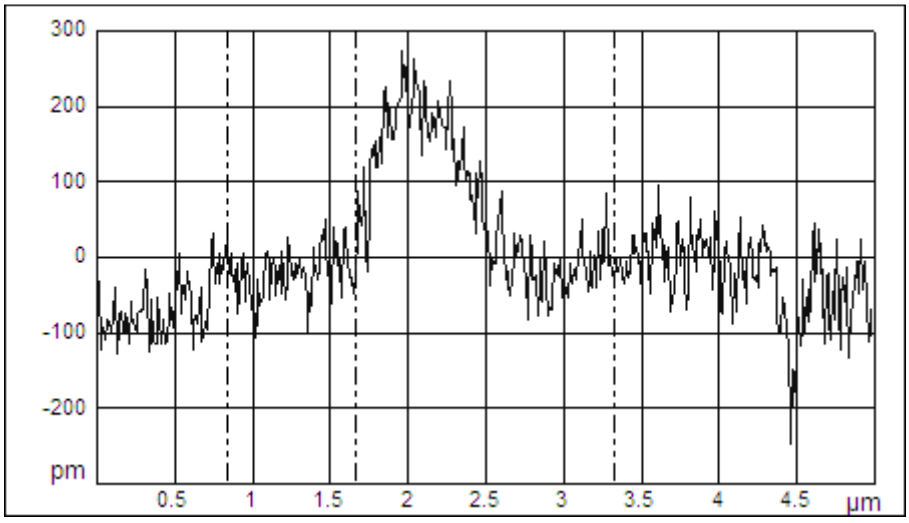

Figure 4-1 Surface roughness profile of silicon substrate

Figure 4-1 shows the surface roughness of a silicon substrate upon which e-beam depositions of different materials were made. It should be noted that the surface roughness scale is in pico-meters (pm = 10^{-12}m) and the highest surface peak is below 300 pm (0.3 nm).

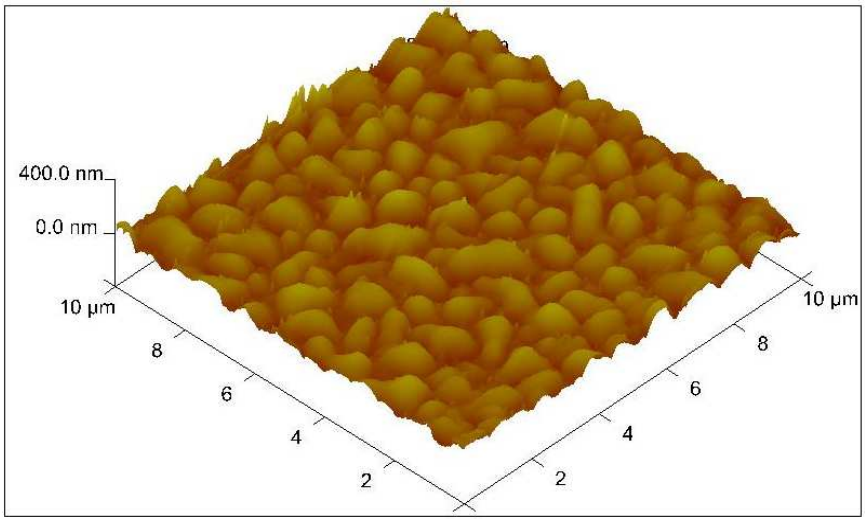

Figure 4-2 Atomic Force Micrograph of copper deposited for 7 min

Figure 4-2 shows the 3D topography of a copper sample, e-beam deposited for 7 min. However; the 3D scan of aluminium, deposited for 7 min, was not clear. Therefore; its surface roughness was shown as a line graph, revealing a peak of 300 nm, as indicated in Figure 4-3.

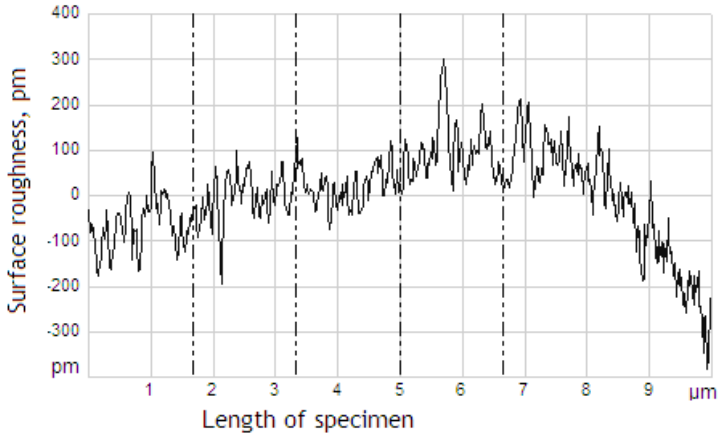

Figure 4-3 Atomic Force Micrograph of aluminium, deposited for 7 min

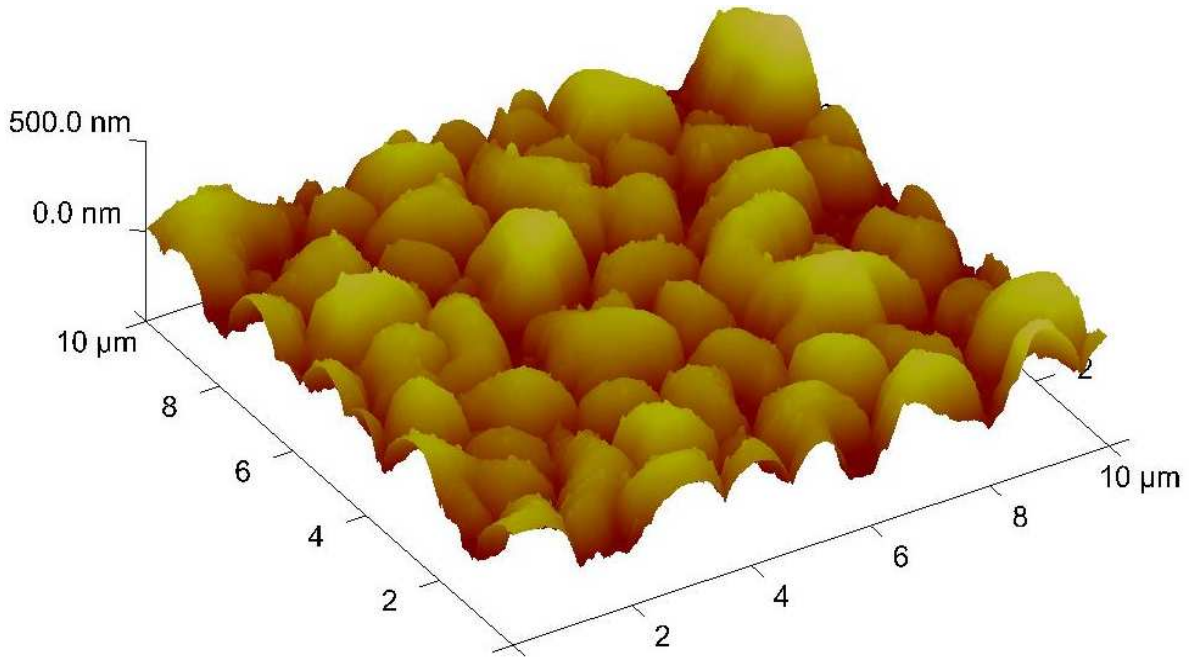

Figure 4-4 Atomic Force Micrograph of copper deposited for 10 min

The 3D Atomic Force Micrograph of copper (e-beam deposited for 10 minutes) reveals well-defined peaks (Figure 4-4) bigger than those of aluminium (Figure 4-5). These big peaks result in copper having the highest *rms* surface roughness value of the three metals, as shown in Table 4.1. As a validation process, the same samples were scanned by an electron microscope. Figure 4-6, and Figure 4-7 of aluminium and copper respectively, were obtained, which revealed the same surface structures.

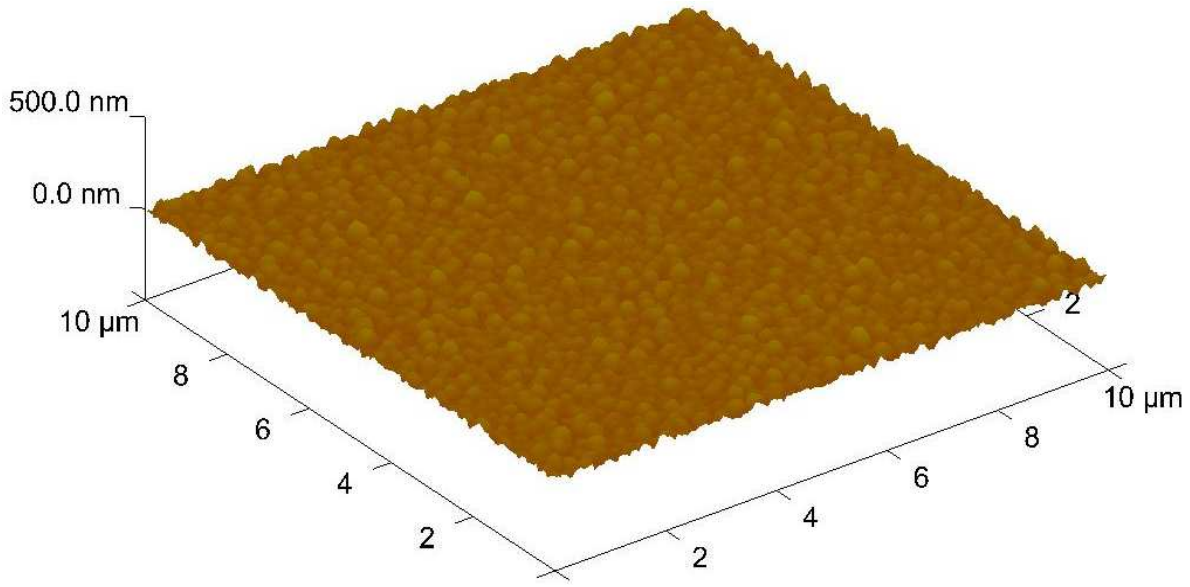

Figure 4-5 Atomic Force Micrograph of aluminium deposited for 10 min

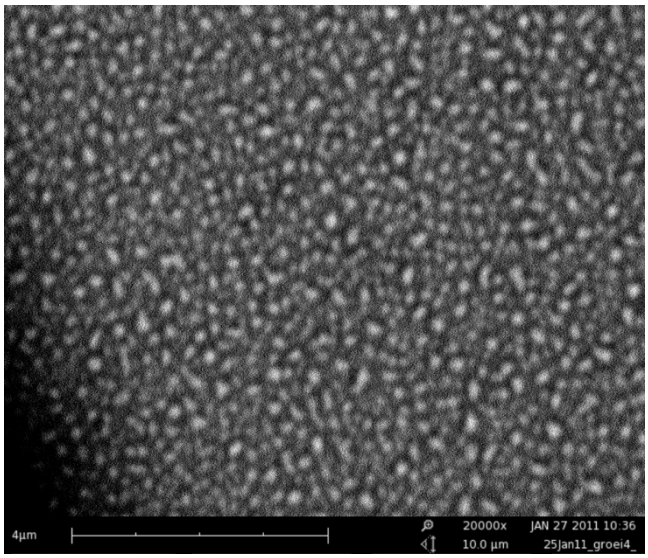

Figure 4-6 Scanning Electron Micrograph for aluminium deposited for 10 min (Courtesy: Electronics laboratory, University of Stellenbosch)

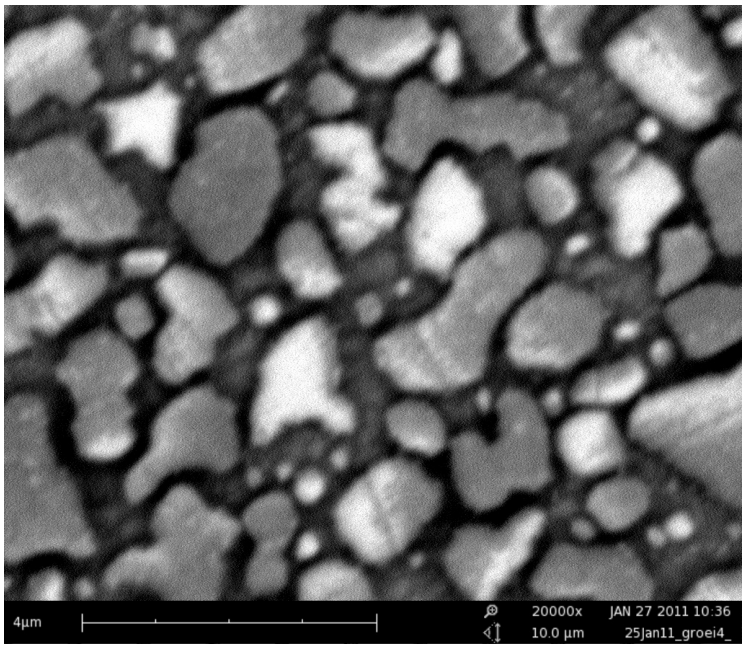

Figure 4-7 Scanning Electron Micrograph for copper deposited for 10 min (Courtesy: Electronics laboratory, University of Stellenbosch)

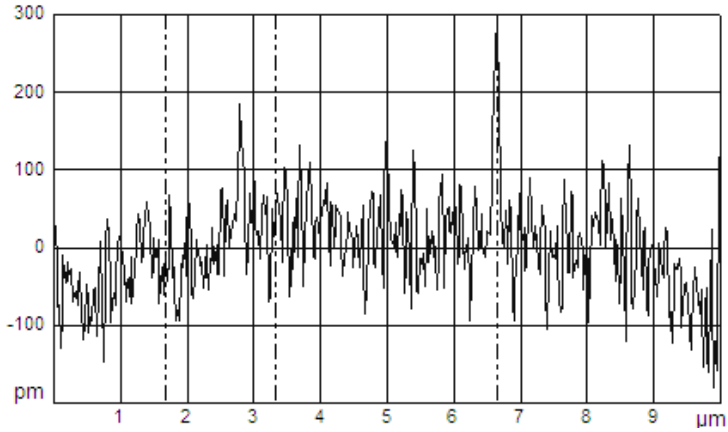

Figure 4-8 Atomic Force Micrograph of silver deposited for 15 min

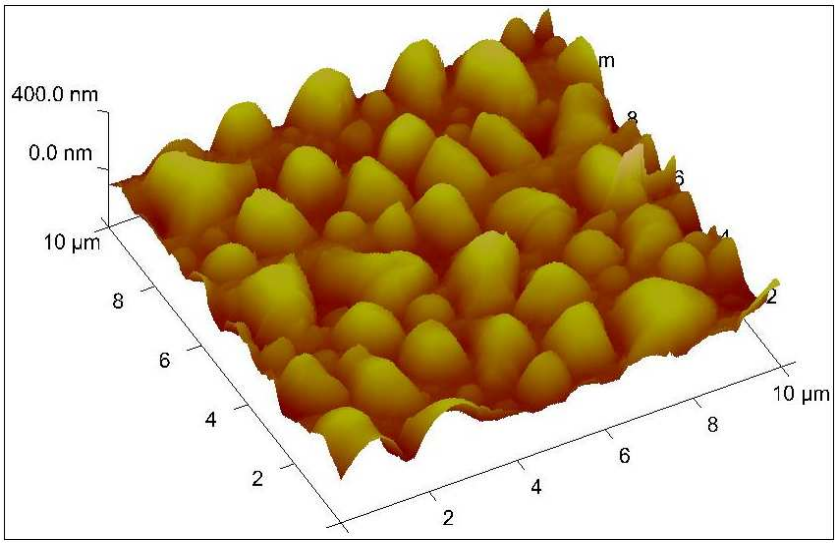

Figure 4-9 Atomic Force Micrograph of copper deposited for 15 min

Another 3D micrograph of 15-minute e-beam deposited copper is shown in Figure 4-9 and its 2D profile is shown in Figure 4-10. It has the biggest peaks when compared to silver (Figure 4-8) and aluminium (with its 3D micrograph in Figure 4.11 and its 2D in Figure 4.12).

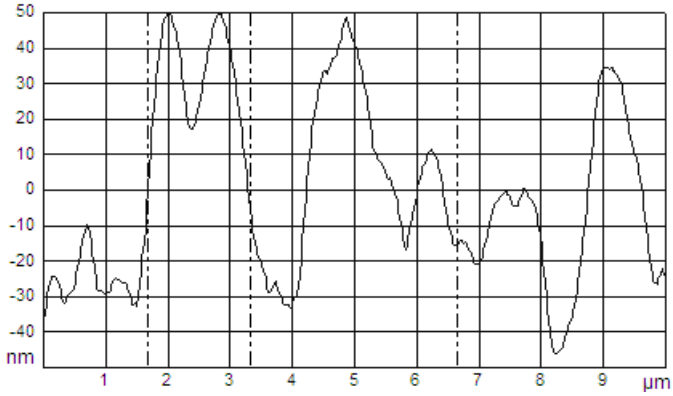

Figure 4-10 Atomic Force Micrograph of copper deposited for 15 min

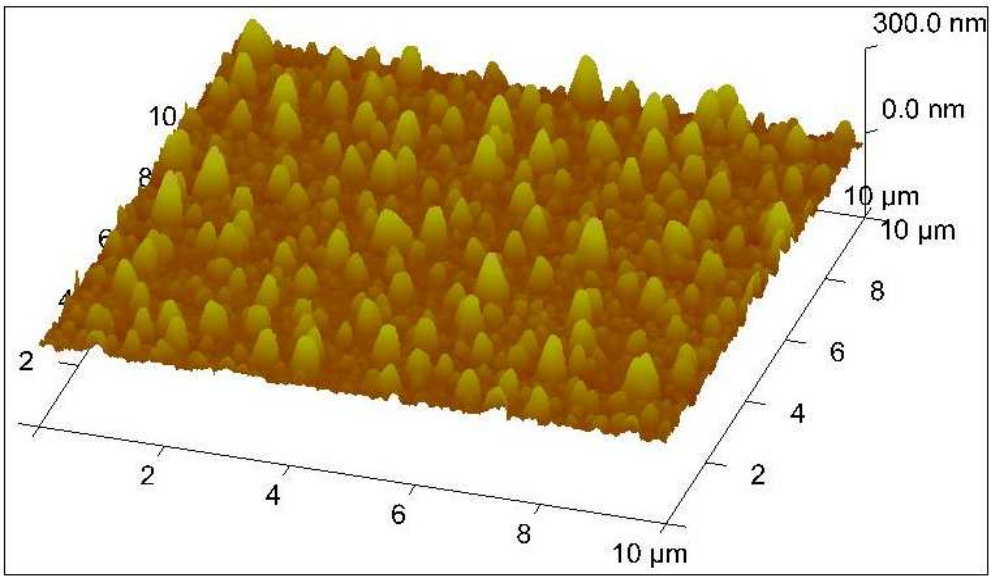

Figure 4-11 Atomic Force Micrograph of aluminium deposited for 15 min

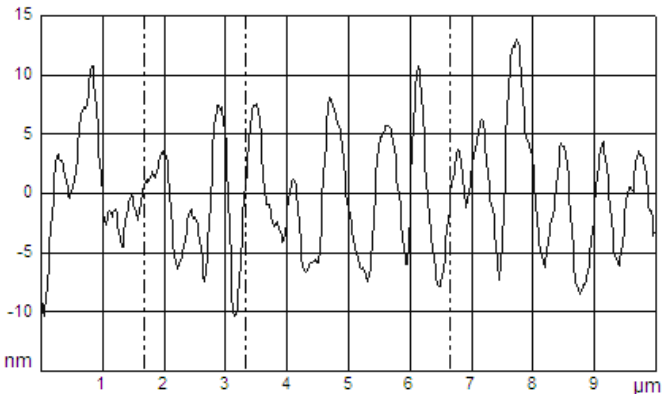

Figure 4-12 Atomic Force Micrograph of aluminium deposited for 15 min

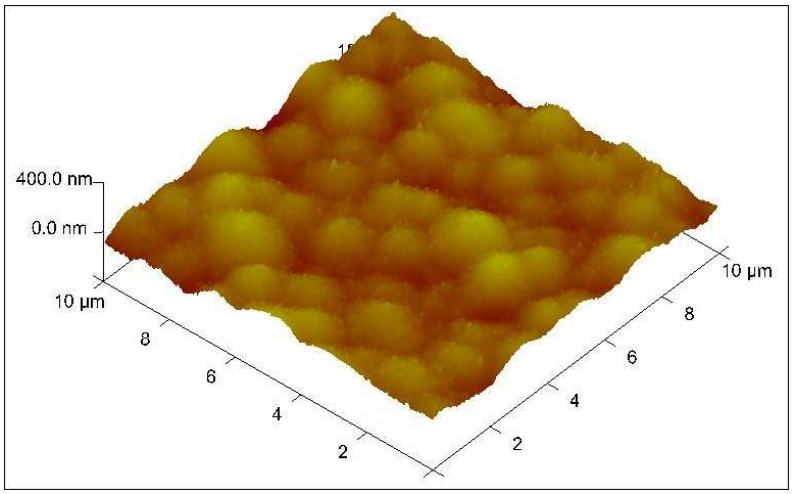

Figure 4-13 Atomic Force Micrograph of copper deposited for 20 min

The Atomic Force Micrograph of copper, deposited for 20 minutes, is shown in Figure 4-13. It has the largest peaks, compared to those of aluminium (Figure 4-14) and silver (Figure 4-15), proving that it has the highest *rms* surface roughness value as indicated in Table 4.1.

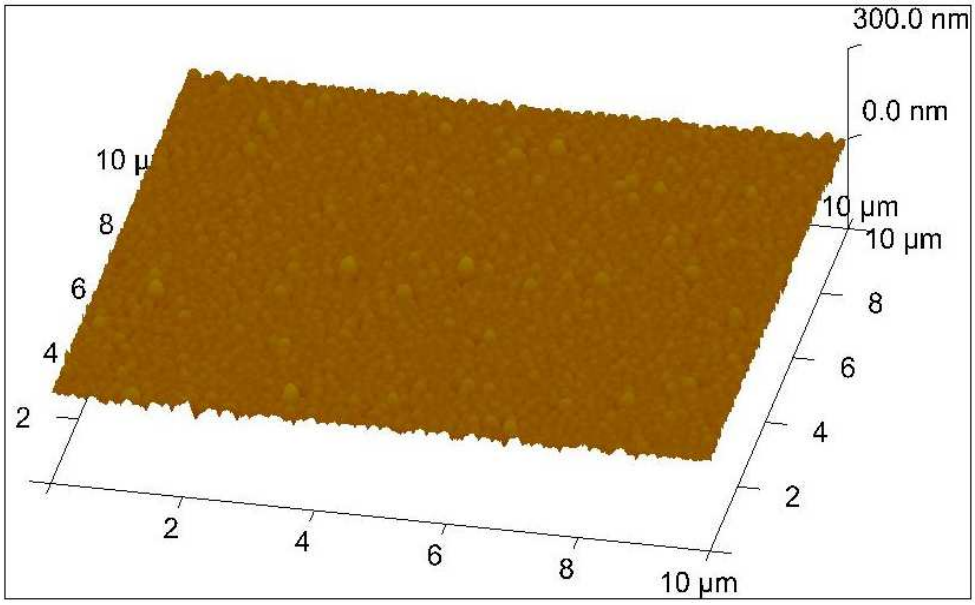

Figure 4-14 Atomic Force Micrograph of aluminium deposited for 20 min

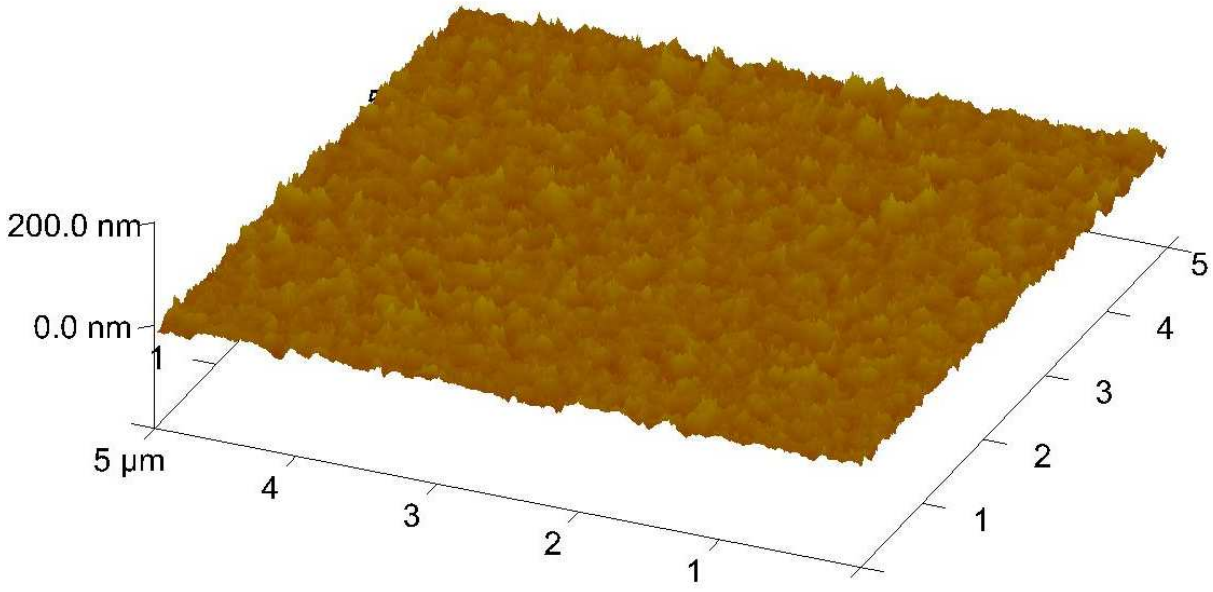

Figure 4-15 Atomic Force Micrograph of silver deposited for 20 min.

The thickness of the layers in Table 4.1 is given in nanometers (nm) and the surface roughness of the generated topographies is shown by *rms* values in nanometers (nm).

Table 4.1 E-beam deposition times, layer thickness and *rms* values

Duration of deposition, *minutes*	Thickness of deposition, *nm*			Surface roughness, *rms* value in *nm*		
	Silver, Ag	Copper, Cu	Aluminium, Al	Silver, Ag	Copper, Cu	Aluminium, Al
2	10.2	13.2	6.0	1.050	2.400	3.310
5	18.6	37.8	6.6	0.684	2.720	1.710
7	42.0	51.0	15.0	0.832	38.300	0.591
10	60.0	65.4	60.0	0.932	51.800	17.500
15	85.8	84.0	62.4	1.010	75.800	28.900
20	117.0	98.4	65.4	1.410	217.000	8.590

The silicon substrate used for e-beam deposits had an *rms* surface roughness value of 0.431 nm.

The chemical and physical properties of the copper, aluminium and silver properties are detailed in Appendix F. The purity of the e-beam deposits was analysed by an X-ray diffraction (XRD) machine and no impurities were detected, as indicated by the XRD graphs in Appendix H. Only the silicon substrate and the e-beam deposited materials were detected in the analysis.

4.2 Theoretical (Numerical Modelling) of Van-der-Waals' Forces with respect to the Measured Surface Roughness: Calculated Van-der-Waals' Forces based on the Rumpf-Rabinovich's Equation.

As a further analysis, all figures from Figure 4.16 to Figure 4-24, numerically model Van-der-Waals' forces, with respect to the measured surface roughness of the e-beam coatings of copper, aluminium and silver. The numerical modelling is performed with respect to the e-beam deposition's durations of 2 min, 5 min, 7 min, 10 min, 15 min and 20 min, chronologically and with reference to the contents of Table 4.1, except for Figure 4-24. The Hamaker coefficients are taken as 500 zJ, 400zJ and 145 zJ for silver, copper and aluminium

respectively, as in Appendix E. A value of 145zJ is used for aluminium as it readily oxidises under atmospheric conditions. The radius of the micro-part interacting with the e-beam generated flat surfaces was taken as 6000 nm in order to shift the Van-der-Waals' forces' graphs into the positive axes for better comparison's sake. The Rumpf-Rabinovich Equation 2.25 was used to numerically model the Van-der-Waals' forces with respect to the measured *rms* surface roughness values. However, the contact term was used only to determine the Van-der-Waals' forces' intensity as discussed earlier in Section 2.6.5 and Section 3.4.

4.2.1 Aluminium and copper

Figure 4-16 shows a comparison of the *rms* surface roughness values for copper and aluminium with reference to Table 4.1. The logarithmic plot of surface roughness and deposition time is indicated. In Figure 4.16, copper has a higher surface roughness value than aluminum. Figure 4-17 includes the corresponding numerical modelling of the Van-der-Waals' forces.

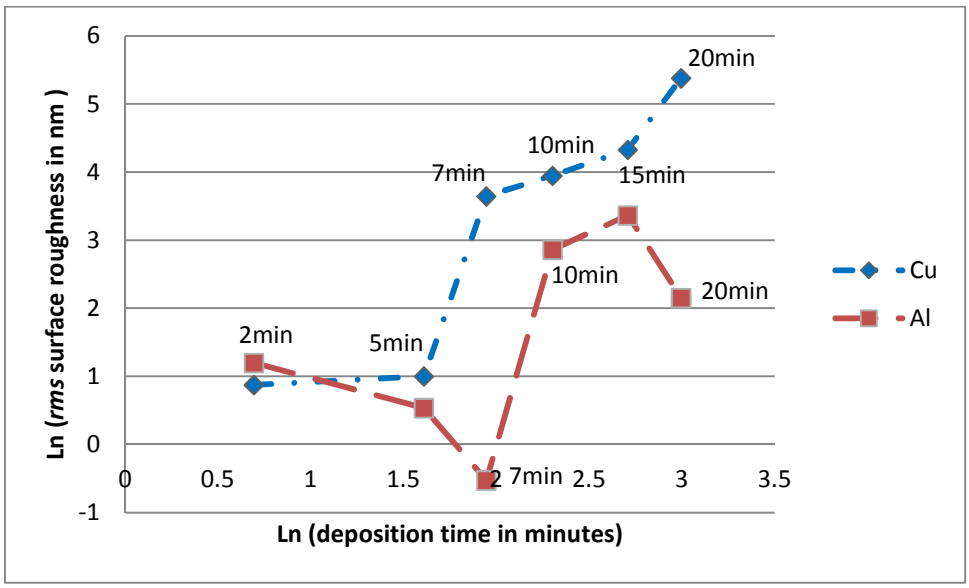

Figure 4-16 Copper's and aluminum's surface roughnesses against deposition time

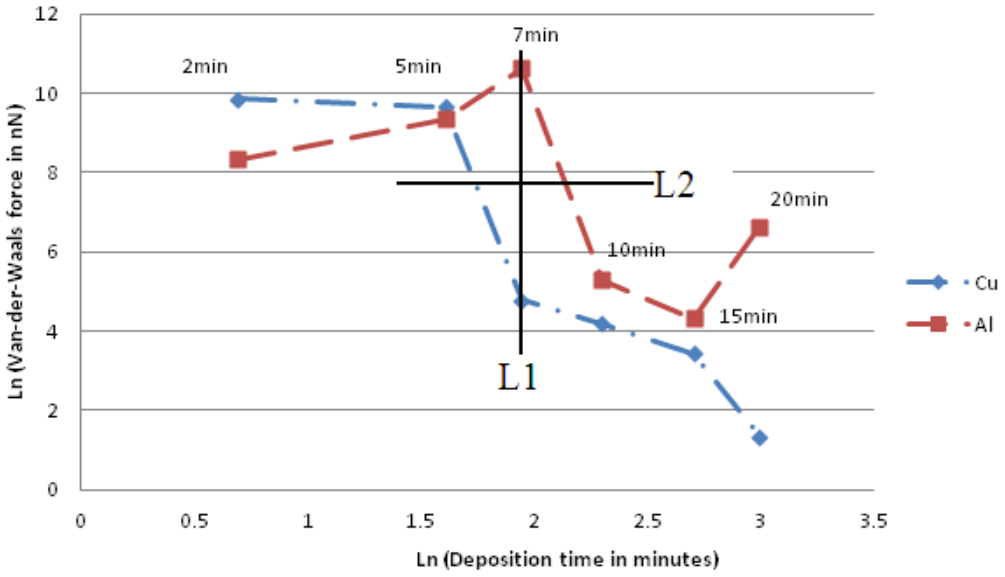

Figure 4-17 Copper's and aluminum's Van-der-Waals forces' intensity against deposition time

An analysis of Figure 4.17 reveals that (in the case of copper) the Van-der-Waals' forces' intensity decreases with an increase in deposition time, since the *rms* values increase. On the other hand, the Van-der-Waals' forces for aluminium (Al) increase during the 2 to 7 minutes' deposition times, and then decrease. In the 10 to 15 minutes' deposition range, there is no significant margin or difference between the Cu and the Al graphs. The 20-minute deposition time shows a widening gap between the two graphs, but the Van-der-Waals' forces are not as significantly different to the 7-minute deposition time. Therefore; our optimal region lies between the 5-minute and 10-minute deposition times.

Further analysis shows that the optimum field lies along line L1 which joins the 7-minute points on both graphs. Consequently, two extremes are identified in which copper (38.3 nm *rms* surface roughness) would be suitable for the pick-up position, and aluminium (17.5 nm *rms)* for the placement position, in a micro-material handling system. In this scenario, an appropriate optimum micro-gripper should have Van-der-Waals' force intensity lying between the two extremes. In Figure 4.17, the Van-der-Waals' forces' intensity of a logarithmic value of 7.71 is found to be the average value of the two extremes where the graphs intersect with L1. Line L2 is drawn perpendicular to L1, passing through the 7.71 value. Through linear interpolation, line L2 intersects the Cu graph at points 1.74; 7.71 and the Al graph at points 2.14 and 7.71. Since the graphs are natural logarithmic plots, it follows that the first point on the Cu graph corresponds to a deposition time of 5.75 minutes and the

second point on the Al graph to a time of 8.82 minutes. Therefore; the micro-gripper can either be copper which has been e-beam deposited for 5.75 minutes or aluminium deposited for 8.82 minutes. Corresponding *rms* values are 8.2 nm for copper and 5.3 nm for aluminium, assuming a linear relationship. However; this assumption may not always be accurate. Incorporation of a third material type may improve the effectiveness of the Van-der-Waals' force actuated micro-material handling operation, as shown in Section 4.2.4.

4.2.2 Aluminum and Silver

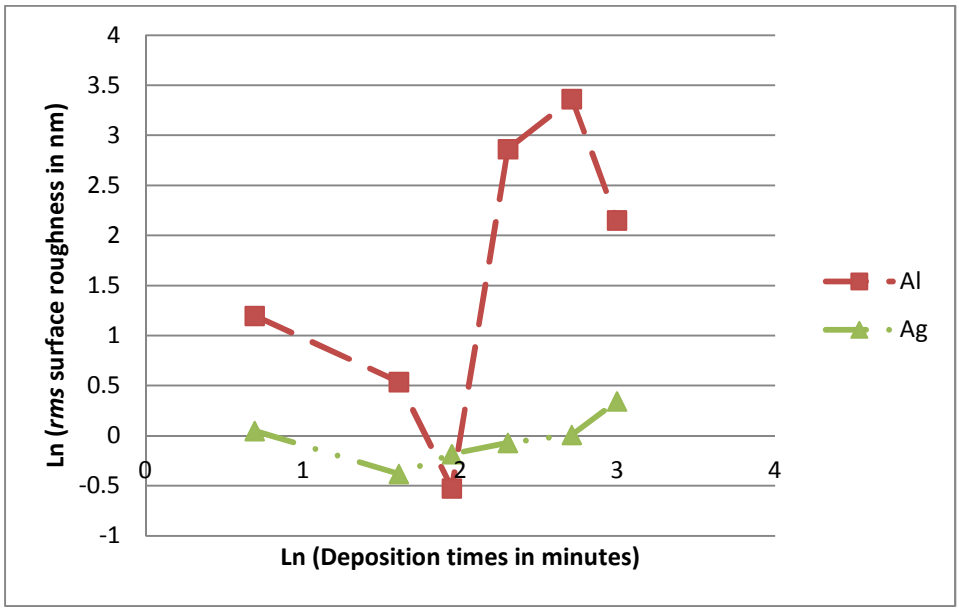

Figure 4-18 Aluminum's and silver's surface roughnesses against deposition time

With reference to Table 4.1, aluminium's (Al) e-beam profiles are generally rougher than the silver's (Ag), and a corresponding logarithmic plot of *rms* surface roughness values against deposition time in Figure 4.18 clearly illustrates this. This means that the silver would exert more Van-der-Waals' forces than aluminum as depicted in Figure 4.19. In a micro-material handling operation, aluminium would be suited to the picking position and silver to the placement position. In this scenario, a 5-minute e-beam deposited aluminium interactive surface would be suitable for the micro-gripper since it is has a medium Van-der-Waals forces' intensity.

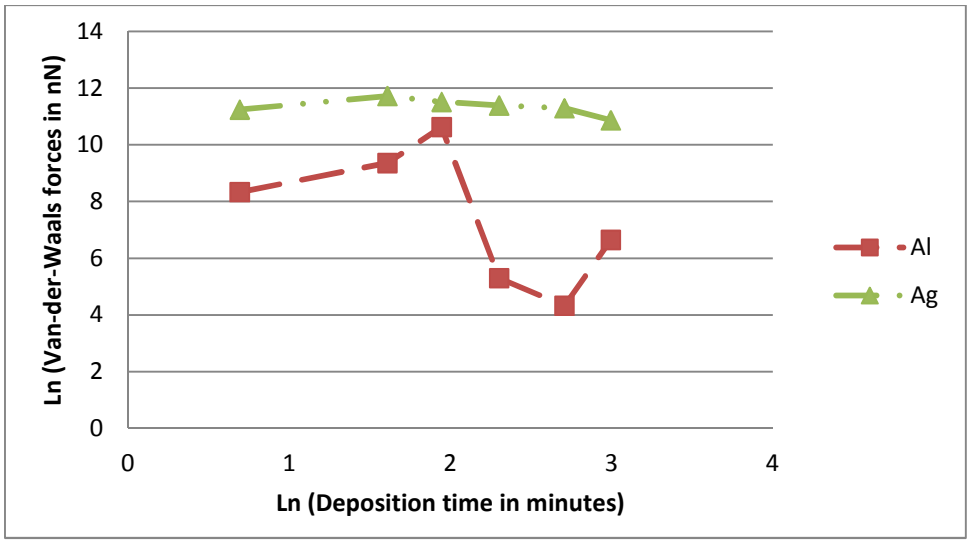

Figure 4-19 Silver (Ag)'s and aluminum (Al)'s Van-der-Waals forces' intensities against deposition time

4.2.3 Copper and silver

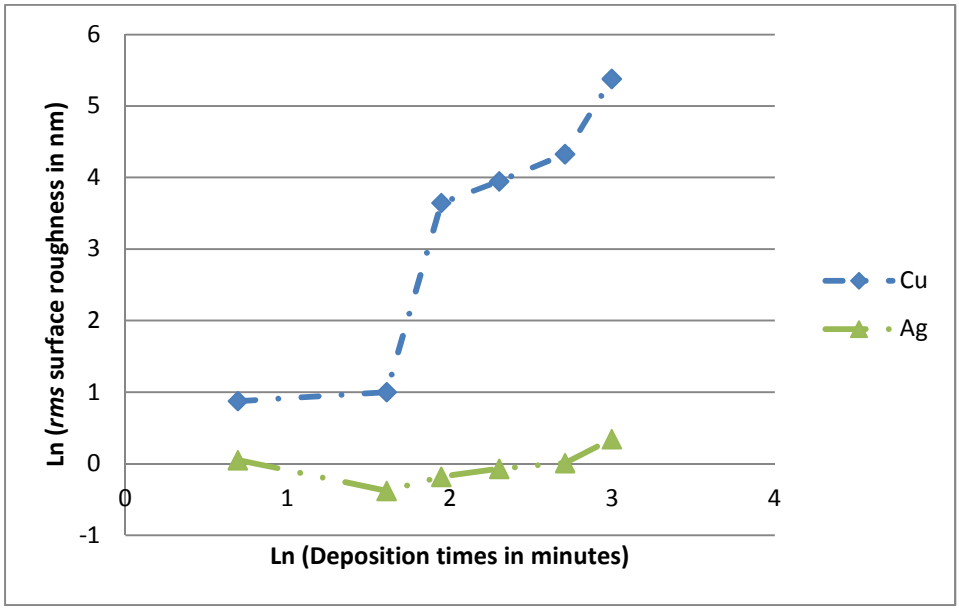

Figure 4-20 Copper's and silver's surface roughnesses against deposition time

A logarithmic plot of the *rms* surface roughness values of copper and silver contained in Table 4.1 is depicted in Figure 4.20. It shows that copper deposits are rougher than silver deposits. Therefore; silver exerts greater Van-der-Waals' forces as numerically modelled in Figure 4.21. In the event that these copper and silver samples are the only ones available for a micro-material handling operation, copper would be suitable for the picking position and silver for the placement position. A 5-minute deposited sample of copper would be suitable

for the gripper's interactive surface since it has a medium Van-der-Waals forces' intensity, as numerically modelled in Figure 4.21.

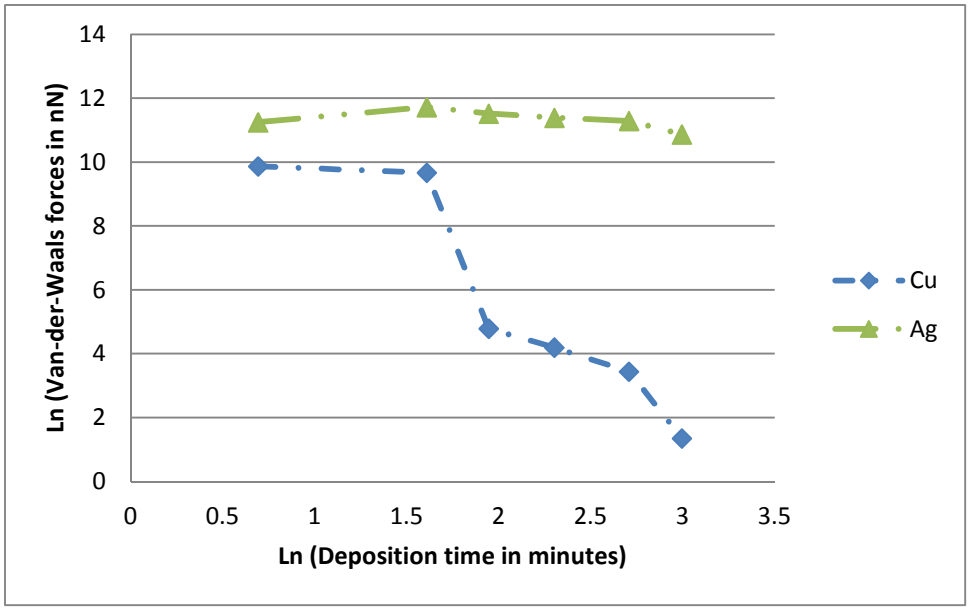

Figure 4-21 Silver (Ag)'s and copper (Cu)'s Van-der-Waals forces' intensities against deposition time

4.2.4 Aluminum, Copper and Silver Numerical Modelling.

Figure 4-22 shows the logarithmic plot of the *rms* surface roughness values of copper, aluminium and silver against e-beam deposition times with reference to the contents in Table 4.1. The *rms* values generally increase with an increase in the e-beam deposition times. Copper's *rms* values are the highest of the three sets, with the exception of the 2-minute deposition. Silver, generally, has the lowest *rms* values and aluminium has moderate values.

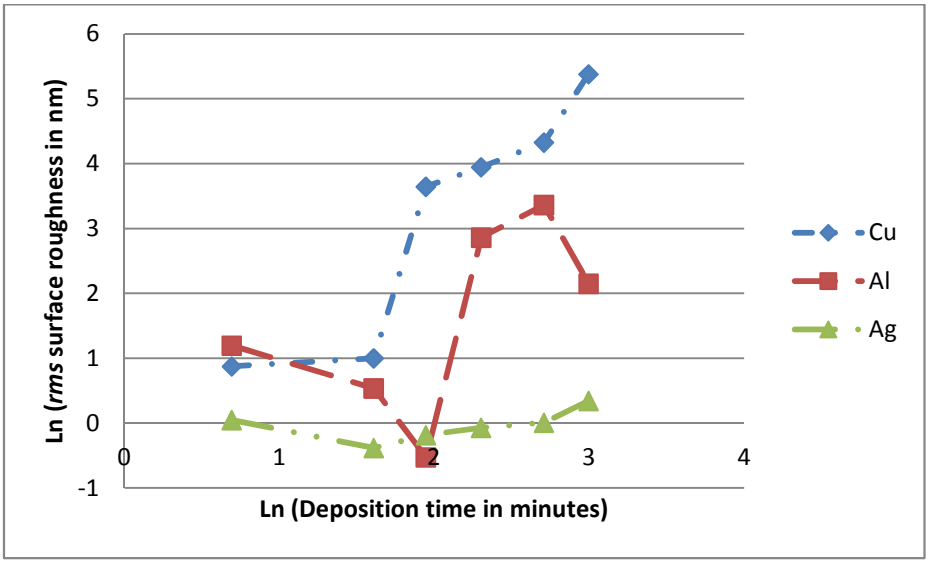

Figure 4-22 Copper's, aluminum's and silver's surface roughnesses against deposition time

Figure 4.23 shows the corresponding numerical modelling of the Van-der-Waals forces' intensity for the three samples.

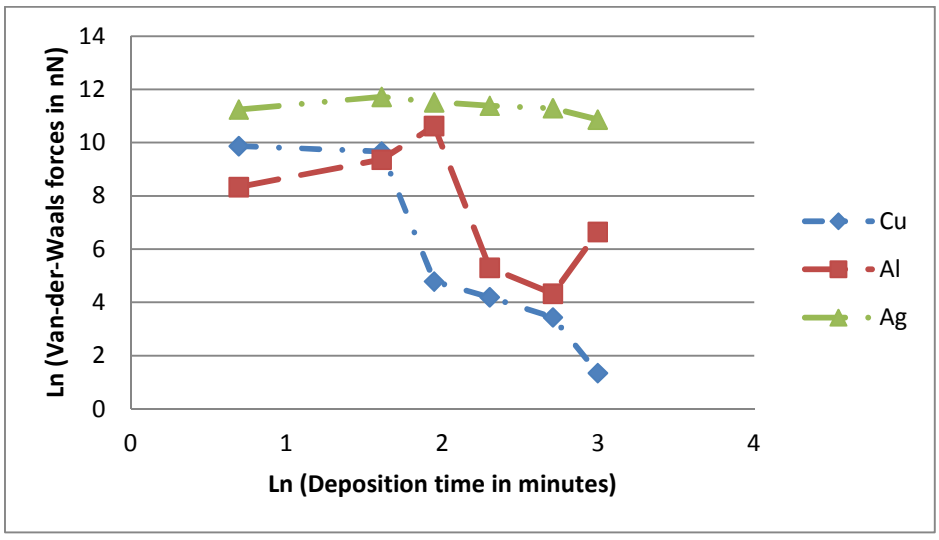

Figure 4-23 Copper's, aluminum's and silver's Van-der-Waals forces' intensities against deposition time

An analysis of Figure 4.23 reveals a significant optimal region lying between the 5-min and 20-min deposition times. This range excludes of the 5 minute deposition time, but includes the 20 minute deposition time. In this range, silver exerts the highest Van der Waals' forces, followed by aluminium with copper being the lowest. Silver would then be suitable for the placement position, aluminium for the gripper and copper for the pick-up position.

Figure 4-24 illustrates the numerical modelling of Van-der-Waal's forces with respect to *rms* surface roughness values, using the Rumpf-Rabinovich Equation 2.25. Basing on the modelling, silver exerts the largest forces as indicated by its force distribution which is concentrated on the top left hand side of the graph due to it having the lowest *rms* values. Since Figure 4-24 is a logarithmic graph, the silver's Van-der-Waals' forces' intensity's centroid is 11.1. Aluminium exerts a medium force since its force distribution is concentrated in the middle of the graph. The aluminium's Van-der-Waals' forces' intensity's centroid is 7.5. Copper exerts the least since its force distribution is concentrated in the lower right hand side of the graph because of the fact that its topography has the largest *rms* surface roughness values. The copper's Van-der-Waals' forces' intensity's centroid is 5.6. Figure 4-24 also gives evidence that *rms* surface roughness values predominate over material type since copper (which has a higher Hamaker coefficient of 400 zJ than that of aluminium of 145 zJ) is inevitably found to exert lower Van-der-Waals forces than aluminium because copper's *rms* surface roughness values are higher than those of aluminium. Therefore; copper is suited for the picking position, aluminium for the gripper and silver for the placement position.

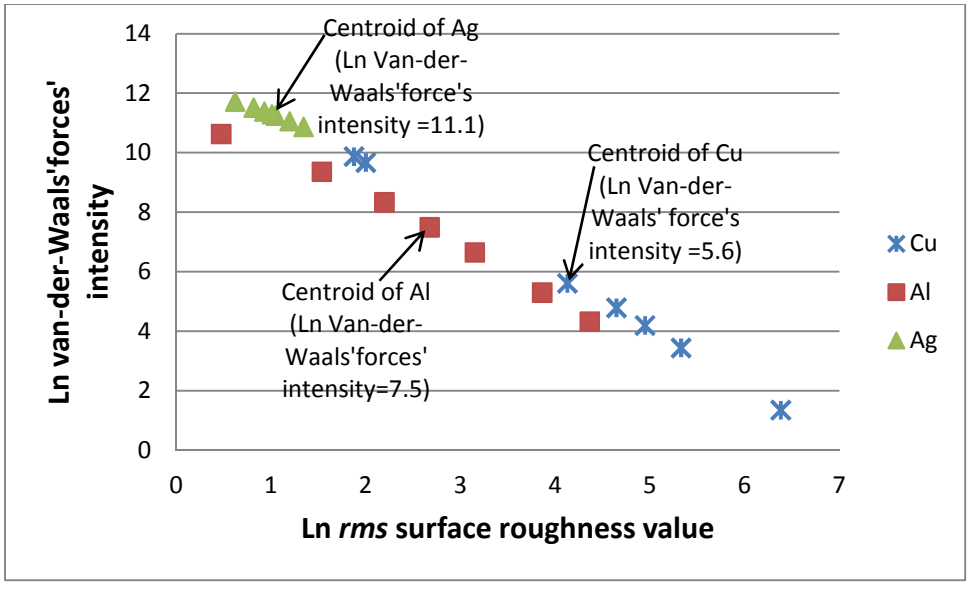

Figure 4-24 Van-der-Waals' forces' intensities numerically modelled with respect to surface roughness of copper (Cu), aluminum (Al) and silver (Ag)

4.3 Measured values of Van-der-Waals' forces and analysis

This section carries the measured values of the Van-der-Waals' forces exerted by the e-beam coatings and polyurethane materials. The measured values and their analysis are presented in order to validate the findings of the numerical modelling conducted in the previous sections. The first sub-section includes extending curves which indicate whether Van-der-Waals' forces are the only forces acting on a given sample. The second sub-section contains the retracting curves which indicate the magnitude of the exerted Van-der-Waals' forces. A reiteration of the alpha-numeric labelling of samples is necessary: the alpha part refers to the chemical symbol of the e-beam-coating material. The first number refers to the e-beam deposition time and the second number refers to the batch number. For example: Cu 20.1 refers to a copper material, e-beam deposited for 20 minutes, batch number 1. Two batches were examined.

4.3.1 Van-der-Waals' forces' Extending Curves.

All the figures, from Figure 4-25 to Figure 4.28, illustrate Van-der-Waals' forces' extending curves (graphs obtained when the AFM probe gradually approaches the specimen until contact is reached) for samples of Cu 5.1, Ag 20.1, Cu 5.2, and Ag 20.2. Extending curves for Cu 20.1, Al 5.2, Al 20.2, Cu 20.2 and Ag 5. 2 are shown in Appendix J. In these figures, the curve marked 1, represents the experimentally measured Van-der-Waals' forces. The curve marked 2 represents the theoretical Van-der-Waals' force obtained using Equation 2.6 for a smooth sample, and the curve marked 3 represents the theoretic force for a rough sample obtained by using Equation 2.29. The dotted line shows the sample's "jump-in" region which corresponds to Equation 2.34. Point "A" corresponds to the force derivative, dF/dH, where $dF/dH = k$. These results are summarised in Table 4.2.

Polyurethane 30 and polyurethane 60 samples are included in Table 4.2. They were observed to have two distinct *rms* surface roughness values, the first corresponding to longer peak-to-peak distances and the second (in brackets) corresponding to the shorter peak-to-peak distances of the asperities on the surfaces.

The experimental results are relatively higher than the theoretical "jump-in" distances possibly due to the following reasons:

1) A spherically modelled surface roughness is used in the development of Equation 2.34, while the examined samples show some non-regular roughness with non-spherical shapes,

2) The chemical compositions and structures of the samples may be different from that of a homogenously pure sample (upon which Equation 2.34 is based).

Table 4.2 Theoretical and experimental jump-in distances, H_j at points "A".

Sample	Surface roughness in *rms* [nm]	$k = dF/DH$ ($H=Hj$), [N/m]	H_j theoretical, [nm] Equation 2.34	H_j experimental, [nm]
Cu 20.1	217	0.27	0	6.2
Cu 5.1	2.72	0.27	2.2	8.3
Cu 5.2	1.5	0.17	5.0	7.9
Cu 20.2	0.9	0.17	5.9	12.2
Al 5.2	1.2	0.17	5.5	14.3
Al 20.2	2.3	0.17	3.7	12.4
Ag 20.1	1.41	0.17	6.4	12.2
Ag 20.2	0.8	0.17	7.8	5.7
Ag 5.2	0.66	0.17	8.0	22
Polyurethane 30	2.0 (0.5)	0.17	6.6	337
Polyurethane 60	3.0 (0.2)	0.17	6.6	250

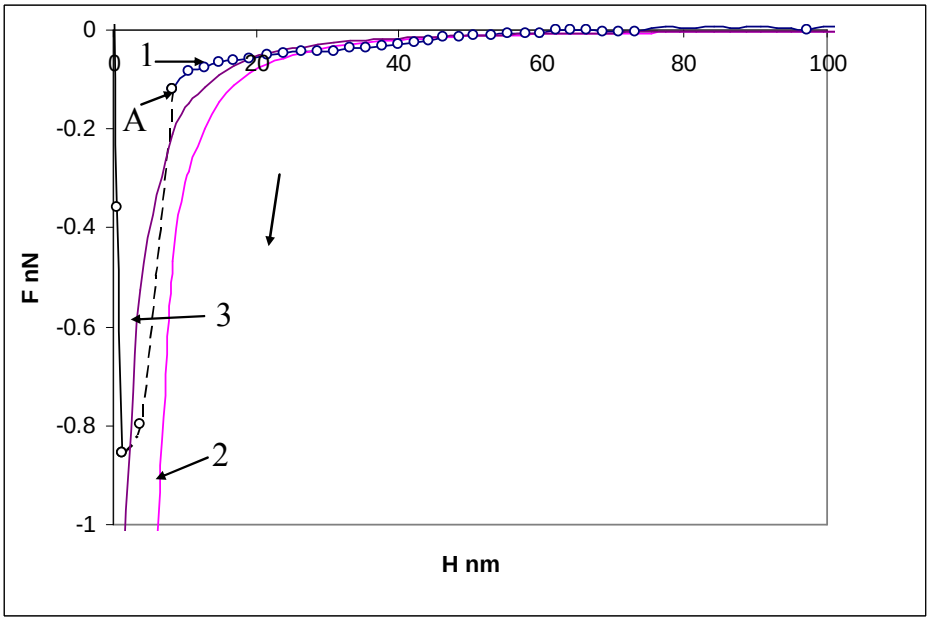

Figure 4-25 Copper (Cu 5.1) extending curves

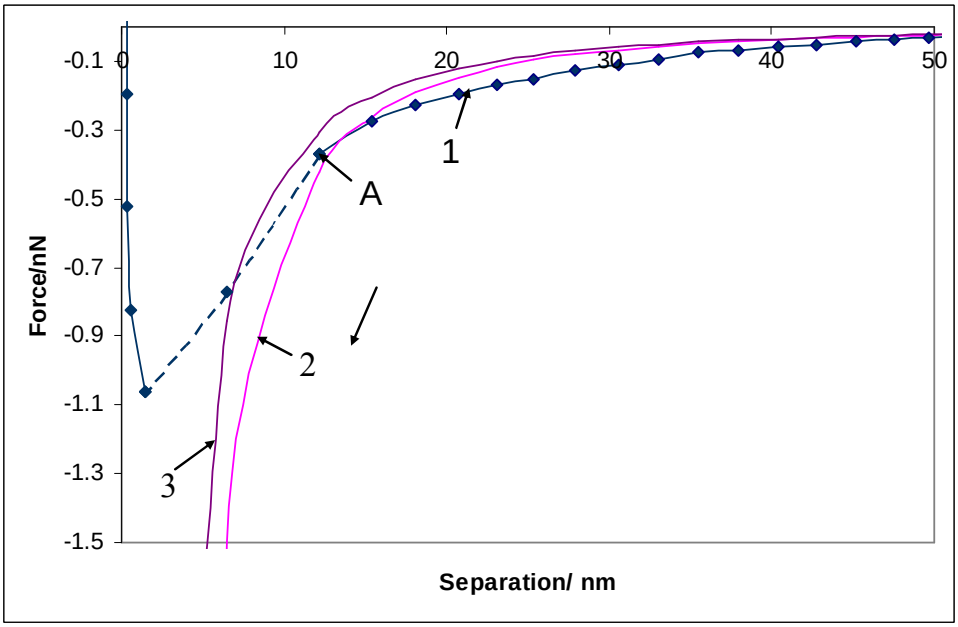

Figure 4-26 Silver (Ag 20.1) extending curves

For all the samples in batch 1, which include those whose extending curves are shown in Figure 4-25 to Figure 4-26, the "jump-in" regions and the position of the point "A" are near or less than the separation distance of 10 nm, which happens to fall under the non-retarded Van-der-Waals' forces region (as stated in Section 2.2.3). Therefore; Van-der-Waals' forces are the predominant forces in this case since the "jump-in" distances do not extend into micro- or millimeter ranges. Batch 2's extending forces shown in Figure 4.27 and Figure 4.28 also

confirm this observation. The rest of the extending forces for other batch 2's samples are shown in Appendix J.

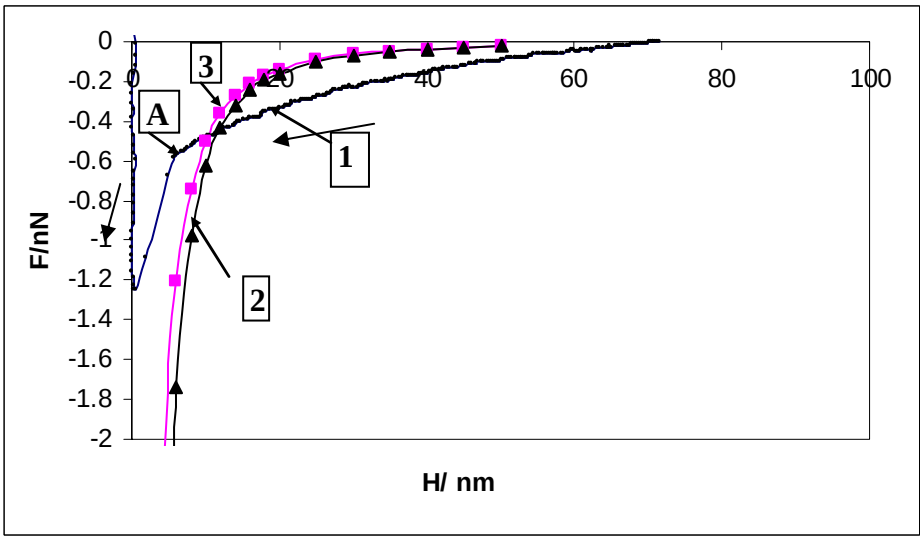

Figure 4-27 Ag 20.2 extending curves

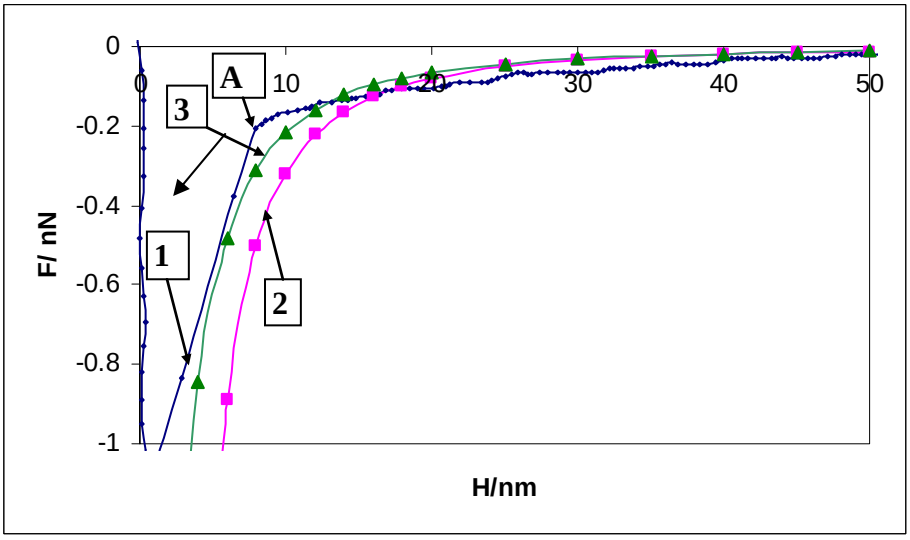

Figure 4-28 Cu 5.2 extending curves

The experimental "jump-in" regions and the position of the point "A" depicted in Figure 4.27 and Figure 4.28 for two batch 2's samples, Ag 20.2 and Cu 5.2 respectively, (also contained in Table 4.2) lie within the short-range separation distance, *H*, of 10 nm, again which happens to fall under the non-retarded Van-der-Waals' forces region (as stated in Section 2.2.3). As for Ag 5.2, polyurethane 30 and polyurethane 60 their jump-in distances are 22 nm, 337 nm and

250 nm respectively, lying in the retarded Van-der-Waals' forces region as discussed in Section 2.2.3. Since the experimental measurements were conducted in a Faraday cage insulated from electrostatic force, magnetic force, electromagnetic forces and other forces; the higher "jump-in" distances were ascribed to special electrostatic mirror image forces (a reflection of Van-der-Waals' forces of one sample on another leading to higher "jump-in" distances) (Danov et al, 2006; Landau et al, 1960). These special electrostatic mirror image forces are more dominant in polyurethane samples than in metallic samples, as indicated in Table 4.2. However; when the interacting surfaces (in this case the AFM spherical silica probe and the specimen) came into contact with one another, these special electrostatic mirror image forces disappeared. These forces did not appear in the Van-der-Waals' forces' retracting curves dealt with in Section 4.3.2. The author (researcher) had to co-author a journal paper on this special finding, as indicated in Appendix A, Abstract 11.

In the figures for Cu 5.1, Cu 20.2, Ag 20.1, Ag 20.2 and Cu.2, the experimental curves marked 1 complied with the numerically modelled Van-der-Waals' forces (of a rough sample interacting with a smooth sphere) marked as curve 2. However; other samples' experimental curves did not match well with the numerical modelling, possibly due to the special electrostatic image forces mentioned earlier. The following section shows the magnitude of the Van-der-Waals' forces exerted by the samples as indicated by their retracting forces.

4.3.2 Van-der-Waals forces' Retracting Curves.

Figure 4-29, Figure 4-30, and Figure 4-31 show retracting curves for Cu 5.1, Cu 20.1, and Ag 20.1, respectively. The retracting curves demonstrate the value of the Van-der-Waals' adhesive forces measured when detaching the AFM silica sphere from the e-beam coatings. The given figures carry graphs showing Van-der-Waals' forces' values close to the statistical mean of the measurements. The statistic distribution of the measured Van-der-Waals' forces for sample Al 20.2, shown in Appendix J has a standard deviation of 7.6 nN (about 25% of the average force). Similar results were obtained for other samples. In addition to that, the possible systematic error due to calibration is about 5%. The rest of the graphs and statistical distributions for Cu 5.2, Cu 20.2, Al 5.2, Al 20.2 and polyurethane samples are given in Appendix J, as well as their surface roughness profiles and distributions.

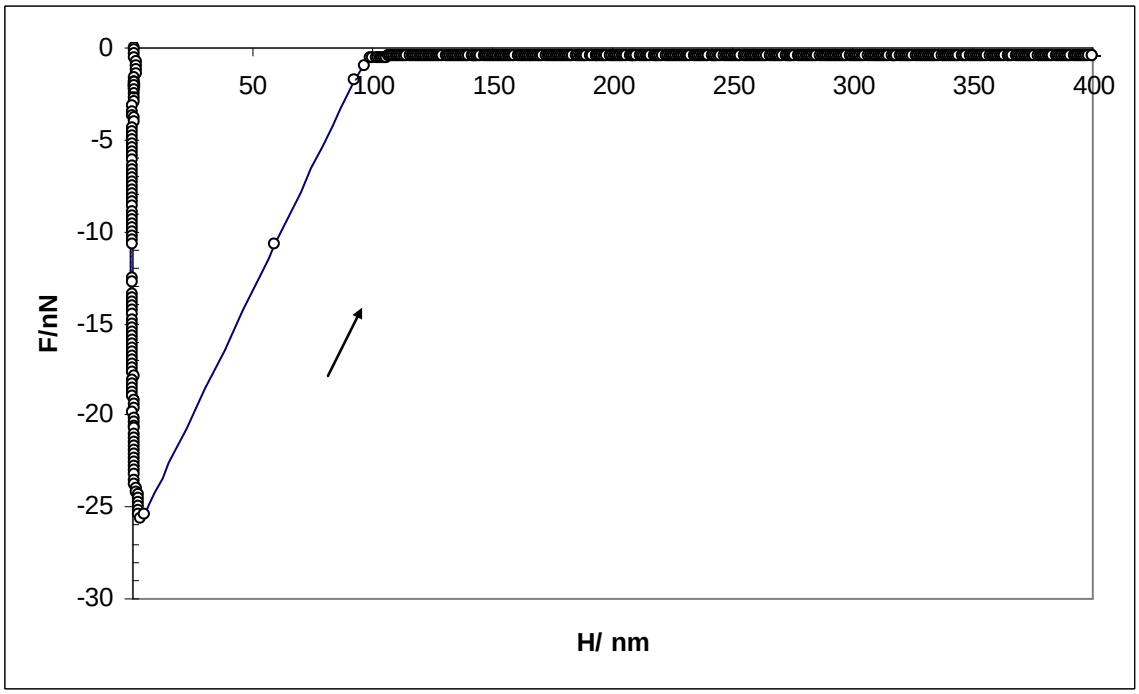

Figure 4-29 Retracting curve for Cu 5.1

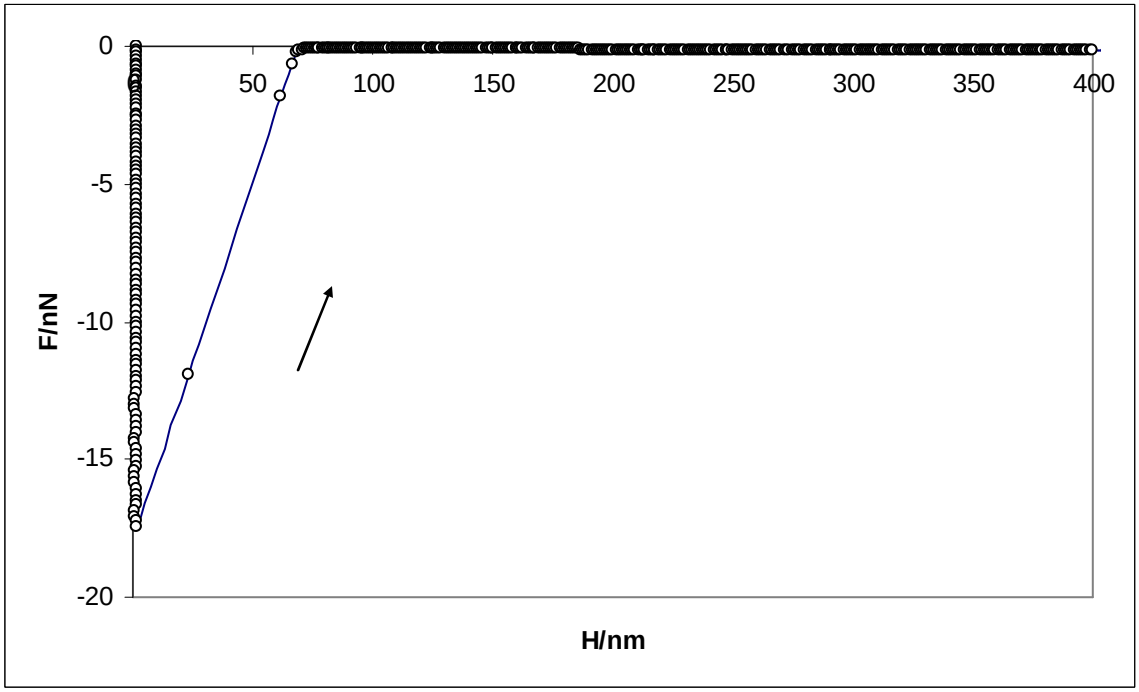

Figure 4-30 Retracting curve for Cu 20.1

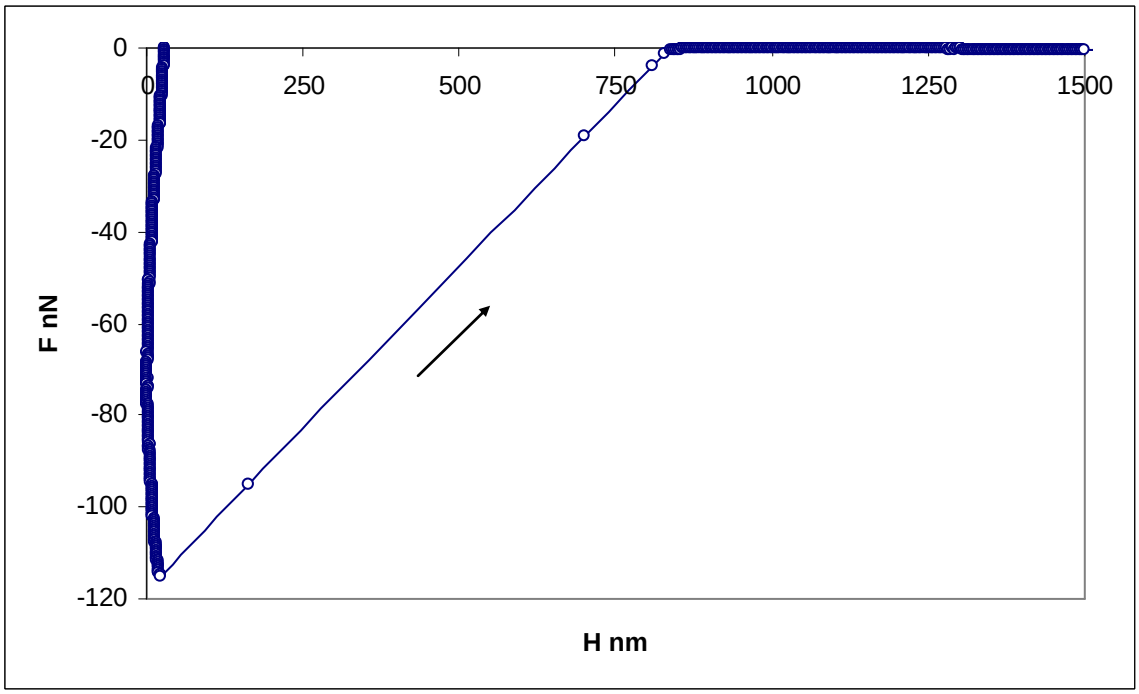

Figure 4-31 Retracting curve for Ag 20.1

The average Van-der-Waals' forces pertaining to Figure 4-29, Figure 4-30, and Figure 4-31 are summarized in Table 4.3. This table also includes a summary of the findings of the second batch of measured samples, the forces and surface roughness statistical distributions thereof shown in Appendix J. Polyurethane 30 and polyurethane 60 samples are included in Table 4.3 with their two distinct *rms* surface roughness values, the first corresponding to longer peak-to-peak distance and the second (in brackets) corresponding to the shorter peak-to-peak distance (also correspondingly shown in brackets in the adjacent column) of the surface surfaces. A comparison between the experimental and theoretical values of the Van-der-Waals forces is made in Table 4.3.

Table 4.3 Average results of Van-der-Waals forces obtained from retracting curves.

Sample	*rms* surface roughness value, [nm]	Peak-to-peak distance of surface roughness, λ, [nm]	Theoretical average Van-der-Waals force, [nN]; obtained using Equation 2-28.	Experimental Van-der-Waals force, [nN]
Cu 20.1	217	100	0.11	17±10
Cu 5.1	2.72	100	19.4	24±12
Cu 5.2	1.5	125	28.2	28±5
Cu 20.2	0.9	100	34.3	32
Al 5.2	1.2	66	14.5	44±5
Al 20.2	2.3	74	7.0	37±8
Ag 20.1	1.41	100	20.7	111±15
Ag 20.2	0.8	80	56.6	25±10
Ag 5.2	0.66	100	93.4	260
Polyurethane 30	2.0 (0.5)	2000 (100)	51	340±10
Polyurethane 60	3.0 (0.2)	3000 (100)	221	630±20

Equation 2.28 is used to calculate the theoretical value of the Van-der-Waals' forces in Table 4.3 as it shows the Van-der-Waals' forces experienced when a micro-part is detached from a rough flat sample (taking peak-to-peak distances of asperities into consideration), as stated in Section 2.6.5. The value of H_0 is taken as equal to 0.3 nm (as indicated in Section 2.6.5); the experimental value of A_H for silica interacting with either copper (Cu) or aluminium (Al) is taken as 7.7 x 10^{-20} J; the value of A_H for silica interacting with silver (Ag) is taken as 1.5 x 10^{-19} J, as mentioned earlier in Section 3.5. In the case of each polyurethane material, double surface roughness profiles were identified. As for the polyurethane 30 the double surface roughness of *rms* values of 2.0 nm and 0.5 nm (given in brackets in Table 4.3) were identified; and these had peak-to-peak distances of 2000 nm and 100 nm (given in brackets) respectively. Same applies to the polyurethane 60 which had double surface roughness of *rms* values of 3.0 nm and 0.2 nm; and peak-to-peak distances of 3000 nm and 100 nm respectively.

The experimental Van-der-Waals' forces are relatively higher than the theoretical values. An investigation was conducted in order to determine whether humidity could be a contributing factor in this phenomenon. The Van-der-Waals' forces were again measured for samples Al 20.2 and Cu 20.2 at a humidity level of 40%. The average values of the forces were 41.8±6.0 nN and 30.0±6.8 nN, for Al 20.2 and Cu 20.2, respectively; which are close to 37±8 nN and 32 nN, respectively; obtained for these samples at 20% humidity level. Therefore; it could be concluded that humidity did not significantly affect the intensity of the exerted Van-der-Waals' forces. It should also be noted that at a humidity level of 40%, the water meniscus radius r is equal to 0.57 nm and is less than the height of asperities for *rms* surface roughness values, ranging between 1 nm and 3 nm, since the capillary force only exists if $2r\cos\theta > 1.82rms$ (Rabinovich et al, 2011). Minor cold welding could be a possible reason for higher experimental Van-der-Waals' forces' values, as compared to theoretical values due to the AFM measuring probe being in contact with the specimen for periods ranging from 3 to 10 seconds under a preload of 1 nN, as stated in Section 3.5. Another reason could be that a smooth spherical surface roughness profile was used in developing Equation 2.28; while the examined specimens reveal some non-regular surface roughness profiles as shown in the figures contained Section 4.1, which are generally not smooth and not uniformly spherical.

4.4 Evaluation of the exerted Van-der-Waals' forces with respect to micro-material handling operations

This section covers the evaluation of the Van-der-Waals' forces exerted by the e-beam deposited samples and the polyurethane materials as to their usability in micro-material handling operations. The metallic e-beam deposited samples' results in Table 4.4 are summarized graphically in Figure 4-32. Samples Cu 20.1, Ag 20.2 are not included in the plot due to their values being inconsistent with others probably as a result of some inconsistent e-beam deposition rates. Polyurethane samples are also not included in Figure 4-32 (however, they are considered at the end of this section) as they are not metals, but rather special polymers which exert higher Van-der-Waals' forces (in some cases 10 times higher than metallic e-beam coatings as indicated in Table 4.3). Figure 4-32 shows that silver exerts the largest Van-der-Waals' forces with a centroid at: rms = 1.035 nm, and Van-der-Waals' forces = 185.5 nN. Aluminium exerts medium Van-der-Waals' forces with a centroid at: rms = 1.75 nm, and Van-der-Waals' forces = 40.5 nN. Copper exerts the least Van-der-Waals' forces with a centroid at: rms = 1.81 nm, and Van-der-Waals' forces = 28 nN.

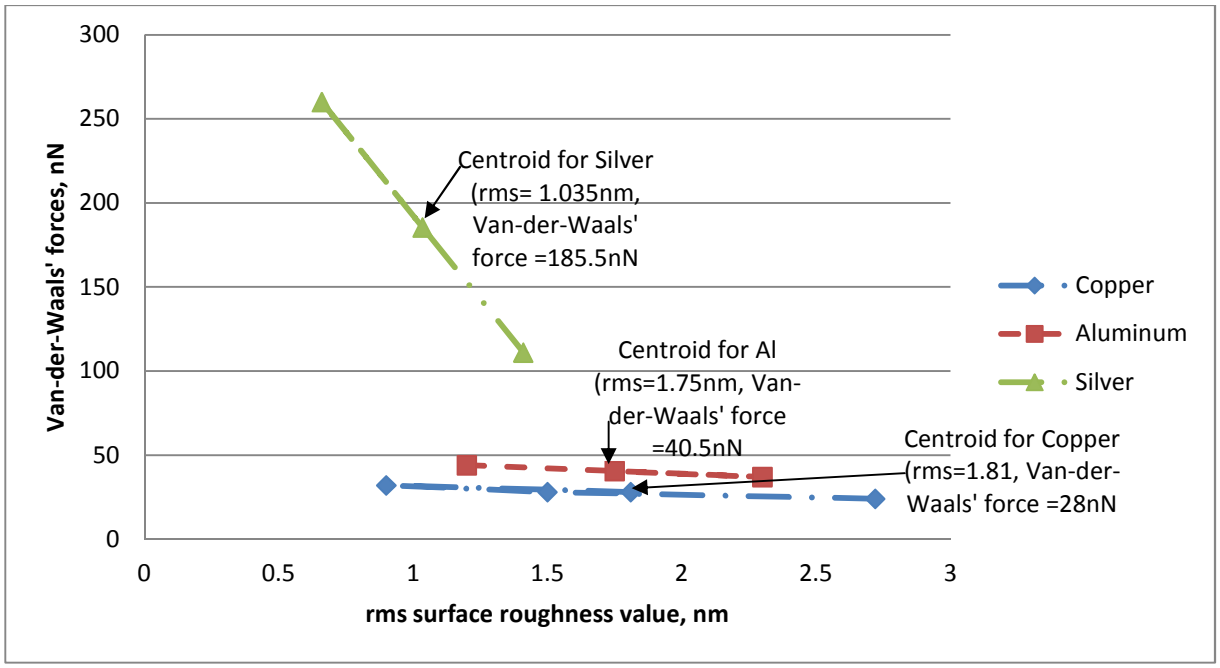

Figure 4-32 Experimental Van-der-Waals' forces exerted by e-beam deposited surfaces of copper (Cu), aluminium (Al) and silver (Ag)

When Figure 4.24 is compared to Figure 4.32 there is a correlation between the numerically modelled and experimental results of Van-der-Waals' forces with respect to surface roughness. Both figures reveal that silver exerts the highest Van-der-Waals' forces, aluminium exerts medium Van-der-Waals' forces, and copper exerts the least Van-der-Waals' forces. Both figures also show that the Van-der-Waals' forces decrease as the *rms* surface roughness values increase. It can be noted in both figures that silver has the lowest *rms* surface roughness values and exerts the highest Van-der-Waals' forces; aluminium has medium *rms* surface roughness values and exerts medium Van-der-Waals' forces; and copper has the largest *rms* surface roughness values and exerts the lowest Van-der-Waals' forces. It should be noted that although the Hamaker coefficient of copper is relatively bigger than that of aluminium, the copper's higher *rms* surface roughness values dominate over material type such that it exerts less Van-der-Waals' forces than aluminium. This is in agreement to the earlier discussion in Section 4.2.4 (centered on Figure 4.24), Section 2.6.5 and Section 2.8 where it is postulated that surface roughness variation overrides material type variation in Van-der-Waals' forces actuated micro-material handling operation. Therefore; in a micro-material handling operation, silver would be suited for the placement position's surface, aluminium for the gripper's surface and the copper for the picking position's surface. Then an

aluminum gripper would pick micro-parts from a copper base and deposit them onto to a silver base.

The AFM silica spherical probe (which has a relatively low Hamaker coefficient of 6.6 x 10^{-20} J and is also naturally stable and relatively hard when compared to metals) was used as a standard base to measure the exerted Van-der-Waals' forces as mentioned earlier in Section 3.5. The fact that van-der-Waals' forces of e-beam generated surfaces were able to attract the silica sphere effectively with significant difference in their exerted forces proves that this type of micro-material handling works effectively with other materials which have the same or higher Hamaker coefficients in practical micro-material handling operations.

However; in order for picking to be feasible, the demarcation is that the gripper should exert a higher Van-der-Waals' force than the combined force of the weight of the micro-part and the Van-der-Waals' forces exerted by the base material. For example, if the 2.5 μm silica sphere used in the AFM cantilever is considered as a micro-part to be handled, and given that its density is 2.648 g/cm^3, then its weight would be 1.7x10^{-3} nN. If the picking position is made of Cu 5.2 which exerts 28 nN, the combined force, including the weight of the micro-part, would be 28.0017 nN. Therefore; a gripper made of Al 20.2 (which exerts 37 nN) could be used to pick the micro-part and release it onto an Ag 5.2 base which exerts 260 nN Van-der-Waals' forces.

Figure 4.33 shows a plot of the Van-der-Waals' forces against the *rms* surface roughness of the previously chosen eight metallic e-beam coated samples contained in Table 4.3. The plot is aimed to find the trend of Van-der-Waals' forces as the surface roughness decreases. Microsoft Office Excel 2007 gives a logarithmic trend of the results as described by Equation 4.1. As surface roughness increases the Van-der-Waals' forces decrease rapidly.

$$F = -115.9\ In(rms) + 113.71 \qquad \text{Equation 4.1}$$

Where *F* is the Van-der-Waals force in *nN*, *rms* is the root-mean-square surface roughness in *nm.*

Therefore, an increase in surface roughness greatly reduces the Van-der-Waals' forces exerted by a given material. This observation is in agreement with the discussion in Section 2.6.5, Section 2.8, Section 4.2.4 centered upon Figure 4.24, and also as shown in Figure 4.32 where it was observed that surface roughness variation (for a given class of materials, for example metals) overrides material type variation as far as the Van-der-Waals' forces exerted by a micro-part are concerned.

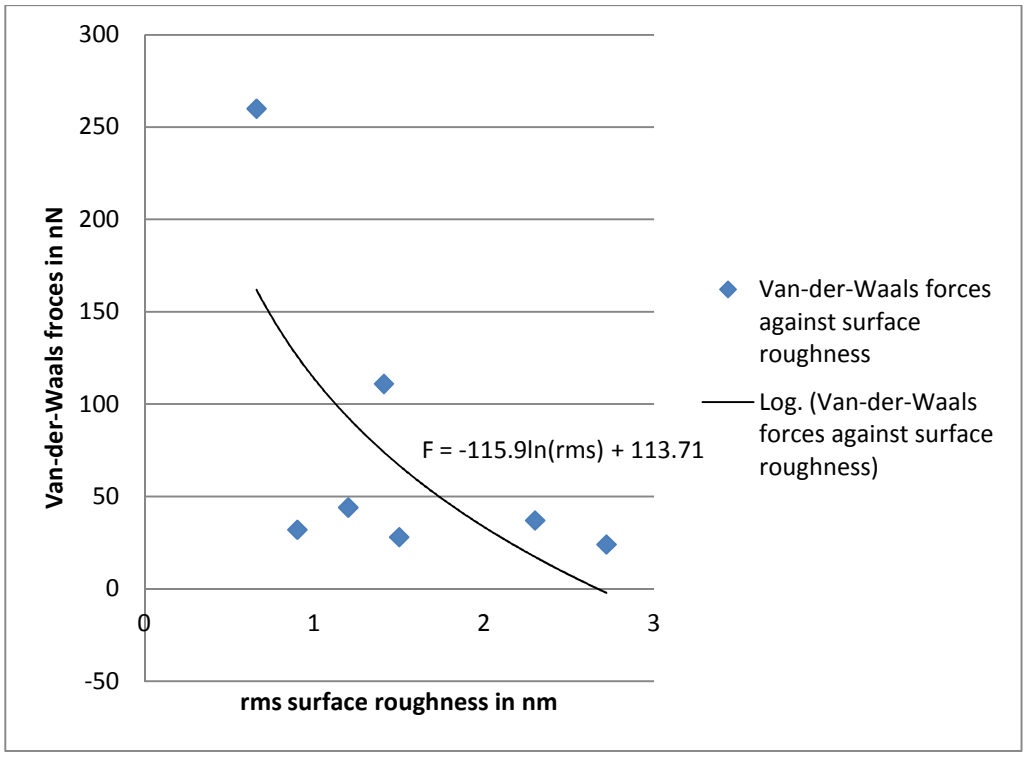

Figure 4-33 Plot of Van-der-Waals forces against surface roughness with a logarithmic trend inserted.

On the other hand, polyurethane 30 and polyurethane 60 exerted high Van-der-Waals' forces of 340±10 nN and 630±20 nN, respectively, when a 2.5µm silica probe was used (Table 4.3). As mentioned earlier, the Van-der-Waals' forces exerted by the polyurethane samples are by far larger than those exerted by the e-beam deposited metallic samples as shown in Table 4.3. Several AFM cantilevers were broken in an attempt to measure these samples' *rms* surface roughness values and Van-der-Waals' forces because the forces were too high. It seems that the short peak-to-peak distances' *rms* surface roughness values were dominant in contributing to the exerted Van-der-Waals' forces in the polyurethane samples. It should be noted that these shorter peak-to-peak distances of 100 nm contributed towards a denser concentration of peaks (which give a lower *rms* surface roughness value) than the longer peak-to-peak distances of 2000 nm and 3000 nm, as shown in Table 4.3. As a result, the 0.5 nm *rms* surface roughness value for polyurethane 30 contributes more to the Van-der-Waals' force of 340±10 nN than the 2.0 nm *rms* surface roughness value, and the 0.2 nm *rms* value for polyurethane 60 contributes more to the Van-der-Waals' force of 630±20 nN than the 3.0 nm *rms* surface roughness value. Therefore; polyurethane 30 would be suitable for the picking up position and polyurethane 60 for the placement position in a micro-material handling operation.

4.5 Applications of polyurethane in micro-material handling utilising Van-der-Waals' forces

Since the polyurethane samples were found to exert larger Van-der-Waals' forces than e-beam deposited metallic samples, this section focuses on the application of Van-der-Waals' force actuated polyurethane micro-grippers in the handling of IC micro-components. Figures 4-34 to 4-46, and Table 4.4 show the results obtained when a flat polyurethane micro-gripper of 8mm radius was first pressed against a flat copper coated circuit board and later detached as explained in Section 3.6. The ripples in the force-time graphs (resonance) could be a result of vibrations of the Motoman SDA 10 robot as it was moved downwards and upwards in the course of each experiment. Figures 4-34 to 4-39, show the plot of preloads (negative) and Van-der-Waals' forces (positive) against time for a polyurethane 30 gripper. It is observed that as the preload increases, the exerted Van-der-Waals force increases until a certain limit is reached.

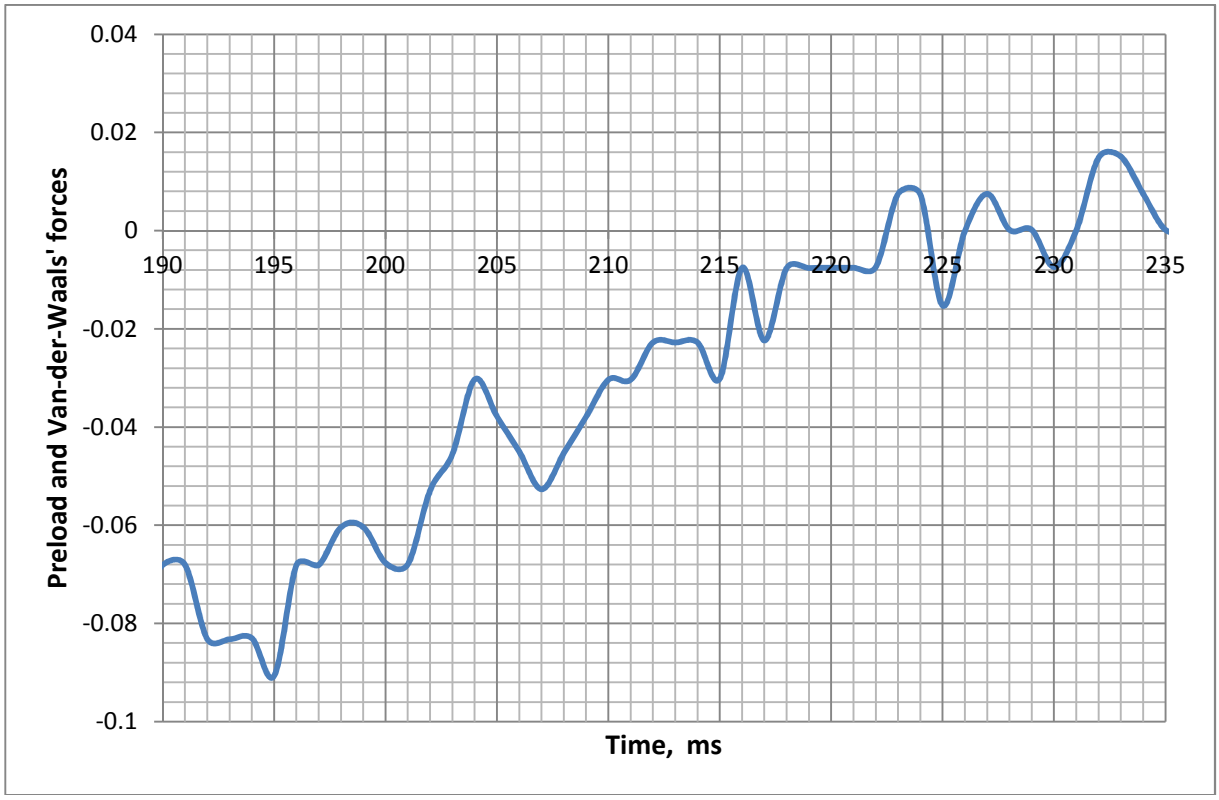

Figure 4-34 Preload of 0.09 ± 0.01 N (maximum) and Van-der-Waals' force of 0.01 ± 0.01 N (maximum) plotted against time for polyurethane 30.

A maximum preload of 0.09 ± 0.01 N as in Figure 4-34 yields a maximum Van-der-Waals' force of 0.01 ± 0.01 N. Figure 4-35 shows that when the maximum preload increases to 0.12 ± 0.01 N the corresponding maximum Van-der-Waals' force exerted by the polyurethane 30 gripper increase to 0.02 ± 0.01 N.

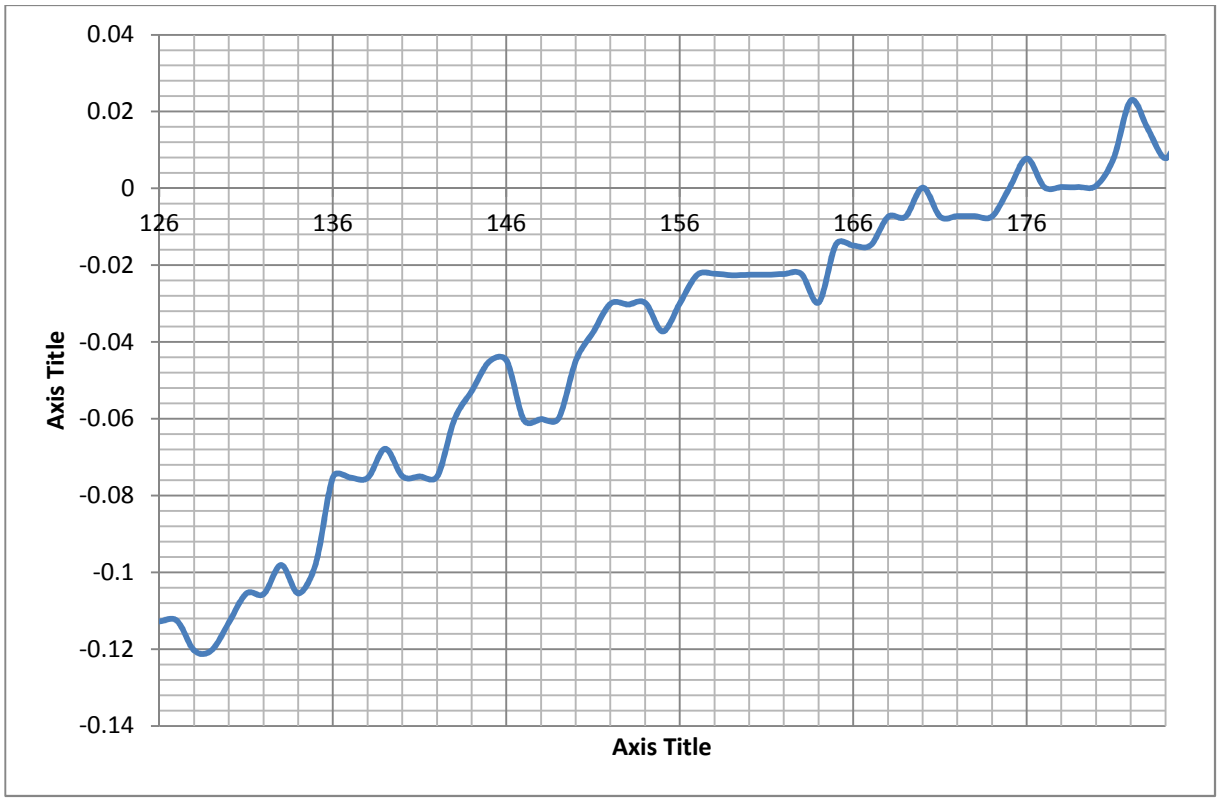

Figure 4-35 Preload of 0.12 ± 0.01 N (maximum) and Van-der-Waals' force of 0.02 ± 0.01 N (maximum) plotted against time for polyurethane 30.

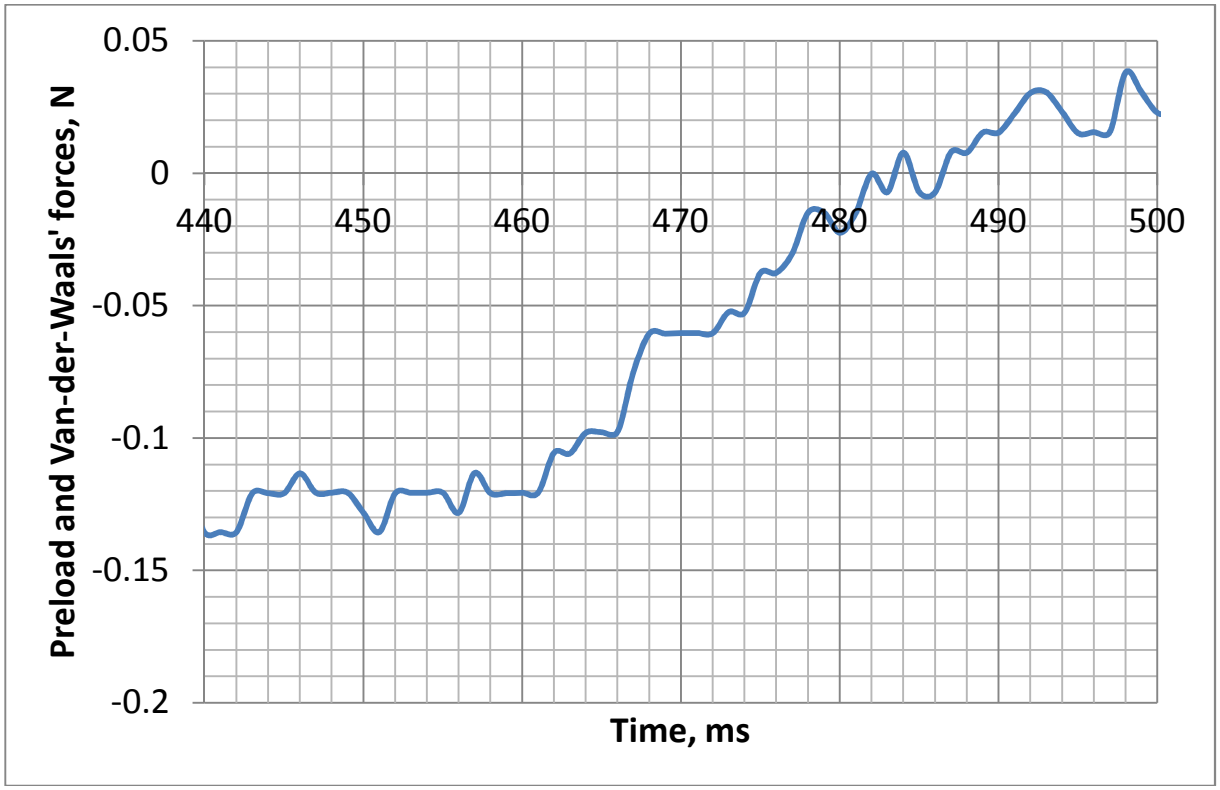

Figure 4-36 Preload of 0.14 ± 0.01 N (maximum) and Van-der-Waals' force of 0.04 ± 0.01 N (maximum) plotted against time for polyurethane 30.

Figure 4-36 shows that when the maximum preload is 0.14 ± 0.01 N the maximum Van-der-Waals force exerted by polyurethane gripper is 0.04 ± 0.01 N. When the preload is increased to 0.18 ± 0.01 N, the corresponding Van-der-Waals' force is also increased to 0.06 ± 0.01 N as indicated in Figure 4-37.

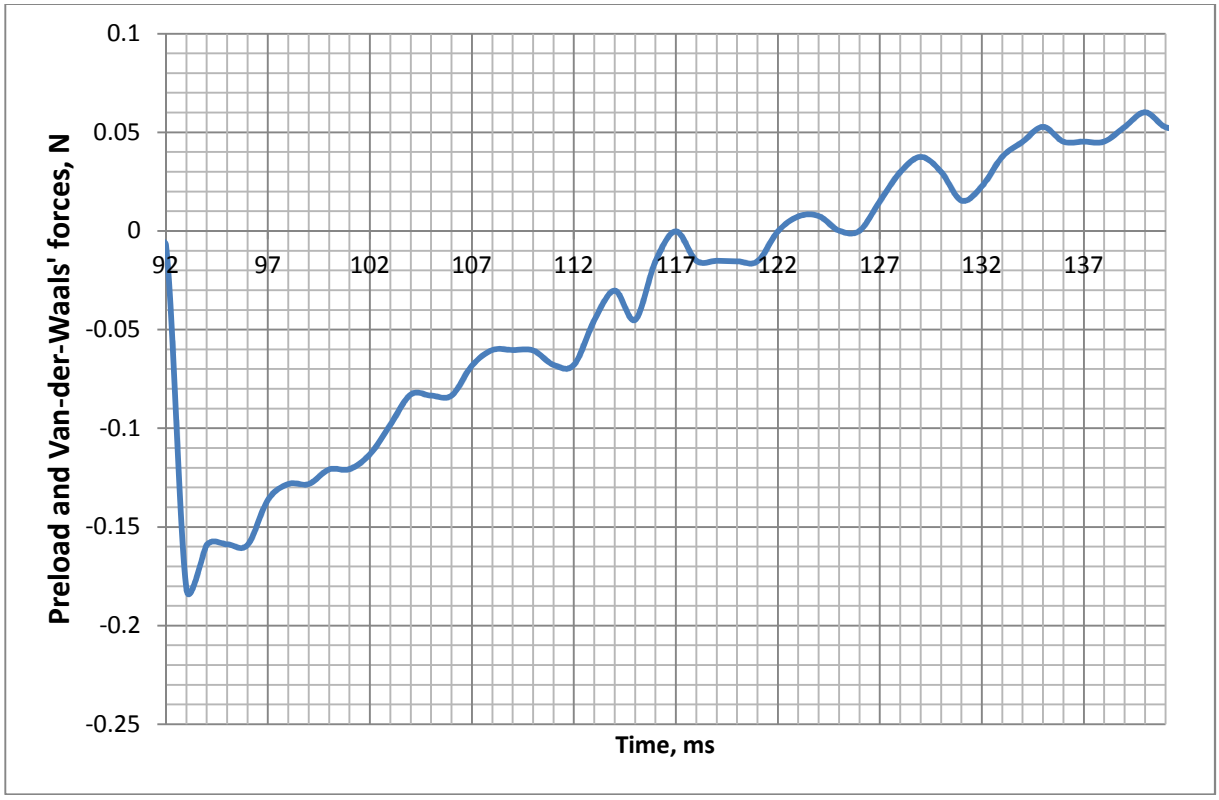

Figure 4-37 Preload of 0.18 ± 0.01 N (maximum) and Van-der-Waals' force of 0.06 ± 0.01 N (maximum) plotted against time for polyurethane 30.

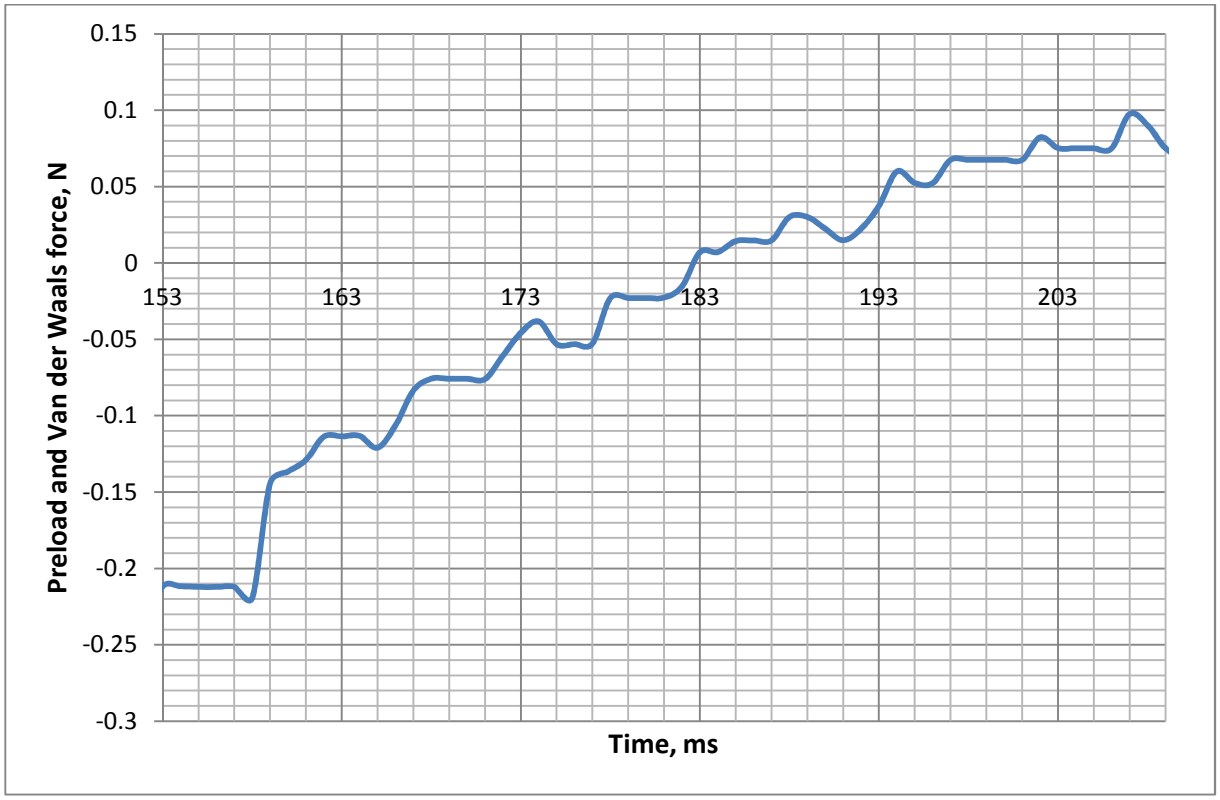

Figure 4-38 Preload of 0.21 ± 0.01 N (maximum) and Van-der-Waals' force of 0.09 ± 0.01 N (maximum) against time for polyurethane 30

When the maximum preload is 0.21 ± 0.01 N as shown in Figure 4-38, the maximum Van-der-Waals' force exerted by the polyurethane 30 gripper is 0.09 ± 0.01 N. However, as the preload increases to 0.25 ± 0.01 N, the exerted Van-der-Waals' force seem not to increase as indicated in Figure 4-39 in which a value of 0.07 ± 0.01 N is indicated.

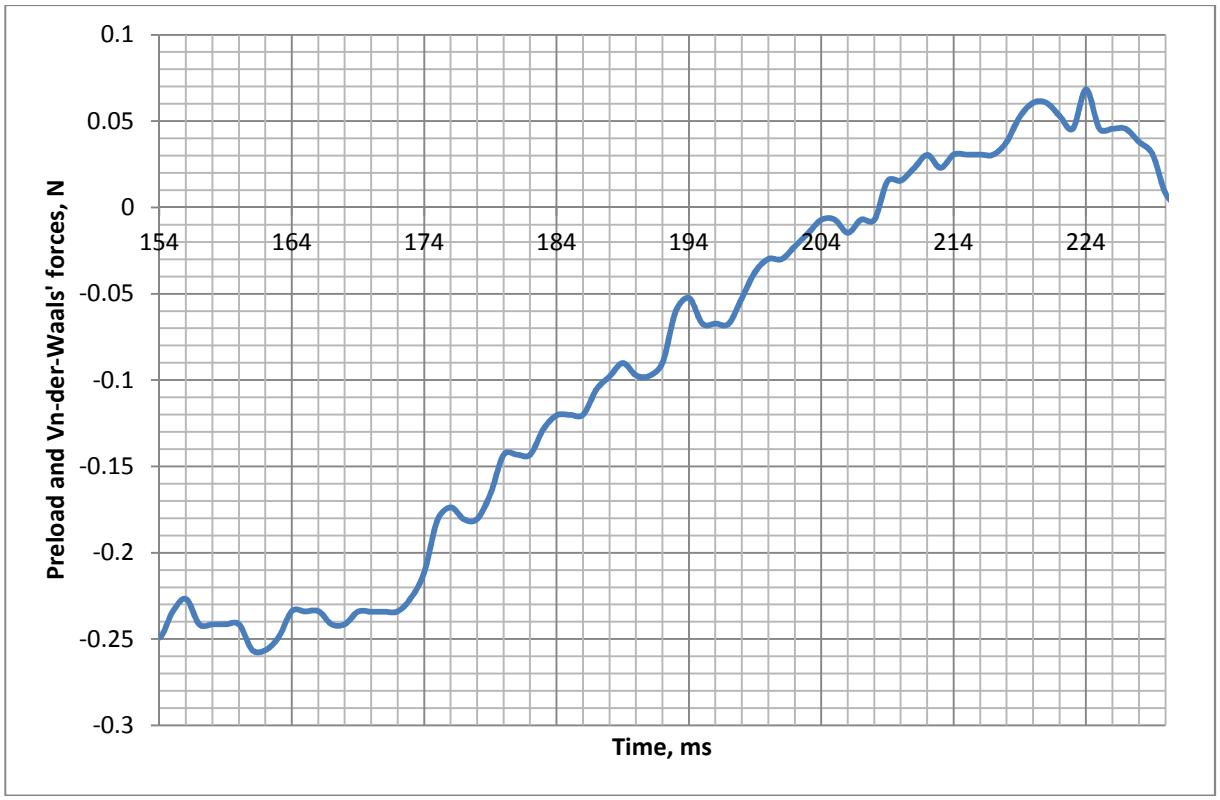

Figure 4-39 Preload of 0.25 ± 0.01 N (maximum) and Van-der-Waals' force of 0.07 ± 0.01 N (maximum) plotted against time for polyurethane 30 showing that there is no significant increase in Van-der-Waals' forces at preloads greater than 0.20 N.

Figure 4-40 shows the plot of the maximum preloads against the maximum Van-der-Waals force exerted before separation of the polyurethane 30 gripper from the copper coated circuit board. From this figure it is seen that as the preload increases, the exerted Van-der-Waals' forces also increase correspondingly. However, there is no significant increase in the exerted Van-der-Waals' forces beyond a preload of 0.2 N under the conditions in which the experiments were conducted.

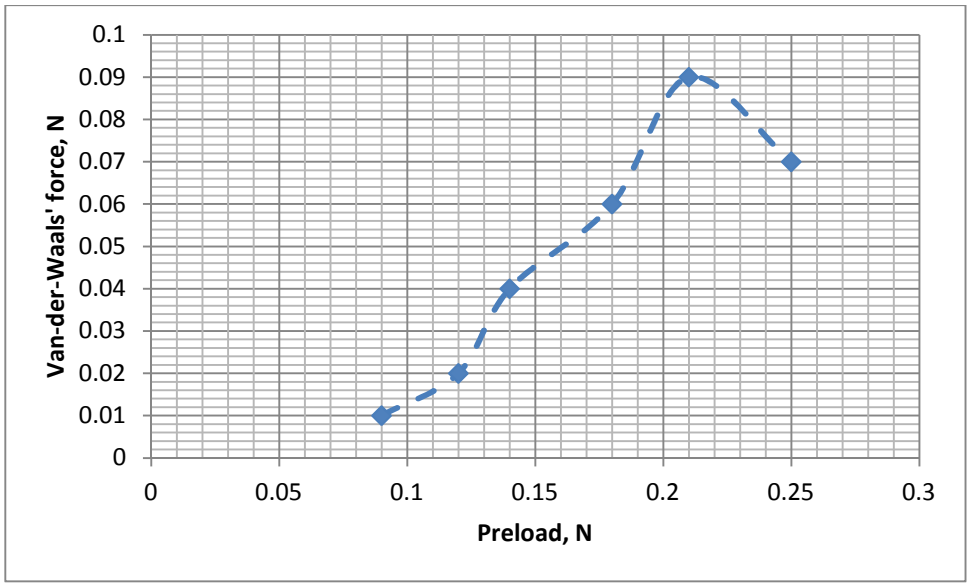

Figure 4-40 Plot of Preload against the exerted Van-der-Waals' forces for polyurethane 30

Figures 4-41 to 4-45 show the plot of preload and the exerted Van-der-Waals' forces against time for polyurethane 60 gripper. Again it is observed that as the preloads increase, the exerted Van-der-Waals' forces correspondingly increase.

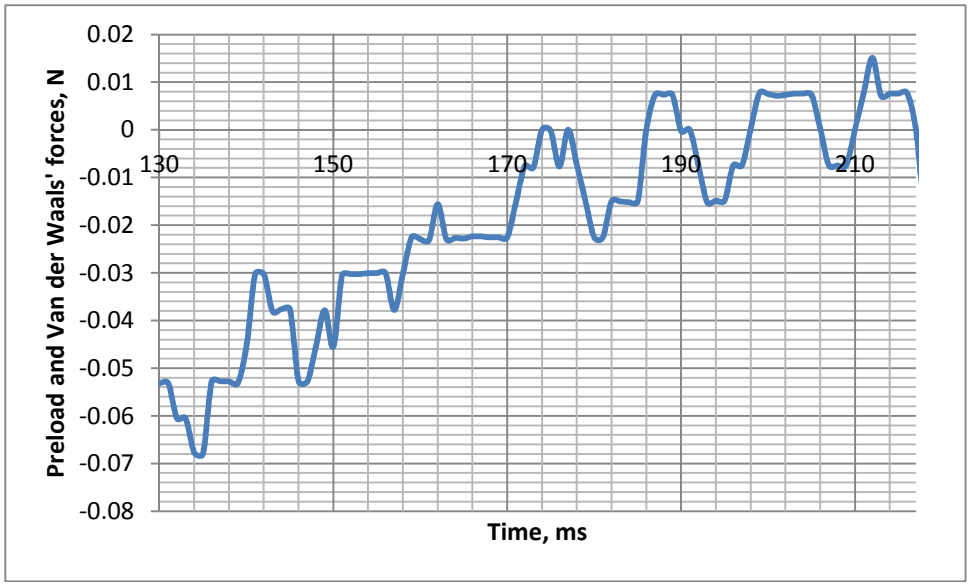

Figure 4-41 Preload of 0.06 ± 0.01 N (maximum) and Van-der-Waals force of 0.01 ± 0.01 N (maximum) plotted against time for polyurethane 60

Figure 4-41 shows that a preload 0.06 ± 0.01 N results in a maximum Van-der-Waals' force of 0.01 ± 0.01 N being exerted by the polyurethane 60. Attempts to measure the exerted Van-der- Waals' forces at preloads of 0.05 N and less failed given the accuracy of the system used. As the preload increases to 0.11 ± 0.01 N as shown in Figure 4-42, the exerted Van-der-Waals' force increase to 0.02 ± 0.01 N.

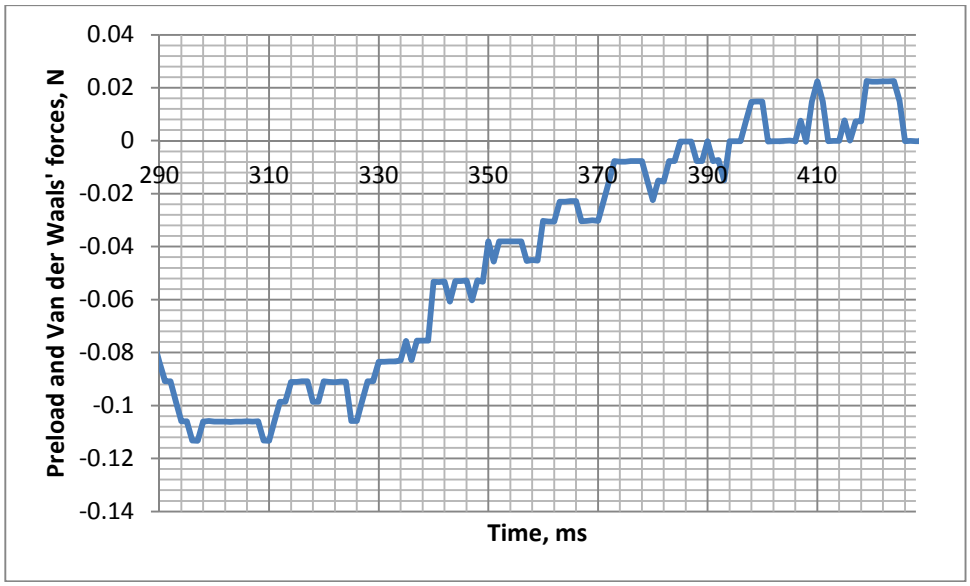

Figure 4-42 Preload of 0.11 ± 0.01 N (maximum) and Van-der-Waals force of 0.02 ± 0.01 N (maximum) plotted against time for polyurethane 60

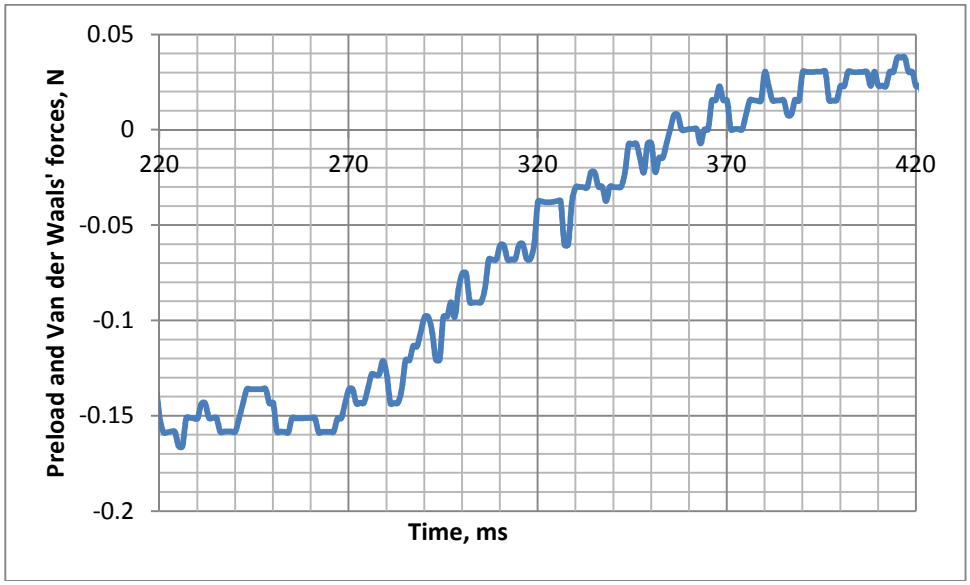

Figure 4-43 Preload of 0.16 ± 0.01 N (maximum) and Van-der-Waals' force of 0.03 ± 0.01 N (maximum) plotted against time for polyurethane 60

When the preload is 0.16 ± 0.01 N, the polyurethane 60 gripper exerts a maximum Van-der-Waals' force of 0.03 ± 0.01 N as indicated in Figure 4-43. An increase of the preload to 0.2 ± 0.01 N results in a corresponding increase of Van-der-Waals' forces to 0.04 ± 0.01 N as indicated in Figure 4-44.

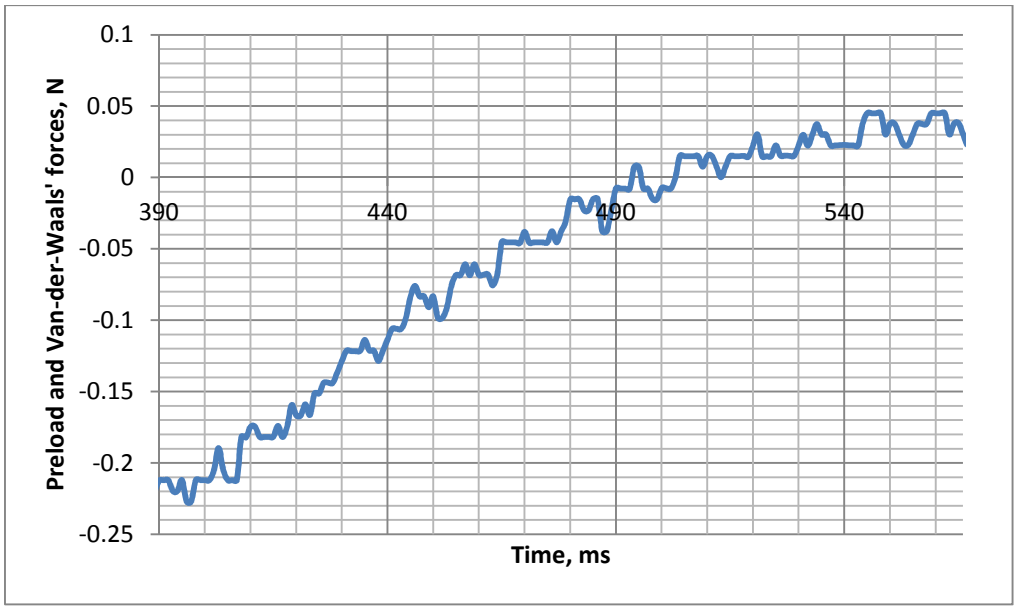

Figure 4-44 Preload of 0.2 ± 0.01 N (maximum) and Van-der-Waals' force of 0.04 ± 0.01 N against time for polyurethane 60

Figure 4-45 shows that when the preload increases to 0.24 ± 0.01 N, the Van-der-Waals' force exerted by the polyurethane 60 do not increase as indicated by its value of 0.04 ± 0.01 N in the graph. This is the same value for the Van-der-Waals force exerted for a preload of 0.2 ± 0.01 N as shown in Figure 4-44.

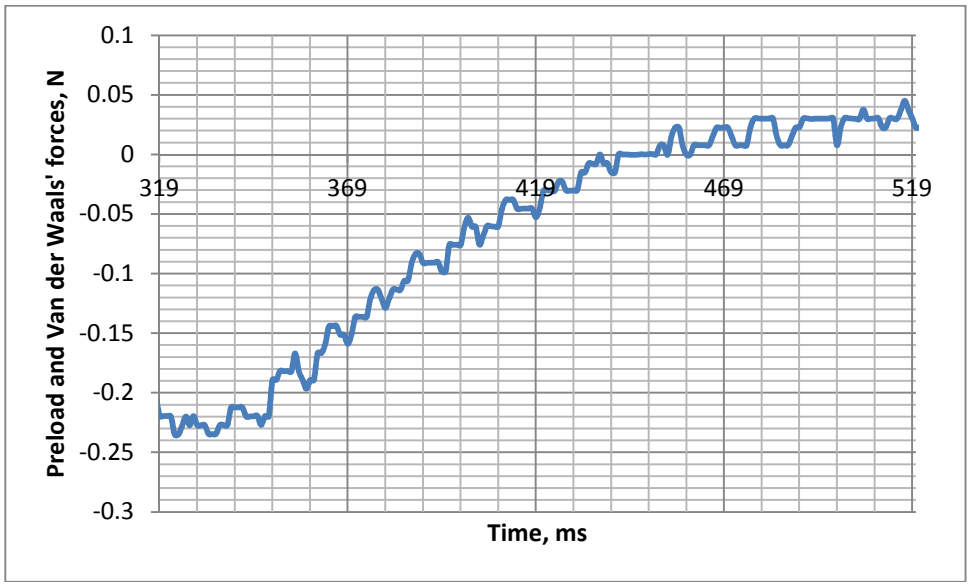

Figure 4-45 Preload of 0.24 ± 0.01 N (maximum) and Van-der-Waals' force of 0.04 ± 0.01 N plotted against time for polyurethane 60 showing that there is no significant increase in Van-der-Waals' forces at preloads greater than 0.20 N.

Figure 4-46 shows a summary of the plot of the preloads against the exerted Van-der-Waals' forces for polyurethane 60. The van-der-Waals' forces increase steadily as the preloads

increase, but no significant increase is observed when the preloads exceeds 2 N. This phenomenon was also observed by Murphy et al (2007) in the preload they used in their wall-climbing robots.

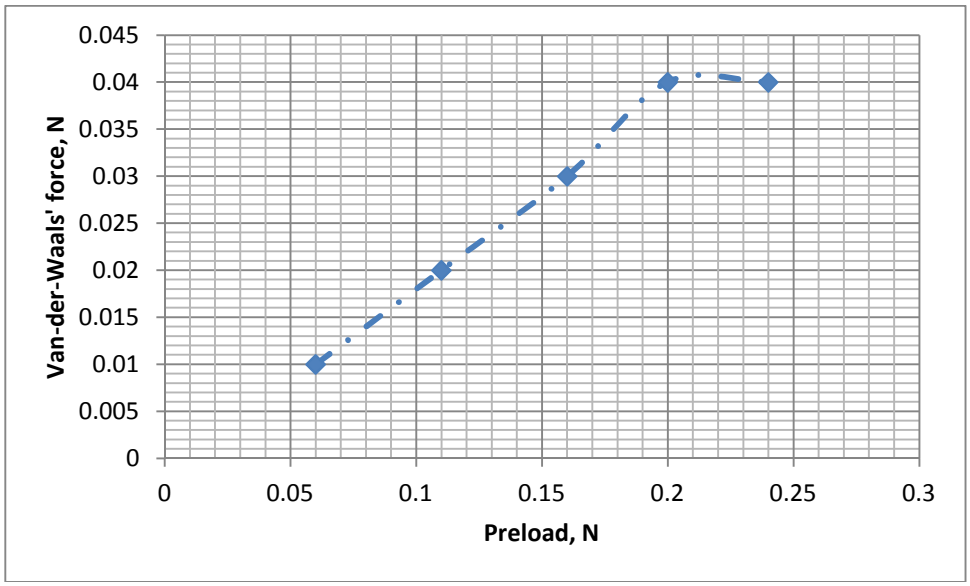

Figure 4-46 Plot of preload against the exerted Van-der-Waals' forces (maximum) for polyurethane 60.

Since a preload of 0.20 ± 0.01 N was found to yield an optimal Van-der- Waals force, Table 4.4 shows the maximum Van-der-Waals' forces recorded at this preload for polyurethane 30 and polyurethane 60 grippers. These grippers were of 8 mm radius. From the recorded values in Table 4.4, the polyurethane 30 gripper exerts an average Van-der-Waals' force of 0.08 ± 0.01 N and the polyurethane 60 gripper exerts less Van-der-Waals' forces averaging 0.03± 0.01 N.

Table 4.4 Van-der-Waals' force measurements (with a tolerance of ± 0.01N) **for polyurethane at a preload of 0.20 ± 0.01 N.**

Polyurethane 30	Polyurethane 60
0.09 N	0.04 N
0.07 N	0.03 N
0.08 N	0.02 N
0.10 N	0.03 N
0.06 N	0.02 N
Average: 0.08 N	Average: 0.03 N

The results in Table 4.4, for preloads of 0.20± 0.01 N, polyurethane 30 exerts higher Van-der-Waals' forces than polyurethane 60 (whereas at preloads of 1 nN, polyurethane 30 exerted lower Van-der-Waals' forces than polyurethane 60 when a silica spherical probe of radius 2.5µm was used as in Table 4.3). A possible reason for this could be that at high preloads, the polyurethane 30 elastically deforms (overriding surface roughness) more so than polyurethane 60, ensuring greater contact area than the latter as the polyurethane 30 (shore hardness 30A) is softer than polyurethane 60 (shore hardness 60A). A larger contact area leads to a higher Van-der-Waals' force being experienced between interacting surfaces. These findings are congruent to the findings of Murphy et al (2007), who found that the soft polyurethane ST1060 with a shore hardness 60A, exerted higher Van-der-Waals' forces than a hard polyurethane ST1087 with a shore hardness 87A.

Since the polyurethane material exerted higher Van-der-Waals' forces than metallic e-beam coatings; experimental applications of Van-der-Waals' forces for micro-material handling purposes were attempted using polyurethane material rather than the latter. Since Attia and Alock (2011), and Cao et al (2004) give the maximum dimension of a micro-part as 10 mm, copper micro-objects of 10 mm x 10 mm x 1mm were used in the experiments. These large micro-parts were used to determine whether the Van-der-Waals' forces can pick them, since they (Van-der-Waals' forces) are normally considered weak. When the experiments were conducted, these micro-parts were picked by both the polyurethane 60 and polyurethane 30 grippers when preloads of 0.20 ± 0.01 N were applied. As they managed to pick them, it follows that any other micro-object with smaller dimensions, for example 50 µm, can be picked by these forces. The anti-static mat and its accessories were used to discharge the equipment of any electrostatic forces.

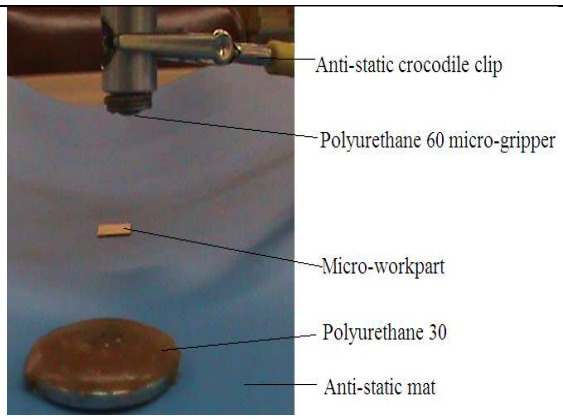

1.Initial arrangement before picking

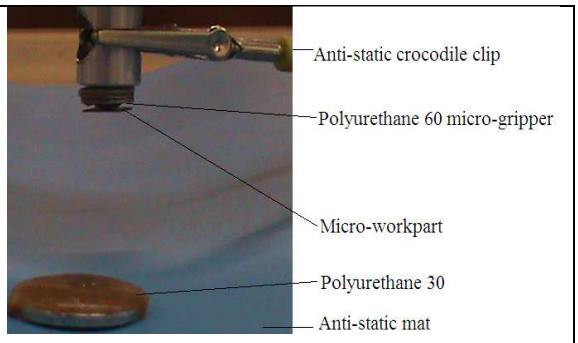

2. Pick-and-transfer by the Van-der-Waals' gripper

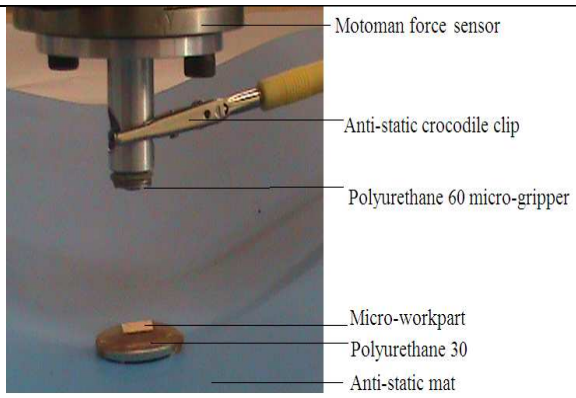

3. Placement of the micro-work part

Figure 4-47 Micro-material handling of copper coated e-beam micro-parts using Van-der-Waals' forces actuated polyurethane gripper

Once again, after applying a preload of 0.20 ± 0.01 N, polyurethane 60 was able to pick and transfer 10 mm x 10 mm x 1mm copper e-beam coated micro-parts (and other micro-objects of smaller dimensions) which were lying on surfaces of wood, perspex and metal; and place them on the polyurethane 30 surface (in agreement with the findings in Table 4.4), as shown in Figure 4.47. All attempts to pick micro-objects from polyurethane 30 by polyurethane 60 failed, proving that the former exerted higher Van-der-Waals' forces than the latter, when preloads of 0.20 ± 0.01 N were applied. Therefore; in a micro-material handling operation, the gripper should be made of polyurethane 60 and the placement position made of polyurethane 30. In assembly operations, the polyurethane 30 would be suitable for the assembly base.

Figure 4-48 shows the application of a 5 mm radius flat micro-gripper, made of polyurethane 30, successfully picking and transferring 10 mm x 10 mm integrated circuit (IC) components to a circuit board, in an assembly operation. The black epoxy material encapsulating the IC components (which also formed the gripping interface) had an average *rms* surface roughness

value of 83.3 nm and its atomic force micrograph is shown Appendix J. Upon placement of the micro-component onto the circuit board, soldering was executed as subsequent stage of the assembly operation. The soldering operation also ensured an effective release of the micro-part from the gripper. It should be noted that the soldering temperature of approximately 183^{o}C for the eutectic alloy of 63% tin and 37% lead used did not affect the polyurethane gripper because the IC component's epoxy covering provide a shield from the heat emitted since epoxy is a high heat resistant material and has a low thermal conductivity (which is less than 0.24 W/m^{o}C, Shokralla and Al-Muaikel (2010)). Furthermore, the polyurethane has a very low thermal conductivity of about 0.042 W/m^{o}C. Again the anti-static mat and its accessories were used to discharge the equipment and the operator of any electrostatic charge.

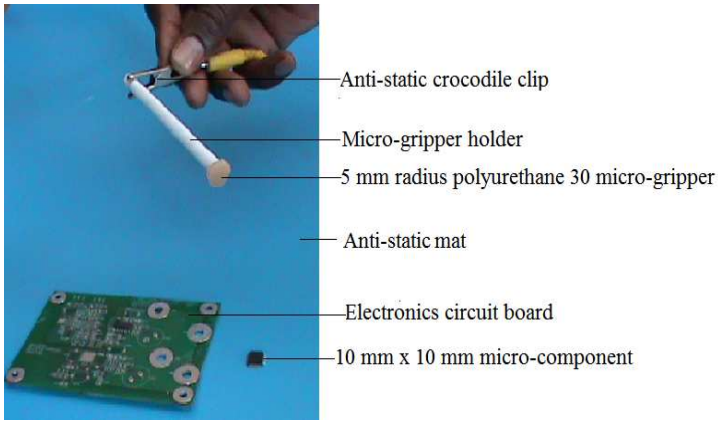

1.Initial arrangement before picking of the black 10 mm x 10 mm IC micro-component by 5 mm radius polyurethane micro-gripper.

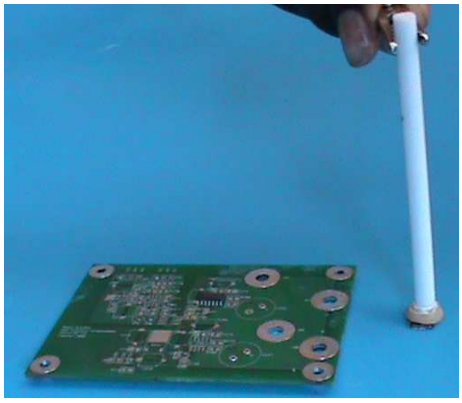

2. Picking contact initiated on 10 mm x 10 mm IC component by polyurethane 30 micro-gripper.

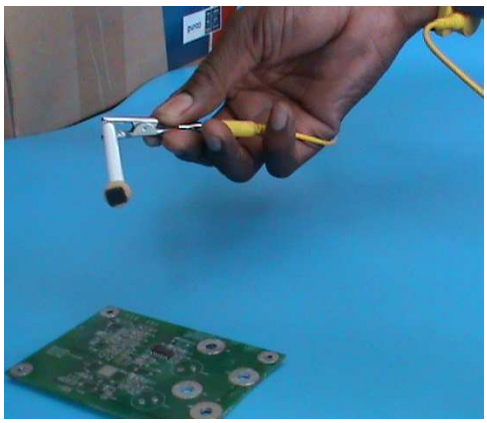

3. Picking and transfer of 10 mm x 10 mm IC component by polyurethane 30 micro-gripper.

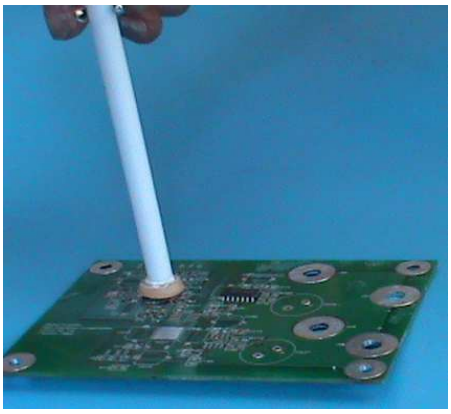

4. Placement of 10 mm x 10 mm IC micro-component on the circuit board by polyurethane 30 micro-gripper.

Figure 4-48, 5mm radius flat polyurethane 30 Van-der-Waals' force actuated gripper used in the assembling of 10 mm x 10 mm IC micro-component onto a circuit board

In a similar operation, a 1 mm radius polyurethane-30 gripper was used to pick, transfer and place a 1 mm x 1 mm IC micro-component onto an electronic circuit board in a micro-assembly operation, as shown in Figure 4.49

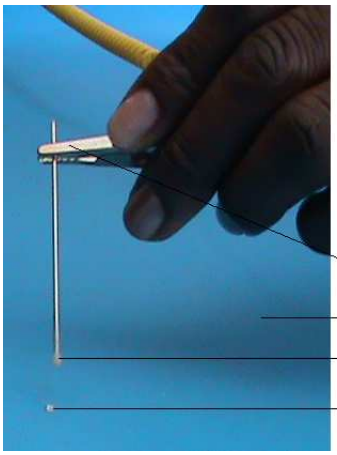

1. 1 mm x 1 mm IC micro-part before being picked by 1mm radius spherical polyurethane 30 micro-gripper.

2. 1 mm x 1 mm IC micro-part picked by 1 mm radius spherical polyurethane 30 micro-gripper.

3. 1 mm x 1 mm IC micro-part transferred by 1 mm radius spherical polyurethane 30 micro-gripper.

4. Placing of the 1 mm x 1 mm IC micro-part by 1 mm radius spherical polyurethane 30 micro-gripper on the circuit board.

Figure 4-49, 1 mm x 1 mm IC micro-part picked and transferred by 1 mm radius polyurethane 30 micro-gripper and placed on an electronic circuit board.

Both polyurethane grades managed to pick micro-parts of 10 mm x 10 mm x 1 mm dimensions repeatedly for 100 times in a dust-free laboratory.

4.6 Sizes and weights of micro-parts picked by Van-der-Waals forces

It should be noted that the sizes and weights of micro-parts to be picked and transferred using Van-der-Waals forces depend on the material type, geometrical configuration and the surface roughnesses of the interacting surfaces. In this research polyurethane 30 flat grippers of 5 mm radius; and of double surface roughness profiles whose *rms* values were 2 nm and 0.5 nm, and whose peak-to-peak distances were 2000 nm and 100 nm respectively (Table 4.3); were used to pick and place copper micro-parts of maximum dimensions of 10 mm x 10 mm x 1 mm whose *rms* surface roughness values were within 1 nm to 3 nm range (Table 4.3). When the density of copper is taken as 8970 Kg/m^3 (Groover, 2011), then the weight of the micro-part is 0.00879957 N. Again the polyurethane 30 flat gripper (of 5 mm radius) actuated by Van-der-Waals' forces was used to pick and place, in an assembly operation, 10 mm x 10 mm x 1.7 mm electronic micro-component which was encapsulated in epoxy material (Figure 4.48). The mass of the electronic micro-component was 0.2 grams (weight of 1.962 x 10^{-3}N). The surface roughness of the epoxy material was 83.3 nm. Murphy et al (2001) found that a 10 mm x 10 mm cross-sectioned directional and hierarchical polyurethane gripper can pick a body of a mass of 1 Kg, which gives a weight of 9.81 N. Since these Van-der-Waals' force actuated polyurethane grippers can pick and place these relatively large micro-parts, they can also pick and place micro-parts of even less dimensions and less weights. In this research, the minimum micro-part picked by Van-der-Waals was a silica sphere of radius 2.5 μm and of *rms* surface roughness value of 0.25 nm (this was the size of the AFM spherical silica probe which was used in determining the exerted Van-der-Waals' forces as in Section 3.5). If the density of silica is taken as 2660 Kg/m^3 (Groover, 2011), then the minimum weight is 1.741×10^{-13} N. This weight was even picked with a copper e-beam coated micro-part with the worst *rms* surface roughness value of 217 nm which exerted an experimentally measured Van-der-Waals force of 17×10^{-9} N (17 nN) as indicated in Table 4.3.

However; the Van-der-Waals' forces exerted by polyurethane are too high for some micro-material handling operations because they do not easily release the micro-parts they would have picked. In addition; since polyurethane materials are polymers, they are softer than metals, which means they may not be useful in the picking and placing of sharp micro-parts as the sharp micro-parts may become imbedded in them. In such cases, hard metallic e-beam generated gripping surfaces would be more suitable.

4.7 Strategies and Decision Support Systems for using Van-der-Waals' forces

Based on the experimental findings and the synthesised literature review in this dissertation, four main strategies of employing Van-der-Waals' forces were developed. These were based on the controllable properties of the interacting surfaces, namely; material type, geometrical configuration (as discussed in Section 2.6.4 where an analysis was conducted) and surface roughness variations. These strategies are referred to as Strategy 1 (material type), Strategy 2 (geometrical configuration), Strategy 3 (surface roughness) and Strategy 4 (a hybrid consisting of at least two of the fundamental strategies just mentioned). The hybrid strategy is further broken into four sub-strategies, categorized as Option 1 (a combination of Strategy 1 and Strategy 2), Option 2 (a combination of Strategy 1 and Strategy 3), Option 3 (a combination of Strategy 2 and Strategy 3) and Option 4 (a combination of Strategy 1, Strategy 2 and Strategy 3). These strategies were developed for a flat surfaced work-part of uniform *rms* surface roughness values on both sides.

In the case where the geometrical configuration and the surface roughness of the interacting materials are correspondingly equal, Strategy 1 would be used. This strategy requires that material types be logically varied in order to improve the reliability of a pick-transfer-place cycle. The micro-gripper should exert a higher Van-der-Waals' force on the micro-part than the picking place. For an effective release to be realised, the material of the placement position should exert higher Van-der-Waals' forces on the micro-part than the micro-gripper. In this case, polyurethane of a shore hardness value 60A (polyurethane 60) was experimentally found to exert lower Van-der-Waals' forces than that of a shore hardness 30A (polyurethane 30), as indicated in Table 4.4. Therefore; the former is suitable for either the picking position or the gripper's interactive surface, and the latter for the placement position. Micro-materials of dimensions 10 mm and below; which included integrated circuit (IC) components; were practically picked by the polyurethane 60 micro-gripper from wooden and metallic bases and placed onto a polyurethane 30 base (as stated earlier) employing this strategy.

In micro-material handling operations where the interacting materials are of the same material type and of equal *rms* surface roughness values, Strategy 2 should be employed. This strategy utilises the logical variation of the geometrical configuration of interacting materials for an effective micro-material operation to be realised. Since Van-der-Waals forces vary directly as the interactive area between the objects involved, this strategy requires the picking position to have less interactive area than the micro-gripper on a given micro-part (as detailed in Section

2.6.4 and as shown in Figure 4.50). Subsequently, the placement position should have a greater interactive area than the micro-gripper for an easy release of the micro-part to be realised.

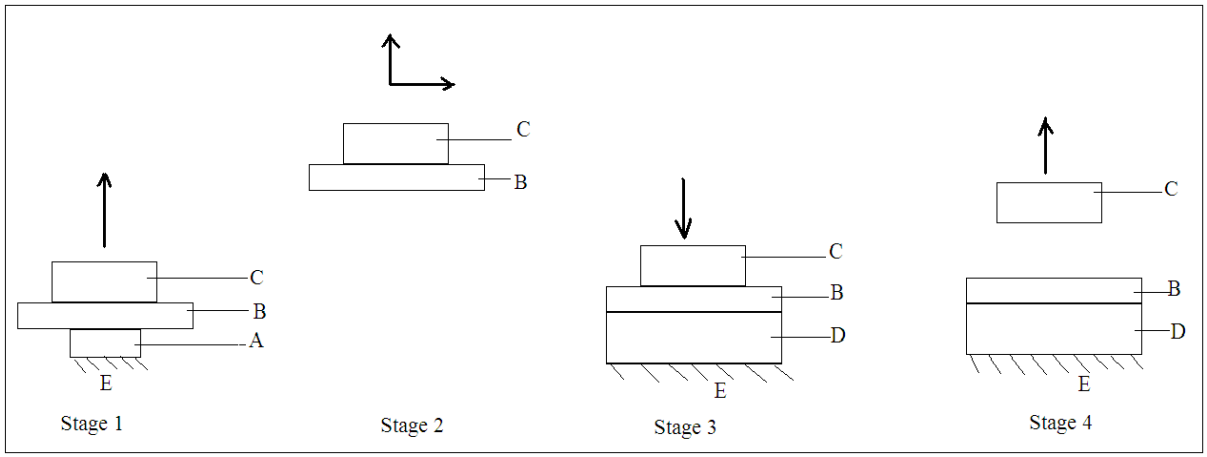

Figure 4-50 Flat geometries in which the interactive contact area is increased for material handling purposes. The arrows show the direction of motion.

In Figure 4.50, the micro-gripper C has a greater interactive area on micro-part B than that of picking position A; and the placement position D has a greater interactive area on B than that of micro-gripper C. It should be noted that both A and D should be fixed and immovable for an effective micro-material handling operation to be realised.

Another option would be to have a spherical picking position, a cylindrical gripper and a flat placement position in order to have a progressive increase in contact area, as discussed in Section 2.6.4 and as shown in Figure 4-40.

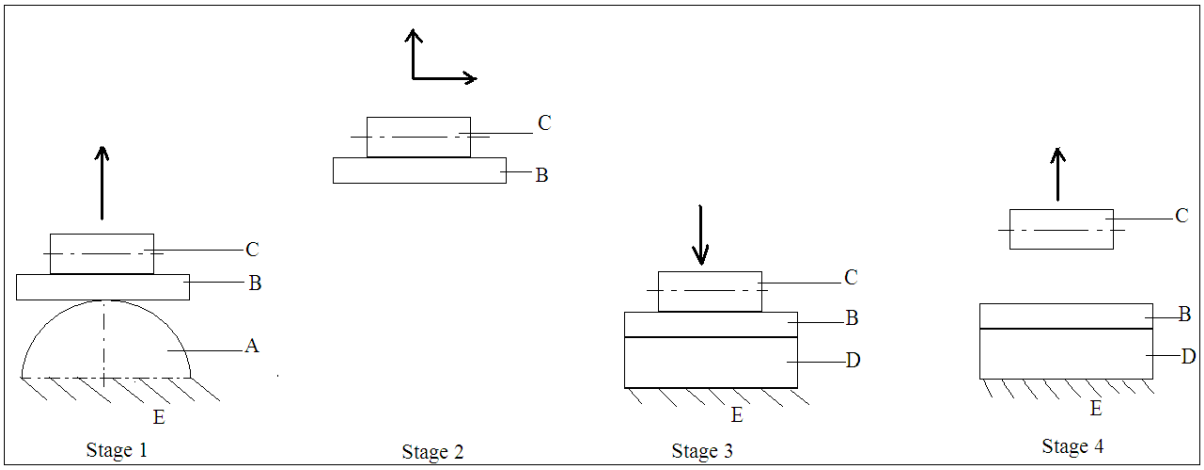

Figure 4-51 Geometrical configuration variation for a micro-material handling operation in which the picking place, A, is spherical; micro-gripper, C, is cylindrical, placement position, D, is flat; and the micro-part, B, to be handled is flat. The arrows show the direction of motion.

In cases where the interacting surfaces are of same material type, same geometry and of equal area; surface roughness variation can be employed as Strategy 3. Since it has been proven that

Van-der-Waals' forces decrease as *rms* surface roughness values increase, the interactive surface area of the picking position should be rougher than that of the micro-gripper, for a micro-part to be picked. For a reliable release to be achieved, the interactive surface area of the micro-part with the placement position should be smoother (have a lower *rms* value) than that of the micro-gripper. The applicability of this strategy can be explained using the validated Ag 20.1 and Ag 5.2 samples of equal interactive area which had empirical *rms* surface roughness values of 1.41 nm and 0.66 nm, respectively, and exerted corresponding Van-der-Waals' forces of 111 nN and 260 nN. The Ag 20.1 can be used for the interactive surface of the picking position and the Ag 5.2 for the placement position.

Nevertheless; some micro-material handling operations would be so complex that one pure strategy may not be reliable. The fourth option would be to use a hybrid strategy, termed Strategy 4, which is a combination of at least two previously mentioned strategies, as shown in the matrix Table 4.5.

Table 4.5 Matrix table for Strategy 4 showing options of hybrid strategies

	Strategy 2 (Geometry)	Strategy 3 (Surface roughness)
Strategy 1 (Material type)	Option 1 (Strategies 1&2)	Option 2 (Strategies 1&3)
Strategy 2 (Geometry)	Not a hybrid	Option 3 (Strategies 2 &3)
Strategy 3 (Surface roughness)	Already considered as Option 3 (Strategies 2 &3)	Not a hybrid
Option 1 (Strategies 1&2)	Already considered as Option 1 (Strategies 1&2)	Option 4 (Strategies 1, 2 &3)

In micro-material handling operations in which the interacting surfaces are of equal *rms* surface roughness values, hybrid strategy Option 1 would be used. This option combines Strategy 1 and Strategy 2. In this case; the picking position, micro-gripper and placement position would be made separately of different materials. Their geometrical configurations are designed so that the interactive area of the micro-part with the picking place, micro-gripper and the placement position, should increase successively as indicated in Figure 4.50 or Figure 4.51; and the interactive Hamaker coefficients of the interacting materials should correspondingly increase; in order to achieve a reliable pick-transfer-place cycle. For example; in this research, a 10 mm x 10 mm IC component was picked from a wooden base

by a 4-mm radius polyurethane 60 gripper and placed onto an 8-mm radius polyurethane 30 base.

When a material handling operation involves surfaces of same geometrical configuration and same interactive area, hybrid strategy Option 2 should be used. Option 2 is a combination of Strategy 1 and Strategy 3. In this option, the interactive surface of the micro-part with the picking place, micro-gripper and the placement position would be made of different materials, of increasing Hamaker coefficients, respectively, and of successively decreasing surface roughness. For example, considering the samples used in this research, a suitable combination would be Cu 5.1, Al 5.2 and Ag 5.2, of decreasing *rms* surface roughness values of 2.72 nm, 1.2 nm and 0.66 nm, respectively. Their empirical Van-der-Waals' forces would accordingly be 24 nN, 44 nN and 260 nN. Therefore; in this option, the interactive surfaces of the picking position, the micro-gripper and the placement position should be Cu 5.1, Al 5.2 and Ag 5.2, respectively.

In cases where the interacting surfaces in a micro-material handling operation are of the same type, Option 3 would be suitable. Option 3 of the hybrid strategies combines Strategy 2 and Strategy 3. In this case, when a similar material is used for all micro-material handling components, then the interactive geometrical areas of the micro-part with the picking position, micro-gripper and placement position should increase successively. However; their *rms* surface roughness values should decrease correspondingly, for an effective micro-material handling operation to be realised. For example; the validated samples of copper namely; Cu 5.1, Cu 5.2 and Cu 20.2; of corresponding *rms* surface roughness values of 2.72 nm, 1.5 nm, 0.9 nm; and their geometrical configurations being spherical, cylindrical and flat, respectively as in Figure 4.51; would correspondingly be used for the picking position, micro-gripper and placement position's interactive surfaces to achieve a reliable micro-material handling system.

In complicated micro-material handling cases where the interacting surfaces are of different materials, geometrical configurations and surface roughnesses, Option 4 would be appropriate. Option 4 of the hybrid strategies combines all the three fundamental strategies: Strategy 1, Strategy 2 and Strategy 3. The choice of material should ensure that the interactive Hamaker coefficients of the micro-part with the picking position, micro-gripper and placement position should increase successively. The geometrical configurations should ensure that the interactive areas of the micro-part with the picking position, micro-gripper and placement position should increase successively. However, *rms* surface roughness values

should decrease correspondingly for a reliable micro-material handling system to be realised. The example in Option 2 can be modified into Option 4 by adding a geometrical configuration element so that the Cu 5.1 picking place is spherical, the Al 5.2 micro-gripper is cylindrical, and the Ag 5.2 placement position is flat as in Figure 4.51.

A decision support system (DSS) is also developed, as illustrated in Figure 4.52, to aid in the identification of the correct strategy to use in a given micro-material handling situation. The first step in the synthesised DSS is task definition. This includes identifying the type of materials to be used, their geometrical configuration and their *rms* surface roughness values. Next is the selection of the correct strategy governed by the pick-transfer-place criteria as stipulated in the strategies discussed.

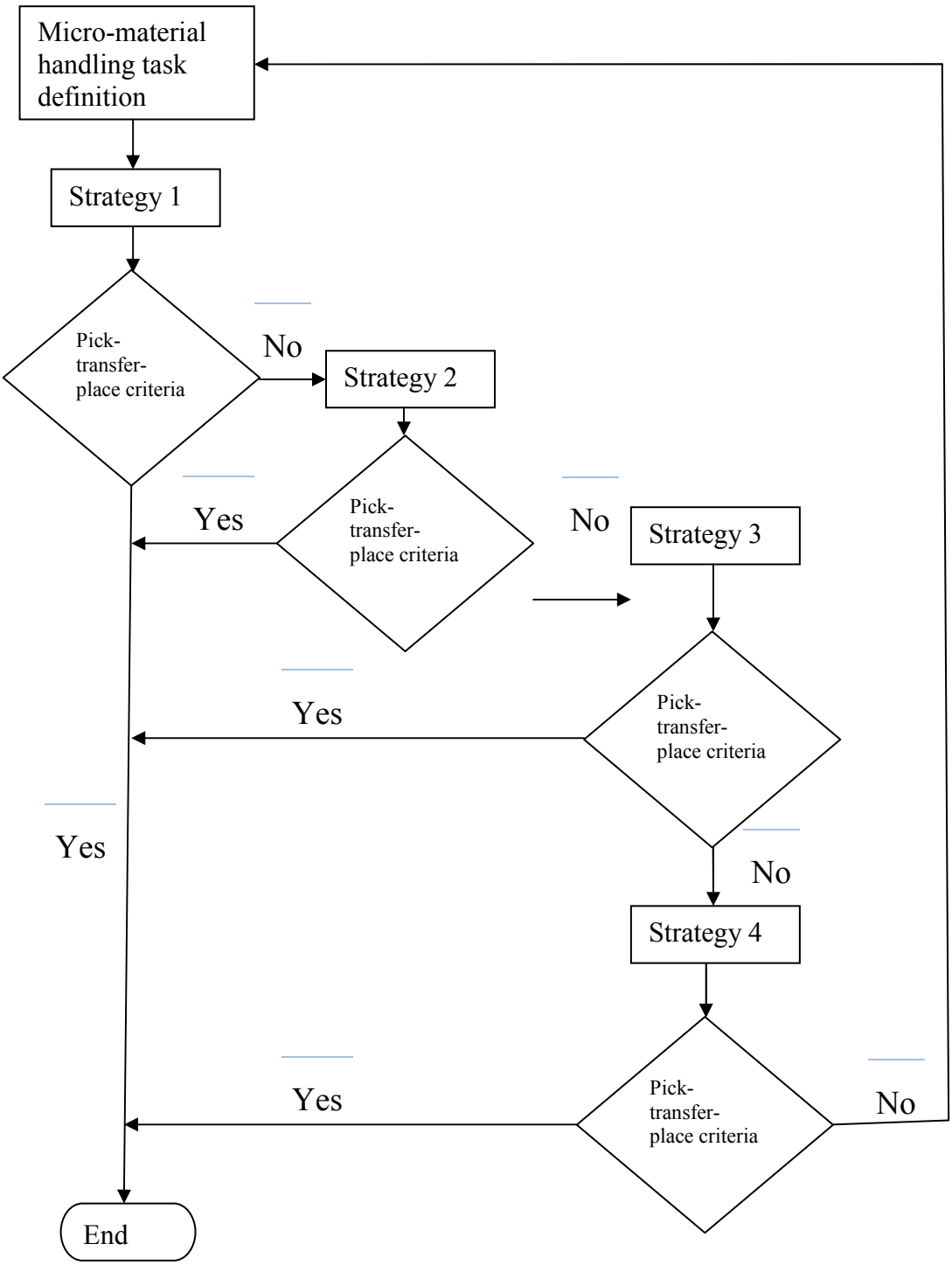

Figure 4-52 DSS for a Van-der-Waals' force actuated micro-material handling strategy

It should be emphasized that for picking to be realised, the combined weight of the micro-part and the Van-der-Waals' forces exerted by the picking position, should be less than the Van-der-Waals' forces exerted by the micro-gripper. The picking position must be firm in order to avoid it being picked together with the micro-part. For an effective release of a micro-part, the placement position should exert greater Van-der-Waals forces than the combined effect of the weight of the micro-part and the gripper's Van-der-Waals' forces. In addition to that, the gripper and the placement position should be firm in order for a transfer of the micro-part to take place.

5 CHAPTER 5: CONCLUSIONS AND RECOMMENDATIONS

This research focused on the application of Van-der-Waals' forces in a micro-material handling system which consists of a picking place, micro-part, micro-gripper and the placement position. It identified material type, geometrical configuration and surface roughness as the main independent parameters of Van-der-Waals' forces as shown in Section 2.6. The research proved true the null hypothesis that Van-der-Waals' forces can be effectively applied in a micro-material handling system as shown in the numerical modelling in Section 4.2 and the experimental measurement of the forces exerted by e-beam deposited samples in Section 4.3. The picking and placing experiments (in Section 4.5) of IC components also proved true this hypothesis.

The research questions have been addressed as follows:
Sub-question 1: What are Van-der-Waals' forces? They are defined in Section 2.2 as adhesive forces which cause particles to adhere to surfaces, or surfaces to adhere to each other, due to spontaneous electrical and magnetic polarisations which occur when surfaces are in close proximity to one another. The Van-der-Waals' forces embody three types of forces: firstly, the force between two permanent dipoles - referred to as Keesom force; secondly, the force between a permanent dipole and a corresponding induced dipole - known as Debye force; and thirdly, the force between two instantaneously induced dipoles - referred to as London dispersion force.

Sub-question 2: Why should they be used in a micro-material handling system? This question is addressed in Section 1.2 and Section 2.3 where it is highlighted that Van-der-Waals' forces can work in almost all conditions including vacuum and aqueous conditions. Although they require clean environments for operational purposes, they have the advantage that they do not strain the micro-workpart, they do not leave residual charges, stresses or oxide layers on the interactive surface. They also do not require any energy supply to activate them for operational purposes.

Sub-question 3: Which parameters greatly influence Van-der-Waals' forces? The parameters which influence the intensity of the exerted Van-der-Waals' forces are identified in Section 2.6 as: material type, geometrical configuration, surface roughness, temperature and humidity. The two latter parameters were found to be less significant than the former three. When the

analytical modelling of geometrical parameters against Van-der-Waals' forces was executed, the flat-flat interactive surfaces were found to exert the greatest force compared to others, based on their large contact area. An analysis of the geometrical configuration with respect to DFMA and DFμA criteria, revealed that a flat surfaced gripper has the highest design efficiency since it (flat gripper) has the lowest part count value and requires the least equipment (jigs and fixtures) to manufacture it. Therefore; in this research, flat surfaced gripping surfaces were used. The experimental measurement of the Van-der-Waals' force exerted by the e-beam deposited samples, proved that surface roughness predominates over material type (as in Section 4.4). Material type was found to be less significant than surface roughness parameters in influencing the exerted Van-der-Waals' forces, since the Hamaker constants are of the order of 10^{-21}J, as shown in Section 2.6 and Appendix E; and *rms* surface roughness values are of the order of 10^{-9} m, as in stated in Sections 4.1, 4.2, 4.3 and 4.4. It has been proven that the rougher the interactive surface, the lower the Van-der-Waals' forces exerted. Nevertheless; polyurethane has been found to exert higher Van-der-Waals' forces than the metals, as indicated in Sections 2.6, 4.3, 4.4, 4.5 and 4.6.

Sub-question 4: What are the components of a micro-material handling system? The components are highlighted in Sections 1.2, 4.3, 4.4, 4.5 and 4.7 as micro-workpart, picking position, micro-gripper and placement position.

Sub-question 5: How can Van-der-Waals' forces be used to realise a reliable micro-material handling operation? This question was addressed in Sections 2.6, 4.2, 4.3, 4.4, 4.5 and 4.7 where it was highlighted that logical variations of material type, geometrical configuration and surface roughness lead to the control of the exerted Van-der-Waals' forces. Therefore; these parameters have to be optimised in order to realise a reliable Van-der-Waals' forces' actuated material handling system. This then led to the development of the strategies of applying Van-der-Waals' forces in micro-material handling operations. In the final analysis, it was observed that surface roughness had the greatest influence on the exerted Van-der-Waals' forces, in the case of metallic e-beam coatings. Therefore; reliable strategies can be based on surface roughness.

Sub-question 6: What strategies should be employed to effectively use Van-der-Waals' forces in a micro-material handling operation? The answering of this sub-question resulted in the solution of the main research question. Four main strategies were identified in Section 4.7 and

a DSS was also developed, based on the main parameters which influence Van-der-Waals' forces. These were: Strategy 1 (material type), Strategy 2 (geometrical configuration), Strategy 3 (surface roughness) and Strategy 4 (a hybrid consisting of at least two of the fundamental strategies just mentioned). The hybrid strategy was further broken into four sub-strategies, categorized as Option 1 (a combination of Strategy 1 and Strategy 2), Option 2 (a combination of Strategy 1 and Strategy 3), Option 3 (a combination of Strategy 2 and Strategy 3) and Option 4 (a combination of Strategy 1, Strategy 2 and Strategy 3). In order for picking to be realized, the weight of the micro-part (together with the Van-der-Waals' forces exerted by the pick-up position) should be less than the Van-der-Waals' forces exerted by the micro-gripper. Again, the picking position should be firm or else it would also be picked together with the micro-part. For the reliable release of a micro-part, the placement position should exert greater Van-der-Waals' forces than the combined effect of the weight of the micro-part and the gripper's Van-der-Waals' forces. Again, the gripper and the placement position should be secured in order for a transfer of the micro-part to take place. Furthermore; for an effective pick-transfer-place cycle to be realised, at least one of the following criteria should be satisfied, depending on the strategy used:

1. The interactive Hamaker coefficient of the micro-part with the picking position, micro-gripper and placement position should increase successively.
2. The interactive surface area of the micro-part with the picking position, micro-gripper and placement position should increase consecutively.
3. The surface roughness values of the interactive surface area of the micro-part with the picking position, micro-gripper and placement position should decrease consecutively.

However; there are limitations to the application of Van-der-Waals' forces in micro-material handling operations. They are short range forces, operating effectively in separation distances falling under the non-retarded region which happens to be in the nano-range and in some cases less than 10 nm. Therefore; in most cases they require contact between interactive surfaces to enable a micro-material handling operation. A clean environment is required which might be expensive to maintain in manufacturing conditions.

Van-der-Waals' forces are advantageous in that they do not leave oxide layers on interacting surfaces, as is the case with surface tension forces on some surfaces; they do not leave residual charges, as is the case with electrostatic force gripping; they do not strain the micro-material, as is the case with vacuum and other mechanically gripping forces. They do not

require an external energy sources for the purposes of gripping, as is the case with vacuum and electrostatic forces. Van-der-Waals' forces' actuated micro-grippers are also beneficial in that they are able to work in vacuum conditions whereas surface tension and vacuum-force actuated micro-grippers cannot. Van-der-Waals' forces are also advantageous in that they can work in aqueous conditions whereas electrostatic forces cannot.

5.1 Unique contribution of the research

The unique contribution of this research is that it proved that Van-der-Waals' forces are usable in micro-material handling operations. The Van-der-Waals' forces were experimentally measured for copper, aluminum, silver and polyurethane specimens. The research revealed how the Van-der-Waals' forces can be used in micro-material handling operations. The research revealed strategies based on material type, geometrical configuration and surface roughness in utilising Van-der-Waals' forces for micro-material handling purposes. It then provided a decision support system for choosing a suitable strategy. The research identified surface roughness as the main parameter influencing the exerted Van-der-Waals' forces and uniquely used e-beam evaporation method to generate characterisable surfaces of uniform surface roughness (in the case of metals) for micro-material handling operations. It distinctly proved that e-beam depositions (conducted over durations within the 2-min and 20-min range) of copper, aluminium and silver have Van-der-Waals' forces as their predominant gripping force at a humidity level of 20%, a temperature of 23^0C, and atmospheric pressure of 101.325 Pa, when no external energy is applied (as observed on their extending curves in Section 4.3.1). The research went on further to indicate that polyurethane material exerts more Van-der-Waals forces than metallic e-beam coatings. In addition the research provided practical examples of the application of Van-der-Waals' forces actuated micro-material handling operations by utilising polyurethane micro-grippers in the assembling of IC components onto electronics circuit boards.

5.2 Recommendations

Since Van-der-Waals' forces can work under various conditions in the micro-range they are recommended for micro-material handling operations in micro-factories. They are recommended for operations where the planes are oriented in any direction (including inverted planes); for micro-parts where the weights are less than the exerted Van-der-Waals' forces. They are usable in micro-material handling operations conducted in confined, small

compartments; for example, brief-case sized micro-factories, as shown in Figure 1.2. This then allows micro-assembly operations to be performed whilst micro-factories are in transit.

Since they can work under vacuum conditions and do not require an external energy sources, they may be recommended for use in remote environments which include space explorations. They may also be used for micro- and nano-robotic operations of patients as they can work in aqueous conditions and do not leave any residual charges, strains and oxides. On the same note, they are recommended for the handling of IC circuits and brittle micro-parts. They are also adaptable to manual and automated operations, which make them versatile in their applications.

Since the Van-der-Waals' forces are dependent on material type, they may be recommended for use in the segregation and sorting of micro-materials. They may also be used in the extraction and purification of minerals, especially when in a powder state.

They are also recommended for intricate clamping operations, for example, in micro-milling operations. They simplify the clamping mechanism in that they do not always rely on moving parts for clamping operations. They are capable of clamping without the use of mechanical-fingers. Hence, the design efficiency of such clamps would be high, since the number of moving parts is greatly reduced. Figure 5-1 shows a comparison of mechanical clamping and Van-der-Waals' forces' clamping, where the latter is proven to have a better design efficiency.

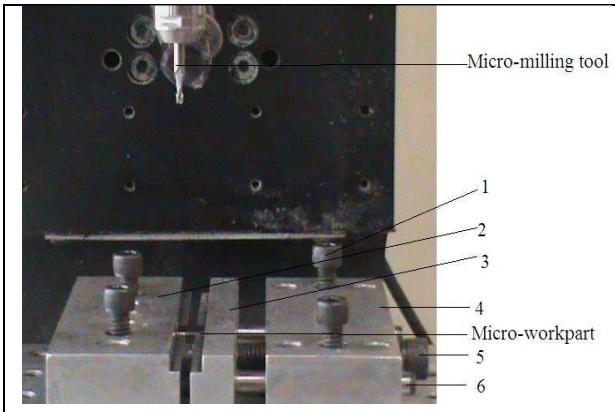

Design 1: Mechanical clamping for micro-milling

Design 2: Polyurethane clamping actuated by Van-der-Waals' forces

Part	No.	Theoretical part count	Assembly time (s)
End plate (left) (item 2)	1	1	8.4
End plate screws (left) (item 1)	2	0	16.6
End plate (right) (item 4)	1	1	8.4
End plate screws (right) (item 1)	2	0	16.6
Lead screw (item 5)	1	0	8.4
Thread leads	-	-	5.0
Middle plate (item 3)	1	0	8.4
Sliding shaft (item 6)	2	0	16.6
Totals	10	2	88.4
Design efficiency = (2 x 3)/88.4 = 6.8%			

Part	No.	Theoretical part count	Assembly time (s)
Base plate (left)	1	1	8.4
Totals	1	1	8.4
Design efficiency = (1 x 3)/8.4 = 35.7%			

Figure 5-1 DFMA and DFμA analysis of two clamping designs

The assembly times used in the comparison in Figure 5.1 are similar to those used in Section 2.5. In Figure 5-1, the mechanical micro-milling clamp has 4 x item number 1 (four items of part number 1 type), 1 x item number 2, 1 x item number 3, 1 x item number 4, 1 x item number 5 and 2 x item number 6, resulting in a total of 10 items. However; items number 2

and 5 are screws and items numbered 3 (middle plate) and 6 (sliding shaft) are not essential, according to DFMA (Boothroyd, 1994) and DFμA (Tietje et al, 2008) principles, as described in Section 2.5. When Equation 2.23 is applied, the mechanical clamp (Design 1) is found to have a design efficiency of 6.8%, 5 times less than that of the polyurethane clamp (Design 2) of 35.7%.

5.3 Future work

Future work involves technological transfer of Van-der-Waals' forces' actuated micro-material techniques to micro-manufacturing industries; for example, the electronics industry. Research on material type, geometrical configuration, and surface roughness combinations which result in the optimisation of the exerted Van-der-Waals' forces still need further exploration. The determination of the percentage of the actual contact area, for a given *rms* surface roughness value of a sample under examination, still needs to be explored. Determination of the peeling off force required to release a micro-part attached by Van-der-Waals' forces from a given surface, also needs investigation.

5.4 Research Outputs and Recognition of the PhD study

The researcher co-authored thirteen peer reviewed papers shown in Appendix A and Appendix L. Ten were accepted and published by end of June 2012, and three were under review. Two were presented and published at accredited regional conferences [(1) SAIIE 2009, (1) SAIIE 2010], four at accredited international conferences [(1) COMA'10, (2) ISEM 2011, (1) CIE 2012], four in accredited journals listed on the South African Index [(2) JNGS, (2) SAJIE]. One submission to 'Journal for New Generation Sciences' (JNGS) is still under review as well as the latest submission to the 'Journal of Colloid and Interface Science' (JCIS). Another latest peer reviewed abstract was accepted for the COMA'13 international conference, 2013.

The researcher also gained international recognition as is evident in his invitation from Chemnitz University of Technology, Germany, where he stayed for three months as a visiting Research Scientist in micro-material handling systems. He worked in the Institute for Machine Tools and Forming Technology under the PT-PIESA (A2) project from the 1st of February to the 29th of April, 2011. The research visit was supported by the German Research Foundation (DFG) as part of the special research field SFB/TR 39. He then submitted a technical report to the DFG as summarized in Appendix C. He also co-authored two

international ISEM 2011 conference papers during the same period with Prof Neugebauer, R; Dr. Koriath, H-J; Dr. Van der Merwe, A. F; and Mr Müller, M.

As a result of this study, collaborative research ventures were established between the Industrial Engineering Department at Stellenbosch with:

1. iThemba Labs, Cape Town, South Africa (Appendix B);
2. Chemnitz University, Germany (Appendix C);
3. Florida University, USA (Appendix D);
4. The National University of Science and Technology (NUST), Zimbabwe.

The researcher was again identified as one of the top three PhD Engineering students graduating in December, 2011 and March, 2012 and was requested to present his research findings at a PhD research colloquium, held on the 2nd of December, 2011.

REFERENCES:

Aksak, B., Murphy, M., and Sitti, M. . (2007). Adhesion of Biologically Inspired Vvertical and Angled Polymer Microfiber Arrays. *Langmuir, 23(6)*, 3322–3332.

Arai F, Ando D., Fukuda T., Nonoda Y., Oota T. (1995). Micro Manipulation Based on Micro Physics. *Proceedings of IEEE/RSJ International Conference on Intelligent Robots Systems*, *2*, pp. 236-241.

Attia, U.M. and Alcock J.R. (2011). A review of the micro-powder injection moulding as a microfabrication technique. *Journal of Micromechanics and Microengineering, 21* (043001), 22 pages

Autum K., Sitti M., Liang Y.A., Peattie A.M., Hansen W. R., Sponberg S., Kenny T.W., Fearing R., Israelachvili J.N., Full, R.J. (2002). Evidence for Van- der- Waals' Adhesion in Gecko Setae. *99*, pp. 12252-12256. National Academy of Sciences (PNAS).

Atsushi, K; Sueyasu, H.; Funayama Y.; Maekawa, T (2011) System for Reconstruction of Three-dimensional Micro-objects from Multiple Photographic Images, Computer-Aided Design, Volume 43, Issue 8, Pages 1045–1055

Bark C. & Binnenboese T. (1998). Gripping with Low Viscocity Fluids. *Proceedings of IEEE International Workshop on MEMS*, (pp. 301-305). Hiedelberg.

Barthel, E. (1998). J. Colloid Interface Sci. *J. Colloid Interface Sci, 200*, 7.

Batsanov, S. S. (2001). Van-derWaals' Radii of Elements. *Inorganic Materials, 37*(9).

Bergstrom, L. (1997). Hamaker Constants of Inorganic Materials. *Advances in Colloid and Interface Science, 70*, 125-169.

Bhushan, B. (2003). Adhesion and Stiction: Mechanisms, Measurement Techniques and Methods for Reduction. *B21*(6), 2262-2296.

Biganzoli F., Fantoni G. (2008). A Self-centering Electrostatic Microgripper. *Journal of Manufacturing Systems , 27*, 136-144.

Bohringer K.F., Fearing R.S., Goldberg K.Y. (1999). Micro-assembly. In N. S. (Ed.), *Handbook of idustrial robotics. 2nd Edition.* Wiley & Sons.

Bohringer K.F., Goldberg K.Y., Cohn M., Howe R., and Pisano A. (1998). Parallel Micro-assembly with Electrostatic Force Fields. *Proceedings of IEEE International Conference on Intelligent Robotics and Automation*, (p. 1204). New York.

Boothroyd, G. & Alting, L. (1992). Design for Assembly and Disassembly. *Annals of the CIRP, 41*(2), 625–636.

Boothroyd, G. (1994). Product Design for Manufacture and Assembly. *Computer-Aided Design, 26*(7).

Bowen W.R., Jenner F. (1995). The Calculation of Dispersion Forces for Engineering Applications. *Advances in colloid and interface science, 56*, 201-243.

Bowen W.R., Lovitt R.W. and Wright C.J.,. (2001). Journal of Mater. Sci. *Journal of Mater. Sci., 36* , 623.

Bradley, R. (1932). Philos. Mag. *13*, 853.

Buhmann, S.Y. & Welsch, D.G. (2007). Review: Dispersion Forces in Macroscopic Quantum Electrodynamics. *Progress in Quantum Electronics, 31*, 51–130.

Butt, H.J., Berger, R., Bonaccurso, E., Chen, Y., Wang, J. (2007). Impact of Atomic Force Microscopy on Interface and Colloid Science. *Advances in Colloid and Interface Science, 133*, 91–104.

Butt, H-J., Cappella, B. and Kappl, M. (2005). Force Measurements with the Atomic Force Microscope: Technique, Interpretation and Applications . *Surface Science Reports , 59*(1-6), 1-152.

Cao J., Krishnan N., Wang Z., Lu H., Liu W.K., Swanson A. (2004). Microforming: Experimental investigation of the Extrusion Process for Micropins and its Numerical Simulation using RKEM. *Journal of Manufacturing Science and Engineering, 126 (4),* 642-652

Casimir H. B. G., Polder D. (1948). The Influence of Retardation on the London-Van- der-Waals' Forces. *Physical Review, 73*(4), 360–372 .

Cooper K., Gupta A. and Beaudoin S., J. . (2001). Electrochem. Soc. *Electrochem. Soc., 148*, 662.

Cooper K., Gupta A. and Beaudoin S., J. (2000). Colloid Interf. Sci. . *Colloid Interf. Sci. , 228*, 213.

Cooper K., Ohler N., Gupta A. and Beaudoin S., J. . (2000). *J. Colloid Interf. Sci.*, 63.

Creton C. and. Leibler L. (1996). J. Polym. Sci. B. *J. Polym. Sci. B, 34*, 545.

Danov K. D., Kralchevsky P. A., Ananthapadmanabhan K. P., Lips A. (2006). Particle-interface Interaction across a Nonpolar Mmedium in Relation to the Production of Particle-stabilized Emulsion, *Langmuir* 22, 106-115.

Debrincat, D.P., Solnordal, C.B., Van Deventer, J.S.J. (2008). Characterisation of Inter-particle Forces within Agglomerated Mmetallurgical powders. *Powder Technology, 182*, 388–397.

DelRio, F.W., De Boer, M.P., Knapp, J.A, Reedy, E.D. (Jr), Clews, P.J., Dunn, M.L. (2005). The Role of Van-der-Waals' Forces in Adhesion of Micromachined Surfaces. *Nature Materials, 4*, 629–634.

Derjaguin B.V., Titijevskaia A.S., Abrikossova I.I., and Malkina, A.D. (1954). Investigation of the Forces of Interaction of Surfaces in Different Media and their Application to the Problem of Colloid Stability. *Discussions of the Faraday Society*, *18*, pp. 24-41.

Derjaguin B.V., Muller V.M. and Toporov, Y.P.. (1975). *Journal of Colloid Interface Sci., 53*, 314.

Derjaguin,B.V., Muller,V.M. and Toporov,Y.P. . (1994). Prog. Surf. Sci. *Prog. Surf. Sci.*, 131-143.

Dini G., Fantoni G. and Failli F. (2009). Grasping Leather Plies by Bernoulli grippers. *CIRP Annals - Manufacturing Technology, 58*, 21–24.

Dzyaloshinskii I.E., Lifshitz E.M., Pitaevskii L.P. (1961). The General Theory of Van-der-Waals' forces. *Advances in Physics, 10*(38), 165-209.

E-beam machine, courtesy of iThemba Labs. (n.d.).

Eichenlaub S., Gelb A., Beaudoin S. (2004). Roughness Models for Particle Adhesion,. *Journal of Colloid and Interface Science, 280*, 289–298.

Eichenlaub, S., Kumar, G., Beaudoin, S. (2006). A Modelling Approach to Describe the Adhesion of Rough, Asymmetric Particles to Surfaces . *Journal of Colloid and Interface Science, 299*, 656–664.

elmics. (2011). http://www.elmics.ru.

Erlandsson, R., Hadziioannou, G., Mate, C.M., McClelland, G.M. and Chaing, S. (1988). J. Chem. Phys. *J. Chem. Phys. , 89*, 5190.

experiment-resources.com. (Accessed 12 November 2011). *http://www.experiment-resources.com/empirical-research.html*.

Fantoni, G. (2003). Assembly of Mini and Microparts: Development of an Electrostatic Feeder. *In Proc. of 6th A.I.Te.M. Int. Conf.*

Fatikow, S., Seyfried, J., Fahlbusch, S., Buerkle, A., Schmoeckel, F. . (2000). A Flexible Microrobot-based Micro-assembly Station. *Journal of Intelligent and Robotic Systems, 27*, 135–169.

Fearing, S. (1995). Survey of Sticking Effects for Micro-parts Handling. *IEEE/RSJ International Workshop on Intelligent Robots & Systems (IROS)*, (pp. 212-217). Pittsburgh.

Feddema J.T., Xavier P., and Brown R. (1999). Micro-assembly Planning with Van-der-Waals' force. *Proceedings of IEEE International Symposium on Assembly and task Planning*, (pp. 32-38). Porto.

Feng S. and Li T. (2006). Predicting Lattice Energy of Organic Crystals by Density Functional Theory with Empirically Corrected Dispersion Energy. *Journal of Chemical Theory and Computation, 2*(1), 149–156.

Ferguson G.S., Chaudhury M.K., Sigal G.B., Whitesides G.M. (1991). Contact Adhesion of Thin Gold Films on Elastomeric Supports: Cold Welding Under Ambient Conditions. *Science, 253*(5021), 776.

Filippov, A.E. & Popov,V. (2006). Optimal Elasticity of Adhesives Mimicking Gecko Foot-hairs. *Physics Letters A, 358*, 309–312.

Fowkes, M. F. (1963). Additivity of Intermolecular Forces at Interfaces, I. Determination of the Contribution to Surface and Interfacial Tensions of Dispersion Forces in Various liquids. *Journal of Physical Chemistry, 67*(12), 2538–2541.

French, R. H. (2000). Origins and Applications of London Dispersion Forces and Hamaker Constants in Ceramics. *Journal of the American Ceramic, 83* (9), 2117–2146.

Fukuda T. & Arai F. (1999). Microrobotics. In *Handbook of Industrial Robotics* (pp. 187–198). New York: John Wiley & Sons, Inc.

Gao, H., Wang, X., Yao, H., Gorb, S., Arzt, E. (2005). Mechanics of Hierarchical Adhesion Structures of Geckoes. *Mechanics of Materials, 37*, 275–285.

Geim, A. K., Dubonos, S. V., Grigorieva, I. V.; Novoselov, K. S.; Zhukov, A. A., Shapoval, S. Y. (2003). Microfabricated Adhesive Mimicking Gecko Foot-hair. Nature Materials. *2*, 461-463.

Glassmaker N. J., Jagota A., Hui, C. Y., Kim, J. (2004). Design of Biomimetic Finterfaces:1. Making contact. *Journal of the Royal Society Interface, 1*(1), 23-33.

Götzinger M. and Peukert W. (2004). Langmuir. *Langmuir, 20*, 5298.

Gotzinger M., Peukert W. (2003). Dispersive Forces of Particle–surface Interactions: Direct AFM measurements and modelling . *Powder Technology, 130*, 102– 109.

Greenwood, J. P. (1997). *Proc. R. Soc. London A*, *453*, p. 1277.

Greenwood, J.A. and Johnson, K.L. (1998). J. Phys. D Appl. Phys. *J. Phys. D Appl. Phys., 31*, 3279.

Groover, M.P. (2011) Principles of Modern Manufacturing. John Wiley & Sons , Asia.

Guoliang C. & Xinhan H. (2004). Research on Vacuum Micro-Gripper of Intelligent Micromanipulation Robots . *Proceedings of the IEEE International Conference on Robotics and Biomimetics.* Shenyang.

Haliyo D.S., Rollot Y., and Regnier. (2001). Dynamical Strategies for the Micro-manipulation by Adhesion. *Proceedings of SPIE Conference on Microrobotics and Micromanipulation*, *4568*, pp. 261-269. Newton.

Halsey T.C. and Toor W. (1990). Fluctuation-induced Couplings between Defect Lines or Particle Chains. *Journal of Statistical Physics, 61*(5-6), 1257-1281.

Hamaker. (1937). The London-Van-der-Waals' Attraction between Spherical Particles. *Physica, IV*(10).

He M., Blum A.S., Aston D.E., Bueviage C., Overney R.M., Luginbuhl R. (2001). Critical Phenomena of Water Bridges in Nanoasperity Contacts. *Journal of Chemical Physics, 114*(3), 1355-1360.

Hertz. (1882). *J. Reine Angew. Math*, 156.

Hesselbach J., Buttgenbach S., Wrege J., Butefisch S., and Graf C. (2001). Centering Electrostatic Microgripper and Magazines for Microassembly Tasks. *In Proc. of SPIE Microrobotics and Micromanipulation*, *4568*, pp. 270–277. Newton.

Hesselbach J., Wrege J., Raatz A. (2007). Micro Handling Devices Supported by Electrostatic Forces. *Annals of the CIRP-Manufacturing Technology, 56*(1), 45-48.

HowStuffWorks. (2007).

http://www.galilmc.com/products/dmc-21x3.php. (n.d.).

Huang X., Chang L. and Ming W. (2010). An Automatic Vacuum Microgripper. *Proceedings of the 8th World Congress on Intelligent Control and Automation.* Jinan.

Huber, G., Gorb, S. N., Hosoda, N., Spolenak, R. Eduard Arzt, E. (2007). Influence of Surface Roughness on Gecko Adhesion. *Acta Biomaterialia, 3*(4), 607–610.

Israelachvili, J. (1972). The Calculation of Van-der-Waals' Dispersion Forces between Macroscopic Bodies. *Proceedings R. Soc. Lond.A.*, *331*, pp. 39-55.

Israelachvili, J. (2011). Van- der-Waals' Forces Between Particles and Surfaces. In J. Israelachvili, *Intermolecular and Surface Forces (Third Edition)* (pp. 253-389). London: Academic Press, Elsevier.

Jayaraman,J. (2003) www.casde.iitb.ac.in/store/events/2003/IAT-Pune-2003/DFMA.ppt, Accessed 4 March 2012

Jacobi N., Cysanak G. (1975). Dispersion Forces at Arbitrary Distances. *Chemical Physics Letters , 30*(3), 367-372.

Johnson, K.L. and Greenwood, J.A. (1997). J. Colloid Interface Sci. *J. Colloid Interface Sci., 192*, 326.

Johnson, K.L., Kendall, K., Roberts, A.D. (1971). Proc. R. Soc. London A. *Proc. R. Soc. London A*(324), 65-76, 301.

Jonat S., Hasenzahl S., Gray A. and Schmidt P.C., J. . (2004). J. Pharm. Sci. *J. Pharm. Sci., 93*, 2635.

Kalkowski G., Risse S., Harnisch G., Guyenot V. (2001). Electrostatic Chucks for Lithography Applications. *Microelectronic Engineering, 57-58*, 219-222.

Kasays T., Myazaki H., Saito S., and Sato T. (1998). Micro Object Handling under sem by Vision-based Automatic Control. *Proceedings of SPIE International Symposium on Microrobotics and Micromanipulation*, *3519.* Boston.

Kim H.C. and Russell T.P. (2001). J. Polym. Sci. B. *J. Polym. Sci. B, 39*, 1848.

Klimov, V.V. & Lebedev, P.N. (2008). *Plasmonic nature of Van der Waals forces between nanoparticles.* Moscow: Russian Academy of Sciences.

Komvopoulos, K. (.-3. (1996). Surface Engineering and Microtribology for Micro-electromechanical Systems. *Wear, 200*, 305-327.

Krishnan, S and Saggere, L (2011) Design and Development of a Novel Micro-clasp Gripper for Micromanipulation of Complex-shaped Objects , *Sensors and Actuators A: Physical,* In Press, Corrected Proof 2011. http://dx.doi.org/10.1016/j.sna.2011.09.030

Lambert P. & Delchambre A. (2003). Forces Acting on Microparts: Towards a Numerical Approach for Gripper Design and Manipulation Strategies in Micro-assembly. *Proceedings of the 1st International Precision approach for gripper design and manufacturing strategies in micro-assembly*, (pp. 79-84). Bad Hofgastein.

Lambert P., Seigneur F., Koelemeijer S., and Jacot J. (2006). A Case Study of Surface Tension Gripping: The Watch Bearing. *J. Micromech. Microeng, 16*(7), 1267–1276.

Lambert, P. (2007). *Capillary Forces in Microassemby: Modelling , Simulation, Experiments, and Case Study.* Springer.

Landau L. D., Lifshitz E.M., Pitaevskii L. P. (1960). *Electrodynamics of Continuous Media. 2nd Edition*. London: Elsevier.

Lewis, J. A. (2000). Colloidal Processing of Ceramics . *Journal of the American Ceramic Society, 83*(10), 2341–2359.

Li, Q., Rudolph, V., Peukert, W. . (2006). London-Van-der-Waals' Adhesiveness of Rough Particles. *Powder Technology, 161*, 248–255.

Lifshitz, E. (1956). The Theory of Molecular Attractive Forces between Solids. *Soviet Physics JETP, 2*(1), 73-83.

London, F. (1942). On Centres of Van-der-Waals' Attraction. *The Journal of Physical Chemistry, 46* (2), 305–316.

Lu Y., Huang J.Y., Wang C., Sun S., Lou J. (2010). Cold Welding of Ultrathin Gold Nanowires . *Nature Nanotechnology*, 213-224.

Luckham, P. F. (2004). Manipulating Forces between Surfaces. *Applications in colloid science and biophysics, Advances in Colloid and Interface Science 111*, 29–47.

Mahanty J. & Ninham B.W. (1976). New York: Academic Press.

Martin,Y., Abraham, D.W. and Wickramasinghe, H.K. (1988). Appl. Phys. Lett. 52 . *Appl. Phys. Lett., 52*, 1103.

Matope, S & Van der Merwe, A. F. (2010). Micro-material Handling Employing Van-der-Waals' forces. *Proceedings of the International Conference on Competitive Manufacturing (COMA 10)*, (pp. 261-267). Stellenbosch.

Matope, S. and Van der Merwe, A.F. (2009). The Physical Design of Micro-Grippers Actuated by Van-der-Waals' Forces for Use in Micro-Material Handling. *Proceedings of the 23rd SAIIE Annual Conference*, (pp. 178-188). Pretoria.

Matope, S. and Van der Merwe, A. F. (2010c). The Application of Van-der-Waals' Forces in Micro-material Handling. *Journal for New Generation Sciences, 8*(1), 122-134.

Matope, S., Van der Merwe, A. F., Nkosi, M., Maaza, M. and Nemutudi R. (2011). Micro-material Handling Employing E-beam Generated Topographies of Copper and Aluminium. *South Africa Journal of Industrial Engineering, 22* (2), 175-188.

Matope, S., Van der Merwe, A.F., Nemutudi R., Nkosi, M., Cele, M., and Maaza, M. (2010). Micro-material Handling through the Manipulation of Van-der-Waals' forces by the Generation of a Predetermined Surface Topology. *24th SAIIE Annual Conference*, (pp. 101-110). Pretoria.

Maugis, D. (1992). Journal of Colloid Interface Sci. *Journal of Colloid Interface Sci., 150*(1), 243-269.

Meine K., Kloss K., Schneider T. and Spaltmann D. (2004). Surf. Interf. Anal. . *Surf. Interf. Anal. , 36*, 694.

Mendez-Vilas A., Gonzalez-Martin M.L., Labajos-Broncano L. and Nuevo M.J. (2002). J.

Menon, C.; Murphy, M.; Sitti, M. (2004). Gecko Inspired Surface Climbing Robots. *Proceedings of the IEEE International Conference on Robotics Biomimetics*, (pp. 431-436).

Michael P. Murphy, Casey Kute, Yi˘git Mengüç and Metin Sitti. (2011). Waalbot II: Adhesion Recovery and Improved Performance of a Climbing Robot using Fibrillar Adhesives. *The International Journal of Robotics Research, 30*(1), 118–133.

Mizes, H., Ott, M., Eklund, E., Hays, D. (n.d.). Small Particle Adhesion: measurement and control . *Colloids and Surfaces A: Physicochemical and Engineering Aspects, 165*, 11–23.

MINAM Position Paper (2010). Paving the ground for the next generation of Micro Nano enabled Products in Europe, pp. 1-18

Mohideen U. & Roy A. (1998). Precision Measurement of the Casimir Force from 0.1 to 0.9 µm. *Physical Review Letters, 81*(21), 4549-4552.

Muller,V.M., Derjaguin, B.V. and Toporov, T.P. (1983). Colloids Surf. *Colloids Surf., 7*, 251.

Muller,V.M., Yushchenko, V.S. and Derjaguin, B.V. (1980). J. Colloid Interface Sci. *J. Colloid Interface Sci, 77*.

Muller,V.M., Yushchenko, V.S. and Derjaguin, B.V. (1983). Journal of Colloid Interface Sci. *Journal of Colloid Interface Sci., 92* .

Munday J. N., Capasso F. (2007). Precision Measurement of the Casimir-Lifshitz Force in a fFuid. *physical Review, A 75*(060102(R)), 060102-1 to 060102-4.

Munday J.N., Capasso F. and Parsegian A. (2009). Measured long-range Repulsive Casimir-Lifshitz Forces. *Nature, 457*, 170-172.

Munday, J.N., Capasso, F., Parsegian, V. A and Bezrukov S.M. (2008). Measurements of the Casimir-Lifshitz Force in Fluids: The Effect of Electrostatic Forces and Debye Screening. *Physical Review. A, 78*(3), 032109-1 to 032109-8.

Murphy M. P., Kute C., Mengüç Y. and Sitti M. (2011). Waalbot II: Adhesion Recovery and Improved Performance of a Climbing Robot using Fibrillar Adhesives . *The International Journal of Robotics Research, 30(1)* , 118–133.

Murphy M., Aksak B., and Sitti M. (2009). Gecko Inspired Directional and Controllable Adhesion. *Small, 5*, 170-175.

Murphy M.P., Kute C., Mengüç Y. and Sitti M. (2011). Waalbot II: Adhesion Recovery and Improved Performance of a Climbing Robot using Fibrillar Adhesives . *The International Journal of Robotics Research, 30*(1), 118–133.

Murphy, M. P. and Sitti, M. (2007). Waalbot: An Agile Small-scale Wall-climbing Robot Uilizing Dry Elastomer Adhesives. *12*(3), 330–338.

Nah S.K., Zhong Z.W. (2007) A Microgripper using Ppiezoelectric Actuation for Micro-Object Manipulation, *Sensors and Actuators A,* 133, pp. 218–224

NanoRobotics Lab. (2011). *http://nanolab.me.cmu.edu/projects/geckohair/hierarchy.shtml.*

Neugebauer R. , Koriath H.-J, Dirkse van Schalkwyk T., Van der Merwe, A.F., Müller M. and Matope, S (2011). (2011a). Micro-milling Work-holding Devices Employing Adhesive Forces,. *Proceedings of the International Conference on Industrial Engineering and Engineering Management for Sustainable Global Development*, (pp. 73-1 to 73-8). Stellenbosch.

Neugebauer R., Koriath H.-J., Muller M. (June 2010). Planar ElectrostaticGgrippers for Precise Handling of Piezoceramic Micro-parts. *Proceedings of the euspen International Conference.* Delt.

Neugebauer, R., Koriath, H-J., Van der Merwe, A. F., Müller M. and Matope, S. (2011). Study on Applicability of Adhesive Forces for Micro-material Handling in Production Technology. *Proceedings of the International Conference on Industrial Engineering and Engineering Management for Sustainable Global Development*, (pp. 55-1 to 55-12).

Ninham, B.W., Parsegian, A.V. and Weiss, G.H. (1970). On the Macroscopic Theory of Temperature-Dependent Van-der-Waals' Forces. *Journal of Statistical Physics, 2*(4).

Okazaki Y., Mishima N., and Ashida K. (2004). Microfactory—Concept, History, and Developments. *Journal of Manufacturing Science and Engineering, 126*, 837-844.

Oliveira, R. (1997). Understanding Adhesion:A Means for Preventing Fouling. *Experimental Thermal and Fluid Science , 14*, 316-322.

Parsegian V.A., Ninham B.M. (1970). Temperature-dependent Van-der-Waals' Forces. *Biophysical journal, 10*(7), 664-674 .

Parsegian, V. (2006). *Van der Waals forces: A handbook for biologists, chemists, engineers, and physicists.* New York: Cambridge University Press.

Pashley, M. (1984). Colloids Surf. *Colloids Surf., 12*, 69.

Peirs, J. (2001). *Design of Micromechatronic Systems: Scale Laws, Technologies, and Medical Apllications.* PhD thesis, KUL, Belgium.

Podczeck, F., Newton J. M., James, M.B. . (1997). Influence of Relative Humidity of Storage Air on the Adhesion and Autoadhesion of Micronized Particles to Particulate and Compacted Powder Surfaces. *Journal Of Colloid And Interface Science , 187*, 484–491.

Qin, Y. (2006). Micro-forming and Miniature Manufacturing Systems—development needs and perspectives. *Journal of Materials Processing Technology, 177* , 8–18.

Quintanilla M.A.S., Castellanos A. and Valverde J.M. (2001). Phys. Rev. E . *Phys. Rev. E , 6403*.

Raatz A. & Hesselbasch J. (2007). High-precision and Micro Assembly. *Proceedings of the International Conference on Competitive Manufacturing, COMA'07*, (pp. 321-326).

Rabinovich Y. I, Adler J. J., Ata A., Singh R.K. , Moudgil B. M. (2000). Adhesion between Nanoscale Rough Surfaces. I. Role of Asperity Geometry. *J. Colloid Interface Surf., 232*, 10-16.

Rabinovich I. Y., Adler J. J., Ata A., Singh K. J., and Moudgil M.B. (2000). Adhesion between Nanoscale Rough Surfaces II. Measurement and Comparison with Theory. *Journal of Colloid and Interface Science, 232*, 10–24.

Rabinovich Y. I., Singh A., Hahn M., Brown S., Moudgil, B.M. "Kinetics of Liquid Annulus Formation and Capillary Forces". *Langmuir* **27** (2011) 13514- 13523.

Reich R.A., Stewart P.A., Bohaychick J., Urbanski,J.A. (2003). Base Oil Properties of Ionic Liquids. (pp. 16-21). Lubrication Engineering.

Rollot, Y., Regnier, S., Guinot, J.C. . (1999). Simulation of Micro-manipulations: Adhesion Forces and Specific Dynamic Models. *International Journal of Adhesion & Adhesives, 19*, 35–48.

Rumpf, H. (1990). *Particle Technology.* London: Chapman & Hall.

Russel W.S., Saville D.A., and Schowalter W.R. (1999). *Colloidal dispersions.* Cambridge: Cambridge University Press.

Salomon, P. (2005). http://www.enablingmnt.com/NEXUS_MNT_Market_Report_III_2005-2009_-_key_results.

Sanchez J. A. . (2010). Handling for Micro-Manufacturing. In *Micromanufacturing Engineering and Technology* (pp. 298-314).

Sanchez-Salmeron, A.J.; Lopez-Tarazon, R.; Guzman-Diana, R.; Ricolfe-Viala, C. (2005). Recent Development in Micro-handling Systems for Micro-manufacturing. *Journal of Materials Processing Technology , 167*, 499–507.

Schaefer D.M., Carpenter M., Gady B., Reifenberger R., DeMejo L.P. and Rimai D.S., J. (1995). Adhesion Science Technology. *Adhesion Science Technology, 9*, 1049.

Scheeper P.R., Voorthuyzen J.A., Olthius W. and Bregveld. (1992). Investigation of Attractive fFrces between PECVD Silicon Nitride Microstructures and an Oxidised Silicon Substrate. *Sensors and Actuators A (Physical), A30*, 231-239.

Schwarz, U. D. (2003). A Generalized Analytical Model for the Elastic Deformation of an Adhesive Contact between a Sphere and a Flat Surface . *Journal of Colloid and Interface Science, 261*(1), 99-206.

Siliconfareast. (2011). *http://www.siliconfareast.com/lith_electron.htm.*

Sitti, M. & Fearing, R. . (2003). Synthetic Gecko Foot-hair Micro/nanostructures as Dry Adhesives. *J. Adhes. Sci. Technol. , 17(5)*, 1055-1074.

Sitti, M. (2003). High Aspect Ratio Polymer Micro/Nano-Structure Manufacturing using Nanoembossing, Nanomolding and Directed Self-Assembly. *Proceedings of the Advanced Intelligent Mechatronics Conference*, *2*, pp. 886-890.

Shokralla S.A. and Al-Muaikel N.S. (2010). Thermal properties of epoxy (DGEBA)/phenolic resin (NOVOLAC) blends *The Arabian Journal for Science and Engineering, Volume 35, Number 1B, pp 7-14.*

Song, J & Srolovitz, D.J. (2008). Mechanism for Material Transfer in Asperity Contact. *Journal of Applied Physics, 104* (12), 124312 (11 pages).

Sonnenberg, J.P. & Schmidt, E. . (2005). Numerical Calculation of London-Van-der-Waals' Adhesion Force Distributions for Different Shaped Particles . *China particuology, 3(1–2)*, 19–22.

Stone, R.B., McAdams, D. A., Kayyalethekkel, V. J. (2004). A Product Architecture-based Conceptual DFA Technique. *Design Studies, 25*(3).

Sulzer J. & Kova I. (2010). Enhancement of Positioning Accuracy of Industrial Robots with a Reconfigurable Fine-positioning Module. *Precision Engineering, 34*, 201–217.

Suresh L. and Walz Y. J. . (1997). Direct Measurement of the Effect of Surface Roughness on the Colloidal Forces between a Particle and Flat Plate. *Journal Of Colloid And Interface Science, 196*, 177–190.

Suresh, L. & Walz, J.Y. (1996). Effect of Surface Roughness on the Interaction Energy between a Colloidal Sphere and a Flat Plate. *Journal of Colloid and Interface Science, 183*, 199-213.

Tabor. (1977). Colloid Interface Sci. . *Colloid Interface Sci. , 58*, 2.

Takahashi, K., Berengueres, J.O.L., Obata, K.J., Saito, S. (2006). Geckos' Foot Hair Structure and their Ability to Hang from Rough Surfaces and Move Quickly. *International Journal of Adhesion & Adhesives, 26*, 639–643.

Takeuchi, M. (2006). Adhesion Forces of Charged Prticles. *Chemical Engineering Science, 61*, 2279 – 2289.

Tan G.-L., Lemon M.F., French R. H. (2003). Optical Properties and London Dispersion Forces of Amorphous Silica Determined by Vacuum Ultraviolet Spectroscopy and Spectroscopic Ellipsometry. *Journal of the American Ceramic Society, 86*(11).

Tanaka, M., Komagata, M., Tsukada, M., Kamiya, H. . (2008). Evaluation of the Particle–particle Iinteractions in a Toner by Colloid Probe AFM. *Powder Technology, 183*, 273–281.

Thoreson, E.J., Mart, J. and Burnham, N.A. (2006). The Role of Ffew-asperity Contacts in Adhesion. *Colloid and Interface Science, 298*(1), 94-101.

Tichem M., Karpuschewski B., and Sarro P.M. (2003). Self-adjustment of Micromechatronic Systems. *CIRP Annals, STC A, 52*(1), 17.

Tietje C. and Ratchev S. (2007) Design for Microassembly – Capturing Process Characteristics. *Proceedings of 4M 2007*.

Tietje C., Leach R., Turitto M., Ronaldo R., Ratchev S. (2008) Application of DFμA Methodology to Facilitate the Assembly of a Micro/nano Measuring Device, *In IFIP International Federation of Information Processing*, Vol. 260, *Micro-Assembly Technologies and Applications*, eds Ratchev S., Koelemeijer S. (Boston) Springer, pp.5-22.

Van der Merwe, A.F. & Matope, S. (2009). The Physical Design of Micro-Grippers Actuated by Van- der Waals' Forces for Use in Micro-Material Handling. *Proceedings of the 23rd SAIIE Annual Conference*, (pp. 178-188). Pretoria.

Van der Merwe, A. F. and Matope, S. (2010). Manipulation of Van-der-Waals' Forces by Geometrical Parameters in Micro-material Handling. *Journal for New Generation Sciences, 8*(3), 152-166.

Van Oss C.J., Good R. J. (1989). Surface Tension and the Solubility of Polymers and Biopolymers: The Role of Polar and Apolar Interfacial Free Energies. *Journal of Macromolecular Science: Part A - Chemistry, 26*(8).

Vandaele V., Lambert P. and Delchambre A. (2005). Non-contact Handling in Microassembly: Acoustical Levitation. *Precision Engineering, 29*, 491–505.

Vogeli B. & von Kanel H. (2000). AFM-study of Sticking Effects of Microparts Handling. *Wear, 238*(1), 20-24.

Weber W. M., Hrenya M. C. (2007). Computational Study of Pressure-drop Hysteresis in Fluidized beds . *Powder Technology , 177*, 170–184.

Weisenhorn A.L., Hansma P.K., Albrecht T.R., Quate C.F. (1989). Forces in Atomic Force Microscopy in Aair and Water. *Applied Physics Letters, 54(26)*, 2651.

Westkamper E., Schraft R.D., Bark C., Vogele C.G, and Weisener T. (1996). Adhesive Gripper - A New Approach to Handling Mems. *In Proceedings of Actuator 96, 5th International Conference on New Actuators*, (pp. 100-103). Bremen.

www.robots.com. (2008). accessed on 09 May.

www.utdallas.edu. (Accessed 23 August, 2011.).

Xie, H.-Y. (1997). The Role of Iinterparticle Forces in the Fluidization of Fine Particles. *Powder Technology, 94*, 99-108.

Xu D., Kenneth M., Liechti, K.M., Ravi-Chandar, K. (2007). On the Modified Tabor Parameter for the JKR–DMT Transition in the Presence of a Liquid Meniscus. *Journal of Colloid and Interface Science*(315), 772–785.

Zesch W., Brunner M., Weber A. (1997). Vacuum Tool for Handling Microobjects with a Nanorobot. *Proceedings of the IEEE International Conference on Robotics and Automation*, *2*, pp. 1761-1766. Albuquerque.

Zhang, H.W., Wang, J.B., Ye, H.F., Wang, L. (2007). Parametric Variational Principle and Quadratic Programming Method for Van-der-Waals' Force Simulation of Parallel and Cross Nanotubes. *International Journal of Solids and Structures, 44*, 2783–2801.

Zhou H.B., Gotzinger M. and Peukert W.,. (2003). Powder Technology. *Powder Technology, 135*, 82.

Zhou Y. and Nelson B.J. (1999). Force controlled gripping. *Proceedings of SPIE Conference on Microrobotics and Microassembly*, *3834*, pp. 211-222. Boston.

A) APPENDIX A: Twelve Research Outputs of the PhD studies in refereed journals and peer reviewed conferences

1. **Matope, S.,** Van der Merwe, A.F., Nemutudi R., Nkosi, M., Cele, M., and Maaza, M. (2010) Micro-material handling through the manipulation of Van-der-Waals forces by the generation of a predetermined surface topology. *Proceedings of the 24th SAIIE Annual Conference*, Glenburn Lodge, Muldersdrift, Gauteng. 6th-8th October 2010, p.101-110. www.saiie.co.za/ocs/index.php/saiie/SAIIE10/paper/download/.../86

ABSTRACT

This paper presents an investigation into the manipulation of Van-der-Waals forces in micro-material handling by the variation of the root mean square (*rms*) surface roughness values of the interacting surfaces. Electron beam evaporation (e-beam) is used in the generation of the required surface topography for the interactive surfaces involved in the picking and placing of micro-work parts. The Rumpf model of *rms* values of roughness is used to determine the Van-der-Waals forces exerted by the generated profiles. The surfaces are generated on a silicon base using e-beam deposition rates ranging from 0.6 to 1.2 Angstroms/second in a vacuum environment of $2x10^{-6}$ millibars. The surfaces with high *rms* were found to be suitable for the pick-up position, and those with low *rms* for the placement position in an effective material handling system.

Key words: Surface topography, Van der Waals forces, micro-material handling.

2. **Matope, S** and Van der Merwe, A. F. (2010) Micro-material handling employing Van-der-Waals forces. *Proceedings of the International Conference on Competitive Manufacturing (COMA 10)*, Stellenbosch University, 3 February -5 February 2010, p.261-267. http://publik.tuwien.ac.at/files/PubDat_184835.pdf

Abstract

This paper focuses on the handling of micro-materials using Van der Waals forces-powered micro-grippers. Analysis of Van der Waals forces' applicability in material handling is done with reference to material type, geometrical parameters and surface

topology. These parameters are embodied in a given material handling system. Optimisation of these parameters is done so as to improve the efficacy of micro-grippers during micro-material handling. Several designs of Van der Waals forces-actuated micro-grippers are then explored in this paper. It was experimentally observed that differentiation of the material types interacting provided an easier option in the manipulation of the grippers. The additional variation of object geometry greatly improved the efficiency of the gripper. In cases were these two options failed, a further variation of the surface roughness of the interacting micro-materials led to a great improvement in the efficacy of the material handling in the micro-range.

Keywords: micro-material, micro-gripper, micro-material handling, Van der Waals forces, employing Van der Waals forces, material type, geometric parameters, surface topology.

3. **Matope, S**. and Van der Merwe, A.F. (2009) The Physical Design of Micro-Grippers Actuated by Van-der-Waals forces for Use in Micro-Material Handling. *Proceedings of the 23rd SAIIE Annual Conference*, Roodevallei Country Lodge, Pretoria. 28th-30th October 2009, p.178-188. Available online at www.saiie.co.za/ocs/index.php/saiie/2009/paper/download/45/6

ABSTRACT

The paper focuses on the physical designs of micro-grippers that are actuated by Van der Waals forces. The designs are developed based on the geometrical and material type parameters of the grippers that are active during micro-material handling. The parameters include surface topology, object geometry, separation distance and material type. It is observed that the smoother the interactive surfaces the more effective are the grippers. Conically shaped grippers are observed to be more manipulatable and effective during operation than other configurations. The robustness of the grippers is increased by varying the type of materials used in their construction. Optimisation of the efficacy of the grippers is improved by manipulating the surface roughness and material type of the picking- and releasing-place of the micro-workparts. The design attributes of the micro-grippers discussed are effective in the range between 1μm to 300μm.

4. **Matope, S.** and Van der Merwe, A. F. (2010) The application of Van-der-Waals forces in micro-material handling. *Journal for New Generation Sciences*, Vol 8, No.1, p. 122-134. http://www.sabinet.co.za/abstracts/newgen/newgen_v8_n1_a9.html

ABSTRACT

This paper investigates the challenges of employing Van-der-Waals forcesin micro-material handling since these forces are dominant in micro-material handling systems. The problems include the creation of a dust-free environment, accurate measurement of the micro-force, and the efficient picking and placing of micro-work pieces. The use of vacuum suction, micro-gripper's surface roughness, geometrical configuration and material type are presented as alternatives to overcome the challenges. An atomic force microscope is proposed for the accurate measurement of the Van der Waals force between the gripper and the micro-work piece.

Keywords: Micro-material handling, Van der Waals forces, micro-work piece, micro-gripper, picking and placing.

5. Van der Merwe, A. F. and **Matope, S**. (2010) Manipulation of Van-der-Waals forces by geometrical parameters in micro-material handling. *Journal for New Generation Sciences,* Vol 8, No.3, pp.152-166. www.sabinet.co.za/abstracts/newgen/newgen_v8_n3_a10.html

ABSTRACT

This paper explores the manipulation of Van der Waals' forces by geometrical parameters in a micro-material handling system. It was observed that the flat-flat interactive surfaces exerted the highest intensity of Van der Waals' forces followed by cone-flat, cylinder-flat, sphere-flat and sphere-sphere interactive surfaces, respectively. A conical micro-gripper proved to be versatile in manipulating the Van der Waals' forces efficiently in a 'picking up' and 'releasing' mechanism of micro-work parts. It was deduced that the pick-up position should be rough and spherical, and the placement position should be smooth and flat for an effective 'pick-and-place' cycle to be realised.

Key words: micro-material handling, Van der Waals' forces, interactive surfaces, geometrical parameters, surface roughness.

6. **Matope, S**., Van der Merwe, A. F., Nkosi, M., Maaza, M. and Nemutudi R. (2011) Micro-material handling employing e-beam generated topographies of copper and aluminum. *South Africa Journal of Industrial Engineering.* Volume No.22, Issue 2, pp. 175-188). www.sabinet.co.za/abstracts/indeng/indeng_v22_n2_a18.html.

ABSTRACT

This paper focuses on the employment of copper and aluminum in a micro-material handling system actuated by Van der Waals forces. Electron beam (e-beam) evaporator deposited both materials on a silicon substrate at a rate of 0.6-1.2 Angstroms/second, vacuum pressure between $2x10^{-6}$ and $3x10^{-6}$mbar and at a current less than 10mA. Veeco NanoMan V Atomic Force Microscope with Nanoscope version 7.3 software were used to analyse the root mean square (*rms*) surface roughnesses of the generated topographies. Rumpf-Rabinovich's *rms* formula was used to determine the Van-der-Waals forces exerted by the surfaces. It was synthesised that an e-beam deposition of 7 minutes duration on both materials produced an optimum micro-material handling solution with copper suitable for the pick-up position and aluminum for the placement position.

Key words: Van der Waals forces, surface roughness, Rumpf-Rabinovich's formula, e-beam evaporation.

7. **Matope, S.,** Van der Merwe, A.F., Nkosi, M., Büttner, U., Maaza, M. and Nemutudi R. (2011) Application of silver, copper and aluminum e-beam deposited layers in micro-material handling. *Journal for New Generation Sciences* (Submitted and is under review).

ABSTRACT

This paper explores how electron beam evaporation (e-beam) depositions of silver, copper and aluminum can be used to optimise the handling of micro-materials. The e-beam depositions were done at a rate within 0.6 – 1.2 Angstrom/s, average vacuum pressure of 2 x 10^{-6} mbar, and current of less than 10mA. Silicon was the substrate. The Veeco NanoMan V Atomic Force Microscope was used to analysis the generated topographies employing Nanoscope version 7.3 software. A cross-examination by a Scanning Electron Microscope (SEM), Phenom TM-FEI model, also validated the observations. Rumpf-Rabinovich method was employed to model the Van der Waals forces' intensity exerted by the surfaces. An optimum micro-material handling system was realised for e-beam

depositions within the 5 min and 20 min range; where copper was suitable for the pick-up position, aluminum for the micro-gripper and silver for the placement position.

Keywords: Van der Waals froces, e-beam deposition, surface roughness, topography, Rumpf-Rabinovich method

8. Dirkse van Schalkwyk T., Van der Merwe, A.F. and **Matope, S** (2011) Micro-milling work-holding devices employing adhesive forces, *Proceedings of the International Conference on Industrial Engineering and Engineering Management for Sustainable Global Development,* Stellenbosch, Capetown, 21st-23rd September 2011, pp. 73-1 to 73-8. www.isem.org.za/index.php/isem/isem2011/paper/download/.../109

ABSTRACT

Micro-materials are very fragile rendering conventional, mechanical work-holding fixtures unsuitable for them since they exert large straining forces. Furthermore, macro-workholding devices occupy a large space which impedes high precision required in micro-milling. Hence this paper focuses on the application of adhesive forces namely; electrostatic, surface tension and Van-der-Waals forces; in work-holding strategies for micro-milling operations. An analysis is given as to their applicability with reference to the material type, geometry, and surface topography of the micro-work parts alongside the micro-milling cutting forces.

Keywords: micro-milling, electrostatic force, surface tension and Van-der-Waals forces, adhesive forces.

9. Neugebauer, R., Koriath, H-J., Van der Merwe, A. F., Müller M. and **Matope, S.** (2011) Study on applicability of adhesive forces for micro-material handling in production technology, *Proceedings of the International Conference on Industrial Engineering and Engineering Management for Sustainable Global Development,* Stellenbosch, Capetown, 21st-23rd September 2011, pp.55-1 to 55-12. www.isem.org.za/index.php/isem/isem2011/paper/view/55

ABSTRACT

Micro-material handling and micro-assembly becomes increasingly important in large-volume manufacturing of products like sensors in automotive applications. Smaller dimensions of the micro-objects lead to problems with regard to the reliability of the

manufacturing process because adhesive forces become predominant over gravity for objects whose dimensions are in the micro-range. In contrast to the common approach of minimizing those adhesive forces, this paper focuses on the use of the three main adhesive forces, Van-der-Waals, electrostatic and surface tension forces, as gripping principles. These forces are compared to conventional vacuum grippers with regard to gripping forces and complexity of application. Modelling of the forces is executed for separation distances in the range of 10 nm to 1 mm and dimensions of 10 µm to 10 mm for selected interactive surfaces of grippers and micro-objects. Even though vacuum forces dominate in magnitude over others within the whole range, application of adhesive forces for micro-part handling can be advantageous. For example, there is no energy supply required in case of Van-der-Waals force grippers. Technological applications of the gripping principles are given as well as their limitations.

Keywords: Vacuum force, electrostatic force, Van-der-Waals force, surface tension and micro-material handling

10. **Matope S.,** Van der Merwe A.F., Rabinovich Y.I. (2012) Micro-material handling employing e-beam coatings of copper and silver. *South Africa Journal of Industrial Engineering,* Vol. 23, No.1, pp 114-121.

ABSTRACT

Van-der-Waals forces and other adhesives force impose great challenges in micro-material handling. Mechanical grippers fail to reliably release micro-parts because of them. Therefore, this paper explores how the problematic Van-der-Waals forces may be utilised for micro-material handling purposes using surface roughnesses generated by e-beam coatings of copper and silver on silicon. An Atomic Force Microscope, model Asylum MFP 3 D-Bio with version 6.22A software, is used to measure the forces exerted by the surfaces. Silver coating of 1.41 nm *rms* surface roughness value is found to exert the highest Van-der-Waals forces, followed by copper coating of 2.72 nm *rms,* and the copper coating of 217 nm *rms* exerts the least. This implies that, in a reliable micro-material handling system, these depositions are suitable for the interactive surfaces of the placement position, micro-gripper, and the pick-up position respectively.

Keywords: Micro-material handling, Van-der-Waals forces, surface roughness, electron beam evaporation coating.

11. **S. Matope**, Y. I. Rabinovich, A.F. Van der Merwe (2012).Van der Waals Interaction of silica with e-beam created metallic thin films. *Journal of Colloid and Interface Science* (submitted and under review)

ABSTRACT

Dispersion force measurements have been done for samples with root mean square (RMS) roughness of more than 10 nm. This paper investigates lower range of roughness to prove or disprove theory of van der Waals force for random surface roughness with RMS in the 0.5- 3 nm range. Metallic films were obtained by coating silicon wafers using electron beam evaporation (e-beam) method. The e-beam deposition rates were within the range of 0.6-1.2 Angstroms/ second at vacuum pressures between $2x10^{-6}$ and $3x10^{-6}$ mbar. The developed coatings had peak- to- peak distance ranges of 80-120 nm and 1-2 μm. The long-range attractive forces between molecularly smooth silica sphere and films were measured by Atomic Force Microscope (AFM). Extending force/distance curves were developed, which in some cases, demonstrated attractive force much larger than theoretically calculated dispersion force. This may be attributed to electrostatic image forces. In other cases, extending curves were comparable with theoretical dispersion forces. The shift of curves for distance 1.82 RMS improved the agreement between experiment and theory. Adhesion forces were found from retracting curves. For peak- to-peak distance near 90 nm, the RMS roughness in the range 0.5- 3 nm reduces the experimental force by 3- 40 times. This effect of the surface roughness agrees with the known approximate formula developed for regular roughness suggesting DMT model and interaction of samples at only unique peak. It is also shown the absence of the capillary force under relative humidity up to 40%. This fact is explained by the thickness of wetting film smaller than the peaks height.

Key words: dispersion force; adhesion force; roughness; e-beam created films..

11. Arderne M., **Matope S.**, Van der Merwe A.F., Nyanga L (2012). Use of Van-der-Waals forces actuated polyurethane micro-grippers in the handling of IC micro-components. *Proceedings of The 42nd International Conference on Computers and Industrial Engineering (CIE42),* 16-18 July 2012, Cape Town (Paper accepted)

ABSTRACT

The handling of integrated circuit (IC) micro-parts is a great challenge in micro-assembly of electronics micro-components. The micro-parts adhere to the two-fingered mechanical grippers commonly used, and in the event that they are released precision is comprised. In some cases the micro-parts are strained or broken during the handling operations. The paper presents a solution through the use of Van-der-Waals forces actuated polyurethane grippers. These grippers are advantageous in that they do not leave residual stresses, charges and strains on the handled IC micro-components. They afford precision position of micro-parts and provide the necessary working space for soldering operations. A motoman robot coupled with polyurethane micro-grippers was used to pick, transfer and place micro-parts ranging from 10 mm down to 500 μm in the micro-assembly of IC micro-components.

Key words: Polyurethane micro-gripper, Van-der-Waals forces, IC micro-components

13. **S. Matope**, S. Read, A. F. Van der Merwe, and M. Mueller (2012). Polyurethane micro-gripper utilizing van-der-Waals forces in micro-assembly. *International Conference on Competitive Manufacturing, COMA'13*. Stellenbosch University January 30, 2013 – February 1, 2013 (Abstract accepted).

ABSTRACT

Handling of micro-parts with dimensions of 10 mm x 10 mm and below is a common issue for electronics and sensor or actuator manufacturing. Particularly if the parts are very thin compared to the lateral dimensions, for example less than 0.3 mm for a 10 mm x 10 mm part, care have to be taken handling those parts. In case of piezo-ceramics, as used for sensors and actuators, common mechanical and vacuum grippers apply high local contact pressures inducing the risk of micro-fractures. Polymer micro parts made from silicone, as used for spacers, are even more difficult to handle due to their flexibility. Given this background, this paper provides a new approach for handling both piezo-ceramic micro parts and silicone spacers with one handling system and one gripper through the use of a polyurethane micro-gripper which is soft and only actuated by van-der-Waals forces. Unlike conventional micro-grippers, polyurethane micro-grippers do neither require power supply nor pressurized air. Gripping and releasing is only performed by differences in van-der-Waals forces of pick and place position. The right choice of material is therefore essential. The paper further reveals that for a given application of production of a piezo-

ceramic sensors, the pick and place areas can be designed to allow for reliable pick and place with the polyurethane micro-gripper.

Keywords: Polyurethane gripper, van-der-Waals force, micro-assembly, piezo-ceramic sensors.

B) APPENDIX B: Collaboration with iThemba Laboratories

UNIVERSITEIT·STELLENBOSCH·UNIVERSITY
jou kennisvennoot • your knowledge partner

22 April 2010

The Material Research Group Head
Materials Research Group
iThemba LABS
PO Box 722
Somerset West
7129

Dear Sir

Re: Collaborative research in the application of Van der Waals forces in micro-material handling.

We would like you to partner with us within the framework of Stephen Matope's PhD research in the "Application of Van der Waals forces in micro-material handling".

We would greatly appreciate any assistance you would render Stephen. We will gladly share the research publications related to this collaboration.

Thank you very much for considering our letter.

Yours sincerely

Dr Andre Van der Merwe
Chairman

Voorsitter Departement Bedryfsingenieurswese • Chairman, Department of Industrial Engineering
Fakulteit Ingenieurswese • Faculty of Engineering
Privaatsak / Private Bag X1, Matieland 7602, Suid Afrika / South Africa, http://www.sun.ac.za
Tel. 021 - 808 4234, Fax 021 - 808 4245, E-pos / E-mail: cjf@sun.ac.za
Int.: Tel. +27 21 808 4234, Fax +27 21 808 4245

C) APPENDIX C: Research scientist's report and Collaboration

The Academic Research Visit Report

by

Mr. Stephen Matope

1 February 2011 to 29 April 2011

Accomplishments/Successes/Outputs

Executive Summary

The researcher visited Chemnitz University of Technology and worked in the Institute for Machine Tools and Production Processes under the PT-PIESA (A2) project as from the 1st of February to the 29th of April 2011. As a researcher in micro-material handling, he contributed to the production and processing of piezoceramic (PZT) sensors. He co-authored (together with Prof Neugebauer R., Dr Koriath H-J., Dr Van der Merwe A. F., Mr Müller M) two papers for an International Conference on Industrial Engineering, Systems Engineering and Engineering Management for Sustainable Global Development (ISEM) to be held on 21st-23rd September 2011. The abstracts were peer reviewed and were accepted in March 2011. The researcher made contributions towards the improvement of the production system of the PZT sensors. These included the employment of cold welding, ultrasonic welding and wire bonding processing techniques to replace soldering so as to improve the tolerance management and minimise the production cycle time. He also recommended the employment grippers (whose operating principle is based on Van-der-Waals forces) in the handling of PZT sensors so as to further minimise the production cycle times. Such grippers are made of polyurethane ST 1060 directional and hierarchical adhesives. The researcher worked with Mr. Muller in the coordination and documentation of the collaborative research initiatives between Chemnitz University and Stellenbosch University. This then culminated in the decisive meeting between the two parties on the 13th of April 2011 where it was agreed to venture into projects on micro-material handling and localised robotic micro-milling for PZT sensors' manufacturing and assemblying.

Collaborative Research document for Chemnitz University of Technology and Stellenbosch University.

The researcher and Mr. Michael Muller worked as coordinators between Chemnitz University of Technology and Stellenbosch University, synergising the contributions from both entities towards the collaborative research. They played a key role in the crafting of the document, articulating and documenting the requirements of the collaboration in respect to the contributions received from the Professors and concerned members.

They identified three research areas namely:

a) Glueless bonding of composites and laminates
    - Innovation: Application of functional surfaces for bonding without adhesive, at the same time achieving higher strength, stiffness and reliability.

b) Novel clamping systems for micro-machining.
    - Innovation: Application of Van-der-Waals forces for clamping workparts of dimensions less than 1 mm. This would employ an actuated clamping system for alignment and releasing of micro-workparts.

c) Robot for micro-machining on large parts
    - Innovation: Mobile fine positioning unit on conventional six-axis robot, and also micro-machining by mobile fine position unit.

The researcher and Mr. Michael Muller presented the proposal to the Professors and concerned members of the Collaborative Research in the meeting held on the 13th of April 2011. Deliberations were made on a joint venture covering these research topics.

The researcher documented the literature, references and important information to be used in the collaborative research and stored the information in the folder entitled: *Stephen_Matope 1Feb-29April 2010.* This folder has been left in the custody of Mr. Mueller for future use.

Acknowledgement

The underlying research is gratefully supported by the German Research Foundation (DFG) as part of the special research field SFB/TR 39. The author thanks the German Research Foundation (DFG) for financing his academic visit at Chemnitz University of Technology from 1 February 2011 to 29 April 2011. He further thanks Professor Neugebauer for inviting and hosting this academic visit.

From: Matope, Stephen, Mr <smatope@sun.ac.za>
Sent: Thursday, September 09, 2010 1:05 PM
To: Van der Merwe, AF andrevdm@sun.ac.za

Subject: RE:Germany Collaboration, Research Cooperation Nanotechnology; Michael Mueller
Dear Dr. Andre F. Van der Merwe
Please find below a draft letter to Prof Michael Muller and his earlier e-mail. Would please mind putting your ideas and then send it to him. Kind regards, Stephen
Dear Prof Michael Muller
We are interested in the cooperation or collaborative research in micro-robotics (with application of nano-coatings) as indicated in your letter.
Currently we have covered some ground in the application of Van-der-Waals forcesin micro-material handling. We identified three crucial parameters namely 1) material type, 2) geometrical nature and 3) surface roughness topology. We have also employed electron beam evaporation (e-beam, a nanotechnology) in the preparation of surfaces with determinable rms surface roughnessness. The e-beam surfaces generated were found to have a characteristic Van-der-Waals forces'exertion intensity during micro-material handling. This leads to the identification of interactive surfaces during the picking and placing of micro-work parts by micro-robots and micro-grippers.
Would you please mind briefing us of the ground you have covered so far in micro-robots and nanotechnology.

Kind regards
Dr Andre F. Van der Merwe

From: Van der Merwe, AF <andrevdm@sun.ac.za> [andrevdm@sun.ac.za]
Sent: Friday, August 27, 2010 9:43 AM
To: Matope, Stephen, Mr <smatope@sun.ac.za>
Subject: FW: Research Cooperation Nanotechnology

Can we discuss this ?

Andre van der Merwe PhD - andrevdm@sun.ac.za

Chairman IE / Director GCC-IBI

Department of Industrial Engineering www.ie.sun.ac.za

Tel: +27 21 808 3734 Fax: +27 21 808 4245

Universiteit Stellenbosch University

Privaat Sak/Private Bag X1 Matieland 7602

Suid-Afrika/South Africa

www.eng.sun.ac.za

* Help save paper - do you really need to print this email ?

-----Original Message-----
From: Michael Müller [mailto:michael.mueller@mb.tu-chemnitz.de]
Sent: 27 August 2010 07:39 AM
To: andrevdm@sun.ac.za
Subject: Research Cooperation Nanotechnology

Dear Dr. Van der Merwe,

I am researcher at the Professor Neugebauer's chair at Chemnitz University of Technology, Germany. We found that you have conducted some research in the field of micro handling and micro robotics. Actually, we found that there is currently an open call for funding of cooperation projects between German and South African Universities and small/medium businesses in both countries. The topics funded are sustainability of

industrial processes, resource efficiency and nano- or biotechnology.

Since we have had research activities in the fields of energy and resource efficiency and micro-robotics (with application of nano-coatings) there might be some basis for cooperation. Personally, I would prefer the latter research field of nanotechnologies, especially aiming on ultra/nano-precision robotics and machines.

If you are generally interested in cooperation please give me feedback as soon as possible. The call is open until 15 Oct 2010 in Germany. Please check your funding opportunities at NRF.

I'm looking forward to your response,

Michael Mueller

--

Dipl.-Ing. Michael Müller

Technische Universität Chemnitz
Fakultät für Maschinenbau
Institut für Werkzeugmaschinen und Produktionsprozesse
Professur für Werkzeugmaschinen und Umformtechnik
Reichenhainer Str. 70
09126 Chemnitz

fon: +49-(0)371-531-37859
fax: +49-(0)371-531-8-37859 (Fax2Mail)
web: http://www.tu-chemnitz.de/mb/iwp

D) APPENDIX D: Collaboration with Florida university

Collaboration with Particle Science and Technology Department headed by Prof Yakov I. Rabinovich at the University of Florida, USA.

From: Matope, Stephen, Mr <smatope@sun.ac.za>
Sent: Friday, May 13, 2011 5:32 PM
To: Rabinovich, Yakov I
Cc: Van der Merwe, AF, Dr <andrevdm@sun.ac.za>
Subject: RE: Application of Van-der-Waals forces and collaboration

Dear Prof Y.I. Rabinovich
Please find attached the material you requested about the 3 samples we sent to you. The third (silver) is a contingent measure since you required different materials.
We courier the samples to the physical address given below:

205 Particle Science & Technology, Gainesville, FL 3261.
Ph: 352.846.1194, Fax: 352.846.1196

Please note the copper samples were deposited about 7 months ago, and the silver 4 months ago.
Thank you in advance for your great help in analysing our samples.
Kind regards
Stephen

From: Rabinovich, Yakov I [yrabinovich@perc.ufl.edu]
Sent: Friday, May 06, 2011 2:38 PM
To: smatope@sun.ac.za
Subject: RE: Application of Van-der-Waals forces and collaboration

Dear Mr. Matope,

You can send me 2 samples. Please, write all details about these samples: materials, roughness (if you know), thickness of deposited metal, which difference is between these samples. I would like to have actually different samples for which the force will be different. I shall try to get results in one-two weeks after obtaining samples.

My address is

Y.I.Rabinovich

206 Particle Science & Technology

PO Box 116135

University of Florida

Gainesville, FL32611-6135

USA

Yours truly

Yakov Rabinovich

-----Original Message-----

From: Matope, Stephen, Mr <smatope@sun.ac.za> [mailto:smatope@sun.ac.za]

Sent: Wednesday, May 04, 2011 11:14 AM

To: Rabinovich, Yakov I

Subject: RE: Application of Van-der-Waals forces and collaboration

Dear Prof Rabinovich

Thank you very much for the response. Would you mind if I send you two samples as you previously suggested so that you can perform the van-der- Waals force measurements. Then I would use the results to convince my University to have the other 18 samples measured and paid for. If you agree, please furnish me with your postal details.

Kind regards

Stephen Matope

PhD Student

Stellenbosch University

South Africa

From: Rabinovich, Yakov I [yrabinovich@perc.ufl.edu]

Sent: Tuesday, May 03, 2011 2:33 PM
To: smatope@sun.ac.za
Subject: RE: Application of Van-der-Waals forces and collaboration

Dear Mr. Matope,
Which measurements would you like to make? I believe it should be contact (adhesion) forces between you samples and silica spheres. But take into account that these forces probably include not only dispersion forces but also donor-acceptor forces and may be polar (dipole/dipole and dipole/non-dipole forces). Electric forces and capillary forces (if humidity is large enough) also should be taken into account. I tell about these forces because price of experiment depends on conditions under which measurements should be done. The topography of each sample should be also measured. As average, I believe that total price should be near five thousand dollars. Is it sensible for you? If yes, then we discuss about form of our agreement (I should consult with our financial department) and you will send me your samples.
Yours truly
Yakov Rabinovich

-----Original Message-----
From: Matope, Stephen, Mr <smatope@sun.ac.za> [mailto:smatope@sun.ac.za]
Sent: Thursday, April 28, 2011 10:44 AM
To: Rabinovich, Yakov I
Subject: RE: Application of Van-der-Waals forces and collaboration

Dear Prof Y. Rabinovich
Would you please advise us of the cost to make the force measurements say for a batch of 10.
Kind regards
Stephen

From: Rabinovich, Yakov I [yrabinovich@perc.ufl.edu]
Sent: Thursday, April 28, 2011 2:24 PM
To: smatope@sun.ac.za
Subject: RE: Application of Van-der-Waals forces and collaboration

Dear Mr. Matope,

I have AFM and can make couple measurements to evaluate one or may be two of your samples. However, I cannot make regular measurements which you need for future paper unless these measurements will be financially supported by grant or by any sponsor (your University?).

Yours truly

Yakov Rabinovich

-----Original Message-----

From: Matope, Stephen, Mr <smatope@sun.ac.za> [mailto:smatope@sun.ac.za]

Sent: Tuesday, April 26, 2011 5:37 AM

To: Rabinovich, Yakov I

Subject: RE: Application of Van-der-Waals forces and collaboration

Dear Prof Rabinovich

In connection with our intended collaborative research, we have e-beam deposited samples of silver, aluminum and copper. We have used your formula as stipulated in the paper we previously sent you. Therefore, we would like to prove our results experimentally by using an Atomic Force Microscope to measure the Van-der-Waals forces exerted by these samples and find a correlation between theory and practice. But unfortunately we don´t have the capacity to measure these forces. Our samples are 18 and are 10mm x10mm each.

We are kindly inquiring whether we can send the samples to you and get the force measurements done and we hope that with the results we can co-author a journal paper with you.

Kind regards

Stephen

PhD Student

Stellenbosch University

South Africa.

From: Matope, Stephen, Mr <smatope@sun.ac.za>

Sent: Monday, April 11, 2011 9:03 PM

To: Rabinovich, Yakov I

Subject: RE: Application of Van-der-Waals forces and collaboration

Dear Prof Rabinovich
Thank you very much for your response which I greatly value.
I will discuss with my study leader, Dr. Andre F. Van der Merwe these crucial points you have raised and then share with you our deliberations. At the same time we would greatly appreciate your hints (any time) as to the direction in which we should go in our intended collaboration since you are an expert in this field.
Once more thank you very much for your precious time in responding to us.
Kind regards
Stephen

From: Rabinovich, Yakov I [yrabinovich@perc.ufl.edu]
Sent: Monday, April 11, 2011 5:52 PM
To: smatope@sun.ac.za
Subject: RE: Application of Van-der-Waals forces and collaboration

Dear Mr. Matope,
Thank you for your mail. I didn't have enough time to see your paper yet. I shall try to answer for your question after I shall read it.
Answer for possibility of collaboration depends on many factors: which task should be solved, what do you need from my side- instruments, experiments, theory (van der Waals force, effect of roughness, effect of humidity, anything else), which financial base could have our collaboration- mutual grant (from any agency in South Africa or USA) or any other? In any case, I wish you good luck in your investigations.
Sincerely yours
Yakov Rabinovich, scientist

-----Original Message-----
From: Matope, Stephen, Mr <smatope@sun.ac.za> [mailto:smatope@sun.ac.za]

Sent: Thursday, April 07, 2011 4:13 AM

To: Rabinovich, Yakov I

Subject: Application of Van-der-Waals forces and collaboration

---

From: Matope, Stephen, Mr <smatope@sun.ac.za>

Sent: Tuesday, March 29, 2011 11:26 AM

To: yrabinovich@erc.ufl.edu

Subject: Re: Application of Van der Waals forces

Dear Professor Yakov I. Rabinovich

I am a South African PhD student at Stellenbosch University and was motivated by your research and I embarked on a research entitled "Intelligent grippers employing Van-der-Waals forces for micro-manufacturing" in 2007.

We have so far written over 8 conference and journal papers (please see Attachment: CV-MATOPE under the Subheading ACADEMIC PAPERS PRESENTED).

We have done e-beam depositions of Copper, Aluminum and Silver on silicon substrates and came up with a journal paper shown in the Attachment (Journal 4)

However, we are limited with laboratory facilities. Hence would you please advise, basing on our conclusion, of the parameters within which a pick-transfer-release operation would experimentally take place for a specific micro-workpart using the surface roughnesses generated.

We are also willing to have collaborative research with you, so please inform us if you are interested.

Yours greatly appreciating your contribution to the world of science and engineering,

Stephen Matope

PhD Candidate

Stellenbosch University

South Africa

Experimental questionnaire of the Van-der-Waals forces exerted by e-beam depositions on a silicon substrate (Sent to Plrof Yakov I. Rabinovich).

2. Aim: Validation of the theoretical calculation of the Van-der-Waals forces intensity by practical and experimental force measurement**.**

3. Required experimental results for the samples

3.1 Defining the type of Van-der-Waals force measurement method (contact mode, tapping mode, non-contact etc)

3.2 Temperature, pressure and humidity level of the experimental environment which insure that surface

3.3 Force distance curves tension force and other forces are eliminated (or reduced) leaving Van-der-Waals forces dominant

3.4 Determination of the Van-der-Waals force values per each given sample when interacting with a silica sphere as indicated in Table 1

Table 1

Material 1	**Material 2**	**Van-der-Waals forces magnitude**
Silica sphere or any other suitable material	F6, Cu (copper deposited for 20 min)	
Silica sphere or any other suitable material	F6, Cu (copper deposited for 20 min)	
Silica sphere or any other suitable material	B2, Copper (copper, e-beam deposited for 5 min)	

3.5 Simple evaluation of the samples according to Table 2. The purpose of this evaluation is to determine whether a picking-and-placing cycle can be achieved as is the requirement in micro-material handling operations.

Table2

Material to be picked silica sphere or any other micro-workpiece	**Substrate sample from which to be picked**	**The picking material sample**	**Theoretical assumption**	**Practical, Experimental result (Picking or No picking)**
Silica sphere	F6, Cu (copper deposited for 20 min)	B2, Copper (copper, e-beam deposited for 5 min)	*Picking will take place*	
Silica sphere	F6, Cu (copper deposited for 20 min)	Holder F, Ag, Silver (silver, e-beam deposited for 20min)	*Picking will take place*	
Silica sphere	B2, Copper (copper, e-beam deposited for 5 min)	Holder F, Ag, Silver (silver, e-beam deposited for 20min)	*Picking will take place*	

Silica sphere	B2, Copper (copper, e-beam deposited for 5 min)	F6, Cu (copper deposited for 20 min)	*No picking will take place*	
Silica sphere	Holder F, Ag, Silver (silver, e-beam deposited for 20min)	F6, Cu (copper deposited for 20 min)	*No picking will take place*	
Silica sphere	Holder F, Ag, Silver (silver, e-beam deposited for 20min)	B2, Copper (copper, e-beam deposited for 5 min)	*No picking will take place*	

4. BACK GROUND OF THE GIVEN SAMPLES

4.1 Hypothesis

The hypothesis on which modelling of Van-der-Waals forces is based when comparing interacting surfaces is that: the higher the Van-der-Waals forces exerted by a material, the more the attraction it exerts on a given micro-work part. Hence, for an effective picking-and-placing cycle to be realised during micro-material handling, the order is as follows: the placement position should exert the highest Van der Waals forces, then followed by the micro-gripper, and finally the pick-up position should exert the least force.

4.2 Method

Initially a washing process of eighteen silicon substrates (*rms* surface roughness values of 0.4-0.7nm) was executed chronologically in an ultrasonic bath of the following liquids: methanol, acetone and trichloroethylene. Later they went through a second cycle of ultrasonic bath in

acetone, methanol, de-ionised water and finally in 20% hydrofluoric acid solution respectively. Each ultrasonic bath was of 5 minutes duration. The substrates were then rinsed in de-ionised water. The purpose of the cleaning was to remove all the oxide layers, greasy materials and other contaminants so as to ensure an impurity-free e-beam deposition
Silver was e-beam deposited on a six silicon substrates for different durations of 2, 5, 7, 10, 15 and 20 minutes. The substrates were mounted onto an indexed sample holder in the e-beam machine. Silver was placed into the e-beam crucible. The e-beam machine was closed and then evacuated for twenty-four hours. The target substrate to be e-beam deposited was indexed into position and deposition was executed as per the prescribed time. The deposition rates were within the range of 0.6-1.2 Angstroms/s, at a vacuum pressure averaging $2x10^{-6}$mbar and at a current less than 10mA. The Veeco NanoMan V Atomic Force Microscope (AFM) was used to analysis the generated topographies using Nanoscope version 7.3 software. This procedure was repeated for copper and aluminum, and the results of the three samples sent to you are shown in Table 1. An extra sample of a different material was added so as to ensure validation as implied in your e-mail to us.

Table 3: E-beam deposition times, layer thickness and *rms* values. The materials deposited are 99.9% pure.

Duration of e-beam deposition, minutes	Index letter	Thickness of deposition, Angstroms	Surface roughness, *rms* value, in nm
5	B2, Copper	378	2.720
20	Holder F, Ag, Silver	1170	1.410
20	F6, Cu	984	217.000

4.3 AFM micrographs

The AFM micrographs of the e-beam depositions of the three samples are shown in Figures 1 to 3

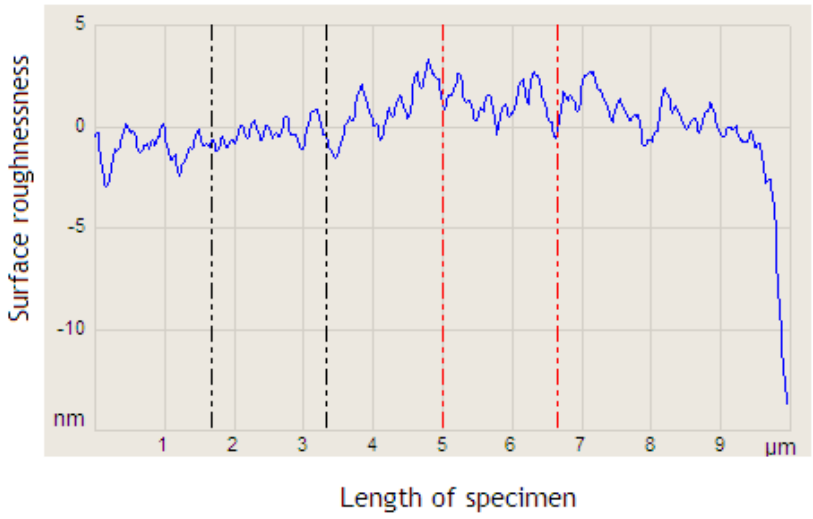

Figure 1. Atomic Force Micrograph of copper deposited for 5 min.

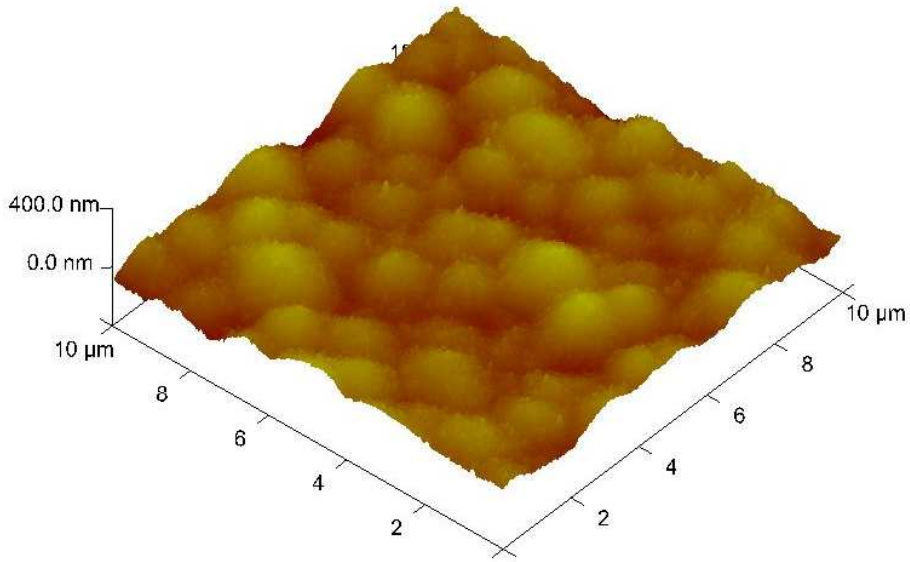

Figure 2. Atomic Force Micrograph of copper deposited for 20 min.

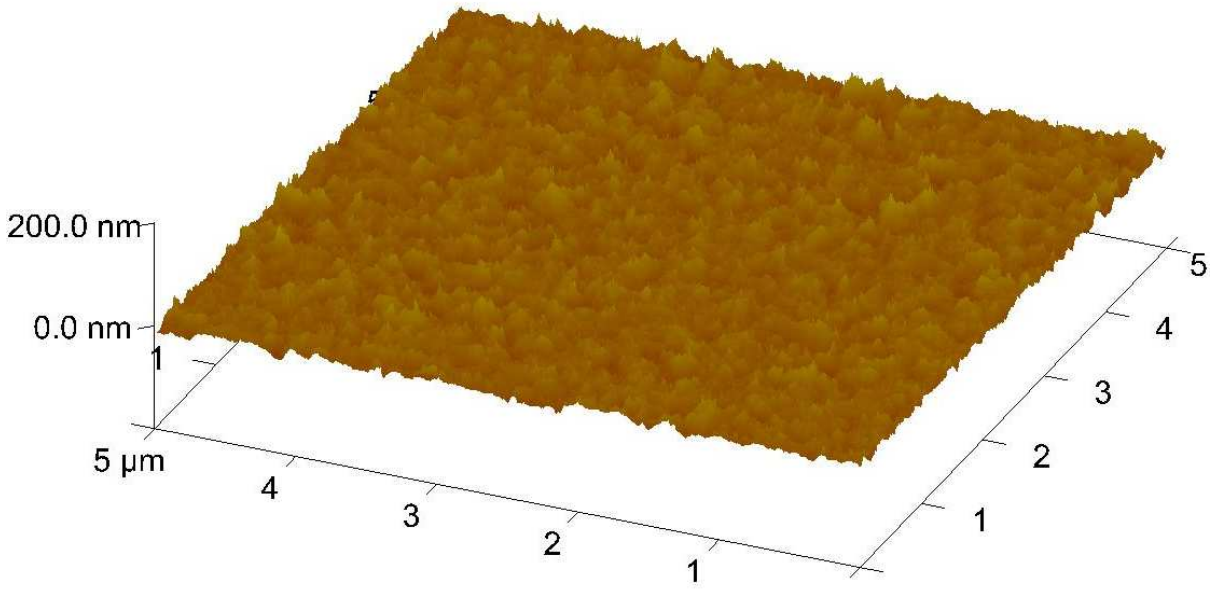

Figure 3. Atomic Force Micrograph of silver deposited for 20 min.

4.4 Modelling and analysis

The Rumpf-Rabinovich's equation (1), depicting the relationship between Van-der-Waals forcesand the surface roughness *rms* values of specific material types (Rabinovich et al, 2000), is used to model the experimental results in Table 1. Equation (1) reveals the relationship between a spherical micro-work part and a flat surface (Rabinovich et al, 2000).

$$F = \frac{A_H R}{6D^2}\left[\frac{1}{1+R/1.48rms} + \frac{1}{\left[1+1.48rms/D\right]^2}\right] \quad \text{.....(1)}$$

Where F is the Van der Waals force, A_H is the Hamaker coefficient (a material property of matter which reflects the intensity of the Van-der-Waals forces exerted by a given substance (Parsegian, 2006), *rms* surface roughness, R is the radius of the spherical micro-work part, D is the separation distance between the micro-work part and the interacting surface.

The two main components in the brackets of the Rumpf-Rabinovich's equation reveal the effect of Van der Waals in non-contact region (2) and contact region (1) as surfaces interact (Li et al, 2006; Komvopoulos, 1996; Suresh & Walz, 1997; Eichenlaub, 2004).

Non-contact component:

$$\frac{1}{1+R/1.48rms} \quad \text{.....(2)}$$

Contact component:

$$\frac{1}{[1+1.48rms/D]^2} \quad \text{.....(3)}$$

In this modelling it is assumed that *D* is 1nm (making the interactive surfaces as close as possible) and *R* is 1 micrometer (a minimum radius taken for a micro-work part in this case). It follows that the non-contact component is very small compared to the contact component because the value of *R* in its denominator is being divided by the nano-range *rms* values. Furthermore, the contact component is a power function, hence it overrides the non-contact component in practical cases. Therefore, in this modelling, the non-contact term is ignored.

Figure 4 shows the modelling of the Van-der-Waals forces intensity exerted by the three materials incorporating the maximum Hamaker coefficients (A_H) in which 500 zJ is for silver, 400 zJ is for copper and 145 zJ is for aluminum (Parsegian, 2006).

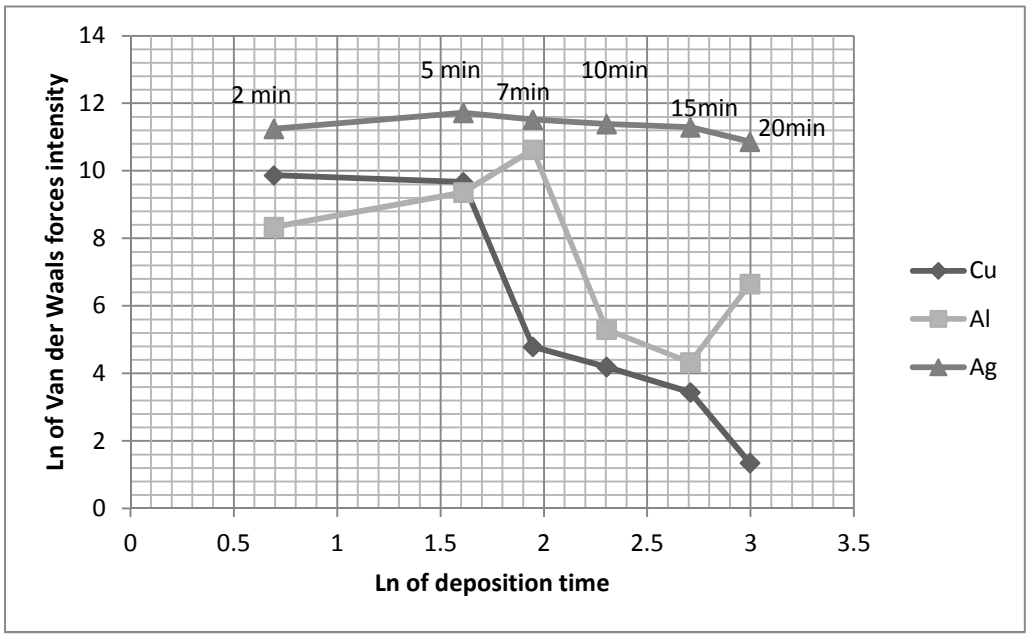

Figure 4 Van-der-Waals forces against deposition time

An analysis of Figure 4 reveals a significant optimisable region lying between the 5 min and 20 min deposition times. This range is exclusive of the 5 min deposition time, but inclusive of the 20 min. In this range silver exerts the highest Van der Waals forces, followed by aluminum, and copper the least. Applying the hypothesis mentioned earlier, silver would then be suitable for the placement position, aluminum for the gripper and copper for the pick-up position.

E) APPENDIX E: Hamaker coefficients

Table E-1, Comparison of Hamaker coefficients (Parsegian, 2006)

For compactness the A are given in zeptojoules (zJ) = 10^{-21}J		
Material	A across water	A across vacuum
Organics		
Polystyrene	13	79
Polycarbonate	3.5	50.8
Hydrocarbon (tetradecane, Level 1)	3.8	47
Polymethyl methacrylate		
Protein	1.47	58.4
Teflon	5-9, 12	n/a
	0.36	Almost = 0
Inorganics		
Diamond	138	296
Mica (monoclinic)	13.4	98.6
Mica (Muscovite)	2.9	69.6
Quartz silicon dioxide	1.6	66
Aluminum oxide	27.5	145
Titanium dioxide rutile	60	181
Potassium chloride (cubic crystal)	4.1	55.1
Water	n/a	55.1
Metals		
Gold	90 to 300	200 to 400
Silver	100 to 400	200 to 500
Copper	300	400

Table E-2 Hamaker's constants for different media for various polymers of different refractive index (French, 2000)

Table I. Nonretarded Hamaker Constants for Ceramic Materials Interacting under Vacuum and across Water at 298 K†

Material	Crystal structure	Hamaker constant ($\times 10^{-20}$ J)	
		Under vacuum	Across water
α-Al_2O_3	Hexagonal	15.2	3.67
$BaTiO_3$‡	Tetragonal	18	8
BeO‡	Hexagonal	14.5	3.35
$CaCO_3$‡	Trigonal	10.1	1.44
CdS	Hexagonal	11.4	3.4
$MgAl_2O_4$	Cubic	12.6	2.44
MgO	Cubic	12.1	2.21
Mica	Monoclinic	9.86	1.34
6H-SiC	Hexagonal	24.8	10.9
β-SiC	Cubic	24.6	10.7
β-Si_3N_4	Hexagonal	18.0	5.47
Si_3N_4	Amorphous	16.7	4.85
SiO_2 (quartz)	Trigonal	8.86	1.02
SiO_2	Amorphous	6.5	0.46
$SrTiO_3$	Cubic	14.8	4.77
TiO_2‡	Tetragonal	15.3	5.35
Y_2O_3	Hexagonal	13.3	3.03
ZnO	Hexagonal	9.21	1.89
ZnS	Cubic	15.2	4.8
ZnS	Hexagonal	17.2	5.74
3Y-ZrO_2	Tetragonal	20.3	7.23

F) APPENDIX F: Properties of e-beam deposited materials

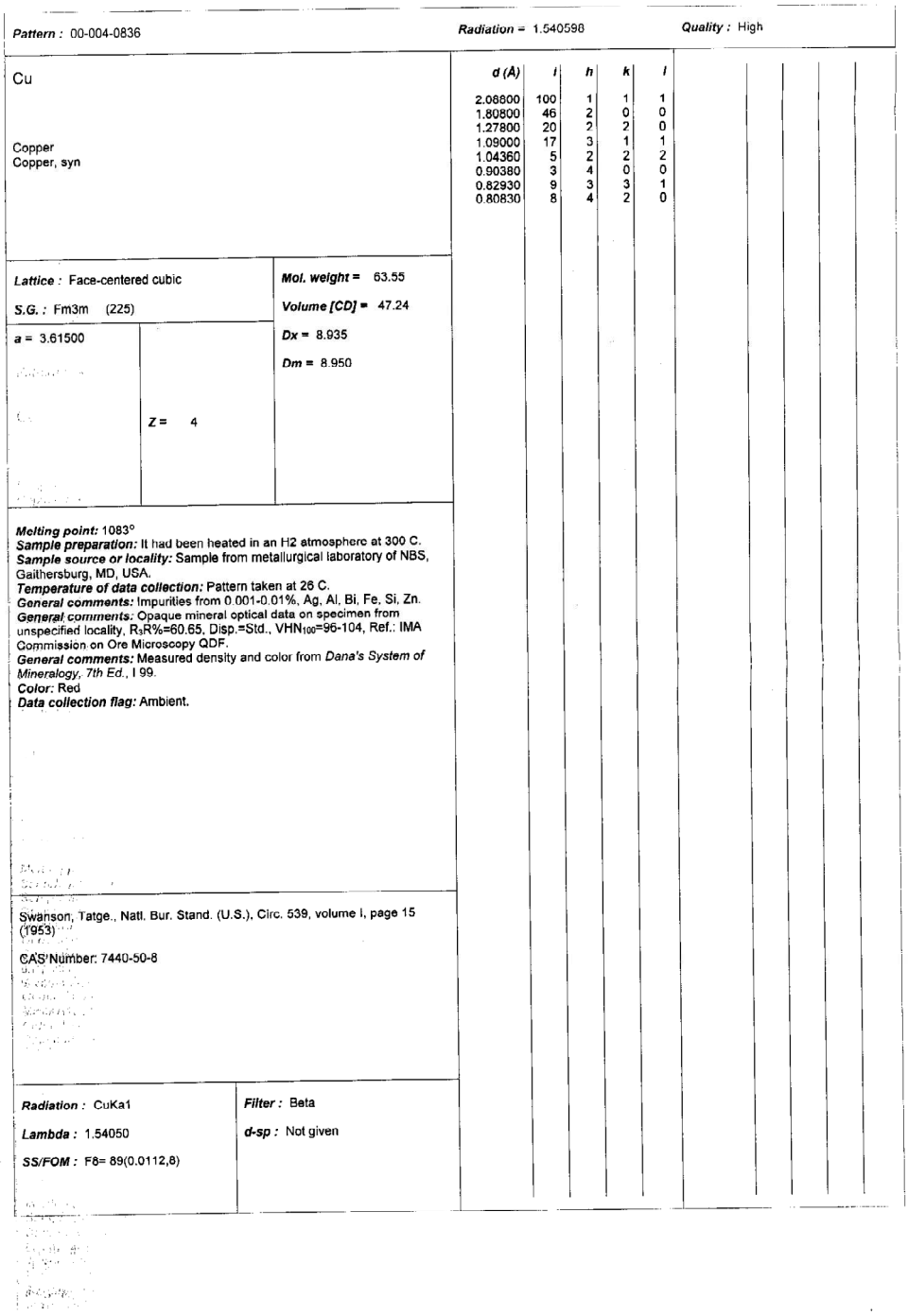

Pattern : 00-004-0836 **Radiation =** 1.540598 **Quality :** High

Cu

Copper
Copper, syn

d (Å)	I	h	k	l
2.08800	100	1	1	1
1.80800	46	2	0	0
1.27800	20	2	2	0
1.09000	17	3	1	1
1.04360	5	2	2	2
0.90380	3	4	0	0
0.82930	9	3	3	1
0.80830	8	4	2	0

Lattice : Face-centered cubic
S.G. : Fm3m (225)

a = 3.61500

Z = 4

Mol. weight = 63.55
Volume [CD] = 47.24
Dx = 8.935
Dm = 8.950

Melting point: 1083°
Sample preparation: It had been heated in an H2 atmosphere at 300 C.
Sample source or locality: Sample from metallurgical laboratory of NBS, Gaithersburg, MD, USA.
Temperature of data collection: Pattern taken at 26 C.
General comments: Impurities from 0.001-0.01%, Ag, Al, Bi, Fe, Si, Zn.
General comments: Opaque mineral optical data on specimen from unspecified locality, R_3R%=60.65. Disp.=Std., VHN_{100}=96-104, Ref.: IMA Commission on Ore Microscopy QDF.
General comments: Measured density and color from *Dana's System of Mineralogy, 7th Ed.*, I 99.
Color: Red
Data collection flag: Ambient.

Swanson, Tatge., Natl. Bur. Stand. (U.S.), Circ. 539, volume I, page 15 (1953)

CAS Number: 7440-50-8

Radiation : CuKa1
Lambda : 1.54050
SS/FOM : F8= 89(0.0112,8)

Filter : Beta
d-sp : Not given

Pattern : 00-004-0783 **Radiation =** 1.540598 **Quality :** Indexed

Ag

Silver
Silver-3C, syn

Lattice : Face-centered cubic
S.G. : Fm3m (225)

a = 4.08620

Z = 4

Mol. weight = 107.87
Volume [CD] = 68.23
Dx = 10.501
Dm = 10.500
I/Icor = 5.20

Color: Light gray metallic
Sample source or locality: Sample obtained from Johnson Matthey Company, Ltd.
General comments: Purity >99.999%.
Analysis: Spectrographic analysis indicated faint traces of Ca, Fe and Cu.
Temperature of data collection: Pattern taken at 27 C.
Optical data: B=0.181
Melting point: 960.6°
General comments: Opaque mineral optical data on specimen from Great Bear Lake, Canada: RR_2R_a=94.1, Disp.=16, VHN_{100}=55-63, Color values .314, .321, 94.2, Ref.: IMA Commission on Ore Microscopy QDF.
Data collection flag: Ambient.

Swanson, Tatge., Natl. Bur. Stand. (U.S.), Circ. 539, volume I, page 23 (1953)

CAS Number: 7440-22-4

Radiation : CuKa1
Lambda : 1.54056
SS/FOM : F9= 65(0.0153,9)

Filter : Beta
d-sp : Not given

d (Å)	i	h	k	l
2.35900	100	1	1	1
2.04400	40	2	0	0
1.44500	25	2	2	0
1.23100	26	3	1	1
1.17960	12	2	2	2
1.02150	4	4	0	0
0.93750	15	3	3	1
0.91370	12	4	2	0
0.83410	13	4	2	2

Pattern : 00-004-0787 ***Radiation =*** 1.540598 ***Quality :*** High

Al

Aluminum
Aluminum, syn [NR]

Lattice : Face-centered cubic
S.G. : Fm3m (225)

a = 4.04940

Z = 4

Mol. weight = 26.98
Volume [CD] = 66.40
Dx = 2.699
I/Icor = 3.62

Color: Light gray metallic
Sample preparation: The material used for the NBS sample was a melting point standard sample of aluminum prepared at NBS, Gaithersburg, MD, USA.
Analysis: The chemical analysis (%): Si 0.011, Cu 0.006, Fe 0.007, Ti 0.0001, Zr 0.003, Ga 0.004, Mo 0.00002, S 0.0001, Al 99.9+ (by difference).
Temperature of data collection: Pattern taken at 25 C.
General comments: Mineral species of doubtful validity, *Am. Mineral.*, **65** 205 (1980).
Data collection flag: Ambient.

Swanson, Tatge., Natl. Bur. Stand. (U.S.), Circ. 539, volume I, page 11 (1953)

CAS Number: 7429-90-5

Radiation : CuKa1
Lambda : 1.54056
SS/FOM : F9= 93(0.0108,9)

Filter : Beta
d-sp : Not given

d (Å)	i	h	k	l
2.33800	100	1	1	1
2.02400	47	2	0	0
1.43100	22	2	2	0
1.22100	24	3	1	1
1.16900	7	2	2	2
1.01240	2	4	0	0
0.92890	8	3	3	1
0.90550	8	4	2	0
0.82660	8	4	2	2

G) Appendix G: e-beam evaporation Experiments

EVAPORATOR LOGSHEET

Experimentalist/s: Stephen & Mthobisi

Experiment Description: Si/Cu

Experiment No.: 1 Crystal (before): 2% (after): 2

Evaporation Date: 25/8/2010 Factor (top): (bottom): 6

Crucible Arrangement: Cu

Holder	~~Sample No~~ time	Element	Thickness	Rate(Å/s)	Current	Temp(°C)	Pressure p1	Pressure p2
A	2min	Cu	110 Å	0.6-1.2	<10mA		2×10^{-6} mbar	
B	5min	Cu	282 Å	0.6-1.2	<10mA		2×10^{-6} mbar	
C	7min	Cu	246 Å	0.6-1.2	<10mA		2×10^{-6} mbar	
D	10min	Cu	374 Å	0.6-1.2	<10mA		2×10^{-6} mbar	
E	15min	Cu	756 Å	0.6-1.2	<10mA		2×10^{-6} mbar	
F	30min	Cu	1254 Å	0.6-1.2	<10mA		2×10^{-6} mbar	

Comments:

EVAPORATOR LOGSHEET

Experimentalist/s: Stephen & Mthobisi

Experiment Description: Si/Ag

Experiment No.: 2 Crystal (before): 2% (after): 3%

Evaporation Date: 27/05/2010 Factor (top): (bottom): 600%

Crucible Arrangement: 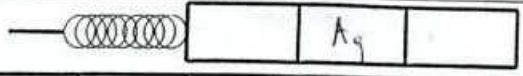

Holder	Time Sample No	Element	Thickness	Rate(Å/s)	Current	Temp(°C)	Pressure P1	P2	P3
A	2min	Ag	~~102Å~~	0.6-1.2	< 16mA		10^{-6}	mbar	
B	5min	Ag	186 Å	0.6-1.2	< 10mA		$<2\times10^{-6}$	mbar	
C	7min	Ag	420 Å	0.6-1.2	< 10mA		10^{-6}	mbar	
D	10min	Ag	600Å	0.6-1.2	< 10mA		10^{-6}	mbar	
E	15min	Ag	858Å	0.6-1.2	< 10mA		10^{-6}	mbar	
F	20min	Ag	1170Å	0.6-1.2	< 10mA		10^{-6}	mbar	

Comments:

EVAPORATOR LOGSHEET

Experimentalist/s: Stephen & Mthobisi

Experiment Description: Si/Al

Experiment No.: 3 Crystal (before): 5% (after): 3%

Evaporation Date: 31/05/10 Factor (top): (bottom): 600Å

Crucible Arrangement: 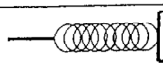 | | | Al

Holder	Sample No	Element	Thickness	Rate(Å/s)	Current	Temp(°C)	Pressure p1	p2	p3
A	2min	Al	60Å	0.6-1.2	<10mA		2X10⁻⁶ mbar		
B	5min	Al	66Å	0.6-1.2	<10mA		3X10⁻⁶ mbar		
C	7min	Al	150Å	0.6-1.2	<10mA		4X10⁻⁶ mbar		
D	10min	Al	600 Å	0.6-1.2	<10mA		2X10⁻⁶ mbar		
E	15min	Al	624Å	0.6-1.2	<10mA		2X10⁻⁶ mbar		
F	20min	Al	654Å	0.6-1.2	<10mA		2X10⁻⁶ mbar		

Comments:

EVAPORATOR LOGSHEET

Experimentalist/s: Stephen & Mthobisi

Experiment Description: Si/Cu

Experiment No.: 4 Crystal (before): 2% (after): 2%

Evaporation Date: 04/06/2010 Factor (top): (bottom): 600%

Crucible Arrangement: Cu | | |

Holder	~~Sample No~~ Time	Element	Thickness	Rate(Å/s)	Current	Temp(°C)	Pressure p1	p2	p3
A	2min	Cu	132 Å°	0.6-1.2	<10mA		3×10^{-6} mbar		
B	5min	Cu	378 Å°	0.6-1.2	<10 mA		3×10^{-6} mbar		
C	7min	Cu	510 Å°	0.6-1.2	<10 mA		3×10^{-6} mbar		
D	10min	Cu	654 Å°	0.6-1.2	<10 mA		$<3\times10^{-6}$ mbar		
E	15min	Cu	840 Å°	0.6-1.2	<10 mA		3×10^{-6} mbar		
F	20min	Cu	984 Å°	0.6-1.2	<10 mA		2×10^{-6} mbar		

Comments:

EVAPORATOR LOGSHEET

Experimentalist/s: MLUNGISI FOR S. MATOPE

Experiment Description: Si / Ag

Experiment No.: Crystal (before): 4% (after): 4%

Evaporation Date: 10/12/10 Factor (top): (bottom): 600%

Crucible Arrangement: Ag

Holder	Sample No	Element	~~Thickness~~ Time (min)	Rate(Å/s)	Current	~~Temp(°C)~~ Thickness	Pressure P1	P2	P3
A		Ag	2 min	0.6 – 1.2 Å/s	160 mA	104 Å	2×10^{-5} mbar		
D		Ag	5 min	0.6 – 1.2 Å/s	130 mA	174 Å	1×10^{-5} mbar		
C		Ag	7 min	0.6 – 1.2 Å/s	160 mA	372 Å	2×10^{-5} mbar		
B		Ag	10 min	0.6 – 1.2 Å/s	130 mA	612 Å	1×10^{-5} mbar		
I		Ag	15 min	0.6 – 1.2 Å/s	150 mA	702 Å	1×10^{-5} mbar		
F		Ag	20 min	0.6 – 1.2 Å/s	140 mA	1586 Å	1×10^{-5} mbar		

Comments:

EVAPORATOR LOGSHEET

Experimentalist/s: Mlungisi & Stephen

Experiment Description: Si/Cu

Experiment No.: 1 Crystal (before): 2% (after): 3%

Evaporation Date: 02/09/2011 Factor (top): (bottom): 600%

Crucible Arrangement:  Cu

Holder	Sample No	Element	Thickness	Rate(Å/s)	Current	Temp(°C)	Pressure P1	P2	P3
A	(2min)	Cu	~84Å	0.6-1.2Å/s	<1mA		1×10^{-6} mbar		2×10^{-6} torr
C	(5min)	Cu	~540Å	0.6-1.2Å/s	<1mA		1×10^{-6} mbar		2×10^{-6} torr
H	(7min)	Cu	~504Å	0.6-1.2Å/s	<1mA		1×10^{-6} mbar		2×10^{-6} torr
B	(10min)	Cu	~888Å	0.6-1.2Å/s	<1mA		1×10^{-6} mbar		2×10^{-6} torr
F	(15min)	Cu	~1500Å	0.6-1.2Å/s	<1mA		1×10^{-6} mbar		2×10^{-6} torr
E	(20min)	Cu	~2656	0.6-1.2Å/s	<1mA		1×10^{-6} mbar		2×10^{-6} torr

Comments:

EVAPORATOR LOGSHEET

Experimentalist/s: MLUNGISI & STEPHEN

Experiment Description: Si | Ag

Experiment No.: 2 Crystal (before): 3% (after): 4%

Evaporation Date: 05/09/2011 Factor (top): (bottom): 600%

Crucible Arrangement: 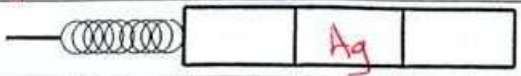

Holder	Sample No	Element	Thickness	Rate(Å/s)	Current	Temp(°C)	Pressure p1	Pressure p2	Pressure p3
H	(2min)	Ag	0.6-1.2Å/s	~150Å	40mA		2×10^{-6} mbar		2×10^{-6}
B	(5min)	Ag	0.6-1.2Å/s	~270Å	40mA		2×10^{-6} mbar		2×10^{-6}
E²	(7min)	Ag	0.6-1.2Å/s	~318Å	50mA		2×10^{-6} mbar		2×10^{-6}
F	(10min)	Ag	0.6-1.2Å/s	~390Å	50mA		2×10^{-6} mbar		2×10^{-6}
C	(15min)	Ag	0.6-1.2Å/s	~750Å	60mA		2×10^{-6} mbar		2×10^{-6}
A	(20min)	Ag	0.6-1.2Å/s	~1030	80mA		2×10^{-6} mbar		2×10^{-6}

Comments:

EVAPORATOR LOGSHEET

Experimentalist/s: Mcungasi & Stephen

Experiment Description: Si / Al

Experiment No.: 3 Crystal (before): 4% (after):

Evaporation Date: 07/09/2011 Factor (top): (bottom): 600%

Crucible Arrangement: Al

Holder	Sample No	Element	Thickness	Rate(Å/s)	Current	Temp(°C)	Pressure P1	Pressure P2	Pressure P3
B	(2min)	Al	~66Å	0.6-1.2Å/s	150mA		2×10^{-5} mbar		2×10^{-9} Torr
H	(5min)	Al	~366Å	0.6-1.2Å/s	150mA		"		"
F	(7min)	Al	~430Å	0.6-1.2Å/s	150mA		"		"
C	(10min)	Al	~726Å	0.6-1.2Å/s	150mA		"		"
G	(15min)	Al	~1440Å	0.6-1.2Å/s	150mA		"		"
E^2	(20min)	Al	~1842Å	0.6-1.2Å/s	150mA		"		"

Comments:

H) APPENDIX H: XRD graphs

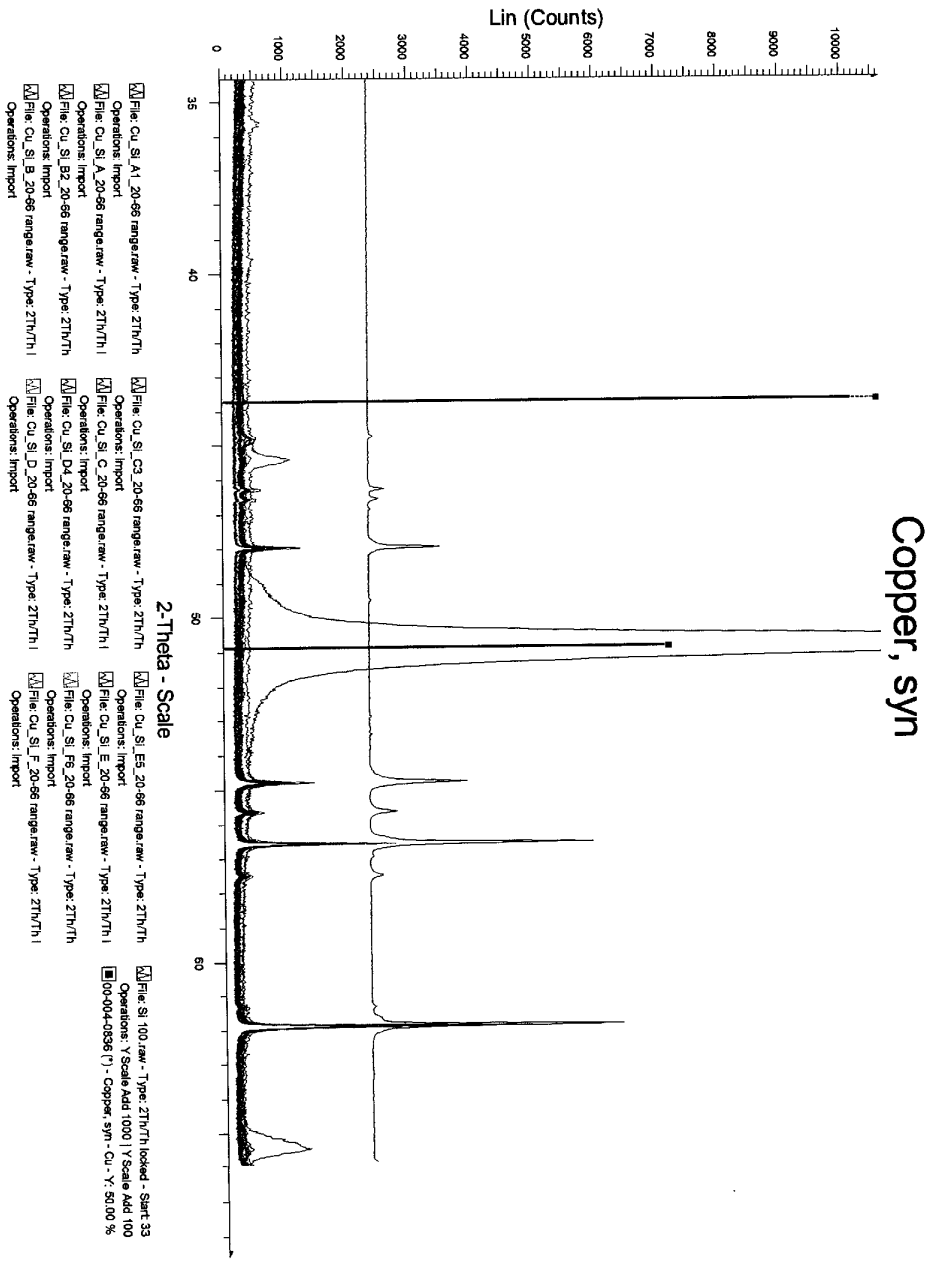

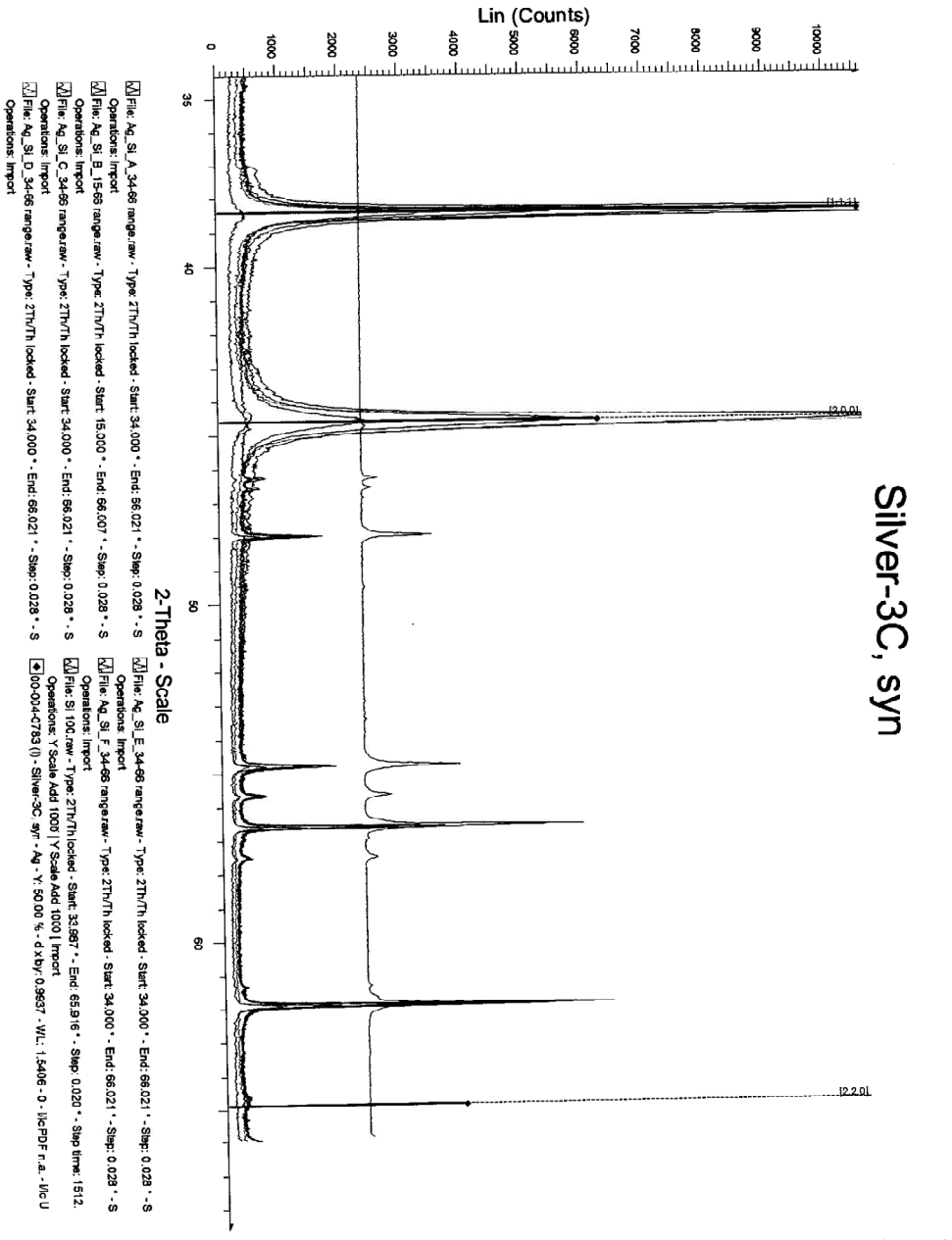

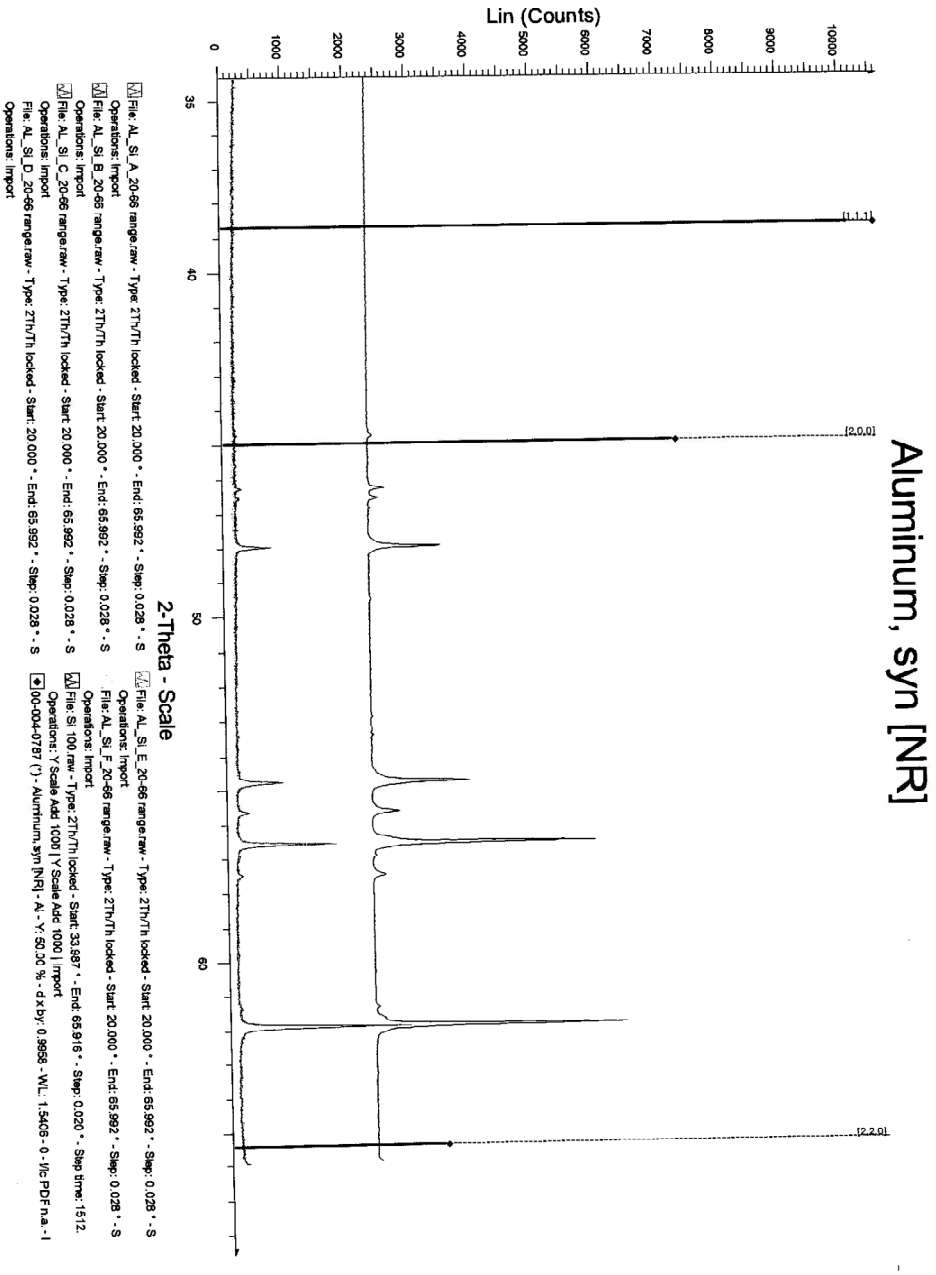

I) APPENDIX I: Polyurethane manufacturer's details

SMOOTH-ON
SINCE 1895

VytaFlex™ Series

Liquid Urethane Rubbers

PRODUCT OVERVIEW

Using Smooth-On's exclusive "V-Polymer" technology, **VytaFlex™** urethane rubbers offer superior physical and performance properties for casting concrete. **VytaFlex™** urethanes are available in 10A 20A, 30A, 40A, 50A and 60A Shore hardness's and feature convenient one-to-one by volume mix ratios. Vacuum degassing is not necessary and **VytaFlex™** rubbers cure with negligible shrinkage to a durable rubber that will last in production.

VytaFlex™ mold rubbers work especially well for casting pigmented / colored concrete. Molds made with VytaFlex™ Series urethanes will render accurate and uniform colored castings.

VytaFlex™ mold rubbers can also be used for a variety of applications including making molds for making special effects, toys and prototypes. Vibrant colors can be achieved by adding So-Strong™ Color Tints, available from Smooth-On. ***Want to cast gypsum or wax?*** Our **ReoFlex** line of urethane rubbers offers better release properties for casting plaster and wax.

TECHNICAL OVERVIEW

	Shore A	Mix Ratio	Color	Spec. Vol.	Spec. Grav.	Mixed Viscosity	Tear (C)	Elong. At Break	Tensile Strength
VytaFlex 10	10	1:1 pbv	Off-White	27.9	1.00	3,100 cps.	30 pli	1,000 %	160 psi
VytaFlex 20	20	1:1 pbv	Clear Amber	27.7	1.00	1,000 cps	58 pli	1,000%	200 psi
VytaFlex 30	30	1:1 pbv	Off-White	27.3	1.02	1,800 cps	78 pli	1,000%	500 psi
VytaFlex 40	40	1:1 pbv	Off-White	26.9	1.03	2,000 cps	82 pli	660%	522 psi
VytaFlex 50	50	1:1 pbv	Off-White	26.7	1.04	2,000 cps	102 pli	400%	588 psi
VytaFlex 60	60	1:1 pbv	Off-White	26.6	1.04	2,000 cps	136 pli	480%	880 psi

~ **Pot Life* VytaFlex 10, 20, 30, 40:** 30 minutes
~ **Pot Life: VytaFlex 50, 60:** 60 minutes

~ **Cure Time/Demold*:** Overnight / 16 hours
Note; Vytaflex 10 should be allowed to cure for 24 hours.
*Values measured at room temperature (72°F/23°C).

Shrinkage: Negligible

J) APPENDIX J: Surface Roughness micrographs and Van-der-Waals Forces graphs of metallic e-beam coatings and polyurethane materials.

This appendix carries the surface roughness profiles and Van-der-Waals forces of examined of metallic e-beam specimens and polyurethane samples

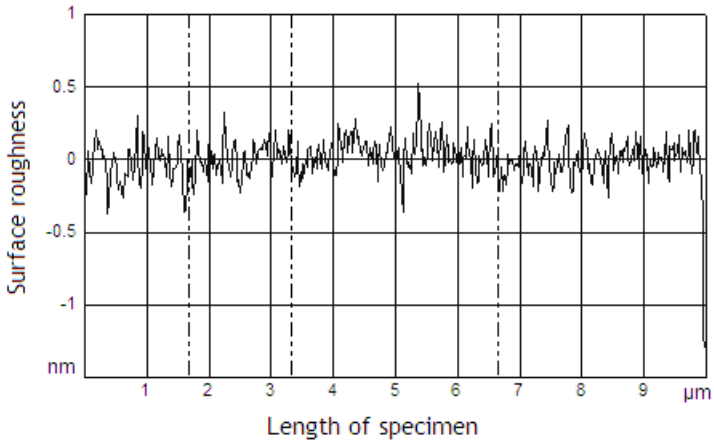

Figure 5-2 Atomic Force Micrograph of copper deposited for 2 min

Figure 5-2 shows the surface profile of an e-beam coating of copper on a 10-µm wide scan. The highest peak is 0.5 nm.

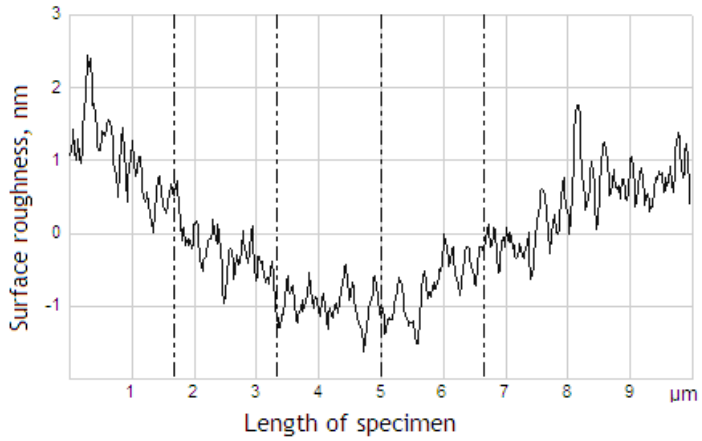

Figure 5-3 Atomic Force Micrograph of aluminum deposited for 2 min.

A 2-min e-beam deposition of aluminum is shown in Figure 5-3. Across a 10 µm wide scan, it is evident that it has a peak of 2.5 nm and a trough of about 1.5 nm. Its peak is greater than that of copper in the in Figure 5-2.

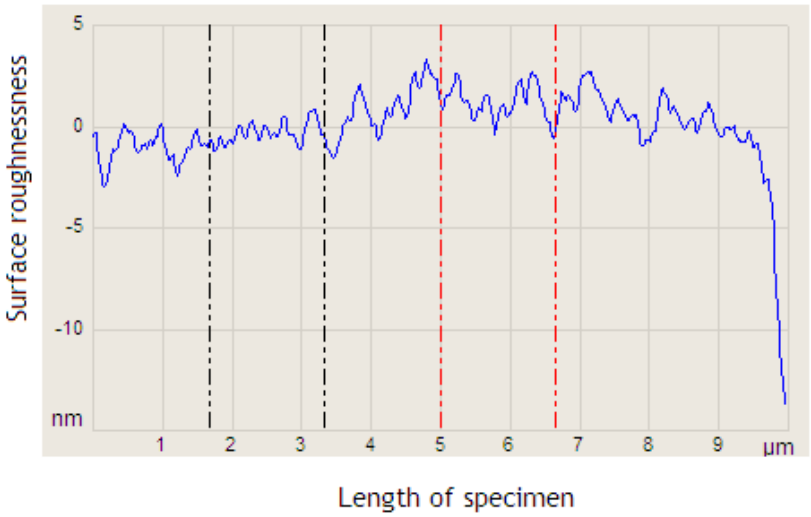

Figure 5-4 Atomic Force Micrograph of copper deposited for 5 min

Figure 5-4 shows the 5-min e-beam deposition of copper revealing peaks and troughs of about 3 nm. These are greater than those for aluminum which was e-beam deposited for 5min as shown in Figure 5-5. The right hand end of the scan coincided with the end of the specimen; hence a continuous drop is indicated.

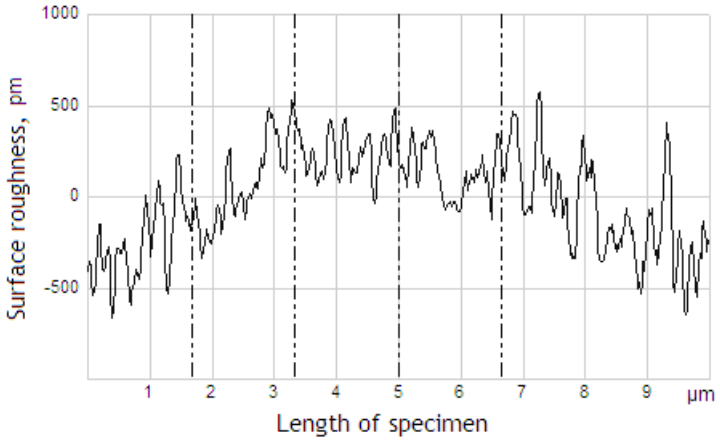

Figure 5-5 Atomic Force Micrograph of aluminum deposited for 5 min

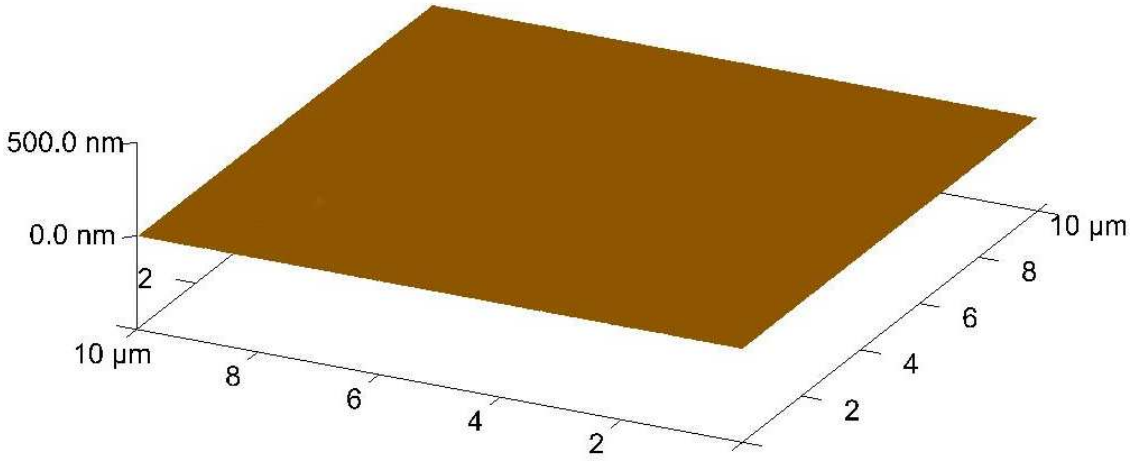

Figure 5-6 Atomic Force Micrograph of Silver deposited for 10 min

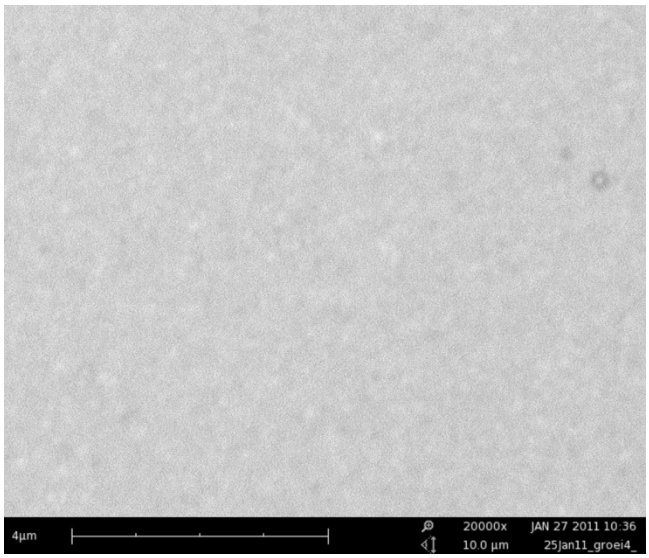

Figure 5-7 Scanning Electron Micrograph for silver deposited for 10 min

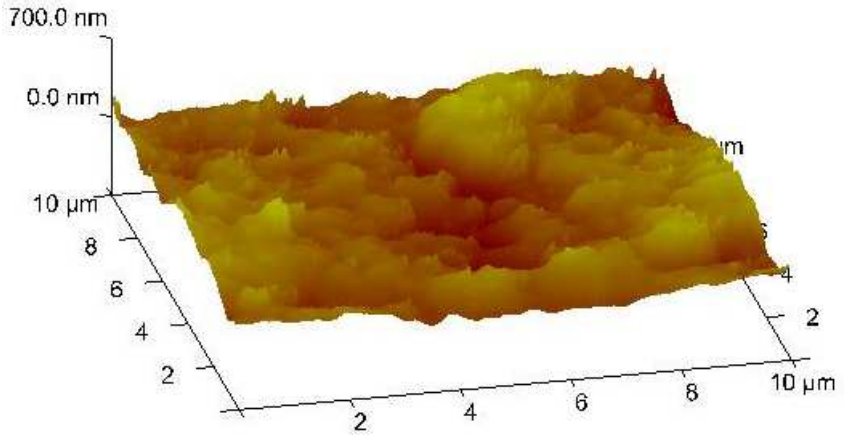

Figure 5-8 Atomic Force Micrograph of epoxy used for encapsulating IC components

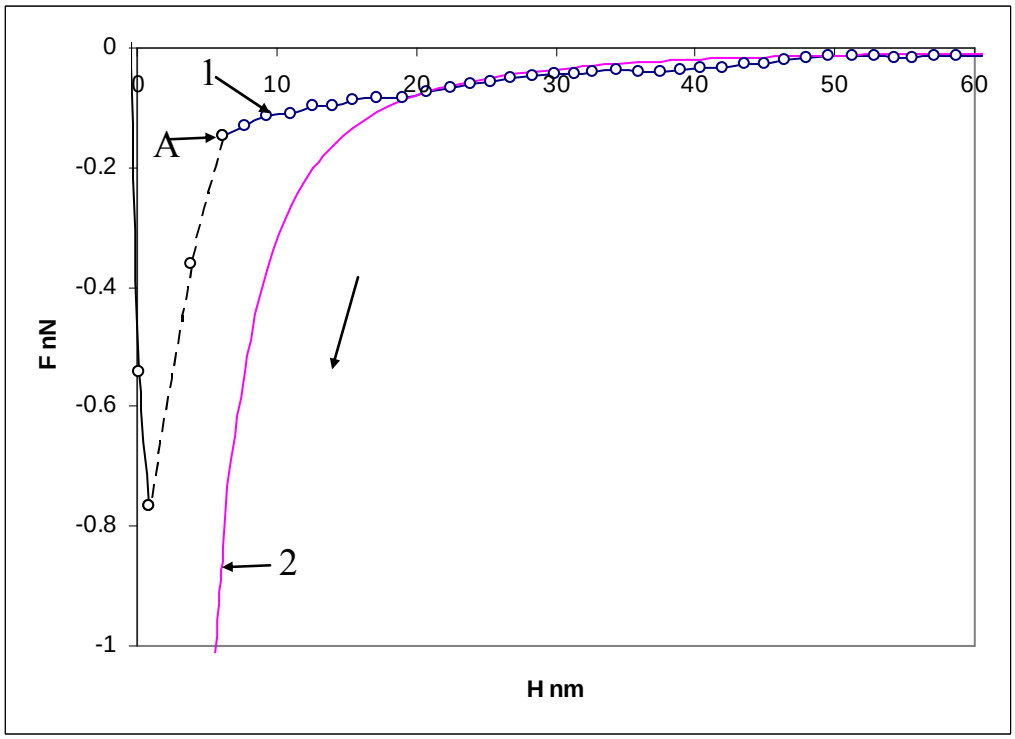

Figure 5-9 Copper (Cu 20.1) extending curves

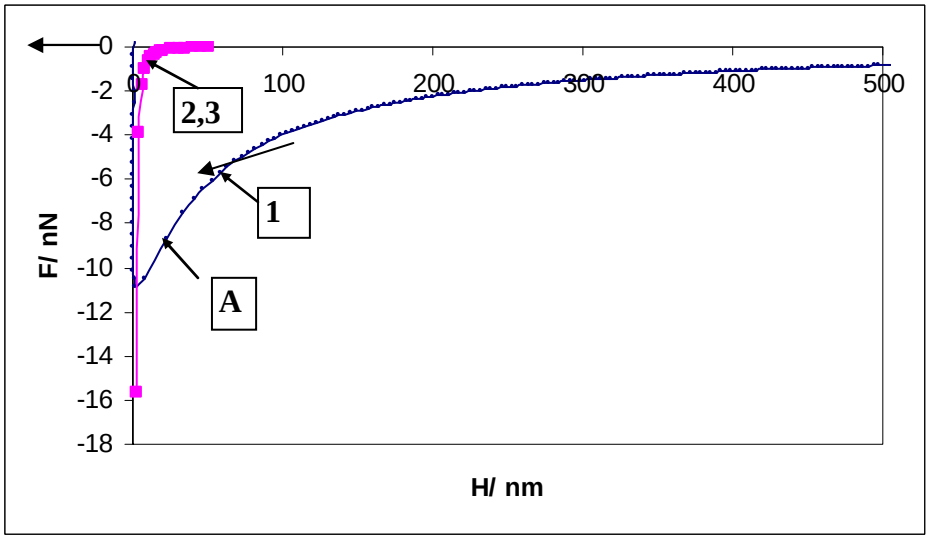

Figure 5-10 Silver (Ag 5.2) extending curves

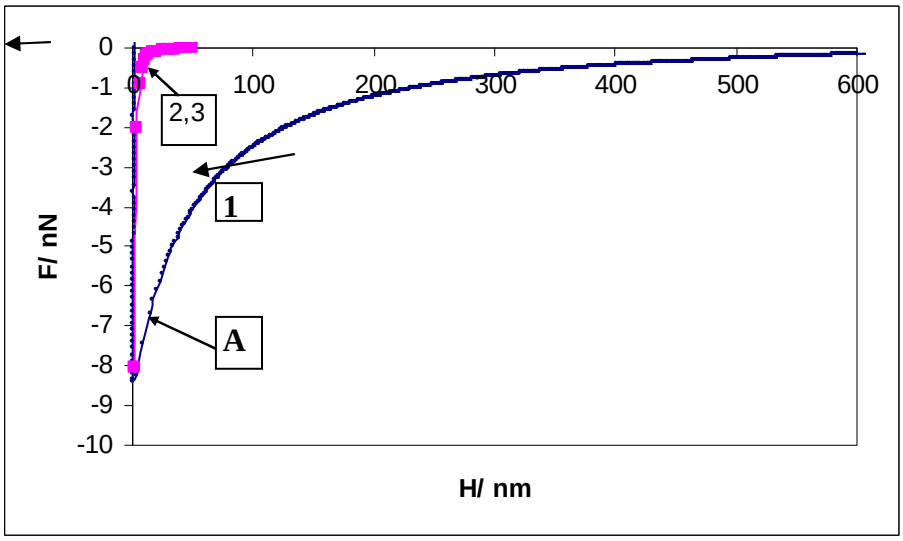

Figure 5-11 Al 5.2 extending curves

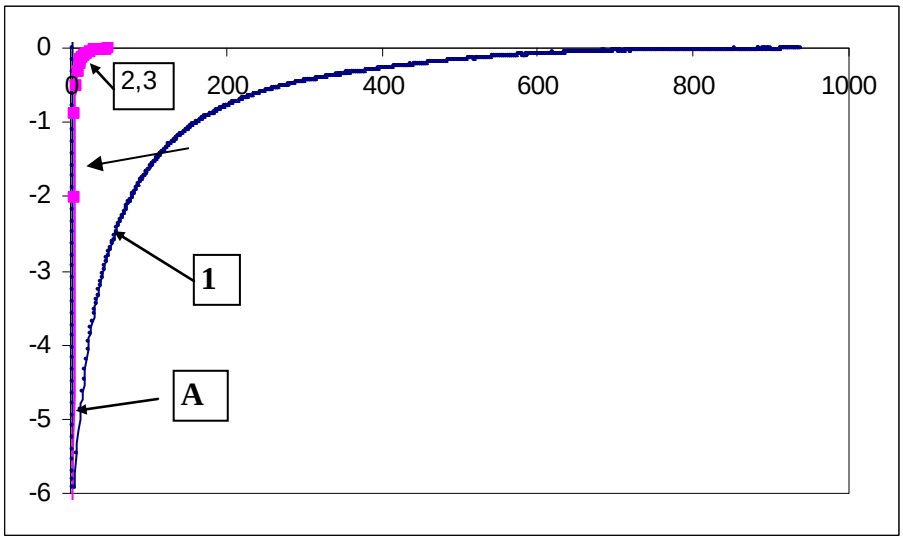

Figure 5-12 Al 20.2 extending curves

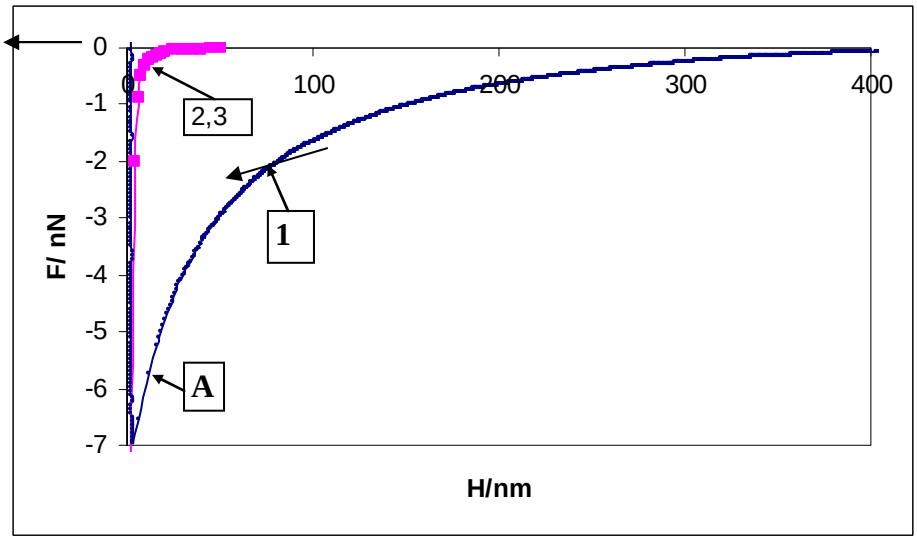

Figure 5-13 Cu 20.2 extending curves

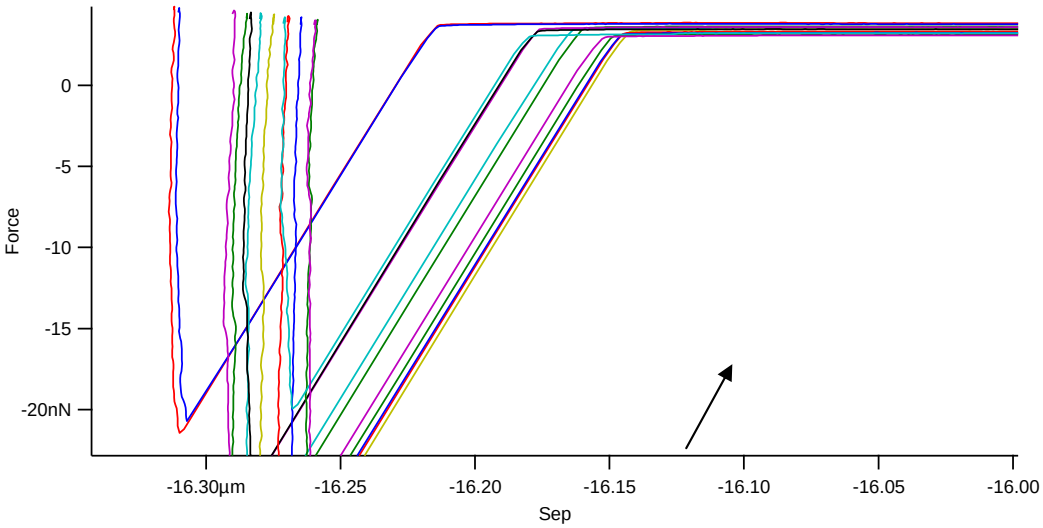

Fig. 1. Cu 5.1 Van-der-Waals force retracting curves

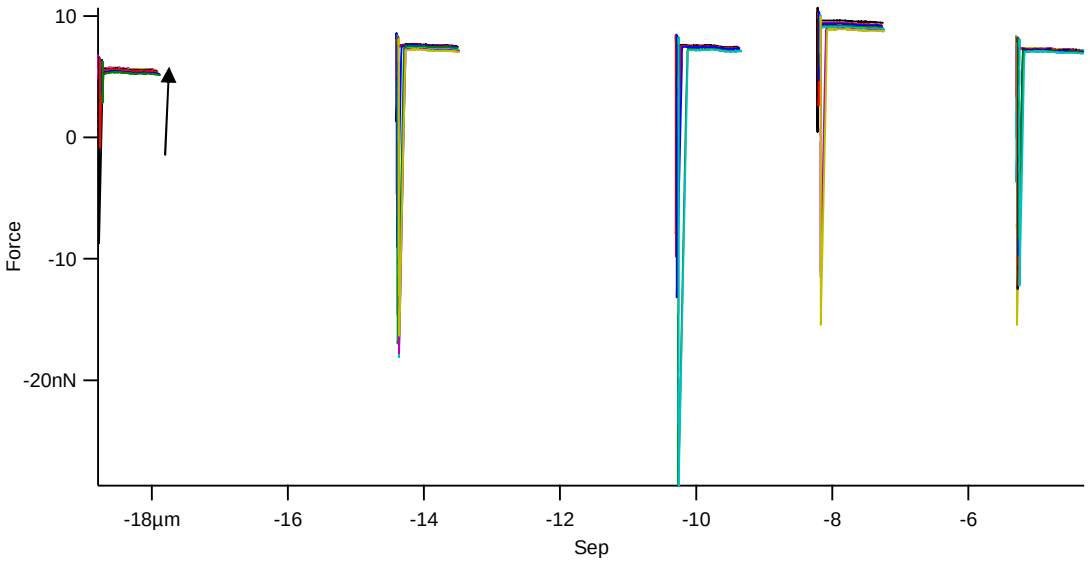

Fig. 2. Cu 20.1 Van-der-Waals force retracting curves

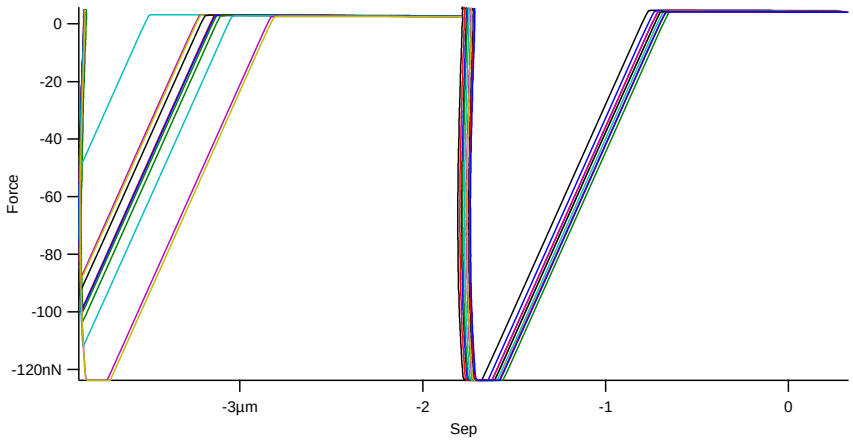

Fig. 3. Ag 20.1 Van-der-Waals force retracting curves

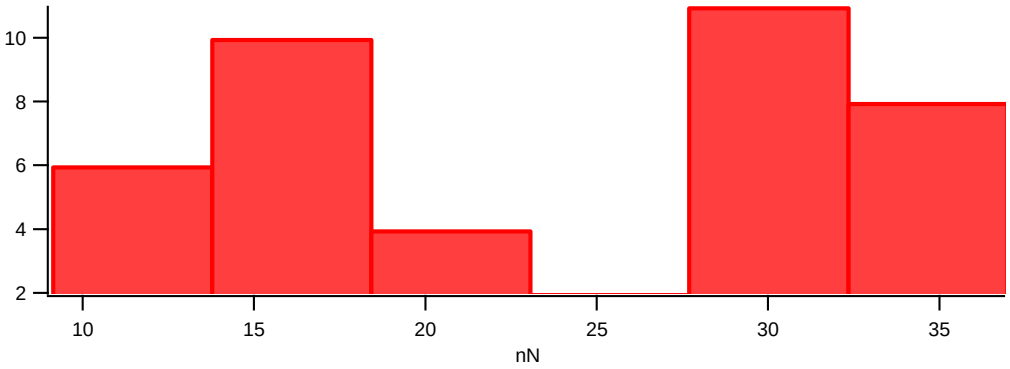

Fig. 4. Cu 5.1 distributions of Van-der-Waals forces

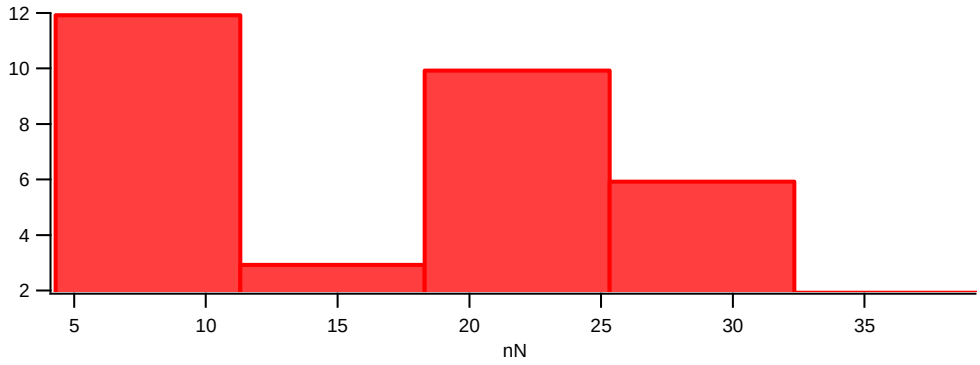

Fig. 5. Cu 20.1 distributions of Van-der-Waals forces

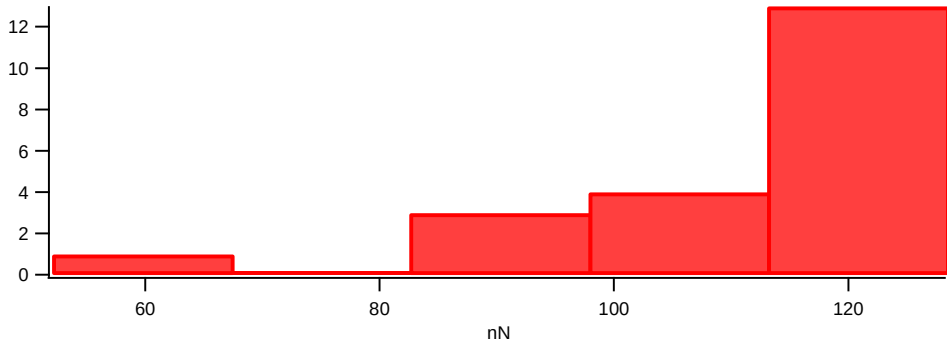

Fig. 6. Ag 20.1 distributions of Van-der-Waals forces

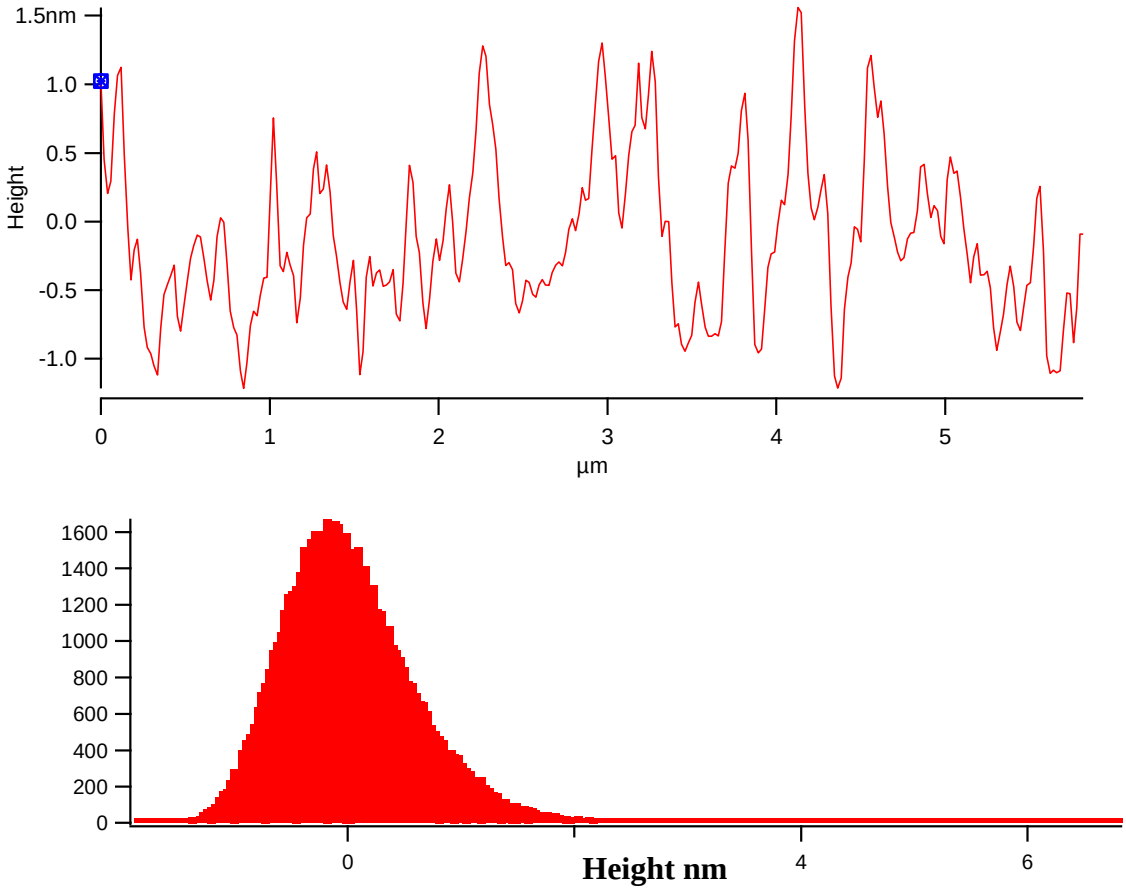

Fig 7. Surface roughness of Ag 5.2

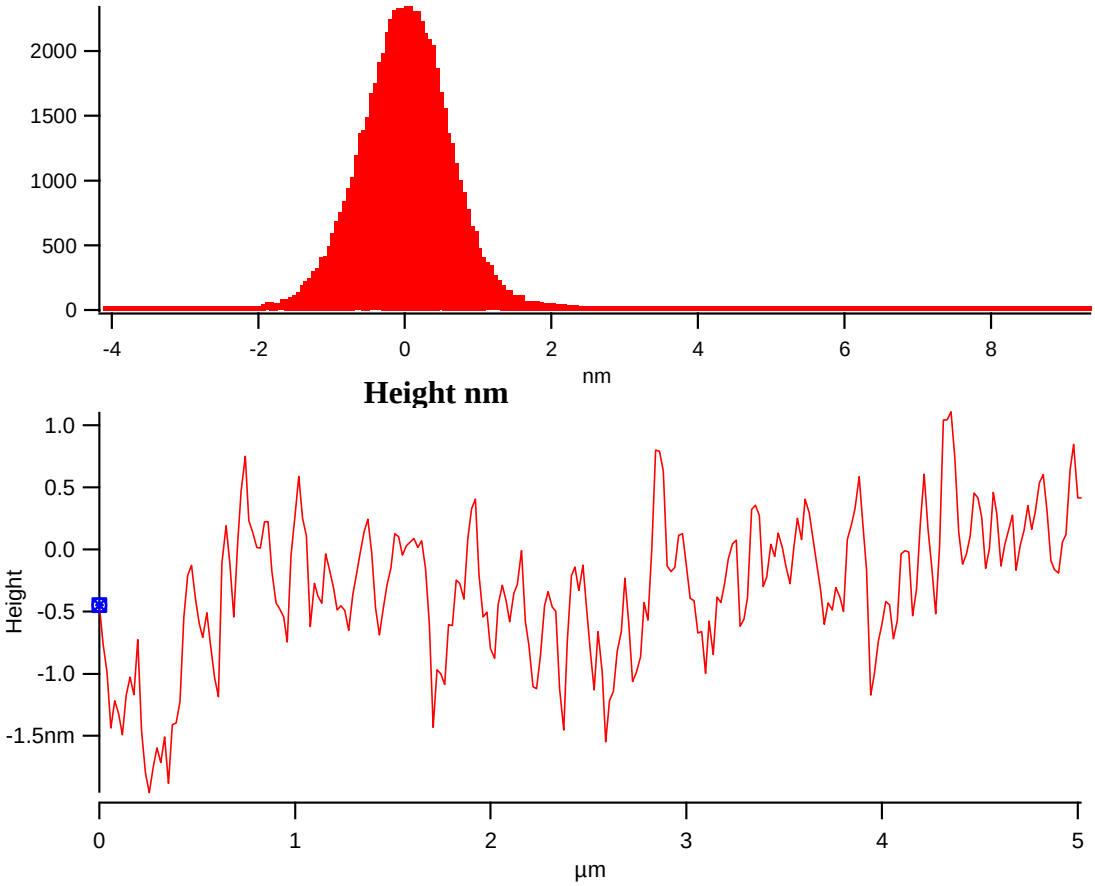

Fig 8. Surface roughness of Ag20.2

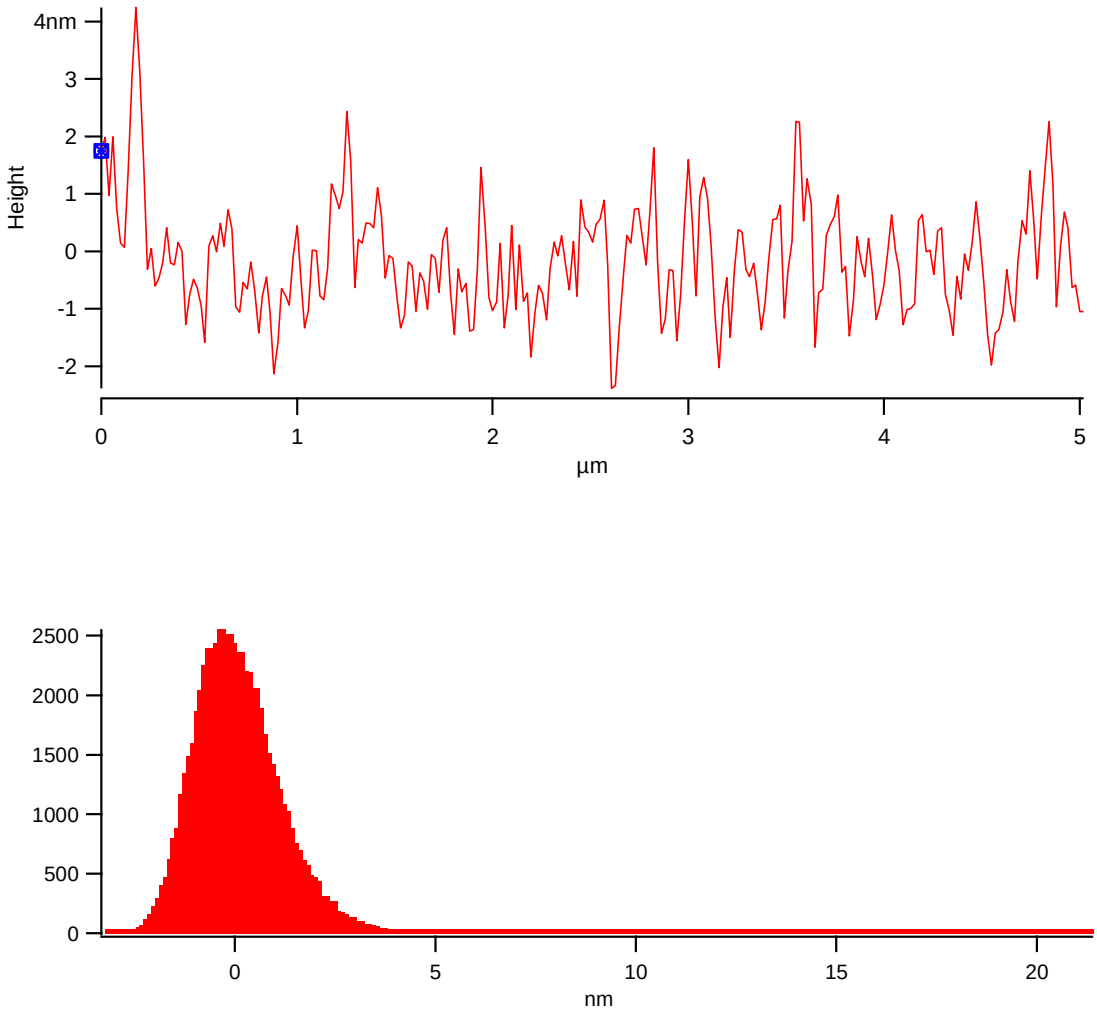

Fig 9. Surface roughness of Al 5.2

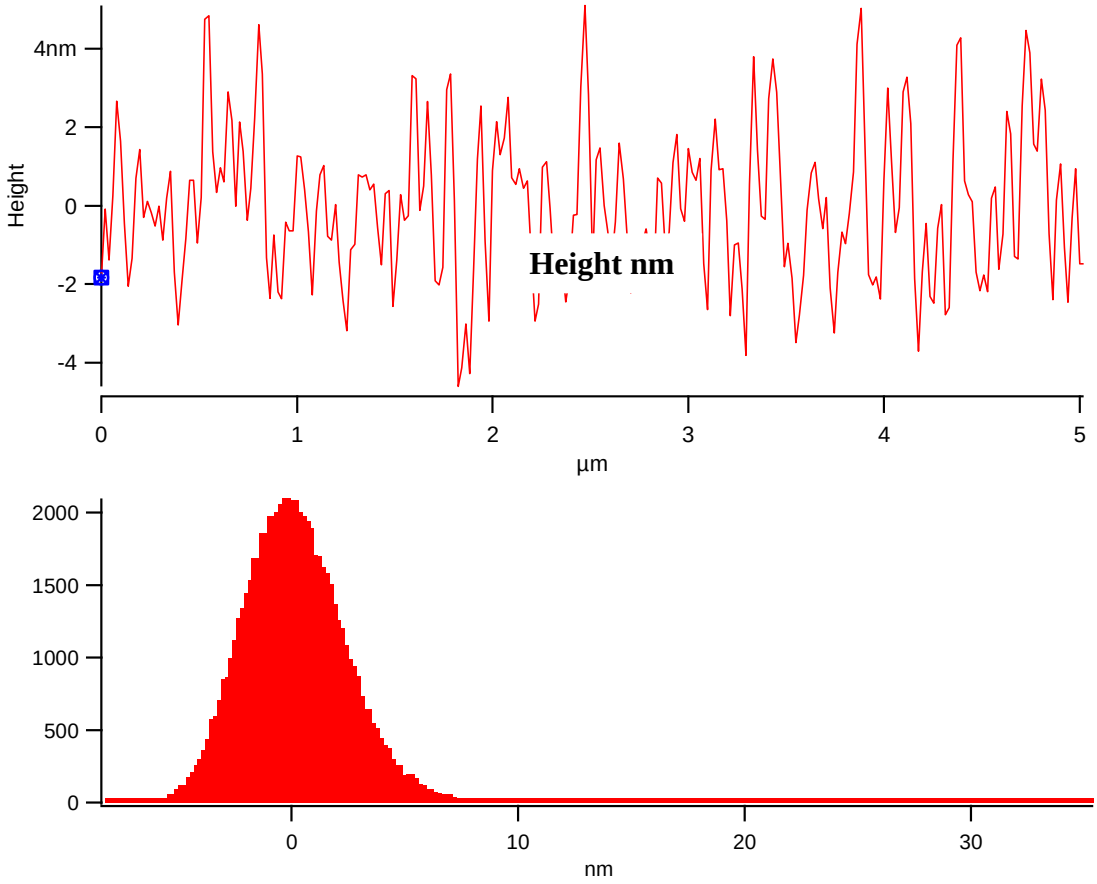

Fig. 10. Surface roughness of Al 20.2

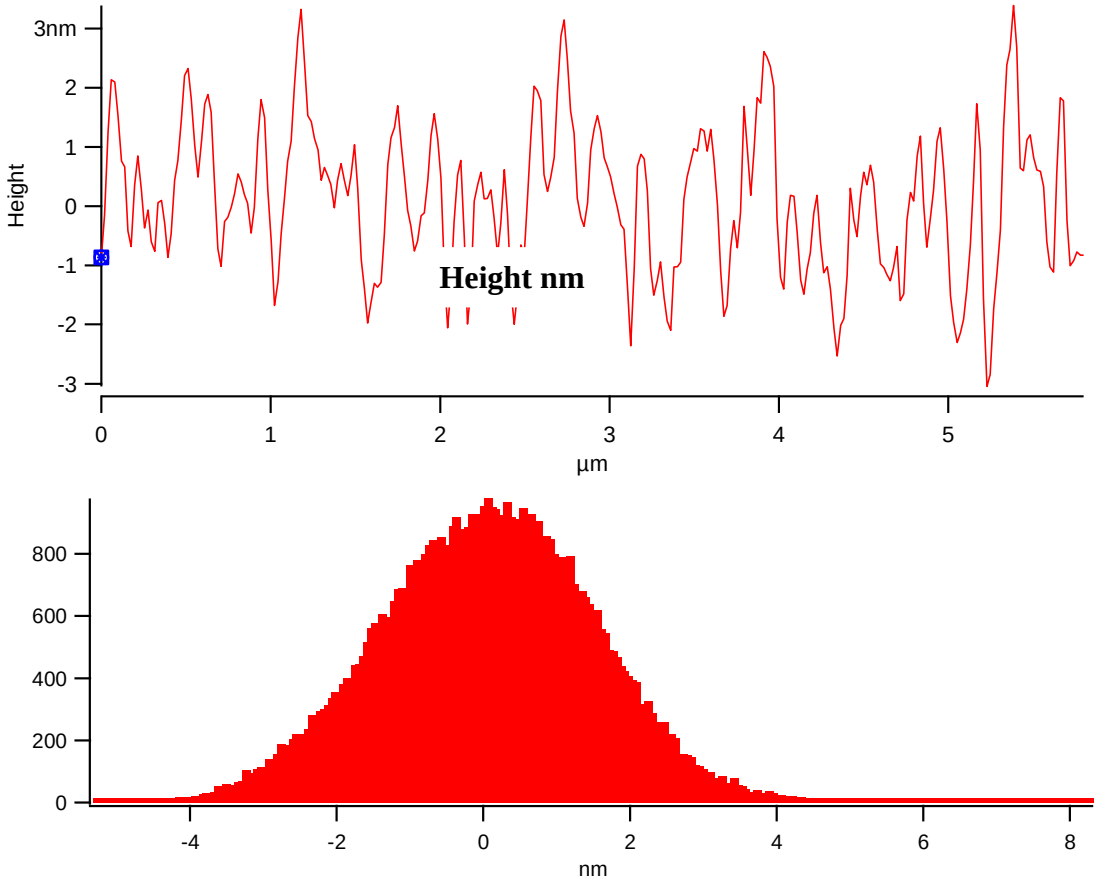

Fig. 11. Surface roughness of Cu 5.2

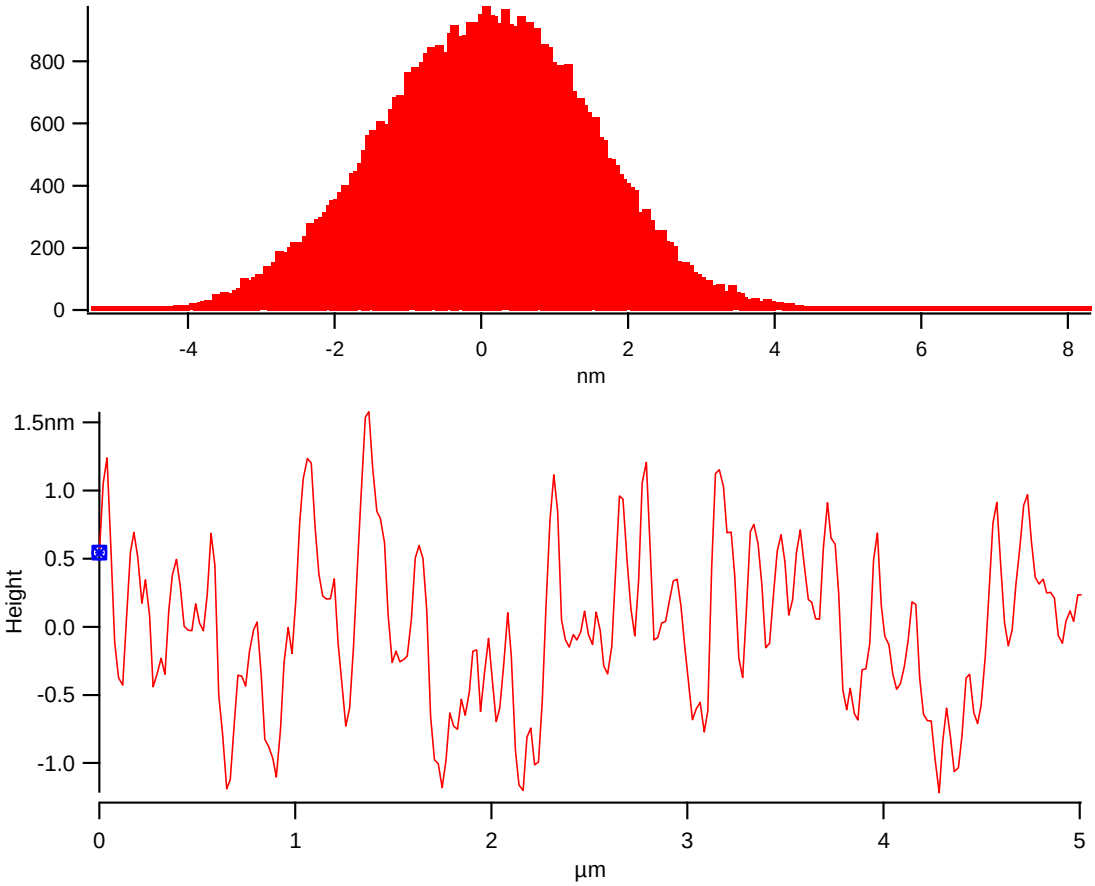

Fig.12. Surface roughness of Cu 20.2

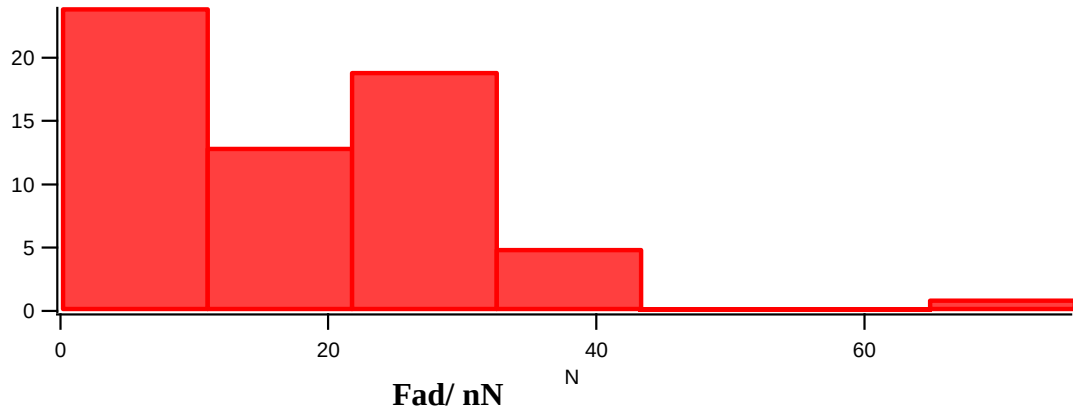

Fig.13 Ag20.2's Van-der Waals force distribution forces with a mean value of 25 nN

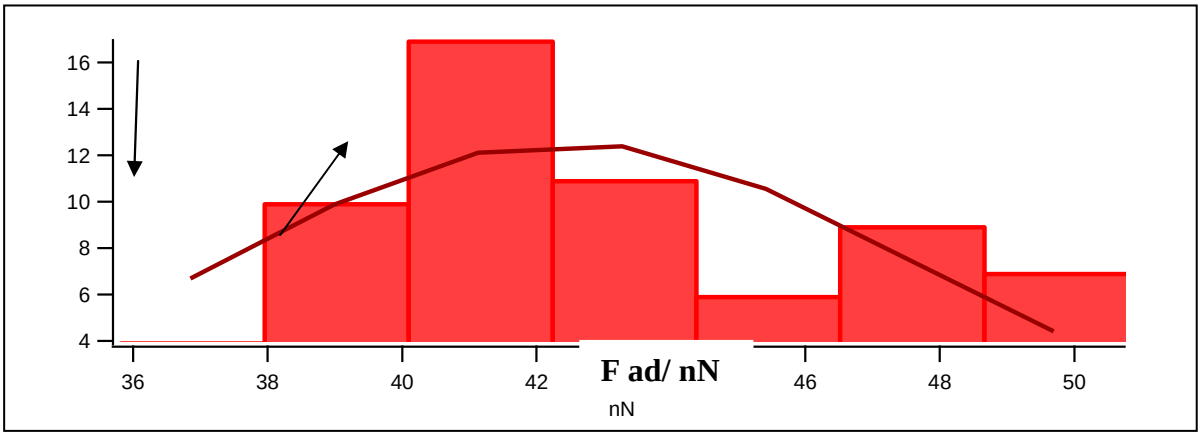

Fig.14 Al 5.2's Van-der Waals force distribution with a mean of 44±5 nN

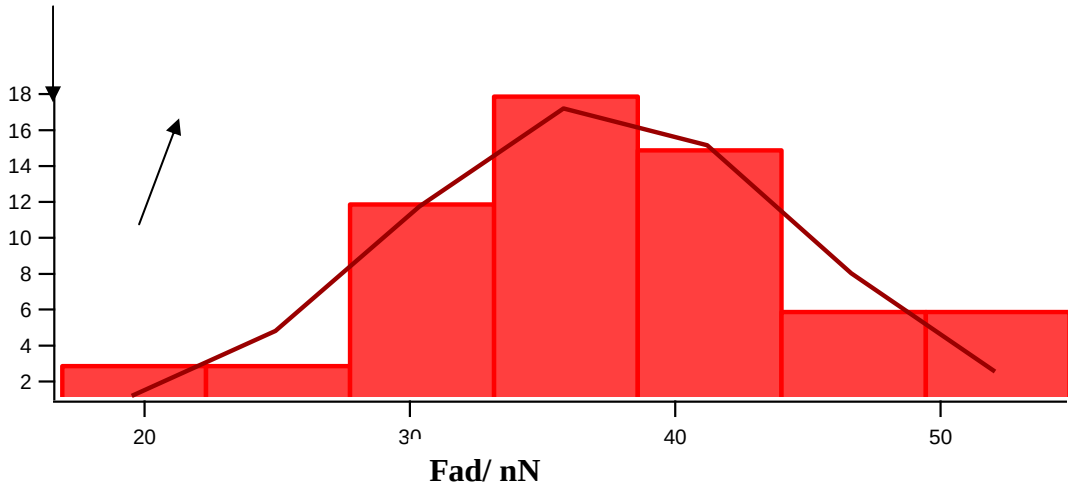

Fig. 15 Al 20.2's Van-der Waals force distribution with a mean of 37±8 nN

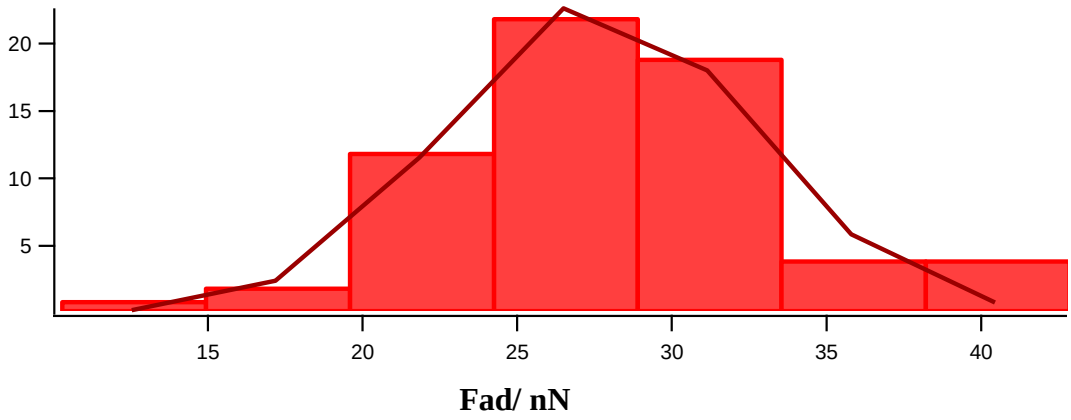

Fig.16 Cu 5.2's Van-der Waals force distribution with a mean of 28±5 nN

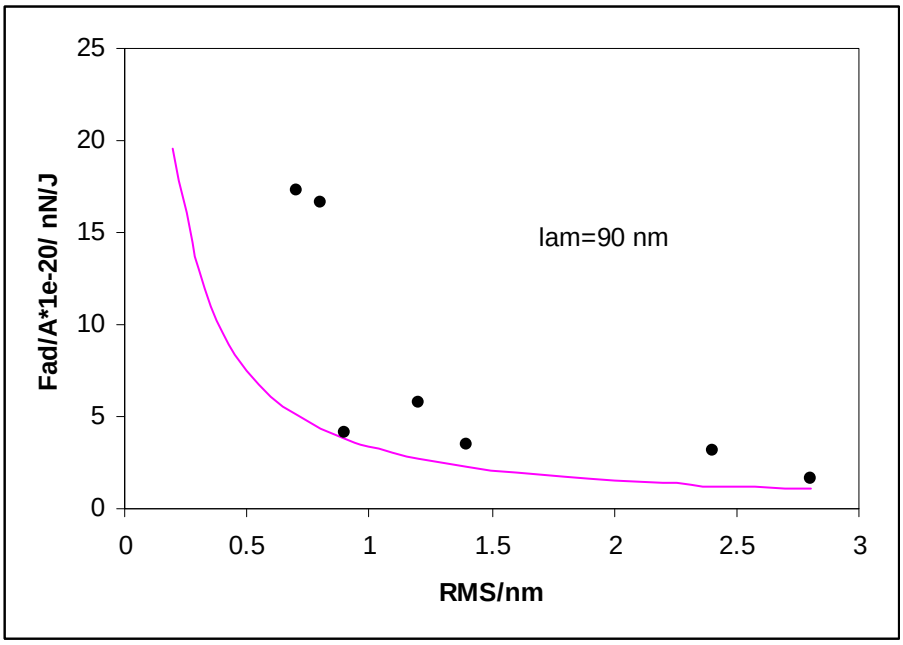

Fig. 18 Van-der Waals force per unit area (Fad /A) vs *rms* surface roughness values

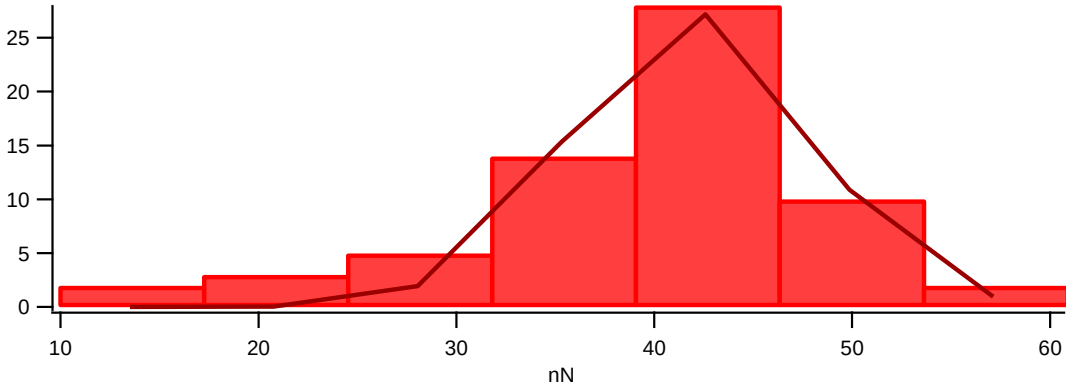

Fig. 19 Al20.2's distribution of Van-der-Waals force in 40% humid atmosphere, the Van-der-Waals forces have a mean value of 41.8±6.0 nN

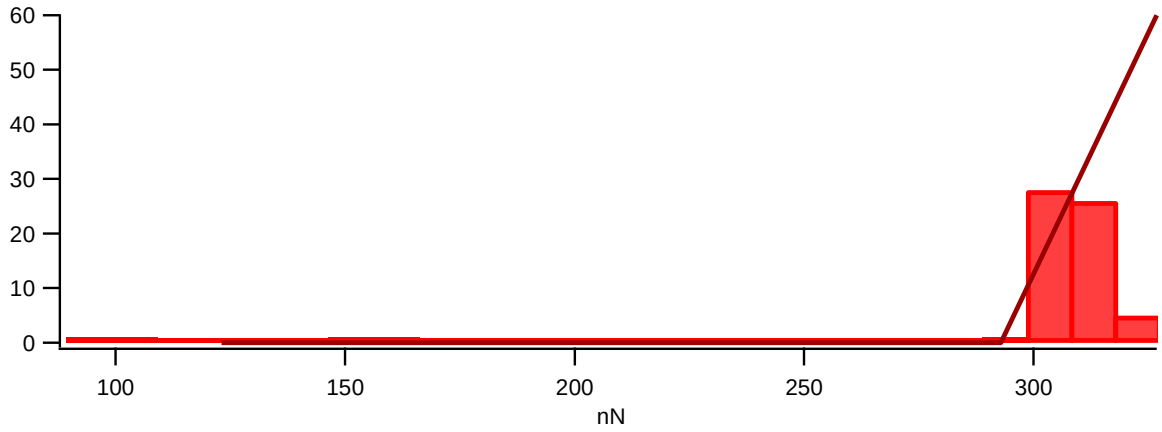

Fig.20 Polyurethane 30's Van-der-Waals force distribution with a mean value of 340±10 nN.

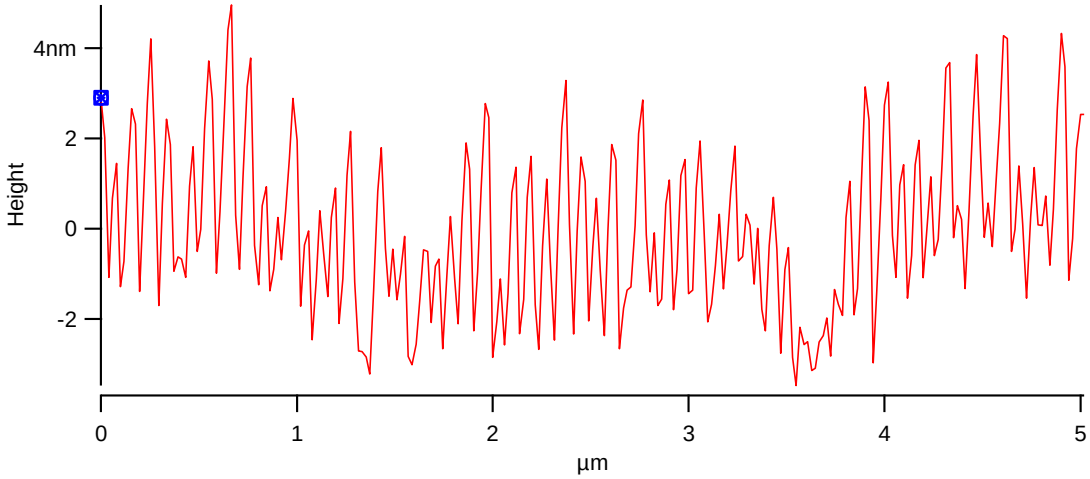

Fig. 21 Polyurethane 30's surface roughness profile

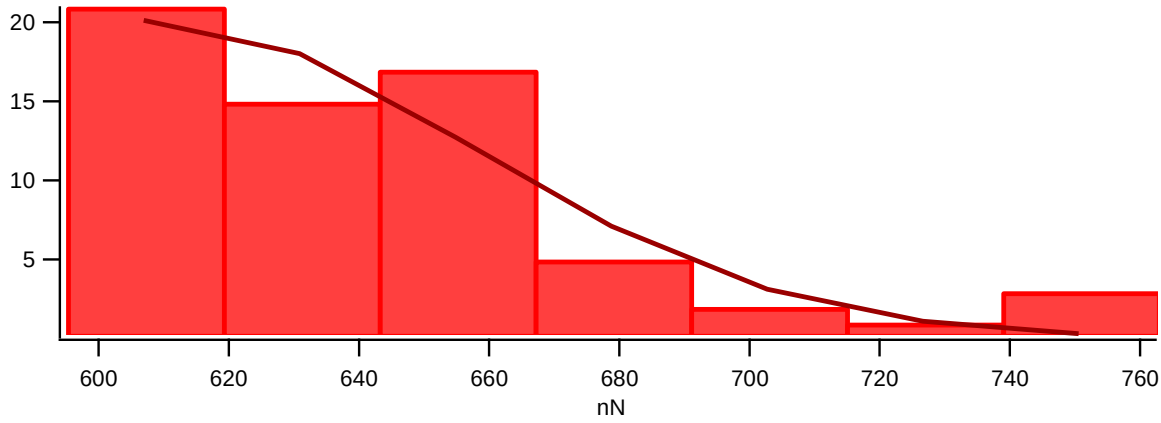

Fig. 22 Polyurethane 60's Van-der-Waals force distribution with a mean value of 630±20 nN

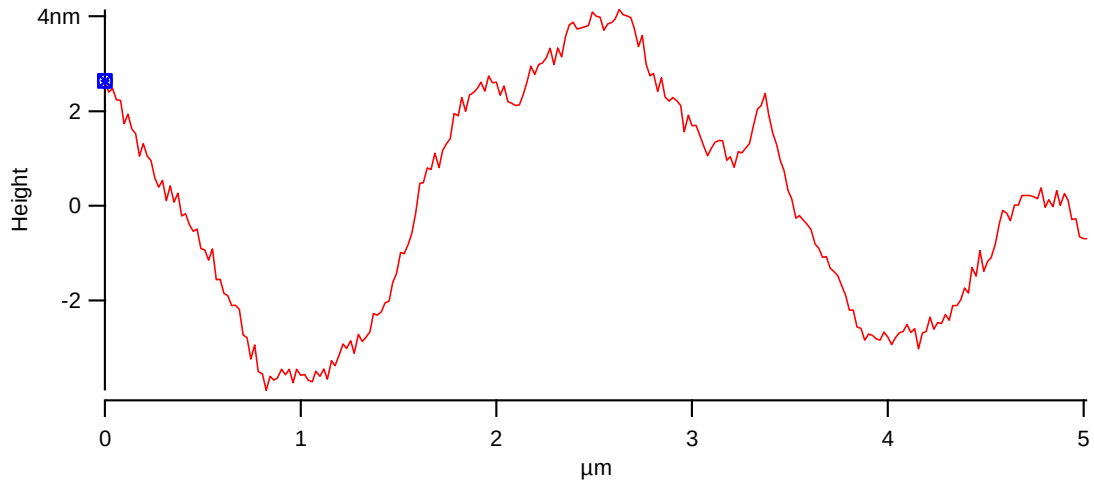

Fig.23 Polyurethane 60's surface roughness profiles

K) APPENDIX K: Experimental samples and equipment

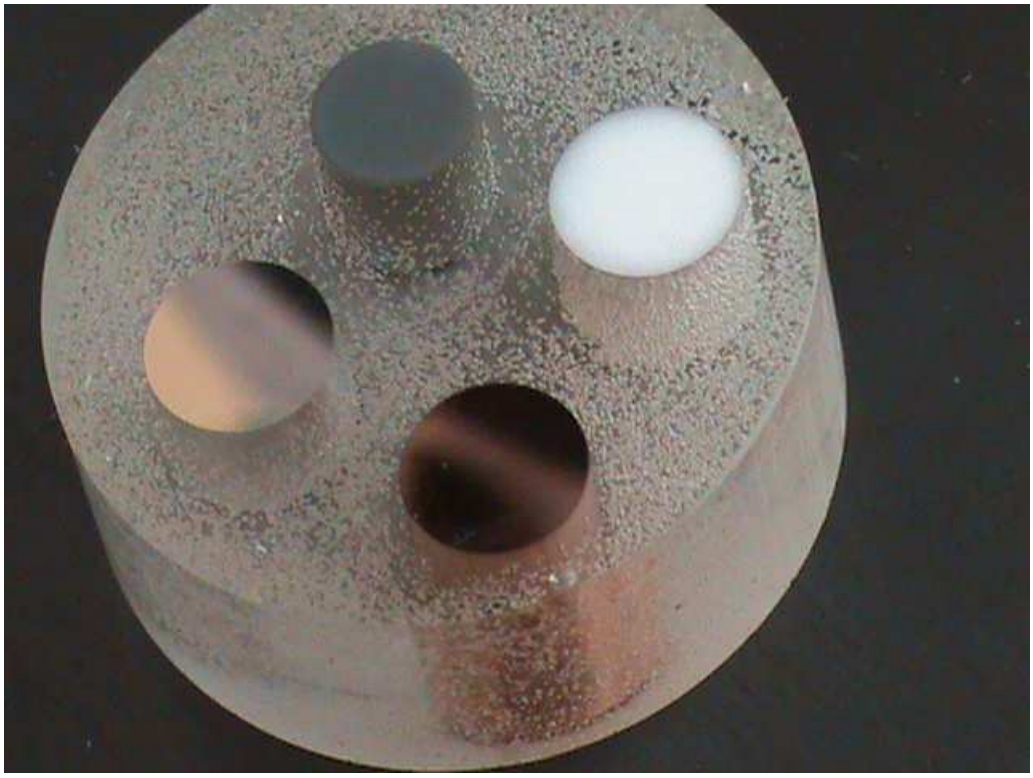

Fig.1 Cured resin used as fixture for four samples

Fig.2 DAP-2 Dia Duo Struers lapping machine with sample (Courtesy: Process Eng. Dept, Univ. of Stellenbosch)

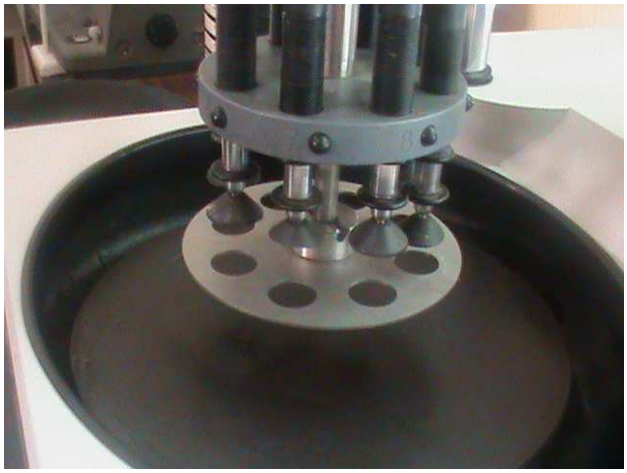

Fig.3 Struers RotoPol-35 lapping Machine (Courtesy: Geology Dept, Univ. of Stellenbosch)

Fig.4 Scanning tunneling microscope (Courtesy: Geology Dept, Univ. of Stellenbosch)

Fig. 5 E-beam deposition machine (Courtesy: iThemba Labs)

Fig.6 Empty e-beam crucible (Courtesy: iThemba Labs)

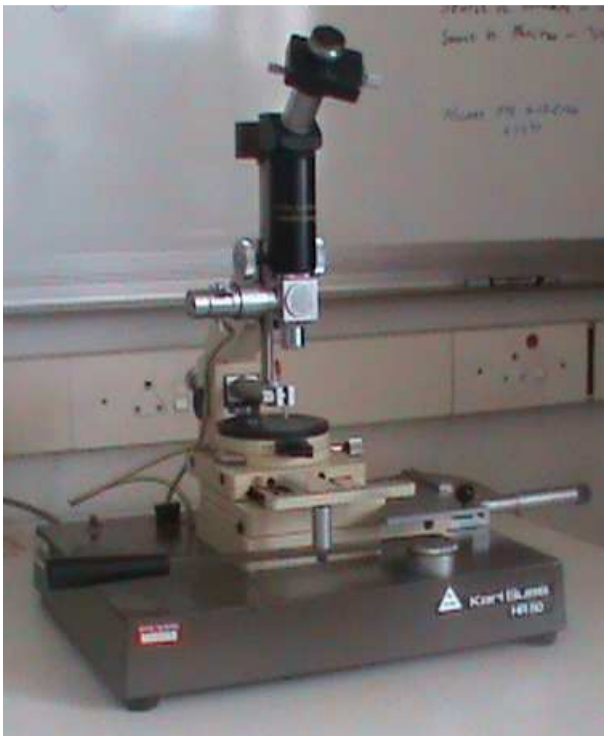

Fig.7 Karl Suss – HR 50 machine (Courtesy: iThemba Labs)

Fig.8 Ultrasonic bath (Courtesy: iThemba Labs)

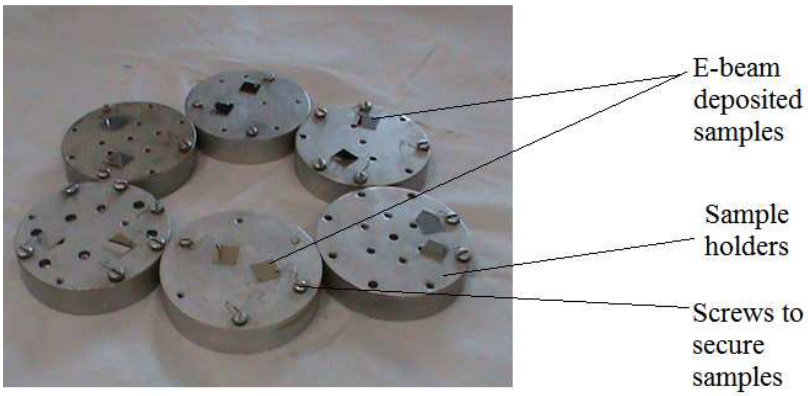

Fig.9 Silicon substrates mounted on aluminium sample holders (Courtesy: iThemba Labs)

Fig. 10 Indexing guide in the e-beam machine (Courtesy: iThemba Labs)

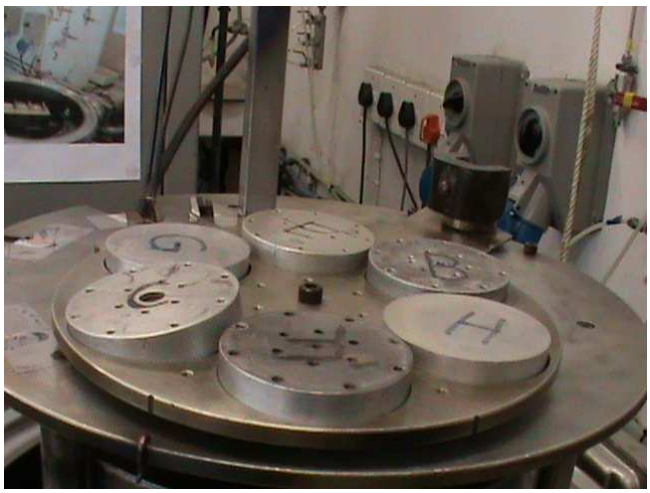

Fig. 11 Sample holders on the indexing guide in the e-beam machine (Courtesy: iThemba Labs)

L) APPENDIX L:Published peer reviewed paper in accredited Journals and conferences